Deconstructing Niche Contributions to Leukemogenesis: Modeling Shwachman-Diamond Syndrome

Noemi Angela Zambetti

Deconstructing Niche Contributions to Leukemogenesis: Modeling Shwachman-Diamond Syndrome

ISBN: 978-94-6299-296-2

Cover: Noemi Zambetti and Ridderprint BV, Ridderkerk, The Netherlands
Layout and printing: Ridderprint BV, Ridderkerk, The Netherlands

The work described in this thesis was performed at the Department of Hematology of the Erasmus Medical Center, Rotterdam, The Netherlands. The work was funded by grants from the Dutch Cancer Society (KWF Kankerbestrijding), the Netherlands Organization of Scientific Research (NWO), and the Netherlands Genomics Initiative. Printing of this thesis was financially supported by the Erasmus University Rotterdam.

Deconstructing Niche Contributions to Leukemogenesis: Modeling Shwachman-Diamond Syndrome

De beenmerg micro-omgeving in het ontstaan van leukemie:
Shwachman-Diamond syndroom als model-ziekte.

Doctoral dissertation

to obtain the degree of Doctor from the
Erasmus University Rotterdam
by command of the
rector magnificus

Prof.dr. H.A.P. Pols

and in accordance with the decision of the Doctorate Board.
The public defense shall be held on

Wednesday, 13 April 2016, at 13:30 hours
by

Noemi Angela Zambetti
born in Bari, Italy

Erasmus University Rotterdam

DOCTORAL COMMITTEE

Supervisor:
Prof.dr. I.P. Touw

Other members:
Prof.dr. H.R. Delwel
Prof.dr. J.N.J. Philipsen
Dr. M.M. von Lindern

Co-supervisor:
Dr. H.G.P. Raaijmakers

To Francesco Gensano, dear friend and inspiring researcher.
Your University fellows miss you dearly.

TABLE OF CONTENTS

Chapter 1

GENERAL INTRODUCTION

1. NORMAL HEMATOPOIESIS

The blood of vertebrates is composed of different cell types that circulate in a fluid extracellular matrix called plasma. These cell types comprise erythrocytes (or red blood cells, RBC), that provide O_2/CO_2 transport, thrombocytes (or platelets, PLT), involved in hemostasis, and leukocytes (white blood cells, WBC), which protect the organism from infections. The lifespan of most blood cells is short compared to the organism they supply, with certain WBC populations having a half-life of 5 hours or less.[1] The lifelong production of new blood cells, or hematopoiesis, is guaranteed by a pool of pluripotent cells that in adult mammals reside in the bone marrow (**Figure 1**). These cells, referred to as hematopoietic stem cells (HSCs), are able to divide and generate both differentiation-committed cells (called progenitors) and other pluripotent HSCs, virtually identical to the parent cell, which will preserve the hematopoietic capacity of the bone marrow over time. Proof that a single HSC can both differentiate and self-renew has been provided in different vertebrate models, showing that asymmetrical division of HSCs results from the specific orientation of cell fate determinants relative to the mitotic spindle.[2-4] However, in homeostatic conditions most HSCs are not actively dividing, but rather preserved in a quiescent state, which is believed to be essential to maintain the genetic integrity of HSCs.[5]

The differentiation of HSCs into mature blood cells occurs in a multistep process in which lineage maturation is associated with progressive restriction of multi-lineage cell potential. HSCs first differentiate into multipotent progenitors (MPPs), which lack self-renewal capacity but retain multi-lineage potential. MPPs further differentiate into oligopotent progenitors, namely the common lymphoid progenitor (CLP) and the common myeloid progenitor (CMP). CLPs are required to produce lymphoid cells, including natural killer (NK) cells, B and T lymphocytes and immature plasmacytoid dendritic cells (DC), which will complete their maturation outside of the blood stream. CMPs, on the other hand, differentiate into either megakaryocyte-erythroid progenitors (MEPs) or granulocyte-macrophage progenitors (GMPs). MEPs can further differentiate into RBCs or megakaryocytes (from which PLTs are produced), whereas GMPs give rise to immature myeloid DCs, monocytes/macrophages and granulocytes. The latter are immune cells characterized by the presence of cytoplasmic granules. Based on how such granules react to histochemical dyes (e.g. May-Grünwald-Giemsa or Wright's staining), granulocytes are further classified into basophils, eosinophils and neutrophils.[6]

Neutrophil maturation

Neutrophilic granulocytes, or neutrophils, represent the most abundant WBC in the human blood and play a central role in the innate immune system, representing the first line of defense in the acute phase of inflammation. In response to chemotactic stimuli, neutrophils migrate from the

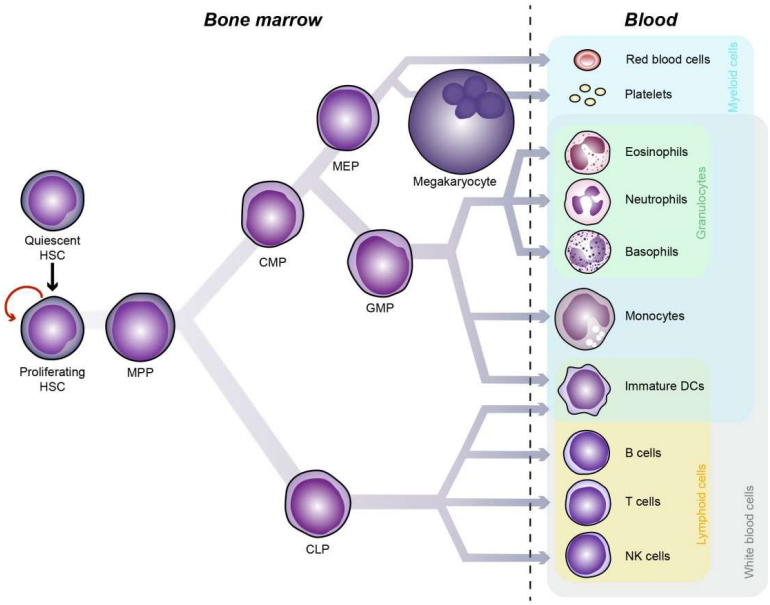

Figure 1. Schematic view of hematopoiesis. Adapted from Reya et al.[7] The production of blood cells requires the expansion and differentiation of otherwise quiescent HSCs. Through progressive differentiation into more committed progenitors, different blood cells are produced in the bone marrow and enter the blood stream. Myeloid cells (blue box) derive from CMPs, whereas lymphoid cells (orange box) originate from CLPs. Note that DCs can differentiate from either CMP or CLP, depending on their subtype. Eosinophils, neutrophils and basophils are collectively referred to as granulocytes (green box), and together with monocytes/macrophages, DCs and lymphoid cells constitute the different subtypes of WBCs (grey box).

blood stream to the inflamed tissues. Here, they participate to the immune defense by different means, that include the degranulation and secretion of antimicrobial peptides, the phagocytosis of opsonized bacteria, the release of cytokines to amplify the immune response, and the secretion of the so-called neutrophil-extracellular traps (NETs), networks of chromatin and proteases that allow the physical containment of pathogens and their killing.[8]

The differentiation of neutrophils from GMPs is associated with nuclear and cytoplasmic changes that morphologically define different maturation stages (**Figure 2**). Myeloblasts are the most primitive cells of the granulocytic lineage and are characterized by loose chromatin and visible nucleoli. The production of primary or azurophilic granules defines the promyelocyte stage: these granules contain different antimicrobial peptides, including myeloperoxidase, elastase,

cathepsins and defensins. At the stage of myelocytes, secondary or specific granules are formed, which contain cytotoxic molecules such as lactoferrin and lysozyme. Myelocytes have a pronounced Golgi apparatus and represent the last dividing cell in the neutrophil maturation lineage. Metamyelocytes are post-mitotic cells with an eccentric, indented nucleus and more condensed chromatin. They are characterized by the production of tertiary granules (gelatinase), containing matrix remodeling enzymes such as MMP8 and MMP9. In humans, band cells have a typical horse-shoe shaped nucleus and a mature cytoplasm. They further differentiate into mature neutrophils, which present a segmented nucleus in humans and a donut-shaped one in mice.[9]

Although in normal myelopoiesis only mature cells are released from the bone marrow into the blood, in case of infections and in certain bone marrow disorders immature myeloid cells circulate in the peripheral blood (left shift). Hematological disorders can also be characterized by dysplastic neutrophil morphology, with hypo- or hypersegmented nuclei, hypogranularity and presence of cytoplasmic inclusions.[10]

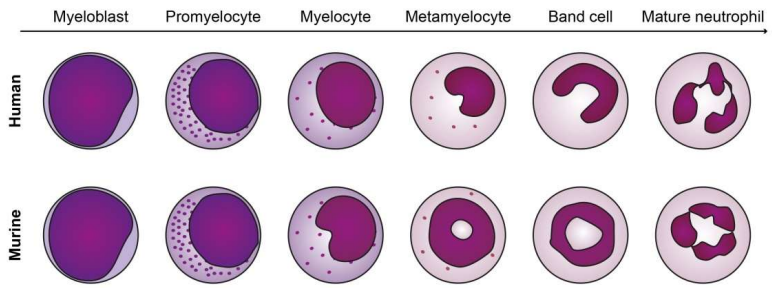

Figure 2. Morphological staging of neutrophil development. Adapted from Pillay et al.[11] Schematic representation of the morphological changes observed during neutrophil development in humans and mice.

2. REGULATION OF HEMATOPOIETIC STEM CELLS BY THE BONE MARROW NICHE

Whether a HSC will proliferate, differentiate or be kept quiescent depends on both cell intrinsic cues, such as the expression of lineage-instructive transcription factors, and extrinsic signals, including growth factors, cytokines, reactive oxygen species, and factors derived from the HSC niche.[12,13]

The HSC niche is defined as the local microenvironment that maintains and regulates HSCs. The supporting nature of the HSC microenvironment was first demonstrated in the late 1970s with seminal work of Michael Dexter, showing that the bone marrow stroma is able to support long-term cultures of hematopoietic cells.[14] The concept of the niche was next formulated by Ray Schofield, who hypothesized the existence of a "fixed tissue" where non-hematopoietic cells maintain HSCs and prevent their differentiation.[15]

The supporting role of the niche results both from the physical interaction with HSCs, and consequently their retention in the microenvironment, and the active secretion of soluble factors that regulate HSC function. The physical adhesion to the niche depends on different proteins, expressed on the HSC plasma membrane, able to bind niche cells or components of the extracellular matrix; these proteins comprise VCAM1,[16] CD44[17] and the integrins α4β1, α6β1 and α9β1.[18-21] Niche cells also secrete cytokines, chemokines and other molecules to maintain HSCs and keep them quiescent. The chemokine CXCL12 (or stromal cell-derived factor 1, SDF-1) binds to the receptor CXCR4 to keep HSCs quiescent and non-motile; its expression is increased by the stromal cells in the presence of different DNA damaging agents and upon parathyroid hormone (PTH) signaling.[22,23] Stem cell factor (SCF, or Kit ligand) is expressed either in a soluble or in a membrane-bound form, the latter being required for HSC maintenance *in vivo*.[24] Other important stroma-derived molecules regulating HSCs are angiopoietin 1, Notch and Wnt ligands and thrombopoietin.[25-28]

The development of transgenic mouse models and the identification of HSC surface markers have contributed to define the cellular components of the bone marrow niche. Emerging data supports a view where different cell types may regulate HSCs both directly and indirectly, i.e. by signaling to other niche components, thus reshaping the definition of niche as a complex network rather than a single cellular entity.[29]

Composition of the bone marrow niche

While the cell types within the hematopoietic lineage and their hierarchy are relatively well defined (**Figure 1**), our understanding of the HSC niche composition is significantly more limited, mostly due to the rarity of HSCs and the difficulty in their identification *in situ*.

The earliest attempts to define the microenvironment of primitive hematopoietic cells relied on fractionation experiments in mice, consisting in separating different areas of the bone marrow and evaluating the frequency of hematopoietic colony-forming units within each fraction.[30] This led to the observation that primitive hematopoietic cells localize preferentially at the endosteum, and suggested that factors or cells located at the bone surface are important to sustain hematopoiesis.[30]

This concept found further support in the early 2000s, with studies defining bone depositing cells (osteoblasts) as candidate components of the HSC niche. In one of these studies, inducing osteoblast proliferation through the activation of the parathyroid hormone receptor signaling resulted in the expansion of the hematopoietic stem and progenitor cell (HSPC) compartment.[26] The same result was achieved in a second study, in which osteoblast proliferation was experimentally induced through the conditional inactivation of the bone morphogenetic protein receptor type IA.[31] Conversely, in a third study, ablating osteoblasts resulted in a severe yet reversible pancytopenia, with reduced numbers of primitive hematopoietic cells.[32]

Collectively, these early reports indicated that osteoblasts influence the HSPC pool size in mice and suggested their role as niche components. In line with this view, cells of the osteoblastic lineage were shown to secrete important niche factors such as CXCL12,[22,33] angiopoietin 1,[25] thrombopoietin[28] and the Notch ligand Jagged-1.[26] Finally, transplanting fetal bone cell populations under the mouse kidney capsule was sufficient to produce ectopic donor-derived niches for the recipient's HSCs, niches that could not be formed by suppressing the expression of the osteogenic transcription factor osterix.[34]

Further advances in the understanding of the niche composition followed the improvements in the HSC identification. The introduction of SLAM family receptors as HSC markers allowed a more accurate definition of the primitive hematopoietic compartment, with one in every 2.1 SLAM-defined cells ($CD48^-$ $CD150^+$ Lin^- $c\text{-}Kit^+$ $Sca\text{-}1^+$) predicted to be a long term-HSC.[35] The availability of these novel markers enabled a better histological assessment of the spatial relationship between HSCs and their microenvironment. In contrast with earlier reports,[30] SLAM marker-based imaging studies revealed that only 14% of the HSCs localized at the endosteum, while 60% were in contact with the sinusoidal endothelium.[35] This opened the possibility that perivascular or endothelial cells could play a role in maintaining HSCs.

Numerous studies supported this concept. First, a population of stromal cells was described that localized both at the endosteum and close to bone marrow sinusoids and expressed high amounts of the HSC supporting factor CXCL12; these cells were renamed CXCL12-abundant reticular (CAR) cells.[36] Other perivascular cells identified by the expression of the intermediate filament Nestin were later found to produce CXCL12 and to be required for homing and maintenance of HSCs.[37] Additionally, endothelial cells seemed to regulate directly HSC expansion and self-renewal via Notch ligands and E-selectin signaling.[38-40] To complete this complex scenario, other cell types in the bone marrow were demonstrated to regulate at different levels HSCs, among which osteoclasts,[41] adipocytes[42] and cells of the nervous system.[42-45]

In an attempt to reach a unifying view among these different (and sometimes discrepant)[47] niche models (**Figure 3**), researchers started interrogating the relative importance of different stromal components by systematically depleting key niche factors from each population and evaluating

the effects of such depletion on HSC biology. Endothelial and perivascular mesenchymal cells, defined respectively by the expression of the angiopoietin- (*Tie2*) and leptin receptor (*Lepr*), were in this way demonstrated to be essential sources of SCF. Deficiency of the ligand in *Tie2*$^+$ and *Lepr*$^+$ cells caused depletion of transplantable HSCs. No effect was observed instead by deleting *Scf* in other cell types, namely hematopoietic (*Vav1*$^+$) cells, Nestin (*Nes*) expressing mesenchymal cells and osteoblasts (identified by expression of the marker *Col2.3*).[48] Similarly, deficiency of CXCL12 in perivascular or endothelial cells had dramatic effects on HSC maintenance, and resulted respectively in HSC mobilization (*Lepr*-cre mice), reduced frequency of HSCs (*Tie2*-cre model), and compromised HSC reconstitution capacity (deletion in *Prx1*$^+$ perivascular mesenchymal cells).[49,50] Conversely, HSC frequencies were not affected when abrogating CXCL12 expression in *Vav1*$^+$, *Nes*$^+$ and osteolineage (*Col2.3*$^+$ and osterix$^+$) cells.[49,50]

While these studies seem to converge on endothelial and perivascular cells as the main producers of key HSC niche factors, they do not formally exclude that other cell types contribute - at least indirectly - to HSC maintenance. This could explain the apparent discrepancy with earlier reports indicating bone lineage cells as essential niche components. In addition, recent data suggests that different putative niche cell types may be connected through unexpected differentiation hierarchies. For instance, perinatal osterix-expressing cells (Osx$^+$), traditionally thought to represent osteoblast progenitors, were found to be a long-lived source of different stromal cell types, including adventitial and *Nes*$^+$ perivascular cells[51,52] (**Figure 3**).

In conclusion, data derived from experiments in mice depicts a complex scenario where the identity and relative importance of the cell types composing the niche remains incompletely understood. Moreover, there is still little knowledge about how these results in mice rely to human biology.

Few studies have analyzed the HSC niche composition in humans to date. An important one identified the adhesion molecule CD146 as marker of a population of perivascular and bone-forming cells that express SCF and CXCL12.[53] More recently, Tormin and colleagues showed that non-hematopoietic cells marked by the nerve growth factor receptor (CD271) are able to support hematopoiesis. This population comprises CD146$^+$ perivascular and CD146$^-$ endosteal subsets, both localizing in proximity to human CD34$^+$ hematopoietic stem and progenitor cells (HSPCs) *in vivo*.[54] The transcriptional study of CD271$^+$ cells confirmed the hematopoietic supporting activity of this population, as shown by the expression of angiopoietin-1 and CXCL12. Transcriptional analysis also indicated that CD271$^+$ cells express markers for different mesenchymal fates, including pericytes (*ACTA2*, *CSPG4*, *PDGFRA*), osteoblasts (osterix, osteonectin, osteopontin, osteocalcin) and adipocytes (*PPARG*, *LPL*, *FABP4*).[55] This promiscuous signature may either reflect single cell multipotency or a heterogeneous nature of the CD271$^+$ cell population. If this were the

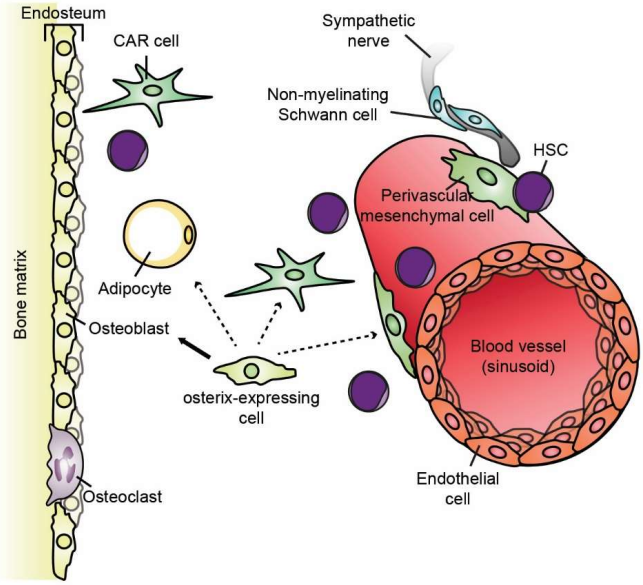

Figure 3. The bone marrow niche: a model in progress. Adapted from Morrison and Scadden.[29] Most of the HSCs in the murine bone marrow are found close to sinusoids (right), while fewer are located near the endosteum (left). Different cell types have been proposed as HSC niche components, among which bone-lining osteoblasts, osteoclasts, adipocytes, cells of the nervous system (non-myelinating Schwann cells), CAR cells and perivascular mesenchymal cells. The latter are further identified by the expression of markers such as *Nes*, *Lepr* and *Prx1*, but the exact hierarchy between these cell types is not completely understood. Moreover, mesenchymal cells expressing Osx, typically considered osteoprogenitors (bold arrow), may differentiate to adipocytes, perivascular adventitial and *Nes*$^{+}$ stromal cells (dashed arrow),[51,52] further complicating the relationships between different niche components.

case, additional markers may be required in the future to better discriminate potential hematopoiesis-supporting subsets.

3. DISORDERS OF HEMATOPOIESIS

The complex network of intracellular and niche-derived signals that regulate HSC biology allows fine-tuning of the blood cell production based on different systemic requirements, but at the same time needs tight regulation in order to ensure the homeostasis of the hematopoietic

system. Alterations of this delicate balance may lead to disorders of hematopoiesis, such as acute myeloid leukemia and bone marrow failure.

Acute myeloid leukemia (AML) is a form of hematopoietic malignancy characterized by uncontrolled proliferation of immature myeloid cells with impaired differentiation capacity. The expanding leukemic clone rapidly outgrows normal HSPCs, leading to decreased production of normal mature blood elements. Clinically, this translates in impaired blood function, with symptoms such as fatigue, increased risk of infections or bleeding episodes, and in the accumulation of myeloblasts in the blood and bone marrow of leukemic patients. The risk of developing acute myeloid leukemia is higher in patients affected by bone marrow failure syndromes.[56]

Bone marrow failure (BMF) is defined as the impaired production of one or multiple hematopoietic lineages. Usually BMF presents itself as a deficiency in one specific blood cell type but can progress to involve all lineages. BMF can be acquired or genetically transmitted; the myelodysplastic syndromes represent the most common forms of acquired BMF syndromes.[57]

Acquired BMF: the myelodysplastic syndromes

The myelodysplastic syndromes (MDS) are a heterogeneous group of malignant hematopoietic stem cells disorders characterized by ineffective, dysplastic hematopoiesis and a variable risk of progression to acute myeloid leukemia. Its etiology is largely unknown, but MDS can occur as a result of environmental exposure to chemotherapy and other mutagenic agents. In addition, MDS may develop in patients suffering from congenital BMF disorders, such as Fanconi anemia and Shwachman-Diamond syndrome.[58]

Clinically, MDS is characterized by cytopenias, which include macro- or normocytic anemia, thrombocytopenia and neutropenia. Based on the presence of uni- or multilineage cytopenia, karyotypic changes and the percentage of circulating blasts, the International Prognostic Scoring System (IPSS) classifies the outcome of newly-diagnosed MDS patients into low, intermediate or high risk of acute myeloid leukemia (AML) development.[59]

The molecular basis of MDS remains incompletely understood. More than 40 recurrent somatic mutations have so far been associated with MDS, implicating - among others - RNA splicing, epigenetics, transcription factor activation and ribosome biogenesis pathways in its pathogenesis.[60] Although these molecular insights may instruct MDS research and potentially suggest novel treatments, it needs to be pointed out that clonal, MDS-associated mutations have been described in otherwise healthy individuals.[61,62] At the same time, patients with idiopatic cytopenia and idiopatic dysplasia often evolve to MDS in the absence of the genetic mutations or

aberrant karyotypes typically associated with MDS.[63] Disease progression in these patients may depend on the acquisition of unknown mutations, but it could also indicate that the pathogenesis of MDS may be complex, with the HSC genetic make-up being an important, but not exclusive determinant factor for MDS development.

Inherited forms of bone marrow failure: the ribosomopathies

Inherited bone marrow failure syndromes (IBMFS) include, among others, Fanconi anemia, severe congenital neutropenia and the disease family of so-called ribosomopathies.

Ribosomopathies are diseases caused by mutations affecting the biogenesis of ribosomes, cellular ribonucleoprotein complexes required for protein translation. In eukaryotes, the biosynthesis of ribosomes is a complex multistep event that requires four types of ribosomal RNA (rRNA), over 80 ribosomal structural proteins, more than 150 different assembly proteins and around 70 small nucleolar RNAs (snoRNA), which cooperate to produce the small (40S) and the large (60S) subunit of ribosomes.

The biogenesis of ribosomes is schematically represented in **Figure 4.** Briefly, rRNAs are first transcribed as precursors by RNA polymerases: in particular, RNA polymerase I (Pol-I) transcribes the 45S multicistronic pre-rRNA, which will generate the 5.8S, 18S and 28S rRNA species, while RNA polymerase III (Pol-III) transcribes the 5S pre-rRNA. These rRNA precursors are further processed in the nucleolus (45S) or in the cytoplasm (pre-5S) to generate the final rRNA components of the ribosomes. Next, the ribosomal proteins are imported in the nucleus and assembled onto rRNAs to form the pre-40S and pre-60S subunits. These precursor subunits are then exported in the cytoplasm to generate the mature 40S and 60S subunits, ready to be assembled in a translation-competent 80S ribosome.

Despite the large number of genes involved in ribosome biogenesis, relatively few have been found mutated in ribosomopathies (**Figure 4** and **Table 1**), probably because a strong selective pressure exists to remove malfunctioning ribosomes. Most of the different ribosomopathies described to date are inherited, but sporadic mutations of ribosomal genes *RPL5*, *RPL10* and *RPL22* have been observed in patients suffering from T cell acute lymphoblastic leukemia,[64,65] and a causative link with impaired ribosome biogenesis has been demonstrated for the **5q- syndrome**.[66,67] This acquired disorder of hematopoietic cells is characterized by a monosomy involving all or part of the long arm of human chromosome 5 and is associated with development of low-risk MDS.[66] Haploinsufficiency of *RPS24*, mapping on 5q, has been demonstrated to participate in the pathogenesis of the macrocytic anemia in 5q- syndrome patients.[67,68]

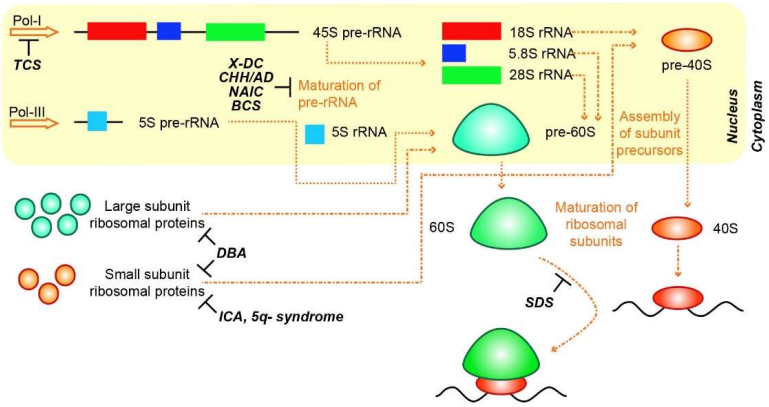

Figure 4. Impairment of ribosome biogenesis in ribosomopathies. Schematic representation of ribosomal biogenesis and indication of the steps affected in different ribosomopathies. TCS: Treacher Collins syndrome. X-DC: X-linked dyskeratosis congenita. CHH: cartilage hair hypoplasia. AD: anauxetic dysplasia. NAIC: North American Indian childhood cirrhosis. BCS: Bowen-Conradi syndrome. SDS: Shwachman-Diamond syndrome. DBA: Diamond-Blackfan anemia. ICA: isolated congenital asplenia.

Interestingly, predisposition to MDS characterizes other (inherited) ribosomopathies, suggesting a specific dependency of myeloid lineage cells for efficient ribosomal biogenesis. An increased risk to develop MDS and progress to AML is observed in patients suffering from X-linked dyskeratosis congenita, Diamond-Blackfan anemia and Shwachman-Diamond syndrome, albeit malignancy occurs in these disorders at different frequencies. Predisposition to cancer, including MDS/AML, is observed in around 4% of Diamond Blackfan anemia patients, less than in other IBMFS.[69]

Perhaps the inherited ribosomopathy with the highest degree of genetic heterogeneity (**Table 1**), **Diamond Blackfan anemia** (DBA) is a pure RBC aplasia disorder characterized by macrocytic anemia, reticulocytopenia and decreased erythroid precursors in the bone marrow.[70] Genetically, DBA is a heterogeneous disease. The first ribosomal gene discovered to be mutated in DBA was *RPS19*, which is indeed mutated in around 25% of patients.[71] Since then, mutations or deletions in other genes encoding for large or small subunit ribosomal proteins have been discovered (**Table 1**), which globally affect more than 50% of all DBA patients.[72] Mutations in the erythroid transcription factor *GATA1* have also been found in rare DBA cases, leading to reduced expression of full length GATA1 isoforms.[73] Interestingly, it has been shown that haploinsufficiency of ribosomal protein genes in DBA leads to reduced GATA1 translation, thus impaired GATA1 activity may represent a common mechanism underlying RBC aplasia in DBA.[74,75] Moreover, reduced translation of specific genes characterized by internal ribosomal entry sites (IRES), some of which

known to be required for erythropoiesis (*Bag1*, *Csde1*), could contribute to the pathogenesis of DBA.[93]

Table 1. Inherited ribosomopathies.

Disease	Mutated gene	Non hematological features	Hematologic defects	Cancer predisposition
Treacher Collins syndrome	*TCOF1,*[76] *POLR1D,*[77] *POLR1C*[77]	Craniofacial deformities, abnormal airways, ear anomalies	None	None
X-linked dyskeratosis congenita	*DKC1*[78]	Skin hyperpigmentation, nail dystrophy, oral leukoplakia	Progressive BMF	MDS, AML, head and neck tumors
Diamond-Blackfan anemia	*RPS7,*[79] *RPS10,*[80] *RPS17,*[81] *RPS19,*[71] *RPS24,*[82] *RPS26,*[80] *RPL5,*[83] *RPL11,*[83] *RPL26,*[84] *RPL35A*[85]	Craniofacial and thumb abnormalities, cardiac defects, growth retardation	Red cell aplasia	Osteosarcoma, MDS and AML (low frequency)
Cartilage hair hypoplasia	*RMRP*[86]	Short limb dwarfism, sparse hair, malabsorption	Lympho- and neutropenia, macrocytic anemia	Non-Hodgkin lymphoma, basal cell carcinoma
North American Indian childhood cirrhosis	*CIRH1A*[87]	Transient neonatal jaundice progressing to biliary cirrhosis	None	None
Shwachman-Diamond syndrome	*SBDS*[88]	Exocrine pancreas insufficiency, short stature, early onset osteoporosis, metaphyseal dysostosis	Neutropenia, anemia, thrombocytopenia	MDS and AML (high frequency)
Anauxetic dysplasia	*RMRP*[89]	Severe short stature, hypodontia, mentalretardation	None	None
Bowen-Conradi syndrome	*EMG1*[90]	Severe growth retardation, craniofacial defects, rockerbottom feet	None	None
Isolated congenital asplenia	*RPSA*[91]	None	Agenesis or hypoplasia of spleen leading to immunodeficiency, Howell-Jolly bodies	None
Aplasia cutis congenita	*BMS1*[92]	Local agenesis of skin	None	None

Tissue specificity in inherited ribosomopathies

While the sporadic nature of T-ALL and 5q- syndrome naturally limits the symptoms of this disease to a single tissue, it would be intuitive to think that a congenital ribosomal defect should homogeneously affect all organs, as protein translation is equally required in every cell of our body. On the contrary, the symptoms of inherited ribosomopathies are rather limited to few or even one tissue, as it is the case for North American Indian childhood cirrhosis, isolated congenital asplenia and aplasia cutis congenita (**Table 1**). Moreover, although affecting the same metabolic process, different ribosomopathies do not share the same tissue specificity, albeit many are associated with development of BMF and increased risk of developing blood cancers (**Table 1**). Solving the central enigma of tissue specificity in ribosomopathies is crucial to the field as it may result in more efficient therapies and perhaps preventive treatments against cancer development in these conditions.

A theory frequently proposed to explain this conundrum considers the symptoms of ribosomopathies as resulting from defects of cell proliferation. In particular, ribosomopathies would affect tissues with a high proliferative rate, like the bone marrow, leading to their aplasia. This concept derives from the regulatory role of ribosome biogenesis in cell cycle progression. In yeast, most of the translational machinery is devoted to the production of ribosomes, thus ribosome biogenesis itself competes with the translation of cell cycle regulators, often characterized by complex mRNA structures and high protein turnover, until threshold concentrations of ribosomes are reached.[94] This represents a control system that couples mitosis with cell growth, allowing the cell to divide only after a sufficient level of protein synthesis. Evidence of impaired cell division upon deficit of ribosomal components is found in metazoans. Haploinsufficiency of ribosomal protein genes in *Drosophila* "minute" mutants induces a developmental delay with an overall decrease in cell mitotic rate, while conditional deletion of ribosomal protein S6 in mouse liver compromises hepatic cell proliferation and thus organ regeneration.[95,96]

While impaired proliferation could explain the hypoplastic phenotypes often observed in ribosomopathies, the limitations of considering this phenomenon as the sole pathogenic factor underlying these diseases should be considered. First, this view would predict that every organ system should be equally compromised during embryogenesis, since at this stage every tissue is rapidly proliferating. Moreover, according to this theory, different ribosomopathies should affect the same tissues (those with the highest proliferative rates), which is in contrast with the heterogeneity of clinical symptoms in ribosomopathies. In the context of hematopoiesis, one would imagine that all blood lineages should be affected by ribosomal biogenesis defects, as all hematopoietic progenitors are fast dividing, while distinct ribosomopathies show different blood cell lineage proclivity.

Alternative explanations for tissue specificity in ribosomopathies have been proposed. First, in contrast with the view of ribosomes as "housekeeping" entities, with constant composition in every cell, the existence of "specialized" ribosomes, different in composition or in mRNA targeting, has been reported. The haploinsufficiency of ribosomal gene *Rpl38* in mouse results in homeotic transformation of distinct axial skeleton regions.[97] Interestingly, the expression pattern of *Rpl38* in mouse embryos is enriched in the same regions and is locally required to translate Homeobox A (*HoxA*) gene transcripts from IRES elements localized in their 5' untranslated regions (5'-UTR).[97,98] As previously indicated, reduced IRES-mediated translation of *Bag1* and *Csde1* has been observed in mouse erythroblast cell lines haploinsufficient for DBA-related genes, leading to impaired erythroid differentiation.[76] Defective translation from IRES has been shown also in primary lymphoblasts and fibroblasts from individuals affected by X-linked dyskeratosis congenita.[99]

Finally, it is possible that ribosomopathy-associated genes may have extra-ribosomal functions restricted to specific cell types. In this regard, it is interesting to note how both cartilage hair hypoplasia (CHH) and anauxetic dysplasia (AD) are caused by mutations in the *RMRP* gene, required for 5.8S rRNA cleavage, albeit only CHH is associated with bone marrow failure and cancer predisposition. Interestingly, RMRP is also required for cell cycle regulation by mediating cyclin B degradation, but accumulation of cyclin B is observed only in CHH, perhaps explaining cancer predisposition in this ribosomopathy.

Role of p53 in ribosomopathies

The tumor suppressor protein p53 is a master regulator of cell fate and induces programs of cell cycle arrest, senescence and apoptosis in response to different stressors. It has emerged that impaired ribosome biogenesis can activate the p53 pathway, resulting in programmed cell death.

In healthy cells, the concentration of p53 is kept low by continuous proteasome degradation, which requires p53 ubiquitination by MDM2. Perturbation of ribosome biogenesis uncouples rRNA transcription and protein synthesis, leading to nucleolar stress and accumulation of unincorporated ribosomal proteins. Several of these proteins (RPL11,[100] RPL23,[101,102] RPL5,[103] RPS7,[104] RPL26[105], and RPS3[106]) have been shown to bind and segregate MDM2, thus inducing activation of the p53 pathway.

Animal models have shown that p53 activation may functionally underlie the pathogenesis of ribosomopathies. Monoallelic loss of *Trp53* rescues craniofacial anomalies in a mouse model of Treacher Collins syndrome by preventing apoptosis of neural crest cells.[107] Similarly, reduced dose of *Trp53* ameliorates RBC counts in mice with heterozygous mutations of *Rps19* and rescues macrocytic anemia in a mouse model of 5q- syndrome.[68,108]

Nevertheless, the relation between p53 and ribosomopathies may be more complex. First, accumulation of p53 protein is not a necessary consequence of ribosomal stress. Heterozygous mutations in 17 different zebrafish ribosomal proteins lead to poor p53 translation rather than its accumulation and induced the formation of tumors similar to those developing upon loss-of-function mutation of p53.[109] Second, the activation of p53 may not be required for disease pathogenesis. For instance, the skeletal patterning defect of *Rpl38* haploinsufficient mice is not rescued by reduced dosage of *Trp53*.[97] Interestingly, alternative models of *Rps19* deficiency in zebrafish and in murine cell lines showed p53-independent defects of erythropoiesis.[76,110] Finally, distinct models of SBDS deficiency reached opposite conclusions about the requirements of p53 activation for pancreatic insufficiency in Shwachman Diamond syndrome.[111,112]

Shwachman-Diamond syndrome

Shwachman-Diamond syndrome (SDS) is an autosomal recessive genetic disease caused by mutation in the gene *SBDS* and characterized by exocrine pancreatic insufficiency, skeletal abnormalities, bone marrow failure (in particular neutropenia), and a strong predisposition to develop MDS and AML.[113,114] The disease occurs with an incidence of around 1:77,000[115] and is typically diagnosed in the first year of life based on the pancreatic phenotype (steatorrhea and nutrient malabsorption) and the recurrence of infections. Differential diagnosis, including genetic testing, is necessary to exclude cystic fibrosis and Pearson disease, also characterized by pancreatic failure and frequent infection episodes.

Clinical manifestations and treatment

Bone defects are common in SDS patients and include short stature, delayed dentition, metaphysial and thoracic dysplasia, and early onset low-turnover osteoporosis, defined as osteopenia caused by a reduced number of osteoblasts and osteoclasts.[116,117] Skeletal defects may regress in time or progress and cause limb deformity and fracturing of the femoral necks.[116] Orthopedic intervention is however rarely required and surgery is mostly limited to cases of rib cage defects impairing the patient's respiratory capacity.

Although severe pancreatic insufficiency is a major concern in newborn and infant SDS patients, this condition often improves with age and pancreatic enzyme supplementation treatment can be stopped in half of the patients at the age of 4.[118] However, it must be pointed out that a progressive involvement of the gastrointestinal tract is possible, most notably diagnosed as hepatic disorders.[119] Neurocognitive deficits have been described in some SDS patients, albeit symptoms varied widely.[120]

The hematological features of SDS are the main cause of morbidity and mortality in the disease. The hallmark of BMF in SDS is neutropenia, observed in at least 90% of the patients.[121] Beside having reduced counts, neutrophils can also show defects of chemotaxis.[122,123] Adaptive immunity may be compromised in SDS, probably contributing to the high frequency of infections in these patients. Different degrees of B and T cell defects have been registered, including low number of B cells and reduced production of antibodies.[124] Anemia and thrombocytopenia are observed in many patients, although they are often intermittent or asymptomatic.[125,126] The bone marrow of SDS patients is often hypocellular, and left-shifted myelopoiesis is a common finding, with 24.7-30% of patients presenting myeloid maturation arrest in the bone marrow.[126,127] Increased vascularity can be observed upon progression to MDS/AML.[128]

Malignant progression of the hematological disease is a major concern in SDS. The estimated cumulative risk of leukemia in SDS patients varies in different reports between 20 and 70%, with higher risk in case MDS is diagnosed.[116,129] The bone marrow cytogenetic abnormalities i(7q) and del(20q), typical of MDS/AML, are often observed in SDS patients in the absence of overt MDS and they largely persist without progressing to malignancy.[121]

The treatment of hematological defects in SDS is typically limited to oral antibiotics, in case of infections, and monitoring of the disease. Patients with anemia or thrombocytopenia rarely require blood transfusions and G-CSF treatment is usually not prescribed for neutropenia, but can be beneficial in case of recurrent infections. Bone marrow smears and biopsies are recommended at the time of diagnosis and every 1-3 years to monitor progression to MDS and AML. HSC transplantation is the elected treatment in case of severe aplastic anemia or leukemia, while chemotherapy is usually not recommended.[114]

Molecular genetics

SDS is considered a monogenic genetic disease, as 90% of patients show mutations in the Shwachman-Bodian-Diamond syndrome gene (*SBDS*), mapping on chromosome 7q11.[89] The two most common mutations, c.183-184TA>CT and c.258+2T>C, are thought to arise from recombination events (gene conversion) between *SBDS* and its paralogous pseudogene copy *SBDSP*, located 5.8 Mb distally from *SBDS*.[89] Patients are mostly compound heterozygous for the two mutations, however other mutations can be observed, resulting in deletions/insertions, premature truncations, frameshifts or amino acidic substitutions.[89,130]

The c.183-184TA>CT mutation introduces an in-frame premature stop (K62X) in *SBDS* mRNA, while c.258+2T>C disrupts the donor splice site of intron 2, and promotes the use of a cryptic upstream donor site at position 251-252.[89] This ultimately results in an 8 bp deletion and a consequent frameshift (C84fsX3), with creation of a premature stop codon (UAA codon at

position 267-269 of the wild type mRNA).[89] Both the truncating and the frameshift mutations have been shown to induce reduction or complete absence of detectable protein levels in patient-derived WBCs, while missense mutations have been proposed to affect the stability and the conformation of SBDS protein.[131,132]

Function of SBDS

Since its association with SDS, it was observed that *SBDS* represented a highly conserved gene with orthologs in archaea, plants and vertebrates.[89] The archaeal *SBDS* ortholog clusters in an operon encoding predicted RNA-processing exosome components and proteins of the large ribosomal subunit.[133] The *bona fide* function of SBDS protein in ribosome biogenesis (**Figure 5**) was first described in yeast, where the SBDS ortholog SDO1 was shown to mediate the release of the nucleolar shuttling factor TIF6 (ortholog of mammalian eukaryotic initiating factor 6, eIF6) from pre-60S ribosomes, allowing the recycling of TIF6, the full maturation of the large subunit and its binding to the 40S.[134] Studies in *Sbds* inducible knock-out mouse models later elucidated the mechanisms of eIF6 release and proved that SBDS couples the GTPase activity of elongation factor-like 1 (EFL1) to a structural conformational change that induces eIF6 release.[132] Reduced ribosomal subunit joining was observed in SDS patients, indicating that *SBDS* mutations impair the eIF6 releasing function of SBDS.[135,136]

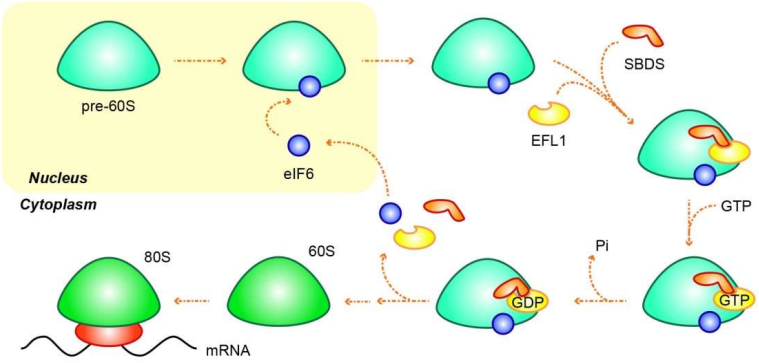

Figure 5. SBDS induces eIF6 release in ribosome biogenesis. Adapted from Menne et al.[134] and Finch et al.[132] SBDS and EFL1 are recruited on the pre-60S subunit. Upon GTPase activity of EFL1, SBDS changes conformation, allowing the release of eIF6 and its recycling in the nucleus, where it works as a shuttling factor for pre-60S.

Beside its role in ribosome biogenesis, other functions have been suggested for SBDS protein. Based on SBDS localization at the mitotic spindle and its binding to microtubules, it was proposed that SBDS is required in mitosis.[137,138] Other studies showed colocalization of SBDS with F-actin and Rac2 in neutrophil cellular protrusions and disruption of actin polarization in SDS neutrophils, indicating a possible role for SBDS in the metabolism of the cytoskeleton.[139] However, it needs to be pointed out that SBDS localization at the cytoskeleton may also reflect localized translation of cytoskeleton proteins. Finally, SBDS may have a general function in the context of cellular stress, as it was shown to improve cellular survival after DNA damage and endoplasmic reticulum stress, perhaps through its binding to RPA70 and DNA-PK.[140]

Pathogenesis of bone marrow failure in SDS

While there is increasing knowledge on the function of SBDS, the consequences of its mutations for BMF pathogenesis remain poorly elucidated, partly due to the difficulties in obtaining viable *in vivo* models of *SBDS* deficiency. Homozygous deletion of *Sbds* in mice induces embryonic death before the time of gastrulation.[141] The missense mutation R126T, rarely associated with SDS, is similarly lethal in homozygous embryos, although it was predicted to be a hypomorphic rather than null mutation.[89,112,142] Transplantation of bone marrow cells after robust lentiviral vector-mediated *Sbds* knock down is equally associated with lethality due to a lack of engraftment, while reducing the viral load during transduction preserves recipient viability but fails to significantly reproduce SDS-associated neutropenia in mice.[143]

Zebrafish models have been used to investigate the consequences of *Sbds* deficiency for development. Impairing *sbds* translation or splicing with morpholinos induced exocrine pancreatic hypoplasia, chondro-osseous abnormalities and reduced numbers of myeloid cells.[121] While it was possible to explain the pancreatic phenotype in terms of reduced expansion of *ptf1a*-expressing progenitors, the mechanisms behind impaired myelopoiesis remained unclear. Moreover, a preferential expression of *sbds* in the gastrointestinal tract could explain the pancreas but not the hematopoietic defects in this model.[144] With respect to tissue specificity, it is also interesting to note that different models of *Sbds* deficiency showed an overall impairment of hematopoiesis but failed to reproduce the neutrophil specificity observed in the clinical spectrum of many SDS patients. The embryonic lethal *Sbds*^{R126T} mouse model showed similar reduction of granulocytic, monocytic and erythroid progenitors by colony-forming unit (CFU) assay.[112] Hematopoietic differentiation of SDS patient-derived induced pluripotent stem cells (iPSCs) similarly failed to show lineage-skewed defects, while an overall reduction in CFU numbers was observed.[145]

Why does *Sbds* deficiency result in neutropenia? Insights from *in vitro* studies suggest that reduced SBDS levels induce programmed cell death. Yamaguchi and colleagues reported that *Sbds* RNA interference induced apoptosis of 32Dcl3 cells upon G-CSF culture, while no effect was observed growing cells in IL-3 proliferation medium.[146] Similarly, primary $CD34^+$ HSPCs from SDS patients were found hypersensitive to proapoptotic Fas stimulation and had increased baseline rates of apoptosis when grown in semisolid differentiation medium.[147,148] While this data suggests that *Sbds* deficiency elicits a stress response in hematopoietic cells, how this general response leads to selective neutrophil defects in SDS has not been clarified yet.

Cancer predisposition in SDS

Another unclear aspect of SDS pathogenesis is how *SBDS* mutations confer increased risk of myeloid malignancies. Because multipolar spindles were found in primary bone marrow stromal cells from SDS patients, it was proposed that *SBDS* mutation may lead to genomic instability.[137] Nevertheless, to date no *in vivo* model has shown development of MDS/AML-like diseases upon hematopoietic cell-restricted SBDS deficiency,[143,149] contradicting the view of *SBDS* as a bona fide DNA repair gene. At the same time, the models argue against a solely cell-autonomous pathogenesis of hematopoietic defects in SDS and open the possibility that extrinsic cues from the microenvironment could contribute to cancer predisposition in this disease.

4. NICHE CONTRIBUTION TO MYELOID DISORDERS

As previously indicated, the bone marrow niche plays an essential role in regulating the number and fate of HSCs. Given its function in ensuring the homeostasis of the hematopoietic tissue, it appears plausible that dysfunctional HSC niches could contribute to hematological disorders, thus changing the traditional view of leukemogenesis as an event solely dependent on intrinsic, genetically-determined characteristics of leukemic cells.

Indeed, intriguing observations in human disease support the importance of the niche for hematologic malignancies. A first example is the inability to obtain engraftment of certain leukemias,[150] as well as human MDS,[151-153] in immunodeficient mice, suggesting that species- or disease-specific states of the bone marrow microenvironment are required for diseased clones to thrive in an otherwise healthy organism. Another observation challenging the view of hematologic malignancies as solely cell-autonomously determined is the emergence of the so-called 'donor cell-derived leukemia' (DCL).[154,155] The term refers to a rare but growingly recognized phenomenon observed upon allogeneic HSC transplantation, a common treatment for hematologic malignancies. While leukemia often relapses in transplanted patients because of

the incomplete eradication of pre-existing malignant clones, rarely it emerges upon transformation of wild-type, grafted hematopoietic cells, while donor individuals seem to remain healthy. Although the persistence of chemotherapy agents or radiation-induced soluble damage signals in the bone marrow have been proposed to explain DCL,[154] a role for the microenvironment in driving this phenomenon is possible. Occult leukemic and pre-leukemic clones may be in fact already present in the graft, and while the efficient immune system in the donor bone marrow can easily eradicate them, this negative selection could be compromised in a dysfunctional HSC niche.

Additionally, it is tempting to hypothesize that the bone marrow microenvironment, profoundly changed by the exposure to primary leukemic cells or by the effect of chemo/radiotherapy, promotes accumulation of genetic mutations in HSC, potentially leading to full-blown malignant transformation. Indeed, chemo- and radiotherapy inflict considerable damage to stromal cells,[156] and stromal layers from MDS/AML display altered transcriptional profile with increased expression of proinflammatory cytokines such as IL-6 and TNF-α.[157,158] Whether a niche-derived proinflammatory environment exists *in vivo* and is relevant for human leukemogenesis remains to be tested.

To summarize, observations in human disease suggest two different, not mutually exclusive models of stromal contribution to hematological malignancies (**Figure 6**). In the first scenario (niche as a facilitating factor), the primary event is the occurrence of a malignant or premalignant HSC clone, which actively modifies the microenvironment in order to obtain a selective advantage over the normal HSCs. Conceptually, this could result either by limiting the niche supporting capacity of normal HSCs or improving that of malignant hematopoiesis. Indeed, mouse models of *MLL-AF9*$^{+}$ AML and myeloproliferative neoplasms (*BCR-ABL*$^{+}$ and *JAK2(V617F)*$^{+}$ inducible knock-in) support this concept. Specifically, they indicated that aberrant HSCs induce depletion of niche cells or downregulation of key niche factors such as CXCL12,[159-161] thus compromising normal hematopoiesis, while maintaining deregulated, diseased HSCs.[159,161]

The second, more provocative scenario considers the bone marrow niche as a true disease initiator, even in the absence of primary genetic events in the hematopoietic compartment. Evidence in support of this theory started accumulating with the observation that mice deficient for the retinoic acid receptor γ developed a myeloproliferative phenotype only when the deficiency involved the bone marrow stroma.[162] Subsequently, a mouse model of primary niche-restricted genetic modification demonstrated that mesenchymal cells can drive leukemogenesis.[163] Targeted deletion of *Dicer1* was induced in osterix-expressing mesenchymal progenitors to achieve broad alteration of the expression landscape in specific cells within the bone marrow niche. This primary genetic alteration was sufficient to induce an MDS-like phenotype, which was reverted by transplanting HSCs from the aberrant niche into wild type

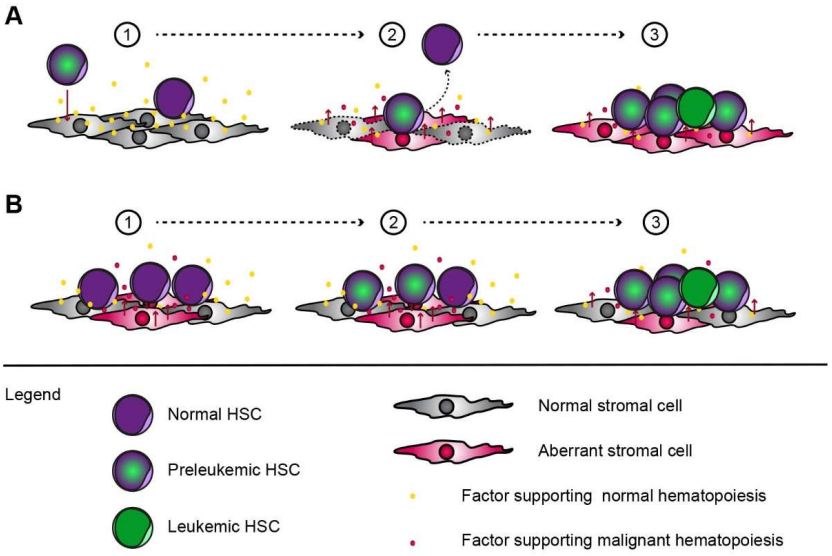

Figure 6. Models of niche contribution to leukemogenesis. (A) Primary event in a HSC. Aberrant HSCs may signal to the niche (A1) causing depletion of stromal cells or modification of their support capacity (A2). While normal hematopoiesis is thus impaired, aberrant HSC expand and their leukemic transformation is facilitated by the niche (A3). (B) Primary event in the niche. Aberrant niche cells (B1) may signal to HSCs and induce a preleukemic transformation (B2). Persistent dysfunction in the niche may facilitate expansion of the preleukemic clone and/or emergence of leukemia (B3).

mice. Notably, AML occurred in a minority of mice, which presented anemia, accumulation of blasts, splenomegaly and sarcomas harboring distinct cytogenetic abnormalities, including monosomies of regions homologous to human 5q. More recently, it was shown that the osteoblast-specific constitutive activation of β-catenin in mice is sufficient to induce AML with common chromosomal aberrations.[164]

While the theory of niche-induced leukemogenesis was proved to be valid in experimental animal models, data supporting its relevance for human disease remain limited. Nuclear accumulation of β-catenin was observed in osteoblasts from MDS/AML patients, reminiscent of the constitutive activation in the mouse model,[164] but the importance of this phenomenon for progression of human disease was not otherwise demonstrated. On the other hand, the relevance of the niche for a leukemia-predisposing syndrome was suggested in the afore-mentioned study of niche-restricted deletion of *Dicer1*. The study showed that aberrant osterix^{+} cells significantly downregulate the expression of *Sbds*, whose deficiency characterizes the human disease SDS.[163]

Indeed, several features of human SDS were recapitulated by conditionally deleting *Sbds* in Osx^{+} cells.[163] First, *Sbds* deficiency in mesenchymal progenitors altered the bone marrow architecture, with increased vasculature and altered cortical bone texture. Second, dysplastic features of the myeloid lineage were observed, while no evidence of dysplasia was previously reported in hematopoietic-restricted mouse models of SDS.[143] Dysplastic morphology was associated with an increased frequency of myeloid and a reduced number of B cells. Finally, a high rate of apoptosis was observed in hematopoietic progenitor cells, similar to what reported in SDS patients.[165] Altogether, the data suggested that extrinsic cues from the niche contribute to disease pathogenesis in SDS. How *Sbds* deficiency in the niche alters HSC biology remained to be investigated.

4. AIM OF THE DISSERTATION

The easiness to isolate hematopoietic cells, including HSPCs, from the peripheral blood and the bone marrow has greatly facilitated the study of human leukemia. Remarkable progress was achieved by analyzing hematopoietic cells alone. Nevertheless, this reductionist approach fails to fully explain the pathogenesis of certain hematopoietic conditions, including cancer predisposition in ribosomopathies.

Recently, the bone marrow microenvironment was recognized as a critical player in blood cancer development and maintenance, suggesting that cell extrinsic cues may underlie leukemogenesis. This dissertation aims at exploring possible contributions of the bone marrow microenvironment to cancer predisposition in preleukemic disorders and identifying candidate underlying mechanisms.

Shwachman-Diamond syndrome was chosen as 'index disease' to study the role of the HSC niche in leukemogenesis based on these considerations:

1. SDS confers a striking predisposition for the development of MDS and AML.
2. SDS is a congenital (constitutive) syndrome, thus both hematopoietic and stromal cells harbor the disease-initiating mutations.
3. Its monogenic nature makes SDS amenable to experimentation.
4. Bone and hematopoietic symptoms coexist in SDS, thus both blood- and bone-lineage niche cells are affected in this disease.
5. While *Sbds* deficiency in hematopoietic cells alone failed to reproduce hematological features of SDS, niche-targeted knock out mice develop a MDS-like disease.
6. The disease belongs to the larger family of ribosomopathies, thus insights on SDS pathology may be relevant for a broader set of illnesses.

To dissect cellular intrinsic and extrinsic contributions to hematological disease in SDS, hematopoietic- and niche-targeted *Sbds* conditional knock out models were obtained in mice based on tissue-selective expression of cre recombinase. In **chapter 2**, the *Cebpa*-cre model targets *Sbds* deletion in murine HSPCs, thus allowing the evaluation of cell intrinsic contributions of hematopoietic cells to bone marrow failure in SDS. In **chapter 3**, the niche-targeting Osx-cre model is used to obtain insights both on the pathogenesis of bone defects in SDS and on the cell extrinsic regulation of HSPCs in this disease, with the hypothesis that the bone marrow microenvironment contributes to SDS progression to MDS/AML. The relevance of the findings for human disease is then evaluated in SDS and MDS patients.

While SDS offers a unique opportunity to study niche contribution to leukemogenesis, it remains a condition affecting a minority of individuals. In contrast, MDS is a more prevalent preleukemic disorder. Moreover, being a disease of the elderly, its incidence is expected to increase in the years to come. Current studies on the MDS niche have largely relied on long term cultures of mesenchymal cells, but analyses of primary cells have not been performed yet, thus whether the niche really contributes to patients disease *in vivo* is still unknown. In **chapter 4**, immunophenotypically-defined HSC niche cells are prospectively isolated from the bone marrow of low-risk MDS patients. RNA sequencing profiling is used to gain insights on possible contributions of stromal cells to MDS. Finally, the results of this thesis are summarized and their importance for the hematologic oncology field is discussed in **chapter 5**.

REFERENCES

1. Tak T, Tesselaar K, Pillay J, Borghans JA, Koenderman L. What's your age again? Determination of human neutrophil half-lives revisited. *J Leukoc Biol*. 2013;94(4):595-601.
2. Wu M, Kwon HY, Rattis F, et al. Imaging hematopoietic precursor division in real time. *Cell Stem Cell*. 2007;1(5):541-554.
3. Zimdahl B, Ito T, Blevins A, et al. Lis1 regulates asymmetric division in hematopoietic stem cells and in leukemia. *Nat Genet*. 2014;46(3):245-252.
4. Tamplin OJ, Durand EM, Carr LA, et al. Hematopoietic stem cell arrival triggers dynamic remodeling of the perivascular niche. *Cell*. 2015;160(1-2):241-252.
5. Nakamura-Ishizu A, Takizawa H, Suda T. The analysis, roles and regulation of quiescence in hematopoietic stem cells. *Development*. 2014;141(24):4656-4666.
6. Beck WS, Leukocytes I. Physiology. In: Beck WS, ed. Hematology, 5th edition. Cambridge MA: The MIT Press; 1998:339-350.
7. Reya T, Morrison SJ, Clarke MF, Weissman IL. Stem cells, cancer, and cancer stem cells. *Nature*. 2001;414(6859):105-111.
8. Brinkmann V, Reichard U, Goosmann C, et al. Neutrophil extracellular traps kill bacteria. *Science*. 2004;303:1532–1535.
9. Provencher Bolliger A, Everds N. Haematology of the mouse. In: Hedrich H, ed. The Laboratory Mouse, 2nd edition. London UK: Academic Press; 2012:331-348.
10. Marionneaux S. Nonmalignant leukocyte disorders. In: Keohane E, Smith L, Walenga J, eds. Rodak's Hematology: Clinical Principles and Applications, 5th edition. St. Louis MO: Elsevier Saunders; 2016:475-497.
11. Pillay J, Tak T, Kamp VM, Koenderman L. Immune suppression by neutrophils and granulocytic myeloid-derived suppressor cells: similarities and differences. *Cell Mol Life Sci*. 2013;70(20):3813-3827.
12. Zhu J, Emerson SG. Hematopoietic cytokines, transcription factors and lineage commitment. *Oncogene*. 2002;21(21):3295-3313.
13. Krause DS. Regulation of hematopoietic stem cell fate. *Oncogene*. 2002;21(21):3262-3269.
14. Dexter TM, Allen TD, Lajtha LG. Conditions controlling the proliferation of haemopoietic stem cells in vitro. *J Cell Physiol*. 1977;91(3):335-344.
15. Schofield R. The relationship between the spleen colony-forming cell and the haemopoietic stem cell. *Blood Cells*. 1978;4(1-2):7-25.
16. Imai K, Kobayashi M, Wang J, et al. Selective transendothelial migration of hematopoietic progenitor cells: a role in homing of progenitor cells. *Blood*. 1999;93(1):149-156.
17. Avigdor A, Goichberg P, Shivtiel S, et al. CD44 and hyaluronic acid cooperate with SDF-1 in the trafficking of human CD34+ stem/progenitor cells to bone marrow. *Blood*. 2004;103(8):2981-2989.
18. Potocnik AJ, Brakebusch C, Fassler R. Fetal and adult hematopoietic stem cells require beta1 integrin function for colonizing fetal liver, spleen, and bone marrow. *Immunity*. 2000;12(6):653-663.
19. Arroyo AG, Yang JT, Rayburn H, Hynes RO. Alpha4 integrins regulate the proliferation/differentiation balance of multilineage hematopoietic progenitors in vivo. *Immunity*. 1999;11(5):555-566.

20. Qian H, Tryggvason K, Jacobsen SE, Ekblom M. Contribution of alpha6 integrins to hematopoietic stem and progenitor cell homing to bone marrow and collaboration with alpha4 integrins. *Blood*. 2006;107(9):3503-3510.
21. Schreiber TD, Steinl C, Essl M, et al. The integrin alpha9beta1 on hematopoietic stem and progenitor cells: involvement in cell adhesion, proliferation and differentiation. *Haematologica*. 2009;94(11):1493-1501.
22. Ponomaryov T, Peled A, Petit I, et al. Induction of the chemokine stromal-derived factor-1 following DNA damage improves human stem cell function. *J Clin Invest*. 2000;106(11):1331-1339.
23. Tzeng YS, Li H, Kang YL, Chen WC, Cheng WC, Lai DM. Loss of Cxcl12/Sdf-1 in adult mice decreases the quiescent state of hematopoietic stem/progenitor cells and alters the pattern of hematopoietic regeneration after myelosuppression. *Blood*. 2011;117(2):429-439.
24. Broudy VC. Stem cell factor and hematopoiesis. *Blood*. 1997;90(4):1345-1364.
25. Arai F, Hirao A, Ohmura M, et al. Tie2/angiopoietin-1 signaling regulates hematopoietic stem cell quiescence in the bone marrow niche. *Cell*. 2004;118(2):149-161.
26. Calvi LM, Adams GB, Weibrecht KW, et al. Osteoblastic cells regulate the haematopoietic stem cell niche. *Nature*. 2003;425(6960):841-846.
27. Kim JA, Kang YJ, Park G, et al. Identification of a stroma-mediated Wnt/beta-catenin signal promoting self-renewal of hematopoietic stem cells in the stem cell niche. *Stem Cells*. 2009;27(6):1318-1329.
28. Yoshihara H, Arai F, Hosokawa K, et al. Thrombopoietin/MPL signaling regulates hematopoietic stem cell quiescence and interaction with the osteoblastic niche. *Cell Stem Cell*. 2007;1(6):685-697.
29. Morrison SJ, Scadden DT. The bone marrow niche for haematopoietic stem cells. Nature. 2014;505(7483):327-34.
30. Lord BI, Testa NG, Hendry JH. The relative spatial distributions of CFUs and CFUc in the normal mouse femur. *Blood*. 1975;46(1):65-72.
31. Zhang J, Niu C, Ye L, et al. Identification of the haematopoietic stem cell niche and control of the niche size. *Nature*. 2003;425(6960):836-841.
32. Visnjic D, Kalajzic Z, Rowe DW, Katavic V, Lorenzo J, Aguila HL. Hematopoiesis is severely altered in mice with an induced osteoblast deficiency. *Blood*. 2004;103(9):3258-3264.
33. Jung Y, Wang J, Schneider A, et al. Regulation of SDF-1 (CXCL12) production by osteoblasts; a possible mechanism for stem cell homing. *Bone*. 2006;38(4):497-508.
34. Chan CFK, Chen CC, Luppen CA, et al. Endochondral ossification is required for haematopoietic stem-cell niche formation. *Nature*. 2009;457(7228):490-494.
35. Kiel MJ, Yilmaz OH, Iwashita T, Yilmaz OH, Terhorst C, Morrison SJ. SLAM family receptors distinguish hematopoietic stem and progenitor cells and reveal endothelial niches for stem cells. *Cell*. 2005;121(7):1109-1121.
36. Sugiyama T, Kohara H, Noda M, Nagasawa T. Maintenance of the hematopoietic stem cell pool by CXCL12-CXCR4 chemokine signaling in bone marrow stromal cell niches. *Immunity*. 2006;25(6):977-988.
37. Mendez-Ferrer S, Michurina TV, Ferraro F, et al. Mesenchymal and haematopoietic stem cells form a unique bone marrow niche. *Nature*. 2010;466(7308):829-834.

38. Butler JM, Nolan DJ, Vertes EL, et al. Endothelial cells are essential for the self-renewal and repopulation of Notch-dependent hematopoietic stem cells. *Cell Stem Cell*. 2010;6(3):251-264.
39. Poulos MG, Guo P, Kofler NM, et al. Endothelial Jagged-1 is necessary for homeostatic and regenerative hematopoiesis. *Cell Rep*. 2013;4(5):1022-1034.
40. Winkler IG, Barbier V, Nowlan B, et al. Vascular niche E-selectin regulates hematopoietic stem cell dormancy, self renewal and chemoresistance. *Nat Med*. 2012;18(11):1651-1657.
41. Kollet O, Dar A, Shivtiel S, et al. Osteoclasts degrade endosteal components and promote mobilization of hematopoietic progenitor cells. *Nat Med*. 2006;12(6):657-664.
42. Naveiras O, Nardi V, Wenzel PL, Hauschka PV, Fahey F, Daley GQ. Bone-marrow adipocytes as negative regulators of the haematopoietic microenvironment. *Nature*. 2009;460(7252):259-263.
43. Katayama Y, Battista M, Kao WM, et al. Signals from the sympathetic nervous system regulate hematopoietic stem cell egress from bone marrow. *Cell*. 2006;124(2):407-421.
44. Mendez-Ferrer S, Lucas D, Battista M, Frenette PS. Haematopoietic stem cell release is regulated by circadian oscillations. *Nature*. 2008;452(7186):442-447.
45. Yamazaki S, Ema H, Karlsson G, et al. Nonmyelinating Schwann cells maintain hematopoietic stem cell hibernation in the bone marrow niche. *Cell*. 2011;147(5):1146-1158.
46. Lucas D, Scheiermann C, Chow A, et al. Chemotherapy-induced bone marrow nerve injury impairs hematopoietic regeneration. *Nat Med*. 2013;19(6):695-703.
47. Li P, Zon Li. Resolving the controversy about N-cadherin and hematopoietic stem cells. *Cell Stem Cell*. 2010;6(3):199-202.
48. Ding L, Saunders TL, Enikolopov G, Morrison SJ. Endothelial and perivascular cells maintain haematopoietic stem cells. *Nature*. 2012;481(7382):457-462.
49. Greenbaum A, Hsu YM, Day RB, et al. CXCL12 in early mesenchymal progenitors is required for haematopoietic stem-cell maintenance. *Nature*. 2013;495(7440):227-230.
50. Ding L, Morrison SJ. Haematopoietic stem cells and early lymphoid progenitors occupy distinct bone marrow niches. *Nature*. 2013;495(7440):231-235.
51. Liu Y, Strecker S, Wang L, et al. Osterix-cre labeled progenitor cells contribute to the formation and maintenance of the bone marrow stroma. *PLoS One*. 2013;8(8):e71318.
52. Mizoguchi T, Pinho S, Ahmed J, et al. Osterix marks distinct waves of primitive and definitive stromal progenitors during bone marrow development. *Dev Cell*. 2014;29(3):340-349.
53. Sacchetti B, Funari A, Michienzi S, et al. Self-renewing osteoprogenitors in bone marrow sinusoids can organize a hematopoietic microenvironment. *Cell*. 2007;131(2):324-336.
54. Tormin A, Li O, Brune JC, et al. CD146 expression on primary nonhematopoietic bone marrow stem cells is correlated with in situ localization. *Blood*. 2011;117(19):5067-5077.
55. Churchman SM, Ponchel F, Boxall SA, et al. Transcriptional profile of native CD271+ multipotential stromal cells: evidence for multiple fates, with prominent osteogenic and Wnt pathway signaling activity. *Arthritis Rheum*. 2012;64(8):2632-2643.
56. Bagby GC, Meyers G. Bone marrow failure as a risk factor for clonal evolution: prospects for leukemia prevention. *Hematology Am Soc Hematol Educ Program.* 2007:40-46.
57. Gerds AT, Scott BL. Last marrow standing: bone marrow transplantation for acquired bone marrow failure conditions. *Curr Hematol Malig Rep*. 2012;7(4):292-299.

58. Shimamura A, Alter BP. Pathophysiology and management of inherited bone marrow failure syndromes. *Blood Rev*. 2010;24(3):101-122.
59. Greenberg P, Cox C, LeBeau MM, et al. International scoring system for evaluating prognosis in myelodysplastic syndromes. *Blood*. 1997;89(6):2079-2088.
60. Papaemmanuil E, Gerstung M, Malcovati L, et al. Clinical and biological implications of driver mutations in myelodysplastic syndromes. *Blood*. 2013;122(22):3616-3627; quiz 3699.
61. Xie M, Lu C, Wang J, et al. Age-related mutations associated with clonal hematopoietic expansion and malignancies. *Nat Med*. 2014;20(12):1472-1478.
62. Busque L, Patel JP, Figueroa ME, et al. Recurrent somatic TET2 mutations in normal elderly individuals with clonal hematopoiesis. *Nat Genet*. 2012;44(11):1179-1181.
63. Steensma DP, Bejar R, Jaiswal S, et al. Clonal hematopoiesis of indeterminate potential and its distinction from myelodysplastic syndromes. *Blood*. 2015.
64. Rao S, Lee SY, Gutierrez A, et al. Inactivation of ribosomal protein L22 promotes transformation by induction of the stemness factor, Lin28B. *Blood*. 2012;120(18):3764-3773.
65. De Keersmaecker K, Atak ZK, Li N, et al. Exome sequencing identifies mutation in CNOT3 and ribosomal genes RPL5 and RPL10 in T-cell acute lymphoblastic leukemia. *Nat Genet*. 2013;45(2):186-190.
66. Vardiman JW, Harris NL, Brunning RD. The World Health Organization (WHO) classification of the myeloid neoplasms. *Blood*. 2002;100(7):2292-2302.
67. Ebert BL, Pretz J, Bosco J, et al. Identification of RPS14 as a 5q- syndrome gene by RNA interference screen. *Nature*. 2008;451(7176):335-339.
68. Barlow JL, Drynan LF, Hewett DR, et al. A p53-dependent mechanism underlies macrocytic anemia in a mouse model of human 5q- syndrome. *Nat Med*. 2010;16(1):59-66.
69. Vlachos A, Rosenberg PS, Atsidaftos E, Alter BP, Lipton JM. Incidence of neoplasia in Diamond Blackfan anemia: a report from the Diamond Blackfan Anemia Registry. *Blood*. 2012;119(16):3815-3819.
70. Flygare J, Karlsson S. Diamond-Blackfan anemia: erythropoiesis lost in translation. *Blood*. 2007;109(8):3152-3154.
71. Draptchinskaia N, Gustavsson P, Andersson B, et al. The gene encoding ribosomal protein S19 is mutated in Diamond-Blackfan anaemia. *Nat Genet*. 1999;21(2):169-175.
72. Horos R, von Lindern M. Molecular mechanisms of pathology and treatment in Diamond Blackfan Anaemia. *Br J Haematol*. 2012;159(5):514-527.
73. Sankaran VG, Ghazvinian R, Do R, et al. Exome sequencing identifies GATA1 mutations resulting in Diamond-Blackfan anemia. *J Clin Invest*. 2012;122(7):2439-2443.
74. Ludwig LS, Gazda HT, Eng JC, et al. Altered translation of GATA1 in Diamond-Blackfan anemia. *Nat Med*. 2014;20(7):748-753.
75. Chlon TM, McNulty M, Goldenson B, Rosinski A, Crispino JD. Global transcriptome and chromatin occupancy analysis reveal the short isoform of GATA1 is deficient for erythroid specification and gene expression. *Haematologica*. 2015;100(5):575-584.
76. Dixon MJ. Treacher Collins syndrome. *Hum Mol Genet*. 1996;5:1391-6.
77. Dauwerse JG, Dixon J, Seland S, et al. Mutations in genes encoding subunits of RNA polymerases I and III cause Treacher Collins syndrome. *Nat Genet*. 2011;43(1):20-2.

78. Heiss NS, Knight SW, Vulliamy TJ, et al. X-linked dyskeratosis congenita is caused by mutations in a highly conserved gene with putative nucleolar functions. *Nat Genet*. 1998;19(1):32-8.
79. Gerrard G, Valgañón M, Foong HE, et al. Target enrichment and high-throughput sequencing of 80 ribosomal protein genes to identify mutations associated with Diamond-Blackfan anaemia. *Br J Haematol*. 2013;162(4):530-6.
80. Doherty L, Sheen MR, Vlachos A, et al. Ribosomal protein genes RPS10 and RPS26 are commonly mutated in Diamond-Blackfan anemia. *Am J Hum Genet*. 2010;86(2):222-8.
81. Cmejla R, Cmejlova J, Handrkova H, Petrak J, Pospisilova D. Ribosomal protein S17 gene (RPS17) is mutated in Diamond-Blackfan anemia. *Hum Mutat*. 2007;28(12):1178-82.
82. Gazda HT, Grabowska A, Merida-Long LB, et al. Ribosomal protein S24 gene is mutated in Diamond-Blackfan anemia. *Am J Hum Genet*. 2006;79(6):1110-8.
83. Gazda HT, Sheen MR, Vlachos A, et al. Ribosomal protein L5 and L11 mutations are associated with cleft palate and abnormal thumbs in Diamond-Blackfan anemia patients. *Am J Hum Genet*. 2008;83(6):769-80.
84. Gazda HT, Preti M, Sheen MR, et al. Frameshift mutation in p53 regulator RPL26 is associated with multiple physical abnormalities and a specific pre-ribosomal RNA processing defect in diamond-blackfan anemia. *Hum Mutat*. 2012;33(7):1037-44.
85. Farrar JE, Nater M, Caywood E, et al. Abnormalities of the large ribosomal subunit protein, Rpl35a, in Diamond-Blackfan anemia. *Blood*. 2008;112(5):1582-92.
86. Ridanpää M, van Eenennaam H, Pelin K, et al. Mutations in the RNA component of RNase MRP cause a pleiotropic human disease, cartilage-hair hypoplasia. *Cell*. 2001;104(2):195-203.
87. Chagnon P, Michaud J, Mitchell G, et al. A missense mutation (R565W) in cirhin (FLJ14728) in North American Indian childhood cirrhosis. *Am J Hum Genet*. 2002;71(6):1443-9.
88. Boocock GR, Morrison JA, Popovic M, et al. Mutations in SBDS are associated with Shwachman-Diamond syndrome. *Nat Genet*. 2003;33(1):97-101.
89. Thiel CT, Horn D, Zabel B, et al. Severely incapacitating mutations in patients with extreme short stature identify RNA-processing endoribonuclease RMRP as an essential cell growth regulator. *Am J Hum Genet*. 2005;77(5):795-806.
90. Armistead J, Khatkar S, Meyer B, et al. Mutation of a gene essential for ribosome biogenesis, EMG1, causes Bowen-Conradi syndrome. *Am J Hum Genet*. 2009;84(6):728-39.
91. Bolze A, Mahlaoui N, Byun M, et al. Ribosomal protein SA haploinsufficiency in humans with isolated congenital asplenia. *Science*. 2013;340(6135):976-8.
92. Marneros AG. BMS1 is mutated in aplasia cutis congenita. *PLoS Genet*. 2013;9(6):e1003573.
93. Horos R, Ijspeert H, Pospisilova D, et al. Ribosomal deficiencies in Diamond-Blackfan anemia impair translation of transcripts essential for differentiation of murine and human erythroblasts. *Blood*. 2012;119(1):262-272.
94. Thomas G. An encore for ribosome biogenesis in the control of cell proliferation. *Nat Cell Biol*. 2000;2(5):E71-72.
95. Morata G, Ripoll P. Minutes: mutants of drosophila autonomously affecting cell division rate. *Dev Biol*. 1975;42(2):211-221.
96. Volarevic S, Stewart MJ, Ledermann B, et al. Proliferation, but not growth, blocked by conditional deletion of 40S ribosomal protein S6. *Science*. 2000;288(5473):2045-2047.

97. Kondrashov N, Pusic A, Stumpf CR, et al. Ribosome-mediated specificity in Hox mRNA translation and vertebrate tissue patterning. *Cell*. 2011;145(3):383-397.
98. Xue S, Tian S, Fujii K, Kladwang W, Das R, Barna M. RNA regulons in Hox 5' UTRs confer ribosome specificity to gene regulation. *Nature*. 2015;517(7532):33-38.
99. Yoon A, Peng G, Brandenburger Y, et al. Impaired control of IRES-mediated translation in X-linked dyskeratosis congenita. *Science*. 2006;312(5775):902-906.
100. Zhang Y, Wolf GW, Bhat K, et al. Ribosomal protein L11 negatively regulates oncoprotein MDM2 and mediates a p53-dependent ribosomal-stress checkpoint pathway. *Mol Cell Biol*. 2003;23(23):8902-8912.
101. Dai MS, Zeng SX, Jin Y, Sun XX, David L, Lu H. Ribosomal protein L23 activates p53 by inhibiting MDM2 function in response to ribosomal perturbation but not to translation inhibition. *Mol Cell Biol*. 2004;24(17):7654-7668.
102. Jin A, Itahana K, O'Keefe K, Zhang Y. Inhibition of HDM2 and activation of p53 by ribosomal protein L23. *Mol Cell Biol*. 2004;24(17):7669-7680.
103. Dai MS, Lu H. Inhibition of MDM2-mediated p53 ubiquitination and degradation by ribosomal protein L5. *J Biol Chem*. 2004;279(43):44475-44482.
104. Chen D, Zhang Z, Li M, et al. Ribosomal protein S7 as a novel modulator of p53-MDM2 interaction: binding to MDM2, stabilization of p53 protein, and activation of p53 function. *Oncogene*. 2007;26(35):5029-5037.
105. Ofir-Rosenfeld Y, Boggs K, Michael D, Kastan MB, Oren M. Mdm2 regulates p53 mRNA translation through inhibitory interactions with ribosomal protein L26. *Mol Cell*. 2008;32(2):180-189.
106. Yadavilli S, Mayo LD, Higgins M, Lain S, Hegde V, Deutsch WA. Ribosomal protein S3: A multi-functional protein that interacts with both p53 and MDM2 through its KH domain. *DNA Repair (Amst)*. 2009;8(10):1215-1224.
107. Jones NC, Lynn ML, Gaudenz K, et al. Prevention of the neurocristopathy Treacher Collins syndrome through inhibition of p53 function. *Nat Med*. 2008;14(2):125-133.
108. McGowan KA, Li JZ, Park CY, et al. Ribosomal mutations cause p53-mediated dark skin and pleiotropic effects. *Nat Genet*. 2008;40(8):963-970.
109. MacInnes AW, Amsterdam A, Whittaker CA, Hopkins N, Lees JA. Loss of p53 synthesis in zebrafish tumors with ribosomal protein gene mutations. *Proc Natl Acad Sci U S A*. 2008;105(30):10408-10413.
110. Torihara H, Uechi T, Chakraborty A, Shinya M, Sakai N, Kenmochi N. Erythropoiesis failure due to RPS19 deficiency is independent of an activated Tp53 response in a zebrafish model of Diamond-Blackfan anaemia. *Br J Haematol*. 2011;152(5):648-654.
111. Provost E, Wehner KA, Zhong XG, et al. Ribosomal biogenesis genes play an essential and p53-independent role in zebrafish pancreas development. *Development*. 2012;139(17):3232-3241.
112. Tourlakis ME, Zhang S, Ball HL, et al. In Vivo Senescence in the Sbds-Deficient Murine Pancreas: Cell-Type Specific Consequences of Translation Insufficiency. *PLoS Genet*. 2015;11(6):e1005288.
113. Shwachman H, Diamond LK, Oski FA, Khaw KT. The Syndrome of Pancreatic Insufficiency and Bone Marrow Dysfunction. *J Pediatr*. 1964;65:645-663.
114. Dror Y, Donadieu J, Koglmeier J, et al. Draft consensus guidelines for diagnosis and treatment of Shwachman-Diamond syndrome. *Ann N Y Acad Sci*. 2011;1242:40-55.

115. Goobie S, Popovic M, Morrison J, et al. Shwachman-Diamond syndrome with exocrine pancreatic dysfunction and bone marrow failure maps to the centromeric region of chromosome 7. *Am J Hum Genet*. 2001;68(4):1048-1054.
116. Mäkitie O, Ellis L, Durie PR, et al. Skeletal phenotype in patients with Shwachman-Diamond syndrome and mutations in SBDS. *Clinical Genetics*. 2004;65(2):101-112.
117. Toiviainen-Salo S, Mayranpaa MK, Durie PR, et al. Shwachman-Diamond syndrome is associated with low-turnover osteoporosis. *Bone*. 2007;41(6):965-972.
118. Mack DR, Forstner GG, Wilschanski M, Freedman MH, Durie PR. Shwachman syndrome: Exocrine pancreatic dysfunction and variable phenotypic expression. *Gastroenterology*. 1996;111(6):1593-1602.
119. Toiviainen-Salo S, Durie PR, Numminen K, et al. The natural history of Shwachman-Diamond syndrome-associated liver disease from childhood to adulthood. *J Pediatr*. 2009;155(6):807-811 e802.
120. Kerr EN, Ellis L, Dupuis A, Rommens JM, Durie PR. The behavioral phenotype of school-age children with shwachman diamond syndrome indicates neurocognitive dysfunction with loss of Shwachman-Bodian-Diamond syndrome gene function. *J Pediatr*. 2010;156(3):433-438.
121. Myers KC, Bolyard AA, Otto B, et al. Variable Clinical Presentation of Shwachman-Diamond Syndrome: Update from the North American Shwachman-Diamond Syndrome Registry. *Journal of Pediatrics*. 2014;164(4):866-870.
122. Aggett PJ, Harries JT, Harvey BA, Soothill JF. An inherited defect of neutrophil mobility in Shwachman syndrome. *J Pediatr*. 1979;94(3):391-394.
123. Rothbaum RJ, Williams DA, Daugherty CC. Unusual surface distribution of concanavalin A reflects a cytoskeletal defect in neutrophils in Shwachman's syndrome. *Lancet*. 1982;2(8302):800-801.
124. Dror Y, Ginzberg H, Dalal I, et al. Immune function in patients with Shwachman-Diamond syndrome. *Br J Haematol*. 2001;114(3):712-717.
125. Dror Y. Shwachman-Diamond syndrome. *Pediatr Blood & Cancer*. 2005;45(7):892-901.
126. Donadieu J, Fenneteau O, Beaupain B, et al. Classification of and risk factors for hematologic complications in a French national cohort of 102 patients with Shwachman-Diamond syndrome. *Haematologica*. 2012;97(9):1312-1319.
127. Aggett PJ, Cavanagh NPC, Matthew DJ, Pincott JR, Sutcliffe J, Harries JT. Shwachmans Syndrome - a Review of 21 Cases. *Archives of Disease in Childhood*. 1980;55(5):331-347.
128. Leung EW, Rujkijyanont P, Beyene J, et al. Shwachman-Diamond syndrome: an inherited model of aplastic anaemia with accelerated angiogenesis. *Br J Haematol*. 2006;133(5):558-561.
129. Alter BP. Diagnosis, genetics, and management of inherited bone marrow failure syndromes. *Hematology Am Soc Hematol Educ Program*. 2007:29-39.
130. Nicolis E, Bonizzato A, Assael BM, Cipolli M. Identification of novel mutations in patients with Shwachman-Diamond syndrome. *Hum Mutat*. 2005;25(4):410.
131. Woloszynek JR, Rothbaum RJ, Rawls AS, et al. Mutations of the SBDS gene are present in most patients with Shwachman-Diamond syndrome. *Blood*. 2004;104(12):3588-3590.
132. Finch AJ, Hilcenko C, Basse N, et al. Uncoupling of GTP hydrolysis from eIF6 release on the ribosome causes Shwachman-Diamond syndrome. *Genes Dev*. 2011;25(9):917-929.

133. Koonin EV, Wolf YI, Aravind L. Prediction of the archaeal exosome and its connections with the proteasome and the translation and transcription machineries by a comparative-genomic approach. *Genome Res*. 2001;11(2):240-252.
134. Menne TF, Goyenechea B, Sanchez-Puig N, et al. The Shwachman-Bodian-Diamond syndrome protein mediates translational activation of ribosomes in yeast. *Nat Genet*. 2007;39(4):486-495.
135. Wong CC, Traynor D, Basse N, Kay RR, Warren AJ. Defective ribosome assembly in Shwachman-Diamond syndrome. *Blood*. 2011;118(16):4305-4312.
136. Burwick N, Coats SA, Nakamura T, Shimamura A. Impaired ribosomal subunit association in Shwachman-Diamond syndrome. *Blood*. 2012;120(26):5143-5152.
137. Austin KM, Gupta ML, Jr., Coats SA, et al. Mitotic spindle destabilization and genomic instability in Shwachman-Diamond syndrome. *J Clin Invest*. 2008;118(4):1511-1518.
138. Orelio C, Verkuijlen P, Geissler J, van den Berg TK, Kuijpers TW. SBDS expression and localization at the mitotic spindle in human myeloid progenitors. *Plos One*. 2009;4(9):e7084.
139. Orelio C, Kuijpers TW. Shwachman-Diamond syndrome neutrophils have altered chemoattractant-induced F-actin polymerization and polarization characteristics. *Haematologica*. 2009;94(3):409-413.
140. Ball HL, Zhang B, Riches JJ, et al. Shwachman-Bodian Diamond syndrome is a multi-functional protein implicated in cellular stress responses. *Hum Mol Genet*. 2009;18(19):3684-3695.
141. Zhang S, Shi M, Hui CC, Rommens JM. Loss of the mouse ortholog of the shwachman-diamond syndrome gene (Sbds) results in early embryonic lethality. *Mol Cell Biol*. 2006;26(17):6656-6663.
142. Shammas C, Menne TF, Hilcenko C, et al. Structural and mutational analysis of the SBDS protein family. Insight into the leukemia-associated Shwachman-Diamond Syndrome. *J Biol Chem*. 2005;280(19):19221-19229.
143. Rawls AS, Gregory AD, Woloszynek JR, Liu FL, Link DC. Lentiviral-mediated RNAi inhibition of Sbds in murine hematopoietic progenitors impairs their hematopoietic potential. *Blood*. 2007;110(7):2414-2422.
144. Venkatasubramani N, Mayer AN. A zebrafish model for the Shwachman-Diamond syndrome (SDS). *Pediatr Res*. 2008;63(4):348-352.
145. Tulpule A, Kelley JM, Lensch MW, et al. Pluripotent stem cell models of Shwachman-Diamond syndrome reveal a common mechanism for pancreatic and hematopoietic dysfunction. *Cell Stem Cell*. 2013;12(6):727-736.
146. Yamaguchi M, Fujimura K, Toga H, Khwaja A, Okamura N, Chopra R. Shwachman-Diamond syndrome is not necessary for the terminal maturation of neutrophils but is important for maintaining viability of granulocyte precursors. *Exp Hematol*. 2007;35(4):579-586.
147. Watanabe K, Ambekar C, Wang H, Ciccolini A, Schimmer AD, Dror Y. SBDS-deficiency results in specific hypersensitivity to Fas stimulation and accumulation of Fas at the plasma membrane. *Apoptosis*. 2009;14(1):77-89.
148. Sen S, Wang H, Nghiem CL, et al. The ribosome-related protein, SBDS, is critical for normal erythropoiesis. *Blood*. 2011;118(24):6407-6417.
149. Leung R, Cuddy K, Wang Y, Rommens J, Glogauer M. Sbds is required for Rac2-mediated monocyte migration and signaling downstream of RANK during osteoclastogenesis. *Blood*. 2011;117(6):2044-2053.

150. Rombouts WJ, Martens AC, Ploemacher RE. Identification of variables determining the engraftment potential of human acute myeloid leukemia in the immunodeficient NOD/SCID human chimera model. *Leukemia*. 2000;14(5):889-897.
151. Nilsson L, Astrand-Grundstrom I, Anderson K, et al. Involvement and functional impairment of the CD34(+)CD38(-)Thy-1(+) hematopoietic stem cell pool in myelodysplastic syndromes with trisomy 8. *Blood*. 2002;100(1):259-267.
152. Benito AI, Bryant E, Loken MR, et al. NOD/SCID mice transplanted with marrow from patients with myelodysplastic syndrome (MDS) show long-term propagation of normal but not clonal human precursors. *Leuk Res*. 2003;27(5):425-436.
153. Thanopoulou E, Cashman J, Kakagianne T, Eaves A, Zoumbos N, Eaves C. Engraftment of NOD/SCID-beta2 microglobulin null mice with multilineage neoplastic cells from patients with myelodysplastic syndrome. *Blood*. 2004;103(11):4285-4293.
154. Wiseman DH. Donor cell leukemia: a review. *Biol Blood Marrow Transplant*. 2011;17(6):771-789.
155. Flynn CM, Kaufman DS. Donor cell leukemia: insight into cancer stem cells and the stem cell niche. *Blood*. 2007;109(7):2688-2692.
156. Greenberger JS, Anderson J, Berry LA, Epperly M, Cronkite EP, Boggs SS. Effects of irradiation of CBA/CA mice on hematopoietic stem cells and stromal cells in long-term bone marrow cultures. *Leukemia*. 1996;10(3):514-527.
157. Flores-Figueroa E, Gutierrez-Espindola G, Montesinos JJ, Arana-Trejo RM, Mayani H. In vitro characterization of hematopoietic microenvironment cells from patients with myelodysplastic syndrome. *Leuk Res*. 2002;26(7):677-686.
158. Medyouf H, Mossner M, Jann JC, et al. Myelodysplastic cells in patients reprogram mesenchymal stromal cells to establish a transplantable stem cell niche disease unit. *Cell Stem Cell*. 2014;14(6):824-837.
159. Schepers K, Pietras EM, Reynaud D, et al. Myeloproliferative neoplasia remodels the endosteal bone marrow niche into a self-reinforcing leukemic niche. *Cell Stem Cell*. 2013;13(3):285-299.
160. Arranz L, Sanchez-Aguilera A, Martin-Perez D, et al. Neuropathy of haematopoietic stem cell niche is essential for myeloproliferative neoplasms. *Nature*. 2014;512(7512):78-81.
161. Hanoun M, Zhang D, Mizoguchi T, et al. Acute myelogenous leukemia-induced sympathetic neuropathy promotes malignancy in an altered hematopoietic stem cell niche. *Cell Stem Cell*. 2014;15(3):365-375.
162. Walkley CR, Olsen GH, Dworkin S, et al. A microenvironment-induced myeloproliferative syndrome caused by retinoic acid receptor gamma deficiency. *Cell*. 2007;129(6):1097-1110.
163. Raaijmakers MH, Mukherjee S, Guo S, et al. Bone progenitor dysfunction induces myelodysplasia and secondary leukaemia. *Nature*. 2010;464(7290):852-857.
164. Kode A, Manavalan JS, Mosialou I, et al. Leukaemogenesis induced by an activating beta-catenin mutation in osteoblasts. *Nature*. 2014;506(7487):240-244.
165. Rujkijyanont P, Adams SL, Beyene J, Dror Y. Bone marrow cells from patients with Shwachman-Diamond syndrome abnormally express genes involved in ribosome biogenesis and RNA processing. *Br J Haematol*. 2009;145(6):806-815.

Chapter 2

Deficiency of the ribosome biogenesis gene *Sbds* in hematopoietic stem and progenitor cells causes neutropenia in mice by attenuating lineage progression in myelocytes

Noemi A. Zambetti,[1] Eric M. J. Bindels,[1] Paulina M. H. Van Strien,[1] Marijke G. Valkhof,[1,2] Maria N. Adisty,[1] Remco M. Hoogenboezem,[1] Mathijs A. Sanders,[1] Johanna M. Rommens,[3] Ivo P. Touw,[1] and Marc H. G. P. Raaijmakers[1]

[1]Department of Hematology, Erasmus Medical Center Cancer Institute, Rotterdam, The Netherlands

[2]Current address: Laboratory for Cell Therapy, Sanquin Research and Landsteiner Laboratory, Amsterdam, The Netherlands

[3]Program in Genetics & Genome Biology, Peter Gilgan Centre for Research and Learning, The Hospital for Sick Children, Department of Molecular Genetics, University of Toronto, Toronto, ON, Canada

Haematologica. 2015 Oct;100(10):1285-93

ABSTRACT

Shwachman-Diamond syndrome is a congenital bone marrow failure disorder characterized by debilitating neutropenia. The disease is associated with loss-of-function mutations in the *SBDS* gene, implicated in ribosome biogenesis, but the cellular and molecular events driving cell specific phenotypes in ribosomopathies remain poorly defined. Here, we established, to our knowledge, the first mammalian model of neutropenia in Shwachman-Diamond syndrome through targeted downregulation of *Sbds* in hematopoietic stem and progenitor cells expressing the myeloid transcription factor CCAAT/enhancer binding protein α (*Cebpa*). *Sbds* deficiency in the myeloid lineage specifically affected myelocytes and their downstream progeny while, unexpectedly, it was well tolerated by rapidly cycling hematopoietic progenitor cells. Molecular insights provided by massive parallel sequencing supported cellular observations of impaired cell cycle exit and formation of secondary granules associated with the defect of myeloid lineage progression in myelocytes. Mechanistically, *Sbds* deficiency activated the p53 tumor suppressor pathway and induced apoptosis in these cells. Collectively, the data reveal a previously unanticipated, selective dependency of myelocytes and downstream progeny, but not rapidly cycling progenitors, on this ubiquitous ribosome biogenesis protein, thus providing a cellular basis for the understanding of myeloid lineage biased defects in Shwachman-Diamond syndrome.

INTRODUCTION

Shwachman-Diamond syndrome (SDS; OMIM 260400) is a rare congenital multi-systemic disorder characterized by exocrine pancreatic insufficiency, skeletal defects and bone marrow failure.[1-3] The hematological hallmark of the disease is neutropenia, which affects 88% to 98% of patients[4,5] and represents, together with leukemic evolution, the main cause of morbidity and mortality in SDS.[1,6-8] Other, less common manifestations are anemia, thrombocytopenia and pancytopenia.[6,7] The disease is caused by biallelic loss of function mutations in the Shwachman-Bodian-Diamond Syndrome gene (*SBDS*).[9] The two most common mutations, 258+2T→C and 183-184TA→CT, result in impaired splicing and a premature stop codon, respectively, and are associated with reduced protein levels of SBDS.[9,10]

SBDS plays an essential role in ribosome biogenesis. In particular, the concerted activity of SBDS and elongation factor-like 1 (EFL1) mediates the removal of eukaryotic initiation factor 6 (eIF6) during the cytoplasmic maturation of the pre-60S subunit, allowing the formation of the 80S ribosome.[10-12] Consistent with this notion, impaired ribosome subunit joining has been demonstrated in SDS patients[12,13] and reduced overall translation was detected in yeast models of SDS.[11] Defects in ribosome biogenesis define a group of pathologies collectively known as ribosomopathies. Causative mutations in genes linked to ribosome biogenesis have been identified in several congenital diseases including Diamond-Blackfan anemia (DBA), dyskeratosis congenita and cartilage-hair hypoplasia. While the hematopoietic system is affected in most of these conditions, leading to some degree of bone marrow failure, pronounced vulnerability of specific cell lineages discerns these disorders, with neutropenia being the specific hallmark of SDS. This reflects the central enigma in the understanding of human congenital ribosomopathies, i.e. how disruption of ribosome biogenesis, a process occurring in all tissues with a proposed generic role in protein synthesis, results in cell and tissue specific disease phenotypes.

It is thought that ribosomes, and hence the proteins related to their biogenesis, are critically important for fast cycling cells, thus leading to impaired function of hematopoietic progenitor cells, resulting in cytopenia, but this view provides no explanation for cell type specificity (neutropenia) in SDS.[14,15]

Identification of the cell types specifically affected by dysfunction of ribosomal genes will thus be critical in deciphering the underlying molecular mechanisms driving disease pathology, ultimately enabling targeted therapies. However, progress in understanding the pathophysiology of SDS is limited by the lack of a robust mammalian model faithfully recapitulating neutropenia. Deficiency of *Sbds* leads to embryonic lethality in full knockout mice[10,16] and transplantation of shRNA-transduced, *Sbds*-deficient murine hematopoietic cells in wild type recipient mice did not result in overt neutropenia, although it impaired myeloid progenitor generation.[17] Targeting *Sbds* in the hematopoietic system via poly(I:C) treatment of *Sbds*$^{fl/-}$*Tg:Mx1-cre* mice resulted in a severe

hepatic phenotype, precluding a thorough investigation of the hematological consequences of *Sbds* deficiency in adult hematopoietic stem cells (HSCs).[10] Thus, *in vivo* targeting of *Sbds* in postnatal mammalian hematopoiesis remains a key challenge for the field.

The basic leucine zipper transcription factor CCAAT/Enhancer-Binding Protein α (C/EBPα) is expressed in a fraction of HSCs and throughout the myeloid lineage,[18-20] thus offering an alternative approach to target hematopoietic stem and progenitor cells and their downstream myeloid lineage progeny in adult mammals.

Here, we generated a novel mouse model of genetic *Sbds* deletion through targeted downregulation of the gene in *Cebpa*-expressing cells, resulting in profound neutropenia. We show that loss of *Sbds* is well tolerated by rapidly cycling myeloid progenitor cells and identify myelocytes and their downstream progeny as the cell types within the hematopoietic hierarchy critically affected by *Sbds* deficiency through induction of cellular stress and apoptosis, thus providing a cellular and molecular basis for neutropenia in SDS.

METHODS

Additional information is provided in the Supplemental Methods.

Mice and Genotyping

Cebpa$^{cre/+}$ R26 EYFP mice and *Sbds*$^{f/+}$ mice have been previously described.[19,21] B6.SJL-*Ptprc*^{a}*Pepc*^{b}/BoyCrl (B6.SJL) mice were purchased from Charles River. Mice and embryos were genotyped by PCR on DNA isolated from toes and forelimbs, respectively, using the primers listed in Table S1 (Life Technologies). Animals were maintained in specific pathogen free conditions in the Experimental Animal Center of Erasmus MC (EDC) and sacrificed by cervical dislocation. All animal work was approved by the Animal Welfare/Ethics Committee of the EDC in accordance with legislation in the Netherlands.

Fetal Liver Cell Transplantation

Fetal livers were isolated from E14.5 embryos. Cell suspensions were centrifuged, resuspended in a minimal volume of ACK lysing buffer (Lonza) and incubated on ice for 4 min to eliminate red blood cells. After centrifugation, cells were resuspended in PBS+0.5% FCS. 7-10-week-old, lethally irradiated (8.5Gy) B6.SJL mice were transplanted with $3x10^5$ fetal liver cells by tail vein injection. Recipients received antibiotics in the drinking water for 2 weeks after transplantation.

RNA Sequencing and GSEA Analysis

cDNA was synthesized and amplified using SMARTer Ultra Low RNA kit (Clontech Laboratories) following the manufacturer's protocol. Amplified cDNA was further processed according to TruSeq Sample Preparation v2 Guide (Illumina) and paired end-sequenced (2x75 bp) on the HiSeq 2500 (Illumina). Demultiplexing was performed using CASAVA software (Illumina) and the adaptor sequences were trimmed with Cutadapt (http://code.google.com/p/cutadapt/). Alignments against the mouse genome (mm10) and analysis of differential expressed genes were performed as previously described.[22] Cufflinks software was used to calculate the number of fragments per kilobase of exon per million fragments mapped (FPKM) for each gene. FPKM values of *Sbds f/f* and *+/+* recipients were then compared to the curated gene sets (C2) and the Gene Ontology gene sets (C5) of the Molecular Signature Database (MSigDB) by GSEA[23] (Broad Institute), using the Signal2Noise metric and 1000 phenotype-based permutations.

Statistical Analysis

Unless otherwise specified, statistical analysis was performed by an unpaired, 2-tailed Student's *t* test or 1-way analysis of variance. All results in bar graphs are reported as mean value ± standard error of the mean.

RESULTS

Cebpa-driven deletion of *Sbds* in the hematopoietic system

To address the functional consequences of *Sbds* deficiency in early hematopoietic progenitors, we crossed *Sbds*-conditional knock-out mice, with loxP sites flanking the second exon of *Sbds*,[21] with *Cebpa*$^{cre/+}$ R26 EYFP mice[19] (**Figure 1A**). In this approach, Cre-mediated deletion of *Sbds* exon 2 in *Cebpa*-expressing cells results in a frameshift and consequently generates a premature stop codon, thus mimicking the effects of the 183-184TA→CT mutation in the human disease.[9] In addition, the R26 EYFP element enables the tracing of *Sbds*-depleted cells and their progeny based on enhanced yellow fluorescent protein (EYFP) expression.

Intercrossings of *Sbds*$^{f/+}$*;Cebpa*$^{cre/+}$*;R26*$^{EYFP/+}$ mice failed to generate any *Sbds*$^{f/f}$*;Cebpa*$^{cre/+}$ viable offspring (**Table S2**). This, together with the small litter sizes, suggested that deficiency of *Sbds* in *Cebpa*-expressing cells is lethal in mice. Because *Cebpa* is expressed in non-hematopoietic tissues, like liver and lungs,[24] we analyzed E14.5 embryos from *Sbds*$^{f/+}$*;Cebpa*$^{cre/+}$ *R26*$^{EYFP/+}$ intercrosses to assess whether the lethal phenotype directly reflected hematopoietic dysfunction. Interestingly,

at this gestational age, *Sbds*$^{f/f}$*;Cebpa*$^{cre/+}$*;R26*$^{EYFP/+}$ (hereafter *Sbds f/f* or mutants) offspring was found at Mendelian frequencies (**Table S2**) and these embryos were morphologically indistinguishable from their littermates. Genomic PCR indicated effective deletion of exon 2 in *Sbds f/f* embryos (**Figure 1A**, **Figure 1B**). We next compared hematopoiesis in *Sbds f/f* embryos with that of *Cebpa*$^{cre/+}$*;R26*$^{EYFP/+}$ controls (hence *Sbds +/+*) and found that *Sbds* recombination was associated with overall conservation of normal hematopoietic architecture in the fetal liver (**Figure 1C**). This suggests that embryonic lethality in this model is not caused by impaired blood cell production. The proportion of EYFP$^+$, Cre-targeted cells in each hematopoietic compartment was also similar in *Sbds f/f* and *+/+* embryos, with the majority of GMPs and Gr1$^+$Mac1$^+$ mature granulocytes expressing EYFP (>90% and >60% of cells, respectively, **Figure 1D**). As expected,[19,20] a small fraction of immunophenotypically defined HSCs, multipotent progenitors (MPPs),

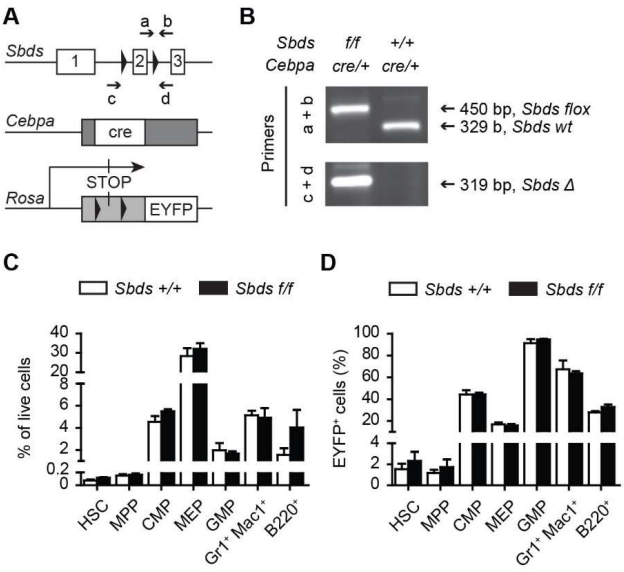

Figure 1. *Sbds*-deletion from myeloid progenitor cells does not perturb the architecture of fetal liver hematopoiesis. (A) Schematic representation of the targeting vectors and the primers used in the study. Primer sequences are listed in Table S1. (B) Genomic analysis of E14.5 embryos confirmed excision of *Sbds* in f/f mice. a + b, genotyping primers. c + d, deletion primers. (C-D) Normal composition of fetal liver (*Sbds +/+*, *n* = 4; *Sbds f/f*, *n* = 6). (C) Frequency of hematopoietic subsets in live cells (7AAD-). (D) Proportion of EYFP$^+$ cells in each hematopoietic population. Data is mean ± s.e.m. Differences between *Sbds +/+* and *f/f* mice are not significant. HSC, Lin$^-$ c-Kit$^+$ Sca1$^+$ (LKS) CD48$^-$ CD150$^+$ cells. Multipotent progenitors (MPP), LKS CD48$^-$ CD150$^-$ cells. Common myeloid progenitor (CMP), Lin$^-$ c-Kit$^+$ Sca1$^-$ CD34$^+$ CD16/32$^-$ cells. Granulocyte-macrophage progenitor (GMP), Lin$^-$ c-Kit$^+$ Sca1$^-$ CD34$^+$ CD16/32$^+$ cells.

megakaryocyte-erythroid progenitors (MEPs) and B220$^+$ lymphocytes also expressed EYFP, indicating targeting of multilineage progenitors in this model.

Transplantation of *Sbds*-deleted fetal hematopoietic cells in adult mice results in neutropenia

To assess whether the deletion of *Sbds* in fetal hematopoietic progenitors would compromise postnatal hematopoiesis, we transplanted fetal liver cells from of E14.5 (CD45.2$^+$) *Sbds f/f* or *+/+* embryos into lethally irradiated (CD45.1$^+$) B6.SJL mice (**Figure 2A**) and monitored hematopoiesis by peripheral blood analysis every 4 weeks. In both *Sbds f/f* and *+/+* recipients more than 90% of circulating blood cells were CD45.2$^+$, indicating high chimerism in reconstituted mice. Mice transplanted with *Sbds*-deficient cells developed profound neutropenia, with an average 5.9-fold reduction of Gr1$^+$ Mac1$^+$ cells in the peripheral blood 5 weeks after transplantation (**Figure 2B**). Neutropenia was stable and persisted during the entire follow-up, i.e. 4 months after transplantation. Consistent with the hypothesis that loss of *Sbds* impairs myelopoiesis, the proportion of EYFP$^+$, Cre-targeted cells in *Sbds f/f* recipients (47.4±10.2%) was lower than that in

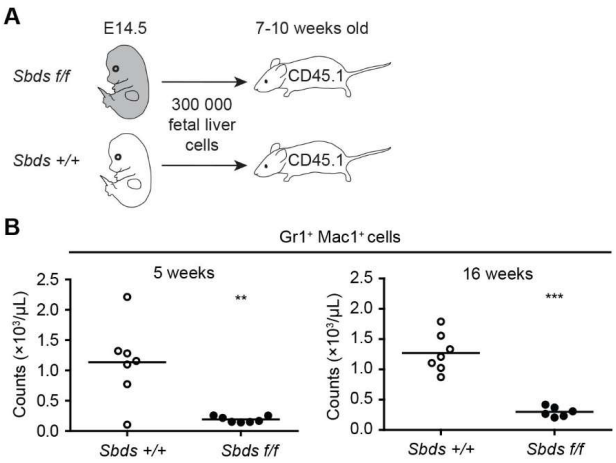

Figure 2. Loss of *Sbds* from C/EBPα-expressing cells causes neutropenia in mice. (A) Experimental design. 300 000 fetal liver cells from either *Sbds +/+* or *f/f* embryos (E14.5) were transplanted into 7 to 10-week-old lethally irradiated CD45.1$^+$ B6.SJL mice (n = 7 per group). (B) Peripheral blood analysis at 5 and 16 weeks after transplantation showed severe reduction of granulocytes (Gr1$^+$ Mac1$^+$ cells) upon *Sbds* deletion. Each circle represents one mouse. The horizontal line depicts average values. WBC, white blood cells. ** P < 0.01, ***P < 0.001.

controls (75.6±17.3%). In addition, numbers of circulating erythrocytes and B-cells were unaltered in steady state hematopoiesis after transplantation, while platelet numbers were increased in transplanted mice (**Figure S1**). Overall, the data indicates that *Sbds* is essential to maintain postnatal granulopoiesis and neutrophil homeostasis.

Sbds-deficiency in the myeloid lineage arrests differentiation at the myelocyte-metamyelocyte stage

To obtain insight into the cellular events caused by *Sbds* deficiency driving the defect in neutrophil development, we sacrificed mice 17 to 19 weeks after transplantation. *Cebpa* is expressed in myeloid progenitor cells and in a subpopulation of early progenitors that retain multilineage differentiation capacity.[19,20] In line with this, EYFP expression was found in a small fraction of immunophenotypically defined hematopoietic stem and progenitor cells (HSPCs) and in all blood lineages ($Gr1^+Mac1^+$ myeloid, $Ter119^+$ erythroid and $B220^+$ lymphoid) at varying frequencies (**Table 1**; **Figure 3A**).

The bone marrow of mice transplanted with *Sbds f/f* fetal liver cells was hypocellular, a common finding in SDS patients[7,25] (**Figure 3B**). Hypocellularity resulted mostly from a marked reduction in $EYFP^+$ $Gr1^+$ $Mac1^+$ neutrophils (86 437 ± 33 601 cells per femur/body gram in *Sbds f/f* recipients and 316 442 ± 47 984 in controls), although also the number of $EYFP^+$ lymphoid and $Ter119^+$ erythroid cells was modestly decreased in mutant mice (**Figure 3C**, **Figure 3D**). Of note, myelodysplastic features were not observed in *Sbds f/f* recipients in the current model, suggesting that hematopoietic cell-extrinsic factors may contribute to myelodysplasia in SDS.[26]

Table 1. Frequency of EYFP+ cells within hematopoietic subsets in the bone marrow.

Population	*Sbds +/+* [a]	*Sbds f/f* [a]
LKS[b]	3.3% (1.61% - 5.82%)	7.4% (1.67% - 11.5%)
CMP[b]	31.2% (24.0% - 41.6%)	22.5% (16.3% - 31.6%)
MEP[b]	8.2% (6.3% - 10.2%)	5.8% (4.92% - 6.79%)
GMP[b]	72.3% (63.7% - 77.6%)	67.7% (62.6% - 72.3%)
$Gr1^+$ $Mac1^+$ [c]	87.9% (86.2% - 89.1%)	76.1% (74.3% - 77.7%)
$B220^+$ [c]	8.8% (5.4% - 13.2%)	4.4% (3.3% - 5.9%)
$Ter119^+$ [d]	3.0% (2.2% - 4.1%)	1.8% (0.7% - 3.2%)

[a]The percentage of $EYFP^+$ cells in different hematopoietic populations is indicated as mean frequency (range). [b]*n* = 7. [c]*Sbds +/+*, *n* = 7; *Sbds f/f*, *n*=6. [d]*Sbds +/+*, *n* = 5; *Sbds f/f*, *n* = 4.

Having established that *Sbds* deletion from multilineage hematopoietic progenitors results in neutropenia, we next sought to define the stages in myeloid lineage progression that were affected by loss of *Sbds*. It is generally assumed that loss of ribosome biogenesis genes affects rapidly proliferating progenitor cells with increased protein translation rates, although *in vivo* experimental support for this view has been lacking in the absence of a mammalian model of *Sbds* deficiency resulting in stable neutropenia. Efficient *Sbds* gene knockdown in EYFP$^+$ cells was first confirmed by quantitative RT-PCR throughout myeloid lineage development (**Figure 3E**), showing near complete deletion of *Sbds* expression at all stages of myeloid development (LKS, CMP, GMP, immature and mature neutrophils). Interestingly, *Sbds* deficiency did not result in reduced numbers of hematopoietic progenitor cells along the myeloid lineage (**Figure 3C**, **Figure 3D**). Rather, a compensatory expansion of some progenitors was observed with numbers of both EYFP$^+$ and EYFP$^-$ GMPs dramatically increased in mice transplanted with *Sbds f/f* cells (average fold change, FC: 5.8 in EYFP$^+$ compartment and 5.9 in EYFP$^-$ cells; **Figure 3D**; **Figure S2**), suggesting the emergence of reactive granulopoiesis in this cohort, defined as adaptation of the hematopoietic system to the increased demand through enhanced myeloid precursor cell proliferation in the bone marrow.[27]

We next aimed to further define the specific cell type in myeloid development that is critically dependent on *Sbds* function. FACS analysis revealed an increased frequency of c-Kit^{int} Gr1^{low} cells, previously identified as myelocytes and metamyelocytes (MC-MMs, **Figure 3F**).[28] Both frequency and absolute count of more mature myeloid cells, characterized by loss of c-Kit expression and bright Gr1 staining, were lower, suggesting an arrest of lineage progression at the MC-MM stage. Morphological assessment of the bone marrow confirmed that terminal granulopoiesis is severely affected in *Sbds f/f* recipients, with accumulation of MC-MMs and reduced frequency of segmented neutrophils (**Figure 3G**; **Figure S3**). Together, the data demonstrates that *Sbds* deletion from hematopoietic progenitor cells critically and specifically affects late stages of myeloid development, in particular the transition MC-MM to mature neutrophils.

Deficiency of *Sbds* deregulates myeloid differentiation programs and prevents cell-cycle-exit in myelocytes and metamyelocytes

To gain insight into the molecular programs associated with the proposed block of myeloid lineage progression at the MC-MM stage, the transcriptome of prospectively FACS-isolated EYFP$^+$ c-Kit^{int} Gr1^{low} (MC-MM) cells was investigated by massive parallel RNA sequencing (RNA-Seq). As expected, *Sbds* expression in this population was significantly reduced in *Sbds f/f* recipients (log_2 FC = -2.39, False Discovery Rate, FDR=6.6x10^{-9}, **Figure 4A**). Consistent with its postulated function in ribosome biogenesis, *Sbds* deficiency significantly (FDR<0.25) affected transcriptional

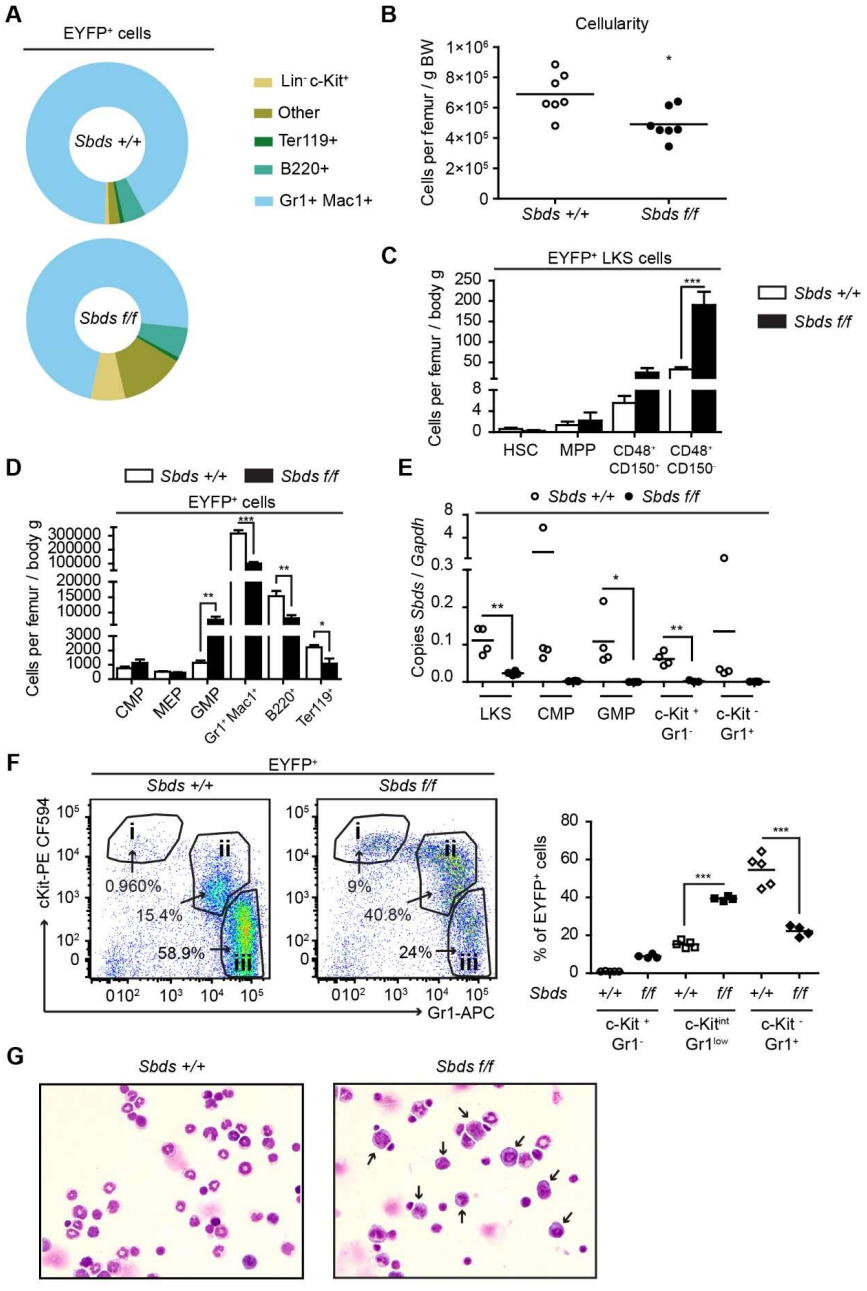
A
EYFP+ cells
Sbds +/+
Sbds f/f
Lin- c-Kit+
Other
Ter119+
B220+
Gr1+ Mac1+
B
Cellularity
Cells per femur / g BW
Sbds +/+
Sbds f/f
C
EYFP+ LKS cells
Cells per femur / body g
HSC
MPP
CD48+ CD150+
CD48+ CD150-
D
EYFP+ cells
CMP
MEP
GMP
Gr1+Mac1+
B220+
Ter119+
E
Copies Sbds / Gapdh
LKS
CMP
GMP
c-Kit + Gr1-
c-Kit - Gr1+
F
EYFP+
cKit-PE CF594
Gr1-APC
0.960%
15.4%
58.9%
9%
40.8%
24%
% of EYFP+ cells
c-Kit + Gr1-
c-Kit int Gr1 low
c-Kit - Gr1+
G

signatures related to translation and ribosome biogenesis (**Figure 4B**; **Table S3** and **S4**). Gene set enrichment analysis (GSEA) highlighted the enrichment of relatively immature hematopoietic signatures in *Sbds f/f* MC-MMs, whereas data sets associated with cell differentiation were enriched in controls, consistent with a defect in maturation (**Figure 4C**; **Table S3**). To specifically define the stage in which myeloid differentiation is impaired, we examined the expression of transcripts encoding constituents of myeloid granules. In myeloid development, primary granules are produced in promyelocytes, whereas secondary granule production starts in myelocytes and gelatinase-containing tertiary granules become apparent in metamyelocytes and in band cells.[29,30] Transcript analysis showed significantly reduced expression of secondary and tertiary granule components, whereas transcripts encoding constituents of primary granules were significantly enriched, indicating that development is specifically arrested in myelocytes, consistent with flow-cytometric findings (**Figure 4D**).

To definitively establish the myelocyte as the cell type in the myeloid lineage critically depending on *Sbds* expression, we next performed cell cycle analysis. Myelocytes represent the last cell in myeloid differentiation capable of mitotic division[31] and cell cycle exit is a required process for terminal granulopoiesis[32]. Ki67 analysis by FACS demonstrated that c-Kit^{int} Gr1^{low} cells indeed failed to exit the cell cycle, congruent with the notion that *Sbds* deficiency attenuates lineage progression in myelocytes (**Figure 4E**, **Figure 4F**). Molecularly, this failure to exit the cell cycle was associated with significant reduced expression of the transcription factor retinoic acid receptor α (RARα) and its downstream transcriptional targets *Itgb2* and p27 (*Cdkn1b*),[33,34] key activators of the terminal myeloid differentiation program and cell cycle exit (**Figure 4G**).

Together, the data demonstrates that loss of *Sbds* from hematopoietic progenitors results in failure of lineage progression specifically in myelocytes, which is associated with attenuation of

Figure 3. *Sbds*-deficiency in hematopoiesis attenuates myeloid lineage progression at the myelocyte-metamyelocyte stage. (A) Donut chart illustrating the percentage of different hematopoietic subsets within the EYFP$^+$ compartment in the bone marrow of *Sbds +/+* and *f/f* recipients. (B) Decreased cellularity upon transplantation of *Sbds*-deficient cells. (C-D) Absolute number of EYFP$^+$ cells in different hematopoietic populations in the bone marrow (*Sbds +/+*, *n* = 7*; Sbds f/f*, *n* = 6, data is mean ± s.e.m). (C) LKS subsets. (D) Reduction of EYFP$^+$ mature granulocytes in *Sbds f/f*-transplanted mice is associated with an increase of granulocyte-macrophage progenitors. (E) Deletion efficacy. Expression of *Sbds* is reduced in LKS and throughout the myeloid differentiation stages in *Sbds f/f* EYFP$^+$ cells. (F) Loss of late myeloid cells in *Sbds f/f* mice. Upper panel, representative plots of EYFP$^+$ cells. Lower panel, percentage of c-Kit$^+$ Gr1$^-$ myeloblasts and promyelocytes (i), c-Kit^{int} Gr1^{low} myelocytes and metamyelocytes (ii) and c-Kit$^-$ Gr1$^+$ band and segmented cells (iii) in EYFP$^+$ cells from *Sbds +/+* and *f/f* cohorts. (G) Accumulation of myelocytes and metamyelocytes (black arrows) in *Sbds*-deficient bone marrow (original magnification x63). * $P < 0.05$, ** $P < 0.01$, *** $P < 0.001$.

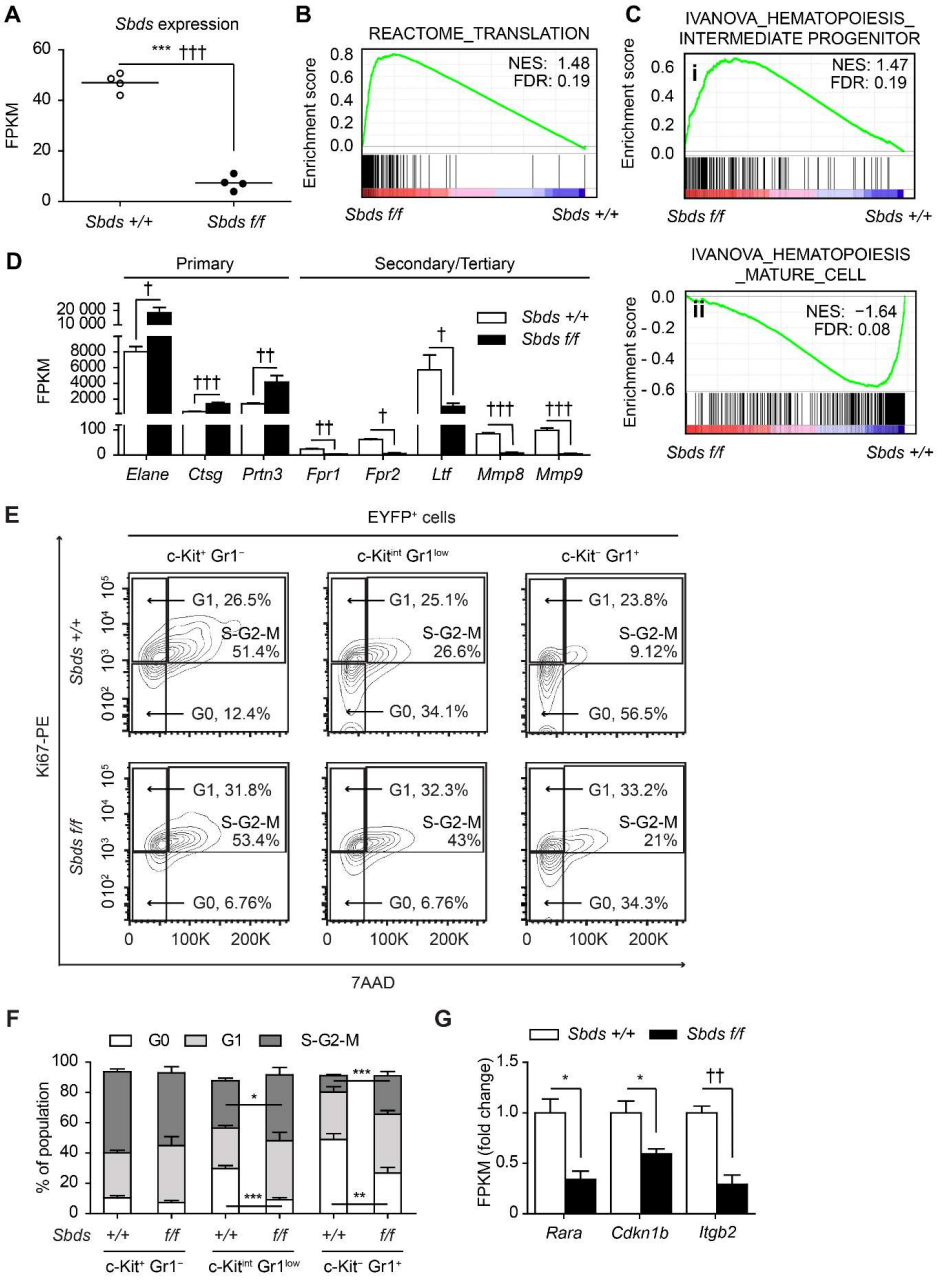
A
Sbds expression
*** †††
FPKM
60
40
20
0
Sbds +/+
Sbds f/f
B
REACTOME_TRANSLATION
NES: 1.48
FDR: 0.19
Enrichment score
0.8
0.6
0.4
0.2
0.0
Sbds f/f
Sbds +/+
C
IVANOVA_HEMATOPOIESIS_
INTERMEDIATE PROGENITOR
i
NES: 1.47
FDR: 0.19
Enrichment score
0.6
0.4
0.2
0.0
Sbds f/f
Sbds +/+
D
Primary
Secondary/Tertiary
Sbds +/+
Sbds f/f
FPKM
20 000
10 000
8000
6000
4000
2000
100
0
Elane
Ctsg
Prtn3
Fpr1
Fpr2
Ltf
Mmp8
Mmp9
IVANOVA_HEMATOPOIESIS
_MATURE_CELL
ii
NES: −1.64
FDR: 0.08
Enrichment score
0.0
- 0.2
- 0.4
- 0.6
Sbds f/f
Sbds +/+
E
EYFP⁺ cells
c-Kit⁺ Gr1⁻
c-Kit^int Gr1^low
c-Kit⁻ Gr1⁺
Sbds +/+
Sbds f/f
Ki67-PE
G1, 26.5%
S-G2-M
51.4%
G0, 12.4%
G1, 25.1%
S-G2-M
26.6%
G0, 34.1%
G1, 23.8%
S-G2-M
9.12%
G0, 56.5%
G1, 31.8%
S-G2-M
53.4%
G0, 6.76%
G1, 32.3%
S-G2-M
43%
G0, 6.76%
G1, 33.2%
S-G2-M
21%
G0, 34.3%
0
100K
200K
7AAD
F
G0
G1
S-G2-M
% of population
100
80
60
40
20
0
Sbds
+/+
f/f
c-Kit⁺ Gr1⁻
c-Kit^int Gr1^low
c-Kit⁻ Gr1⁺
G
Sbds +/+
Sbds f/f
FPKM (fold change)
1.5
1.0
0.5
0
Rara
Cdkn1b
Itgb2

myeloid differentiation signatures and cellular events.

Loss of *Sbds* results in activation of the p53 tumor suppressor pathway and apoptosis in late stage myeloid cells

Finally, we shought to better define the underlying cellular and molecular mechanisms of the arrest in lineage progression at the stage of myelocytes. Activation of p53 has been proposed as a common mechanism in the pathogenesis of different ribosomopathies, including DBA, Treacher Collins syndrome and 5q- syndrome[35]. In SDS, overexpression of p53 in immature cells has been described in bone marrow biopsies from SDS patients[36] but the consequences of p53 activation for disease pathogenesis have not been experimentally defined. Transcriptional activation of the p53 pathway was observed in *Sbds f/f* MC-MMs by GSEA analysis (**Figure 5A**). Specifically, RNA sequencing demonstrated a significant increase in transcripts for p53 itself and many of its downstream targets, including the cell cycle regulators *Cdkn1a* (p21) and *Zmat3* (Wig1) and the pro-apoptotic genes *Bbc3* (PUMA), *Bax*, *Tnfrsf10b* (Death Receptor 5) and *Cycs* (cytochrome c, somatic) (**Figure 5B**). FACS analysis confirmed intracellular accumulation of the p53 protein, specifically at late stages of myelopoiesis (MC-MM and c-Kit $^{-}$ EYFP+ populations) in *Sbds f/f* recipients (FC = 1.78 and 1.53, respectively, **Figure 5C**). In line with this activation of the p53 tumor suppressor pathway and increased expression of pro-apoptotic genes, an increased rate of apoptosis (annexin V^{+} 7AAD^{-} cells) was found in p53-overexpressing c-Kit^{int} and c-Kit^{-} EYFP^{+} populations (**Figure 5D**). Of note, no significant p53 accumulation or apoptosis was observed in

Figure 4. *Sbds* deficiency results in failure of cell cycle exit and secondary granule formation in myelopoiesis. (A) Expression of *Sbds* in c-Kit^{int} Gr1^{low} EYFP^{+} cells by RNA-Seq (n = 4). Each circle represents one mouse. (B-C) GSEA plots showing enrichment of data sets relating to translation (B) and immature hematopoietic features (Ci) in c-Kit^{int} Gr1^{low} EYFP^{+} cells from *Sbds f/f* recipients and enrichment of maturation signatures in the *Sbds +/+* group (Cii). Genes in the datasets are represented by black bars distributed according to their differential expression between *Sbds f/f* and *Sbds +/+* cohorts. NES: Normalized Enrichment Score. (D) Reduced expression of genes encoding secondary and tertiary granule proteins in *Sbds f/f* c-Kit^{int} Gr1^{low} EYFP^{+} cells with enrichment of transcripts encoding primary granules components. (E-F) *Sbds* deficiency impairs cell cycle exit in myelopoiesis (*Sbds +/+*, n = 5; *Sbds f/f*, n = 4). (E) Gating strategy in representative FACS plots. (F) Percentage of cells in G0 (Ki67^{-} 7AAD^{low}), G1 (Ki67^{+} 7AAD^{low}) and S-G2-M (Ki67^{+} 7AAD^{high}) in each YFP^{+} population. (G) Downregulation of *Rara*, *Cdkn1b* (p27) and *Itgb2* in recipients of *Sbds*-deficient cells (n = 4). Data is mean ± s.e.m. * P < 0.05, ** P < 0.01, ***P < 0.001. † *FDR* < 0.05, †† *FDR* < 0.01, ††† *FDR* < 0.001.

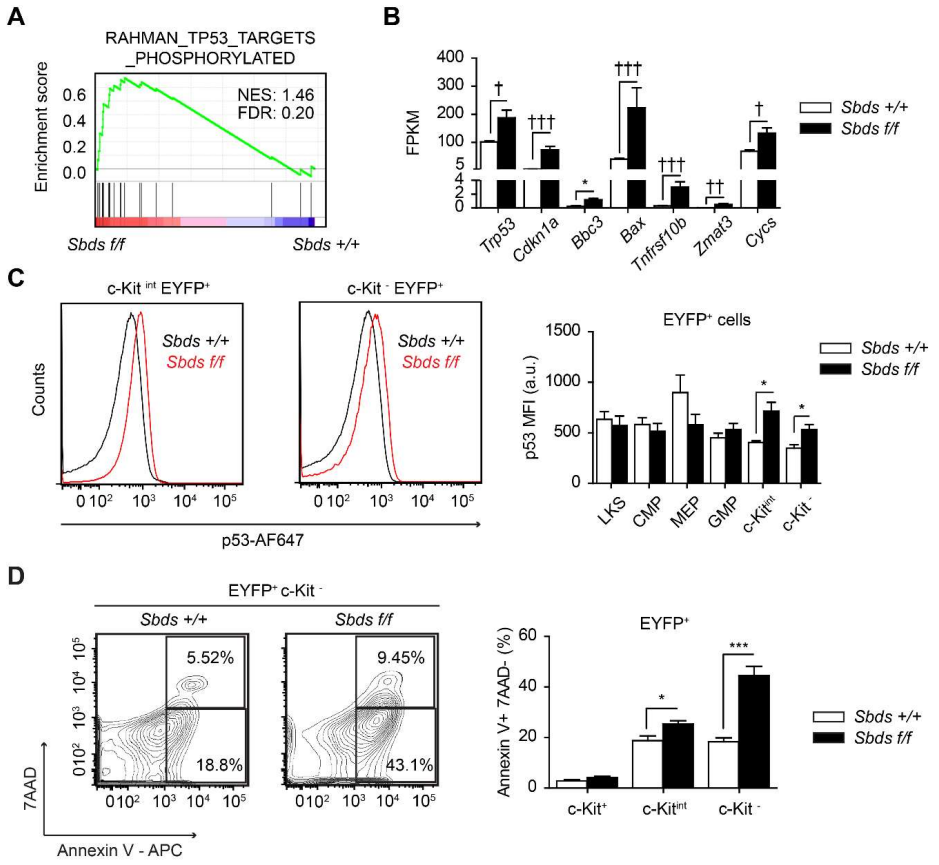

Figure 5. Activation of p53 and apoptosis in late stages of *Sbds*-deficient myeloid development. (A) Enrichment of p53 signatures in the transcriptome of MC-MMs from *Sbds f/f* recipients (n = 4). (B) Increased transcript levels of *Trp53* and its downstream transcriptional targets in RNA-Seq data. (C) Accumulation of p53 protein in late stages of myelopoiesis. Left, representative histograms. Right, mean fluorescence intensities in different EYFP+ populations (*Sbds +/+*, n = 5; *Sbds f/f*, n = 4). (D) Increased rates of apoptosis in late myeloid cells upon *Sbds* deletion (n = 4). Left, representative plot. Right, frequency of annexin V+ 7AAD- apoptotic cells in different stages of myelopoiesis. Data in bar graphs is mean ± s.e.m. $^{*}P < 0.05$, $^{***}P < 0.001$. †FDR < 0.05, †††FDR < 0.001.

more immature progenitors (cKit$^+$ EYFP$^+$ cells). Collectively, the findings indicate that *Sbds* deficiency in the myeloid lineage specifically attenuates lineage progression at the myelocyte stage through activation of cellular stress pathways and induction of p53-associated apoptosis.

DISCUSSION

Neutropenia is the principal hematological manifestation of SDS, but the cellular and molecular mechanisms underlying this specific disease phenotype remain poorly understood. Here, we established a mammalian model of *Sbds* deficiency-induced neutropenia, revealing a critical dependency of myelocytes and their downstream progeny on the function of this ribosomal biogenesis gene through induction of p53-associated apoptosis, thus providing a cellular and molecular basis for the understanding of neutropenia in this disease.

Several findings in our study point towards myelocytes as the differentiation stage critically impaired by *Sbds* deficiency. First, the data indicates that myelocytes accumulate in *Cebpa*-cre *Sbds* mutant mice and fail to exit the cell cycle, a process typically occurring at the myelocyte stage and required for terminal differentiation towards mature neutrophils.[31,32] Secondly, massive parallel transcriptional profiling of prospectively isolated MC-MMs revealed specifically reduced expression of genes encoding constituents of secondary and tertiary granule proteins, the production of which specifically marks the transition from promyelocytes to myelocytes in myeloid development.[29,30] Finally, *Sbds* deficiency in myelocytes was associated with reduced expression of the myeloid transcription factor RARα and its downstream transcriptional targets. RARα is an important regulator of myelopoiesis with a putative role in terminal granulocyte differentiation.[37] *In vitro* differentiation studies show that RAR deficiency blocks lineage progression at the myelocyte stage[38] and *in vivo* inhibition of endogenous retinoids results in accumulation of immature myeloid cells in wild type mice.[37]

While *Sbds* deletion in the myeloid lineage specifically attenuated lineage progression downstream of myelocytes, deficiency of *Sbds* did not functionally affect rapidly cycling hematopoietic progenitor cells (HPCs). This finding was initially unanticipated since HPCs are thought to have a relatively high rate of protein synthesis in comparison to HSCs and other cells of the hematopoietic hierarchy[39] and it seemed therefore reasonable to predict that rapidly cycling progenitors are more sensitive to defects of ribosome biogenesis and protein translation. In line with this view, reduced frequency or altered activity of HPCs have been previously suggested to drive cytopenia in both DBA and SDS,[40-42] albeit this does not provide a satisfactory explanation for lineage specificity in these diseases. In our model, the efficacy of *Sbds* deletion was comparable throughout myeloid development (*Cebpa*-expressing LKS, CMP, GMP and the myelocyte compartment), yet the size of the progenitor pool in the bone marrow increased, while

the number of mature neutrophils was reduced. This finding seems congruent with observations in zebrafish, where deletion of *Sbds* induces loss of neutrophils, but does not affect spi1 (PU.1) positive progenitors.[43]

The resulting left-shifted myelopoiesis in our model is reminiscent of that observed *in vitro* upon granulocytic differentiation of *Sbds*-knockdown hematopoietic cells, resulting in an accumulation of MC-MMs,[17] and of the maturation defect that characterizes a subset of SDS patients.[5,7,25,44] While our findings provide a basis for understanding the myeloid lineage specificity of ribosomal dysfunction in SDS, in translating these findings to human disease it is important to point out that pluripotent hematopoietic stem cells are incompletely targeted in this model. *Cebpa*-driven deletion of *Sbds* occurred in a small subset of immunophenotypically defined, multipotent HSCs, reflected in a modest decrease in erythroid and lymphoid cells in the EYFP+ compartment of mutant mice. It is therefore reasonable to assume that *Sbds* deficiency in the hematopoietic system does not exclusively, but rather predominantly, affects the myeloid lineage. It is conceivable that in human disease composite effects of *Sbds* deficiency in pluripotent HSCs, potentially reducing numbers of (normally functioning) hematopoietic progenitor cells,[42,44,45] synergize with a specific impairment of lineage progression in late myeloid differentiation phases to impair granulopoiesis. Incomplete HSC targeting may also explain the apparent absence of homing defects, previously reported in a transplant model of *Sbds* downregulation in HSC.[17] This notion may help understand why we have been able to establish a stable model of neutropenia, where incomplete targeting of HSCs allowed durable and robust engraftment of hematopoiesis enabling the detailed analysis of long-term myeloid lineage progression in mutant mice.

Identification of the cells driving neutropenia within the *Sbds*-deficient hematopoietic hierarchy allowed us to begin defining the cellular and molecular events underlying neutropenia in SDS. Our study describes activation of the p53 pathway and an associated increase in apoptotic rates specifically in myelocytes and their downstream progeny. The data seems congruent with observations in human disease where an intrinsic propensity for apoptosis is seen in hematopoietic cells after 7-day culture of CD34+ cells in medium containing G-CSF[46] with a lack of correlation between colony numbers and apoptosis rate, indicating that the number of CFU-C is not affected in SDS patients. Activation of the p53 pathway has been suggested to represent a molecular commonality in ribosomopathies and perhaps congenital neutropenias[47] but experimental support for this view in SDS has been lacking. Our findings do not, however, exclude the possibility that other mechanisms are involved in the failure in cell cycle progression and neutropenia in SDS.

It is conceivable that the loss of function of *Sbds* affects the translation of specific transcription factors driving terminal myeloid differentiation, including those upstream of RARα. In particular, the mRNA of specific transcription factor isoforms may be characterized by distinct 5'-UTRs, some

of them predicted to have a complex secondary structure.[48] These complex 5'-UTRs are typically associated with high demands for translation initiation factors and may thus confer particular sensitivity to conditions of translational stress. Such a mechanism of reduced translation efficiency has recently been shown to affect GATA1 protein levels in the pathogenesis of DBA.[49] Alternatively, the high and specific demand of protein synthesis and cotranslational assembly into secretory granules, which characterizes and defines myelocytes and their downstream progeny, may cause specific translational stress, resulting in activation of cellular alarm pathways and downstream events including impaired differentiation. In this context, it is interesting to note previous observations in induced pluripotent stem cell models of SDS, indicating granule abnormalities in pancreatic and myeloid cells,[50] and in a mouse model of pancreatic-specific *Sbds* deficiency, showing reduced *in vivo* zymogen granule formation in acinar cells,[21] perhaps pointing towards impaired secretory granule maturation as a common mechanism underlying tissue specificity in SDS.[50] Our current model will allow the interrogation of these potential mechanisms which is ultimately anticipated to result in novel, targeted therapeutic strategies for SDS.

ACKNOWLEDGEMENTS

The authors would like to thank Dr Marieke van Lindern and Roberto Avellino for valuable scientific discussions; Dr Kirsten van Lom, Marije Havermans, Dr Elwin Rombouts, Peter van Geel for technical assistance; and members of the Erasmus MC animal core facility EDC for the help with animal care. This work was supported by grants from the Dutch Cancer Society (KWF Kankerbestrijding), Amsterdam, The Netherlands (grant EMCR 2010-4733).

AUTHORSHIP

N.A.Z., M.H.G.P.R. and I.P.T. designed the study; J.M.R. provided the *Sbds*–conditional knock out mice; N.A.Z., P.M.H.V.S., M.G.V., M.N.A. and E.M.J.B. performed the experiments; E.M.J.B., R.M.H. and M.A.S. provided bioinformatics support; N.A.Z., P.M.H.V.S., M.G.V. and M.H.G.P.R analyzed the data; N.A.Z. and M.H.G.P.R. wrote the manuscript.

Disclosures: The authors report no potential conflicts of interest.

REFERENCES

1. Shwachman H, Diamond LK, Oski FA, Khaw KT. The Syndrome of Pancreatic Insufficiency and Bone Marrow Dysfunction. *Journal of Pediatrics*. 1964;65:645-663.
2. Huang JN, Shimamura A. Clinical spectrum and molecular pathophysiology of Shwachman-Diamond syndrome. *Current Opinion in Hematology*. 2011;18(1):30-35.
3. Tamary H, Alter BP. Current diagnosis of inherited bone marrow failure syndromes. *Pediatric Hematology and Oncology*. 2007;24(2):87-99.
4. Mack DR, Forstner GG, Wilschanski M, Freedman MH, Durie PR. Shwachman syndrome: Exocrine pancreatic dysfunction and variable phenotypic expression. *Gastroenterology*. 1996;111(6):1593-1602.
5. Ginzberg H, Shin J, Ellis L, et al. Shwachman syndrome: phenotypic manifestations of sibling sets and isolated cases in a large patient cohort are similar. *Journal of Pediatrics*. 1999;135(1):81-88.
6. Dror Y. Shwachman-Diamond syndrome. *Pediatric Blood & Cancer*. 2005;45(7):892-901.
7. Donadieu J, Fenneteau O, Beaupain B, et al. Classification of and risk factors for hematologic complications in a French national cohort of 102 patients with Shwachman-Diamond syndrome. *Haematologica-the Hematology Journal*. 2012;97(9):1312-1319.
8. Myers KC, Bolyard AA, Otto B, et al. Variable Clinical Presentation of Shwachman-Diamond Syndrome: Update from the North American Shwachman-Diamond Syndrome Registry. *Journal of Pediatrics*. 2014;164(4):866-870.
9. Boocock GR, Morrison JA, Popovic M, et al. Mutations in SBDS are associated with Shwachman-Diamond syndrome. *Nature Genetics*. 2003;33(1):97-101.
10. Finch AJ, Hilcenko C, Basse N, et al. Uncoupling of GTP hydrolysis from eIF6 release on the ribosome causes Shwachman-Diamond syndrome. *Genes & Development*. 2011;25(9):917-929.
11. Menne TF, Goyenechea B, Sanchez-Puig N, et al. The Shwachman-Bodian-Diamond syndrome protein mediates translational activation of ribosomes in yeast. *Nature Genetics*. 2007;39(4):486-495.
12. Wong CC, Traynor D, Basse N, Kay RR, Warren AJ. Defective ribosome assembly in Shwachman-Diamond syndrome. *Blood*. 2011;118(16):4305-4312.
13. Burwick N, Coats SA, Nakamura T, Shimamura A. Impaired ribosomal subunit association in Shwachman-Diamond syndrome. *Blood*. 2012;120(26):5143-5152.
14. De Keersmaecker K, Sulima SO, Dinman JD. Ribosomopathies and the paradox of cellular hypo- to hyperproliferation. *Blood*. 2015;125(9):1377-1382.
15. Ruggero D, Shimamura A. Marrow failure: a window into ribosome biology. *Blood*. 2014;124(18):2784-2792.
16. Zhang S, Shi M, Hui CC, Rommens JM. Loss of the mouse ortholog of the shwachman-diamond syndrome gene (Sbds) results in early embryonic lethality. *Molecular and Cellular Biology*. 2006;26(17):6656-6663.
17. Rawls AS, Gregory AD, Woloszynek JR, Liu FL, Link DC. Lentiviral-mediated RNAi inhibition of Sbds in murine hematopoietic progenitors impairs their hematopoietic potential. *Blood*. 2007;110(7):2414-2422.

18. Zhang P, Iwasaki-Arai J, Iwasaki H, et al. Enhancement of hematopoietic stem cell repopulating capacity and self-renewal in the absence of the transcription factor C/EBP alpha. *Immunity*. 2004;21(6):853-863.
19. Wölfler A, Oorschot AADV, Haanstra JR, et al. Lineage-instructive function of C/EBP alpha in multipotent hematopoietic cells and early thymic progenitors. *Blood*. 2010;116(20):4116-4125.
20. Ye M, Zhang H, Amabile G, et al. C/EBPa controls acquisition and maintenance of adult haematopoietic stem cell quiescence. *Nature Cell Biology*. 2013;15(4):385-394.
21. Tourlakis ME, Zhong J, Gandhi R, et al. Deficiency of Sbds in the Mouse Pancreas Leads to Features of Shwachman-Diamond Syndrome, With Loss of Zymogen Granules. *Gastroenterology*. 2012;143(2):481-492.
22. Gröschel S, Sanders MA, Hoogenboezem R, et al. A Single Oncogenic Enhancer Rearrangement Causes Concomitant EVI1 and GATA2 Deregulation in Leukemia. *Cell*. 2014;157(2):369-381.
23. Subramanian A, Tamayo P, Mootha VK, et al. Gene set enrichment analysis: a knowledge-based approach for interpreting genome-wide expression profiles. *Proc Natl Acad Sci U S A*. 2005;102(43):15545-15550.
24. Flodby P, Barlow C, Kylefjord H, Ahrlund-Richter L, Xanthopoulos KG. Increased hepatic cell proliferation and lung abnormalities in mice deficient in CCAAT/enhancer binding protein alpha. *Journal of Biological Chemistry*. 1996;271(40):24753-24760.
25. Aggett PJ, Cavanagh NPC, Matthew DJ, Pincott JR, Sutcliffe J, Harries JT. Shwachmans Syndrome - a Review of 21 Cases. *Archives of Disease in Childhood*. 1980;55(5):331-347.
26. Raaijmakers MH, Mukherjee S, Guo S, et al. Bone progenitor dysfunction induces myelodysplasia and secondary leukaemia. *Nature*. 2010;464(7290):852-857.
27. Manz MG, Boettcher S. Emergency granulopoiesis. *Nature Reviews Immunology*. 2014;14(5):302-314.
28. Satake S, Hirai H, Hayashi Y, et al. C/EBP beta Is Involved in the Amplification of Early Granulocyte Precursors during Candidemia-Induced "Emergency" Granulopoiesis. *Journal of Immunology*. 2012;189(9):4546-4555.
29. Borregaard N, Sehested M, Nielsen BS, Sengelov H, Kjeldsen L. Biosynthesis of Granule Proteins in Normal Human Bone-Marrow Cells - Gelatinase Is a Marker of Terminal Neutrophil Differentiation. *Blood*. 1995;85(3):812-817.
30. Borregaard N, Cowland JB. Granules of the human neutrophilic polymorphonuclear leukocyte. *Blood*. 1997;89(10):3503-3521.
31. Bainton DF, Ullyot JL, Farquhar MG. The development of neutrophilic polymorphonuclear leukocytes in human bone marrow. *Journal of Experimental Medicine*. 1971;134(4):907-934.
32. Wang QF, Cleaves R, Kummalue T, Nerlov C, Friedman AD. Cell cycle inhibition mediated by the outer surface of the C/EBPalpha basic region is required but not sufficient for granulopoiesis. *Oncogene*. 2003;22(17):2548-2557.
33. Walkley CR, Purton LE, Snelling HJ, et al. Identification of the molecular requirements for an RAR alpha-mediated cell cycle arrest during granulocytic differentiation. *Blood*. 2004;103(4):1286-1295.
34. Bush TS, St Coeur M, Resendes KK, Rosmarin AG. GA-binding protein (GABP) and Sp1 are required, along with retinoid receptors, to mediate retinoic acid responsiveness of CD18 (beta 2 leukocyte

integrin): a novel mechanism of transcriptional regulation in myeloid cells. *Blood*. 2003;101(1):311-317.
35. Fumagalli S, Thomas G. The role of p53 in ribosomopathies. *Seminars in Hematology*. 2011;48(2):97-105.
36. Elghetany MT, Alter BP. p53 protein overexpression in bone marrow biopsies of patients with Shwachman-Diamond syndrome has a prevalence similar to that of patients with refractory anemia. *Archives of Pathology & Laboratory Medicine*. 2002;126(4):452-455.
37. Kastner P, Lawrence HJ, Waltzinger C, Ghyselinck NB, Chambon P, Chan S. Positive and negative regulation of granulopoiesis by endogenous RARalpha. *Blood*. 2001;97(5):1314-1320.
38. Labrecque J, Allan D, Chambon P, Iscove NN, Lohnes D, Hoang T. Impaired granulocytic differentiation in vitro in hematopoietic cells lacking retinoic acid receptors alpha1 and gamma. *Blood*. 1998;92(2):607-615.
39. Signer RAJ, Magee JA, Salic A, Morrison SJ. Haematopoietic stem cells require a highly regulated protein synthesis rate. *Nature*. 2014;509(7498):49-54.
40. Perdahl EB, Naprstek BL, Wallace WC, Lipton JM. Erythroid Failure in Diamond-Blackfan Anemia Is Characterized by Apoptosis. *Blood*. 1994;83(3):645-650.
41. Dutt S, Narla A, Lin K, et al. Haploinsufficiency for ribosomal protein genes causes selective activation of p53 in human erythroid progenitor cells. *Blood*. 2011;117(9):2567-2576.
42. Dror Y, Freedman MH. Shwachman-Diamond syndrome: An inherited preleukemic bone marrow failure disorder with aberrant hematopoietic progenitors and faulty marrow microenvironment. *Blood*. 1999;94(9):3048-3054.
43. Provost E, Wehner KA, Zhong XG, et al. Ribosomal biogenesis genes play an essential and p53-independent role in zebrafish pancreas development. *Development*. 2012;139(17):3232-3241.
44. Mercuri A, Cannata E, Perbellini O, et al. Immunophenotypic Analysis of Hematopoiesis in Patients suffering from Shwachman-Bodian-Diamond Syndrome. *Eur J Haematol*. 2014.
45. Saunders EF, Gall G, Freedman MH. Granulopoiesis in Shwachman's syndrome (pancreatic insufficiency and bone marrow dysfunction). *Pediatrics*. 1979;64(4):515-519.
46. Dror Y, Freedman MH. Shwachman-Diamond syndrome marrow cells show abnormally increased apoptosis mediated through the Fas pathway. *Blood*. 2001;97(10):3011-3016.
47. Glaubach T, Minella AC, Corey SJ. Cellular stress pathways in pediatric bone marrow failure syndromes: many roads lead to neutropenia. *Pediatr Res*. 2014;75(1-2):189-195.
48. Yost CC, Denis MM, Lindemann S, et al. Activated polymorphonuclear leukocytes rapidly synthesize retinoic acid receptor-alpha: a mechanism for translational control of transcriptional events. *Journal of Experimental Medicine*. 2004;200(5):671-680.
49. Ludwig LS, Gazda HT, Eng JC, et al. Altered translation of GATA1 in Diamond-Blackfan anemia. *Nature Medicine*. 2014;20(7):748-753.
50. Tulpule A, Kelley JM, Lensch MW, et al. Pluripotent stem cell models of Shwachman-Diamond syndrome reveal a common mechanism for pancreatic and hematopoietic dysfunction. *Cell Stem Cell*. 2013;12(6):727-736.

SUPPLEMENTAL METHODS

Peripheral Blood Measurements

Peripheral blood was collected by submandibular bleeding in K2EDTA-coated microtainers (BD). Hematological parameters were analyzed using a Vet ABC counter (Scil Animal Care).

Flow Cytometry

Bone marrow cells were isolated as previously reported.[1] Red blood cells (RBC) from bone marrow and fetal liver were lysed with ACK lysing buffer (Lonza) before FACS staining. Peripheral blood cells were first stained for surface markers and next RBC-depleted using IOTest 3 Lysing Solution (Beckman Coulter). Bone marrow, blood and fetal liver cells were stained in PBS+0.5%FCS for 20 min on ice. To identify bone marrow lineage positivity (Lin+), cells were co-stained with biotin-labelled antibodies against Gr1 (RB6-8C5), Mac1 (M1/70), Ter119 (TER-119), CD3e (145-2C11), CD4 (GK1.5), CD8 (53-6.7) and B220 (RA3-6B2) (all from BD), followed by incubation with Pacific Orange-conjugated streptavidin (Life Technologies). For fetal liver analysis, anti-Mac1 was excluded from the lineage cocktail as this marker is expressed in fetal hematopoietic stem cells.[2] In addition to the lineage cocktail, the following antibodies were used to identify HSPCs: Pacific Blue anti-Sca1 (D7), AF700 or PE anti-CD48 (HM48-1), PE-Cy7 anti-CD150 (TC15-12F12.2), PE anti-CD34 (HM34) (all from Biolegend), APC or PE-CF594 anti-c-Kit (2B8) and APC-Cy7 anti-CD16/32 (2.4G2) (all from BD). To analyze differentiated cells, we used APC anti-Gr1 (RB6-8C5), PE-Cy7 anti-Mac1 (M1/70) (both from Biolegend) and eFluor450 anti-B220 (RA3-6B2, eBioscience). Erythroid subsets were identified by staining with PE anti-CD71 (C2, BD) and Ter119 (TER-119, Biolegend). Dead cells were excluded based on 7-AAD staining (Biolegend). Apoptotic cells were identified with APC annexin V (BD) according to the manufacturer's protocol. For cell cycle and p53 analysis, cells were stained for surface markers, then permeabilized using Cytofix/Cytoperm Fixation/Permeabilization Solution Kit (BD) following the manufacturer's recommendations and finally stained with PE anti-Ki67 (B56, BD) and 7-AAD (cell cycle analysis) or with AF647 anti-p53 (1C12, Cell Signaling Technology). For all FACS analysis, events were recorded using a BD LSR II Flow Cytometer and analyzed with FlowJo 7.6.5 software (Tree Star). Cells were sorted with a BD FACSAria III.

Bone Marrow Morphology

For morphological studies, cytospin preparations were obtained from 5x105 bone marrow cells per transplanted mouse and stained with May-Grünwald-Giemsa as previously reported.[3]

Quantitative PCR

Cells were sorted in TRIzol Reagent (Life Technologies) and RNA was extracted following the manufacturer's instructions, with addition of 25 µg linear polyacrylamide (Genelute LPA; Sigma Aldrich) as RNA carrier. Genomic DNA was eliminated by treatment with RQ1 RNase-free DNase (Promega). First strand cDNA was synthesized from poly(A)+-selected RNA using SuperScript III First-Strand Synthesis System (Life Technologies). Real-Time PCR reactions were prepared with Fast SYBR Green Master Mix (Life Technologies) using the primers listed in Online Supplementary Table S1 and run on a 7500 Fast Real-Time PCR System (Life Technologies).

SUPPLEMENTAL TABLES

Table S1. Oligonucleotide primers used in this study.

Application	Target	Allele	Primer ID	Sequence	Amplicon size (bp)
Genotyping	*Sbds*	Wild type	a	CCAGGGTCACGTTAATACAAACC	329
			b	TGAGTTTCAATCCTCAGCATCC	
		Floxed	a	CCAGGGTCACGTTAATACAAACC	450
			b	TGAGTTTCAATCCTCAGCATCC	
		Recombined	c	TAAAACAAAGCTGCGGTCAAGA	319
			d	ATCCTCAGCATCCCGAACAA	
	Cebpa	Wild type	e	GCTCTAAGACCCAGCAGGC	272
			f	CGGCTCCACCTCGTAGAAGTC	
		Cre	g	CGCTAAGGATGACTCTGGT	487
			h	GTCTCAAGGAGAAACCACCAC	
	Rosa26	Wild type	i	ACCTTTCTGGGAGTTCTCTGCTG	488
			j	GGAGCGGGAGAAATGGATATG	
		EYFP	i	ACCTTTCTGGGAGTTCTCTGCTG	200
			k	GCGAAGAGTTTGTCCTCAACC	
		Recombined	i	ACCTTTCTGGGAGTTCTCTGCTG	400
			l	GCTCCTCGCCCTTGCTCA	
Quantitative RT-PCR	*Gapdh*	N/A	m	AGGTCGGTGTGAACGGATTTG	123
			n	TGTAGACCATGTAGTTGAGGTCA	
	Sbds	N/A	o	GCGCTTCGAAATCGCCTG	167
			p	TCTGGTCGTCTGTCCCAAATG	

Table S2. Complete loss of *Sbds* in *Cebpa*-expressing cells is lethal during mouse development.

Crossing	Time of DNA isolation	Genotype	Expected frequency†	No. of pups
Sbds$^{f/+}$ *Cebpa*$^{cre/+}$ x *Sbds*$^{f/+}$ *Cebpa*$^{cre/+}$	P7	*Sbds*$^{+/+}$ *Cebpa*$^{+/+}$	1/12	7/59
P = 0.0018		*Sbds*$^{+/+}$ *Cebpa*$^{cre/+}$	1/6	18/59
11 crossings		*Sbds*$^{f/+}$ *Cebpa*$^{+/+}$	1/6	8/59
Average litter size = 5.36		*Sbds*$^{f/+}$ *Cebpa*$^{cre/+}$	1/3	23/59
		Sbds$^{f/f}$ *Cebpa*$^{+/+}$	1/12	3/59
		Sbds$^{f/f}$ *Cebpa*$^{cre/+}$	1/6	0/59
Sbds$^{f/f}$ *Cebpa*$^{+/+}$ x *Sbds*$^{f/+}$ *Cebpa*$^{cre/+}$	P7	*Sbds*$^{f/+}$ *Cebpa*$^{+/+}$	1/4	11/33
P = 0.0043		*Sbds*$^{f/+}$ *Cebpa*$^{cre/+}$	1/4	8/33
5 crossings		*Sbds*$^{f/f}$ *Cebpa*$^{+/+}$	1/4	14/33
Average litter size = 6.25		*Sbds*$^{f/f}$ *Cebpa*$^{cre/+}$	1/4	0/33
Sbds$^{f/+}$ *Cebpa*$^{cre/+}$ x *Sbds*$^{f/+}$ *Cebpa*$^{+/+}$	P7	*Sbds*$^{+/+}$ *Cebpa*$^{+/+}$	1/8	5/36
P = 0.1047		*Sbds*$^{+/+}$ *Cebpa*$^{cre/+}$	1/8	4/36
5 crossings		*Sbds*$^{f/+}$ *Cebpa*$^{+/+}$	1/4	9/36
Average litter size = 7.20		*Sbds*$^{f/+}$ *Cebpa*$^{cre/+}$	1/4	9/36
		Sbds$^{f/f}$ *Cebpa*$^{+/+}$	1/8	9/36
		Sbds$^{f/f}$ *Cebpa*$^{cre/+}$	1/8	0/36
Sbds$^{f/+}$ *Cebpa*$^{cre/+}$ x *Sbds*$^{f/+}$ *Cebpa*$^{cre/+}$	E14.5	*Sbds*$^{f/+}$ *Cebpa*$^{+/+}$	1/4	12/49
P = 0.018		*Sbds*$^{f/+}$ *Cebpa*$^{cre/+}$	1/4	9/49
5 crossings		*Sbds*$^{f/f}$ *Cebpa*$^{+/+}$	1/4	17/49
Average litter size = 9.80		*Sbds*$^{f/f}$ *Cebpa*$^{cre/+}$	1/4	11/49

Cumulative frequencies of litters obtained from intercrossing *Sbds*$^{f/+}$ *Cebpa*$^{cre/+}$ *R26*$^{YFP/+}$ mice. The genotype of the parents and the offspring is shown. The R26 genotype is omitted for simplicity. †*Cebpa*$^{cre/cre}$ mice are not viable due to the complete absence of *Cebpa* coding sequence in the Cre allele[4]. *P* values refer to Pearson's chi-squared test.

Table S3. Transcriptional signatures for translation and lineage progression in *Sbds*-deficient MC-MMs.

Data set	Enrichment	Size	ES	NES	NOM p-val	FDR q-val
Translation						
BILANGES_RAPAMYCIN_SENSITIVE_VIA_ TSC1_AND_TSC2	Mutants	72	0.698	1.611	<0.001	0.232
BILANGES_SERUM_RESPONSE_ TRANSLATION	Mutants	35	0.701	1.550	0.035	0.166
PENG_RAPAMYCIN_RESPONSE_DN	Mutants	243	0.613	1.511	<0.001	0.175
REACTOME_TRANSLATION	Mutants	140	0.788	1.477	<0.001	0.193
BILANGES_SERUM_AND_RAPAMYCIN_ SENSITIVE_GENES	Mutants	64	0.79	1.431	0.021	0.210
MENSSEN_MYC_TARGETS	Mutants	52	0.676	1.397	<0.001	0.245
REACTOME_SRP_DEPENDENT_ COTRANSLATIONAL_PROTEIN_TARGETIN G_TO_MEMBRANE	Mutants	102	0.826	1.391	0.021	0.248
REACTOME_ACTIVATION_OF_THE_MRNA _UPON_BINDING_OF_ THE_CAP_BINDING_COMPLEX_AND_EIFS _AND_ SUBSEQUENT_BINDING_TO_43S	Mutants	54	0.759	1.390	<0.001	0.246
Undifferentiated state						
BHATTACHARYA_EMBRYONIC_STEM_ CELL	Mutants	85	0.575	1.601	<0.001	0.203
JUBAN_TARGETS_OF_SPI1_AND_FLI1_DN	Mutants	90	0.582	1.572	<0.001	0.154
MUELLER_PLURINET	Mutants	295	0.535	1.539	<0.001	0.157
PARK_HSC_AND_MULTIPOTENT_ PROGENITORS	Mutants	50	0.504	1.480	0.086	0.192
IVANOVA_HEMATOPOIESIS_ INTERMEDIATE_PROGENITOR	Mutants	147	0.637	1.469	<0.001	0.193
BYSTRYKH_HEMATOPOIESIS_STEM_CELL _AND_BRAIN_QTL_CIS	Mutants	64	0.524	1.403	<0.001	0.240
SCHURINGA_STAT5A_TARGETS_DN	Mutants	15	0.478	1.397	0.026	0.246
RAMALHO_STEMNESS_UP	Mutants	207	0.531	1.386	<0.001	0.249
XU_RESPONSE_TO_TRETINOIN_AND_ NSC682994_DN	Mutants	15	0.750	1.383	<0.001	0.246

Table S3. Transcriptional signatures for translation and lineage progression in *Sbds*-deficient MC-MMs. *(Continued)*

Data set	Enrichment	Size	ES	NES	NOM p-val	FDR q-val
Myeloid differentiation						
LIAN_NEUTROPHIL_GRANULE_ CONSTITUENTS	Controls	24	-0.556	-1.719	<0.001	0.062
JAATINEN_HEMATOPOIETIC_STEM_CELL_ DN	Controls	214	-0.561	-1.718	<0.001	0.061
IVANOVA_HEMATOPOIESIS_MATURE_ CELL	Controls	294	-0.582	-1.644	<0.001	0.082
PID_AMB2_NEUTROPHILS_PATHWAY	Controls	40	-0.532	-1.612	<0.001	0.108
REACTOME_DEGRADATION_OF_THE_ EXTRACELLULAR_MATRIX	Controls	27	-0.529	-1.601	<0.001	0.110
BROWN_MYELOID_CELL_DEVELOPMENT _UP	Controls	168	-0.665	-1.590	<0.001	0.122
TAVOR_CEBPA_TARGETS_UP	Controls	49	-0.503	-1.580	<0.001	0.123
PID_INTEGRIN_A9B1_PATHWAY	Controls	25	-0.575	-1.567	<0.001	0.137
KEGG_HEMATOPOIETIC_CELL_LINEAGE	Controls	80	-0.460	-1.557	<0.001	0.144
SA_MMP_CYTOKINE_CONNECTION	Controls	15	-0.629	-1.542	<0.001	0.160
XU_RESPONSE_TO_TRETINOIN_UP	Controls	15	-0.605	-1.478	<0.001	0.188
NAKAJIMA_EOSINOPHIL	Controls	27	-0.640	-1.477	0.027	0.189
BIOCARTA_CCR3_PATHWAY	Controls	23	-0.670	-1.467	<0.001	0.193
ZHOU_INFLAMMATORY_RESPONSE_LPS_ UP	Controls	373	-0.380	-1.443	<0.001	0.224
KAMIKUBO_MYELOID_CEBPA_NETWORK	Controls	80	-0.457	-1.417	<0.001	0.249

Curated data sets significantly enriched in *Sbds f/f* (mutants) or *+/+* (controls) are shown (FDR<0.25, GSEA comparison to the C2 MSigDB collection). ES: enrichment score. NES: normalized enrichment score. NOM p-val: nominal p-value. FDR q-val: False Discovery Rate q-value.

Table S4. Enrichment of GO-terms for ribosome biogenesis in *Sbds*-deficient MC-MMs.

Data set	Enrichment	Size	ES	NES	NOM p-val	FDR q-val
REGULATION_OF_TRANSLATIONAL_ INITIATION	Mutants	28	0.681	1.520	<0.001	0.183
TRANSCRIPTION_FROM_RNA_ POLYMERASE_III_PROMOTER	Mutants	17	0.703	1.523	0.032	0.187
RIBOSOME_BIOGENESIS_AND_ASSEMBLY	Mutants	17	0.859	1.525	<0.001	0.201
NUCLEOLUS	Mutants	119	0.700	1.551	<0.001	0.207
RIBONUCLEOPROTEIN_COMPLEX	Mutants	141	0.672	1.589	<0.001	0.213
RIBONUCLEOPROTEIN_COMPLEX_ BIOGENESIS_AND_ASSEMBLY	Mutants	83	0.664	1.552	<0.001	0.217
PROTEIN_RNA_COMPLEX_ASSEMBLY	Mutants	64	0.601	1.492	<0.001	0.217
RRNA_METABOLIC_PROCESS	Mutants	15	0.845	1.589	<0.001	0.231
TRANSLATIONAL_INITIATION	Mutants	36	0.640	1.455	<0.001	0.237
NUCLEOLAR_PART	Mutants	17	0.783	1.467	<0.001	0.241
RIBOSOME	Mutants	38	0.825	1.435	<0.001	0.242

GO gene sets related to ribosome maturation and translation are significantly enriched in *Sbds f/f* (mutants) (FDR<0.25, GSEA comparison to the C5 MSigDB collection). ES: enrichment score. NES: normalized enrichment score. NOM p-val: nominal p-value. FDR q-val: False Discovery Rate q-value.

SUPPLEMENTAL FIGURES

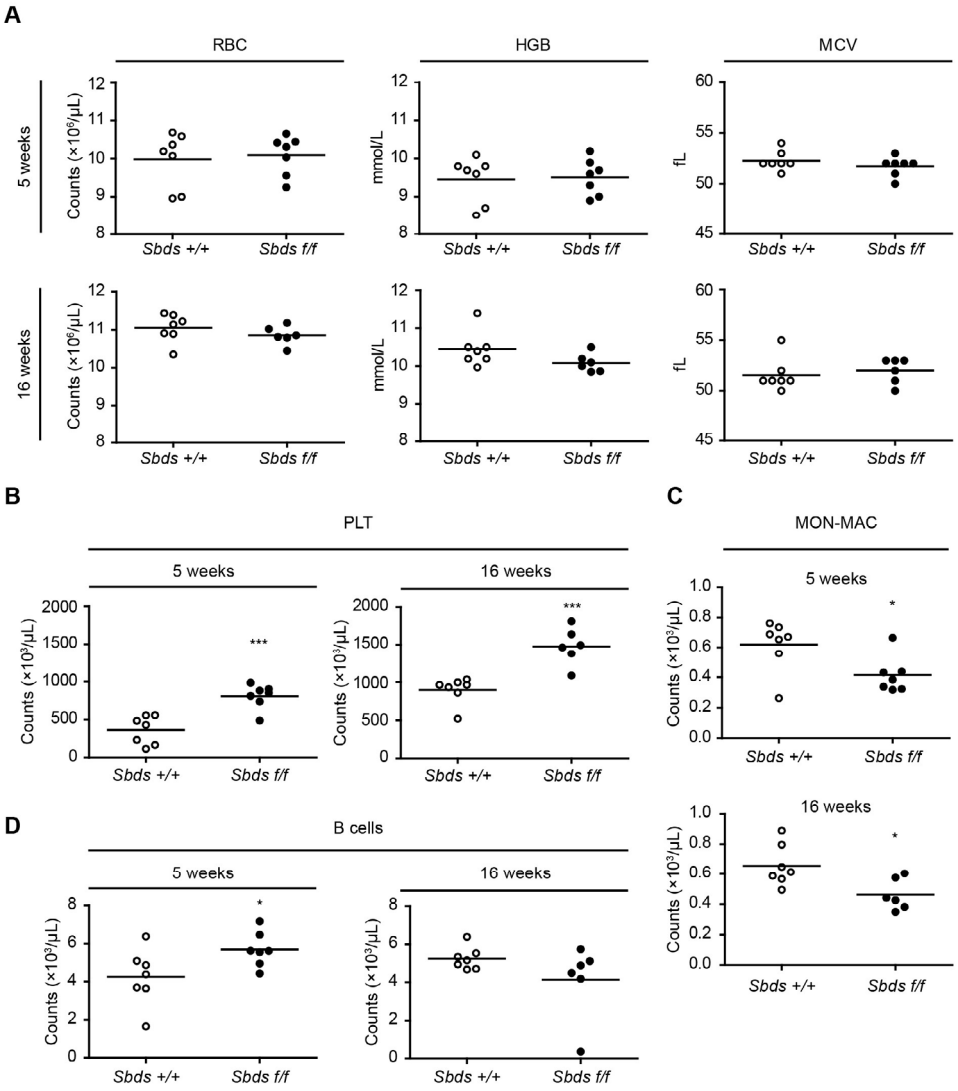

Figure S1. Effects of *Sbds* deletion from *Cebpa*-expressing hematopoietic cells on peripheral blood cell numbers. (A) Normal levels of red blood cells counts (RBC), hemoglobin (HGB) and mean corpuscular volume (MCV) in mice injected with *Sbds +/+* or *f/f* cells. (B) Platelet counts (PLT) in the peripheral blood. (C) Numbers of B220^{+} lymphocytes (B cells) in the peripheral blood. Each circle represents one recipient mouse. Data is presented at 5 and 16 weeks after transplantation. **P* < 0.05. ****P* < 0.001.

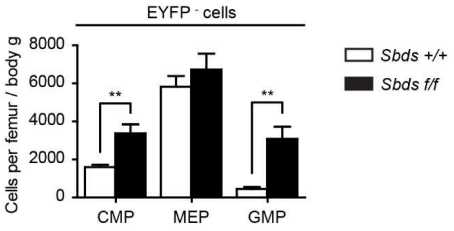

Figure S2. Expansion of EYFP- progenitors in *Sbds f/f* recipients. Absolute counts of EYFP$^-$ progenitors in transplanted mice. Data is mean ± s.e.m. $^{**}P < 0.01$.

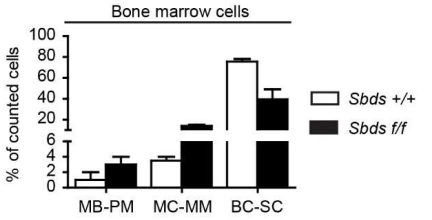

Figure S3. Increased frequency of MC-MMs and loss of mature neutrophils in *Sbds f/f* recipients. Evaluation of myeloid differentiation stages in bone marrow cytospins from *Sbds f/f* and *+/+* recipients (*n* = 2). MB-PM: myeloblasts-promyelocytes. MC-MM: myelocytes-metamyelocytes. BC-SC: band cells-segmented cells. Data is mean ± s.e.m.

SUPPLEMENTAL REFERENCES

1. Raaijmakers MH, Mukherjee S, Guo S, et al. Bone progenitor dysfunction induces myelodysplasia and secondary leukaemia. *Nature*. 2010;464(7290):852-857.
2. Morrison SJ, Hemmati HD, Wandycz AM, Weissman IL. The Purification and Characterization of Fetal Liver Hematopoietic Stem-Cells. *Proc Natl Acad Sci U S A*. 1995;92(22):10302-10306.
3. Nishimoto N, Arai S, Ichikawa M, et al. Loss of AML1/Runx1 accelerates the development of MLL-ENL leukemia through down-regulation of p19(ARF). *Blood*. 2011;118(9):2541-2550.
4. Wölfler A, Oorschot AADV, Haanstra JR, et al. Lineage-instructive function of C/EBP alpha in multipotent hematopoietic cells and early thymic progenitors. *Blood*. 2010;116(20):4116-4125.

Chapter 3

Mesenchymal inflammation induces genotoxic stress in hematopoietic stem and progenitor cells in leukemia predisposition syndromes

Noemi A. Zambetti,[1,7] Zhen Ping,[1,7] Si Chen,[1,7] Keane J. G. Kenswil,[1] Maria A. Mylona, [1] Mathijs A. Sanders,[1] Remco M. Hoogenboezem,[1] Eric M. J. Bindels,[1] Maria N. Adisty, [1] Cindy S. van der Leije,[2] Theresia M. Westers,[3] Eline M. P. Cremers,[3] Johannes P. T. M. van Leeuwen,[2] Bram C. J. van der Eerden,[2] Ivo P. Touw,1 Taco W. Kuijpers,[4] Roland Kanaar,[5] Arjan A. van de Loosdrecht,[3] Thomas Vog[1,6] and Marc H. G. P. Raaijmakers.[1]

[1]Department of Hematology, Erasmus MC Cancer Institute, Rotterdam 3015CN, The Netherlands

[2]Department of Internal Medicine, Erasmus MC Cancer Institute, Rotterdam 3015CN, The Netherlands

[3]Department of Hematology, VU University Medical Center, Cancer Center Amsterdam, Amsterdam 1081HV, The Netherlands

[4]Department of Pediatric Hematology, Immunology and Infectious Diseases, Emma Children's Hospital, Academic Medical Centre (AMC), University of Amsterdam (UvA), Amsterdam 1105AZ, The Netherlands

[5]Department of Genetics, Cancer Genomics Center, Department of Radiation Oncology, Erasmus MC Cancer Institute, Rotterdam 3015CN, The Netherlands

[6]Institute of Immunology, University of Münster, Münster 48149, Germany

[7]Co-first author

Manuscript submitted

SUMMARY

Mesenchymal niche cells may drive tissue failure and malignant transformation in the hematopoietic system but the molecular mechanisms and their relevance to human disease remain poorly defined. Here, we show that perturbation of mesenchymal cells in a mouse model of the preleukemic disorder Shwachman-Diamond syndrome induces mitochondrial dysfunction, oxidative stress and activation of DNA damage responses in hematopoietic stem and progenitor cells. Massive parallel RNA sequencing of highly purified mesenchymal cells in the mouse model and a range of human preleukemic syndromes identified S100A8/9-TLR4 inflammatory signaling as a common driving mechanism of genotoxic stress, which could be attenuated by TLR4 blockade. S100A8/9 expression in mesenchymal cells predicted outcome in myelodysplastic syndromes, the principal human preleukemic condition, independent of known prognostic variables. Collectively, findings reveal a concept of mesenchymal niche-induced genotoxic stress in heterotypic stem and progenitor cells through inflammatory signaling as an actionable determinant of disease outcome in human preleukemia.

GRAPHICAL ABSTRACT

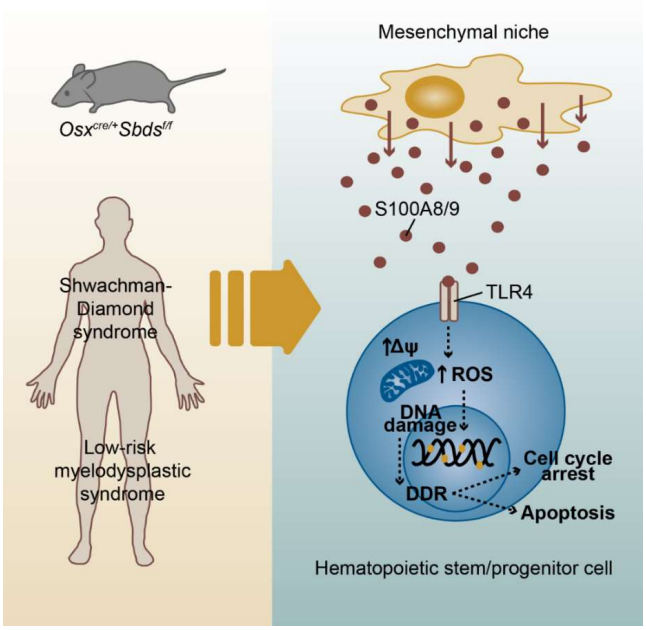

INTRODUCTION

Genotoxic stress results in the accumulation of DNA lesions in hematopoietic stem and progenitor cells (HSPCs) over the lifespan of an organism, contributing to tissue failure and malignant transformation.[1,2] The pathophysiological insults underlying genomic stress in HSPCs, however, remain incompletely understood. Perturbed signaling from their surrounding microenvironment may be implicated, but this has not been experimentally defined.

Components of the bone marrow microenvironment have emerged as key regulators of normal and malignant hematopoiesis.[3-7] We, and others, have shown that primary alterations of the mesenchymal niche can induce myelodysplasia and promote the emergence of acute myeloid leukemia (AML) with cytogenetic abnormalities in HSPCs,[8,9] thus introducing a concept of niche-driven oncogenesis in the hematopoietic system.

To provide insights into the mechanisms that underlie this concept, as well as their relevance for human disease, we modeled the human leukemia predisposition disorder Shwachman-Diamond syndrome (SDS), caused by constitutive homozygous or compound heterozygous loss of function mutations in the *SBDS* gene, required for ribosome biogenesis.[10,11] SDS is characterized by skeletal defects in conjunction with a striking propensity to develop myelodysplastic syndrome (MDS) and AML at a young age, with a cumulative probability of >30% at the age of 30 years and a median onset at 18 years.[12,13] Hematopoietic cell intrinsic loss of *Sbds* does not result in MDS or leukemia,[14,15] supporting the notion that cell-extrinsic factors contribute to malignant transformation. Deletion of *Sbds* from mesenchymal cells in the bone marrow induced apoptosis in HSPCs and myelodysplasia, but the molecular mechanisms driving these observations and their relevance for human disease remained to be defined.[8]

Here, we identify the endogenous damage-associated molecular pattern (DAMP) molecules S100A8 and S100A9, secreted from mesenchymal niche cells, as drivers of mitochondrial dysfunction, oxidative stress and DDR activation in HSPCs, with clinical relevance to the pathogenesis and prognosis of human bone marrow failure and leukemia predisposition syndromes.

RESULTS

Deletion of *Sbds* from mesenchymal progenitor cells (MPCs) recapitulates skeletal abnormalities of human SDS

SDS is characterized by bone abnormalities including low-turnover osteoporosis with reduced trabecular bone volume, low numbers of osteoblasts, and reduced amount of osteoid, leading to

increased risk of fractures.[16] The cellular subsets driving these abnormalities and the underlying molecular mechanisms have remained largely undefined. We have previously shown that Cre-mediated deletion of *Sbds* from osterix^{+} MPCs (*Sbds*$^{f/f}$ *Osx*$^{cre/+}$ mice, hereafter OCS$^{f/f}$ or mutants) disrupts the architecture of the marrow and cortical bone.[8] Here, we first sought to better define the skeletal defects in these mice and their relevance to human disease.

OCS$^{f/f}$ mice presented growth retardation and reduced femur length compared to control *Sbds*$^{f/+}$ *Osx*$^{cre/+}$ (OCS$^{f/+}$) mice (**Figure 1A** and **1B**) as observed in human patients.[17,18] The runted phenotype was associated with a significantly limited lifespan, with lethality observed after the age of 4 weeks. Analyses were therefore performed in three week-old mice. The femur trabecular area was profoundly reduced in OCS$^{f/f}$ mice, with decreased bone volume, low number of trabeculae, increased trabecular spacing and reduced numbers of osteoblasts compared to controls (**Figure 1C**-**1G**, and **1I**). The cortical bone of OCS mutants was also affected, as indicated by low bone mineral density values (**Figure 1C**-**1D** and **1H**), attenuating the mechanical properties of the bone, which was found less resistant to fracture in three-point bending tests (**Figure 1J**). A tendency for reduced stiffness in the long bones was also observed (**Figure 1K**). Taken together, the structural and mechanical defects indicate that *Sbds* deficiency in MPCs causes osteoporosis with a propensity for fracturing, in line with observations in SDS patients.[16,18,19] Impaired osteogenesis did not reflect a contraction of the bone progenitor cell pool as shown by frequency of CFU-F and Osx::GFP^{+} cells (**Figure S1A** and **S1B**), but rather impairment of terminal osteogenic differentiation as suggested by transcriptional profiling of prospectively isolated osterix-expressing (GFP^{+}) cells (**Figure S1C**). Transcriptional data confirmed deregulated expression of genes related to ribosomal biogenesis and translation (**Figure S1D** and **S1E**), in line with the established role of *Sbds* in ribosome biogenesis. Collectively, this data supports a view in which bone abnormalities in SDS are caused by deficiency of *Sbds* in MPCs, which attenuates terminal differentiation towards matrix-depositing osteoblastic cells with a compensatory increase in the most primitive mesenchymal compartment.

Sbds deficiency in the hematopoietic niche induces mitochondrial dysfunction, oxidative stress and activation of the DNA damage response in HSPCs

Having established that the OCS mice represent a *bona fide* model for bone abnormalities in human disease, we next investigated the hematopoietic consequences of these environmental alterations. HSPC number was unaltered in OCS mice (**Figure S2A**-**S2C**) and HSPCs displayed global preservation of their transcriptional landscape after exposure to the *Sbds*-deficient environment (**Figure S2D**-**S2F**).

Transcriptional network analysis, however, revealed significant overlap with signatures previously

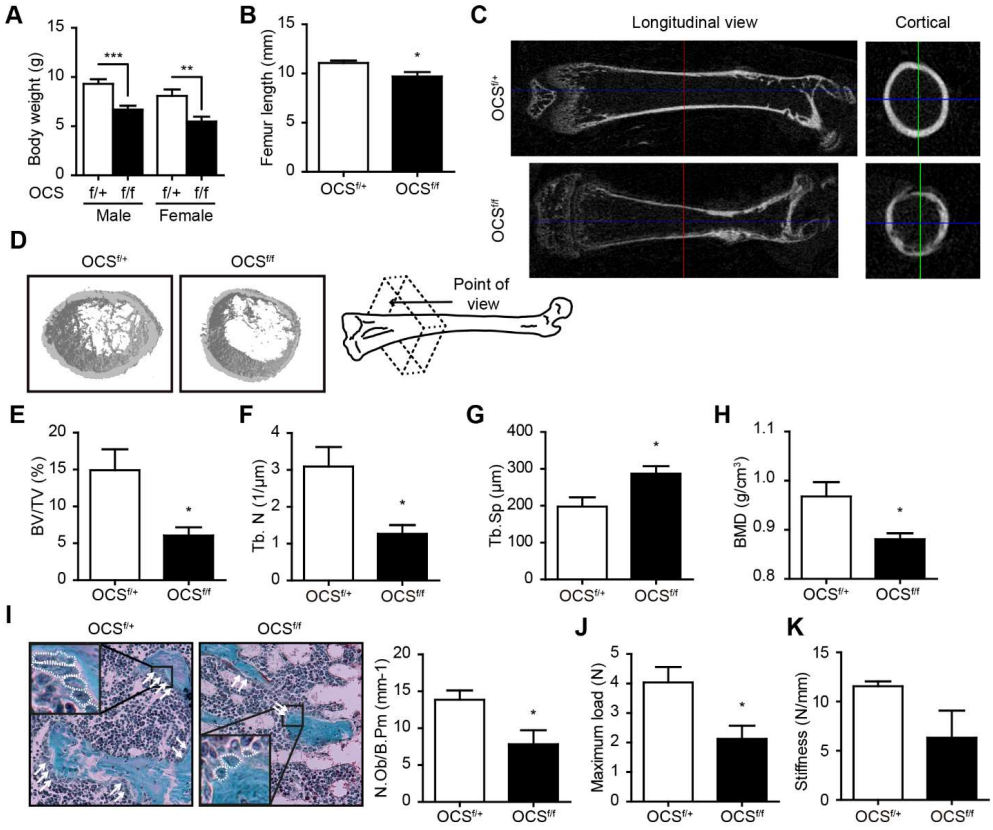

Figure 1. Deletion of *Sbds* in MPCs recapitulates skeletal defects in human SDS. (A-B) Impaired growth in OCS$^{f/f}$ mice: (A) body weight (n = 9) and (B) femur length (n = 5). (C-H) Femur µCT analysis of OCS$^{f/+}$ (n = 5) and OCS$^{f/f}$ (n = 4) mice. (C) Representative 2D-images. Left: longitudinal view. Right: cortical bone. (D) 3D-image. (E) Bone volume per tissue volume (BV/TV). (F) Trabecular number (Tb. N). (G) Trabecular spacing (Tb. Sp). (H) Cortical bone mineral density (BMD). (I) Goldner osteoblast staining (OCS$^{f/+}$, n = 6; OCS$^{f/f}$, n = 8). Left: representative images (arrows: osteoblasts; with white dashed line in the magnified region). Right: number of osteoblasts per bone perimeter (N.Ob/B.Pm). (J-K) 3-point bending test indicating (J) reduced resistant to fracture and (K) increased stiffness of OCS$^{f/f}$ bone (OCS$^{f/+}$, n = 5; OCS$^{f/f}$, n = 4). *P<0.05. **P< 0.01. ***P<0.001. Data are mean ± SEM. See also Figure S1.

defined as predicting leukemic evolution of human CD34^{+} cells,[20] including pathways signaling mitochondrial abnormalities (**Figure 2A**; **Table S1**). Mitochondrial dysfunction was confirmed by measuring the mitochondrial membrane potential (Δψ), indicating hyperpolarization of the

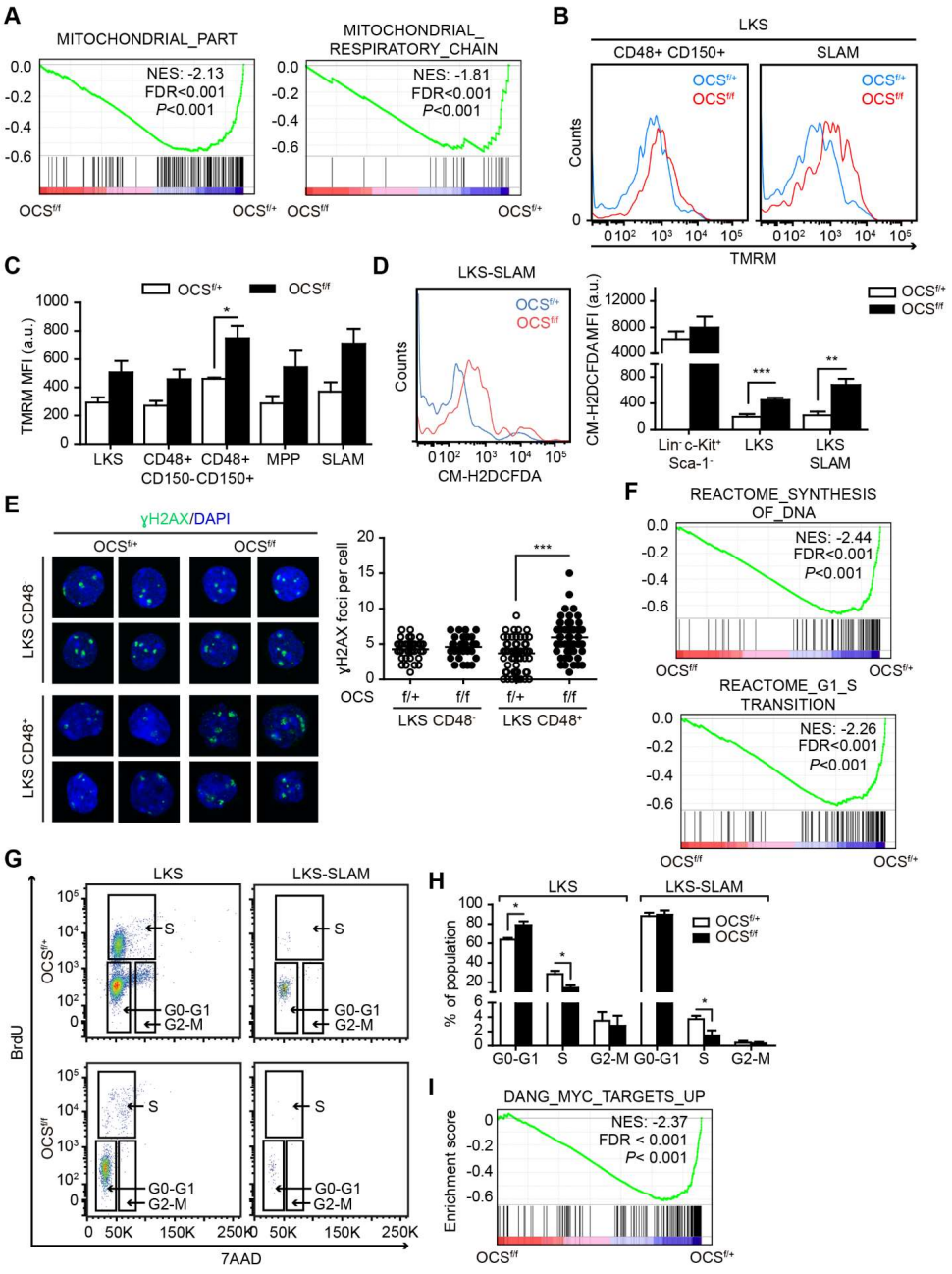
A
MITOCHONDRIAL_PART
NES: -2.13
FDR<0.001
P<0.001
MITOCHONDRIAL_
RESPIRATORY_CHAIN
NES: -1.81
FDR<0.001
P<0.001
OCSf/f
OCSf/+
B
LKS
CD48+ CD150+
SLAM
Counts
TMRM
C
TMRM MFI (a.u.)
LKS
CD48+ CD150-
CD48+ CD150+
MPP
SLAM
D
LKS-SLAM
CM-H2DCFDA
CM-H2DCFDA MFI (a.u.)
Lin- c-Kit+ Sca-1-
E
γH2AX/DAPI
LKS CD48-
LKS CD48+
γH2AX foci per cell
OCS
F
REACTOME_SYNTHESIS
OF_DNA
NES: -2.44
FDR<0.001
P<0.001
REACTOME_G1_S
TRANSITION
NES: -2.26
FDR<0.001
P<0.001
G
LKS
LKS-SLAM
BrdU
7AAD
G0-G1
S
G2-M
H
% of population
I
DANG_MYC_TARGETS_UP
NES: -2.37
FDR < 0.001
P< 0.001
Enrichment score

mitochondria (**Figure 2B** and **2C**). Mitochondrial hyperpolarization can result in reverse electron transfer, leading to the production of superoxide radicals, which can be further converted into other reactive oxygen species (ROS).[21] In line with this, a marked increase in intracellular ROS levels was found in OCS mutant HSPCs (**Figure 2D**). ROS can undermine the genomic integrity of HSPCs by inducing DNA damage,[22-24] to which normal HSPCs react by activating the DNA damage response (DDR) and repair pathways.[1] Indeed, $CD48^+$ LKS cells from $OCS^{f/f}$ mice displayed increased foci of Ser139-phosphorylated H2AX histone (γH2AX), which form at the sites of DNA damage (**Figure 2E**). Congruent with genotoxic effects of the mutant microenvironment, HSPCs displayed transcriptional modulation of DDR and DNA repair pathways (**Table S2**), including nucleotide excision repair programs, associated with ROS-induced lesions[25] and signatures related to the master regulator of DDR and cell checkpoint activation ataxia telangiectasia and Rad3-related (ATR). Activation of the G1-S cell cycle checkpoint, resulting in cell cycle arrest, was further demonstrated by depletion of G1-S transcriptional signatures (**Figure 2F; Table S1**), *in vivo* BrdU labeling (**Figure 2G** and **2H**) and downregulation of the Myc pathway, a critical regulator for this restriction point and the coordination of S–G2–M progression (**Figure 2I**; **Table S3**). Apoptosis of mutant HSPCs, as an alternative outcome of checkpoint activation, was earlier demonstrated.[8] Together, the data indicate that the *Sbds*-deficient environment induces mitochondrial dysfunction, oxidative stress, DNA damage and genotoxic stress in HSPCs leading to activation of DDR pathways and G1-S checkpoint activation, reminiscent of a model in which mitochondrial dysfunction underlies an escalating cycle of increased ROS and genotoxic damage.[26]

Short term exposure to the genotoxic environment did not attenuate HSPC function in DNA repair proficient cells, as demonstrated by competitive transplantation experiments (**Figure S3A**-**S3C**), suggesting efficient DNA-repair or elimination of functionally impaired HSPCs by DDR-driven apoptosis and cell cycle arrest. Congruent with this notion, alkaline comet assays on sorted HSPCs failed to demonstrate structural DNA damage (**Figure S3D** and **S3E**).

Figure 2. *Sbds*-deficient mesenchymal cells induce genotoxic stress in HSPCs. (A) Transcriptional network analysis indicating mitochondrial dysregulation in mutant HSPCs. NES: Normalized Enrichment Score. (B-C) Increased mitochondrial potential (TMRM) in HSPCs: (B) representative plots; (C) mean fluorescence intensity (MFI) (n = 3). (D) ROS quantification by CM-H2DCFDA ($OCS^{f/+}$, n = 6; $OCS^{f/f}$, n = 7). (E) γH2AX foci quantification in HSPCs from mutants (n = 2; pooled data). (F-I) Activation of DNA damage response in mutant HSPCs. (F) Transcriptional repression of G1-S checkpoint progression. (G, H) *In vivo* BrdU staining confirming impaired S-phase transition (n = 4). (I) Downregulation of Myc signaling. GSEA data shown is from $CD48^-$ LKS cells †††FDR<0.001. **P*<0.05. ***P*<0.01. ****P*<0.001. Data in bar graphs are mean± SEM. See also Figure S2, S3 and Table S1, S2 and S3.

Activation of the p53 pathway drives bone abnormalities but not genotoxic stress in OCS mice

Next, we sought to define the molecular programs underlying the bone and hematopoietic alterations in OCS mice. A proposed common molecular mechanism for the pathogenesis of ribosomopathies involves activation of the p53 tumor suppressor pathway.[27] The p53 protein was overexpressed in GFP$^+$ MPCs in OCS mutants, with activation of downstream transcriptional pathways and upregulation of canonical targets (**Figure 3A**-**3C**).

To assess the pathophysiological role of p53 activation in MPCs, we intercrossed OCS with *Trp53*-floxed mice,[28] generating a double conditional knock-out model where the deletion of p53 is localized in the *Sbds*-deleted stromal compartment (*Sbds*$^{f/f}$ *Trp53*$^{f/f}$ *Osx*$^{cre/+}$ mice; hence OCS$^{f/f}$ p53$^{\Delta}$) (**Figure 3D**). Genetic recombination of the *Trp53* locus was detected only in bone cells-containing samples, demonstrating the tissue specificity of p53 deletion in this model (**Figure 3E**). Genetic deletion of p53 from *Sbds*-deficient MPCs rescued the osteoporotic phenotype (**Figure 3F-3J**), but not cortical bone mineralization, growth, or hematopoietic parameters (**Figure 3K** and data not shown), implicating p53-independent molecular mechanisms in the induction of cellular stress in HSPCs.

Identification of the damage-associated molecular pattern genes *S100A8* and *S100A9* as candidate niche factors driving genotoxic stress in human leukemia predisposition syndromes

To identify human disease-relevant niche factors driving genomic stress in HSPCs, we compared the transcriptomes of GFP$^+$ MPCs from OCS mice to those from prospectively FACS-isolated mesenchymal CD271$^+$ niche cells[29] from human SDS patients (**Figure 4A**; **Table S4**). The mesenchymal nature of CD271$^+$ cells was confirmed by CFU-F capacity and differential expression of mesenchymal, osteolineage and HSPC-regulatory genes (**chapter 4**).

RNA sequencing showed the presence of *SBDS* mutations (**Figure 4B**; **Figure S4**; **Table S4**) associated with reduced *SBDS* expression (**Figure 4C**), confirming molecular aspects of SDS in previous studies.[11,30] Identical transcriptional signatures of disrupted ribosome biogenesis and translation were found in human niche cells (**Figure 4D**) and in GFP$^+$ cells from OCS mice (**Figure S1E**), confirming faithful recapitulation of human molecular disease characteristics in the mouse model. Forty genes were differentially expressed both in the mouse model and human SDS, 25 of which were overexpressed, with a remarkable abundance of genes encoding proteins implicated in inflammation and innate immunity (**Figure 4E**).

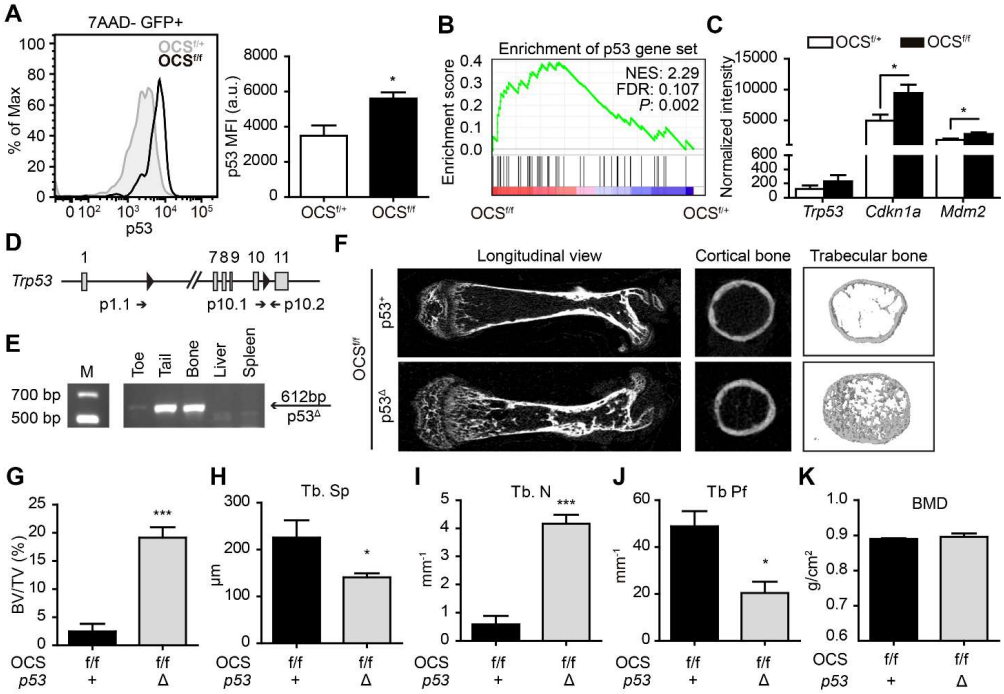

Figure 3. Activation of p53 in MPCs drives skeletal abnormalities in OCS mutants. (A) p53 protein (FACS) accumulates in GFP$^+$ cells from OCS$^{f/f}$ mice (n = 3). (B-C) Activation of p53 in mutant GFP$^+$ cells as demonstrated by (B) enrichment of a p53 GSEA signature and (C) overexpression of canonical p53 targets (n = 3). (D) Schematic representation of the p53 floxed allele with indication of primers used to assess genotypes (p10.1-p10.2) and genomic deletion (p1.1-p10.2). (E) Specific deletion of p53 in bone-containing tissue in OCS$^{f/f}$ p53$^{\Delta}$ mice (genomic PCR). (F-J) µCT analysis indicating normalization of bone mass in OCS$^{f/f}$ mice upon genetic deletion of p53 (p53$^+$, n = 3; p53$^{\Delta}$, n = 5). Tb. Pf , Trabecular bone pattern factor. (K) Bone mineral density in OCS$^{f/f}$ mice is not rescued by p53 deletion. MFI: mean fluorescence intensity. *P < 0.05. ***P <0.001. Data are mean ± SEM.

To further delineate candidate genes driving genomic stress and leukemic evolution from this gene set, we performed whole transcriptome sequencing of CD271$^+$ cells in two related human bone marrow failure and leukemia predisposition disorders: (1) low-risk MDS, the principal human preleukemic disorder in which cell cycle exit (senescence), accumulation of ROS, DNA damage and apoptosis have been described,[31-33] reminiscent of HSPC phenotypes in OCS mice, and (2) DBA, like SDS, a ribosomopathy characterized by bone marrow failure, but with a much lower propensity to evolve into AML (<1% with longer latency than observed in SDS and MDS)[34] (**Table S4**). We reasoned that genes specifically overexpressed in mesenchymal niche cells from

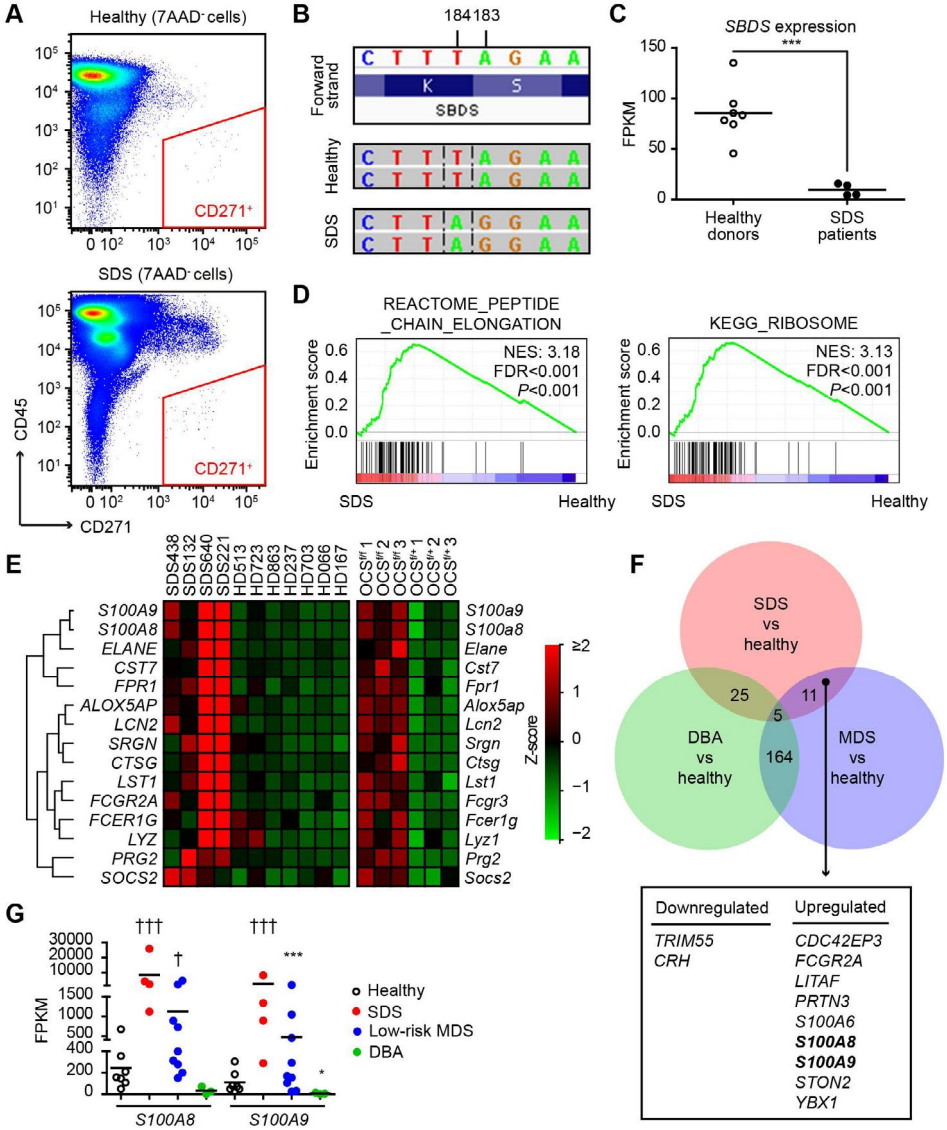
A
Healthy (7AAD- cells)
CD271+
SDS (7AAD- cells)
CD45
CD271
B
184183
Forward strand
K
S
SBDS
Healthy
SDS
C
SBDS expression
***
FPKM
Healthy donors
SDS patients
D
REACTOME_PEPTIDE _CHAIN_ELONGATION
NES: 3.18
FDR<0.001
P<0.001
KEGG_RIBOSOME
NES: 3.13
FDR<0.001
P<0.001
Enrichment score
SDS
Healthy
E
SDS438
SDS132
SDS640
SDS221
HD513
HD723
HD863
HD237
HD703
HD066
HD167
OCS#1
OCS#2
OCS#3
OCS#+1
OCS#+2
OCS#+3
S100A9
S100A8
ELANE
CST7
FPR1
ALOX5AP
LCN2
SRGN
CTSG
LST1
FCGR2A
FCER1G
LYZ
PRG2
SOCS2
S100a9
S100a8
Elane
Cst7
Fpr1
Alox5ap
Lcn2
Srgn
Ctsg
Lst1
Fcgr3
Fcer1g
Lyz1
Prg2
Socs2
Z-score
F
SDS vs healthy
DBA vs healthy
MDS vs healthy
25
11
5
164
Downregulated
TRIM55
CRH
Upregulated
CDC42EP3
FCGR2A
LITAF
PRTN3
S100A6
S100A8
S100A9
STON2
YBX1
G
FPKM
Healthy
SDS
Low-risk MDS
DBA
S100A8
S100A9

disorders with as strong propensity for leukemic evolution (SDS and MDS) might represent strong candidate drivers of genotoxic stress. Eleven such genes were found (**Figure 4F**), among which the damage-associated molecular pattern (DAMPs) *S100A8* and *S100A9*, significantly (P<0.05) differentially expressed in GFP$^+$ cells from OCS mutant mice (**Figure 4E**-**4G**).

S100A8/9 induces genotoxic stress in murine and human HSPCs

S100A8 and *S100A9* belong to a subclass of proinflammatory molecules referred to as damage-associated molecular pattern (DAMP) or alarmins. DAMPs are endogenous danger signals that are passively released or actively secreted in the microenvironment after cell death, damage or stress and bind pattern recognition receptors (PRR) to regulate inflammation and tissue repair.[35]

S100A8 and S100A9 proteins were overexpressed in mouse *Sbds*-deficient MPCs (**Figure 5A** and **5B**) and increased plasma concentration of S100A8/9 indicated secretion of the heterodimer (**Figure 5C**). Its canonical receptor TLR4[36] is expressed in murine HSPCs (**Figure S2G**) and the canonical downstream signaling NF-κB and MAPK pathways were activated in HSPCs from OCS$^{f/f}$ mice (**Figure S2H**). Exposure of HSPCs (LKS) cells to recombinant murine S100A8/9 resulted in a replication-independent increase in DNA damage (number of γH2AX foci) (**Figure 5D** and **5E**) and apoptosis (**Figure 5F**), associated with activation of TLR signaling (**Figure 5G**; **Table S5**), recapitulating the *in vivo* HSPC phenotype.[8] *In vivo*, blockage of TLR4 by neutralizing antibodies resulted in a reduction of γH2AX foci in LKS cells (**Figure 5H**). Translating these findings to human disease, exposure of human cord blood CD34$^+$ HSPCs to human recombinant S100A8/9 at clinically relevant concentrations[37] (Supplemental Experimental Procedures) resulted in DNA damage (increased γH2AX foci), apoptosis and impaired HSPC function (CFU-C) (**Figure S5**).

Figure 4. Identification of *S100A8* and *S100A9* as candidate drivers of genotoxic stress in leukemia predisposition syndromes. (A) Representative mesenchymal CD271$^+$ FACS gating. (B) Pathognomonic 183-184 TA>CT mutation in niche cells from a representative SDS patient (IGV plot). (C) Reduced *SBDS* expression in SDS niche cells. (D) Disruption of ribosome biogenesis and translation in SDS CD271$^+$ cells (GSEA). (E) Inflammation-related transcripts are upregulated in niche cells from SDS patients and OCS$^{f/f}$ mice. (F) Significantly differentially expressed genes in SDS (n = 4), MDS (n = 9) and DBA (n = 3) in comparison to normal CD271$^+$ cells. (G) Expression of *S100A8* and *S100A9* in mesenchymal cells from SDS, low-risk MDS, and DBA patients. *P<0.05. ***P<0.001. †††FDR-adjusted P<0.001. See also Figure S1, S4 and Table S4.

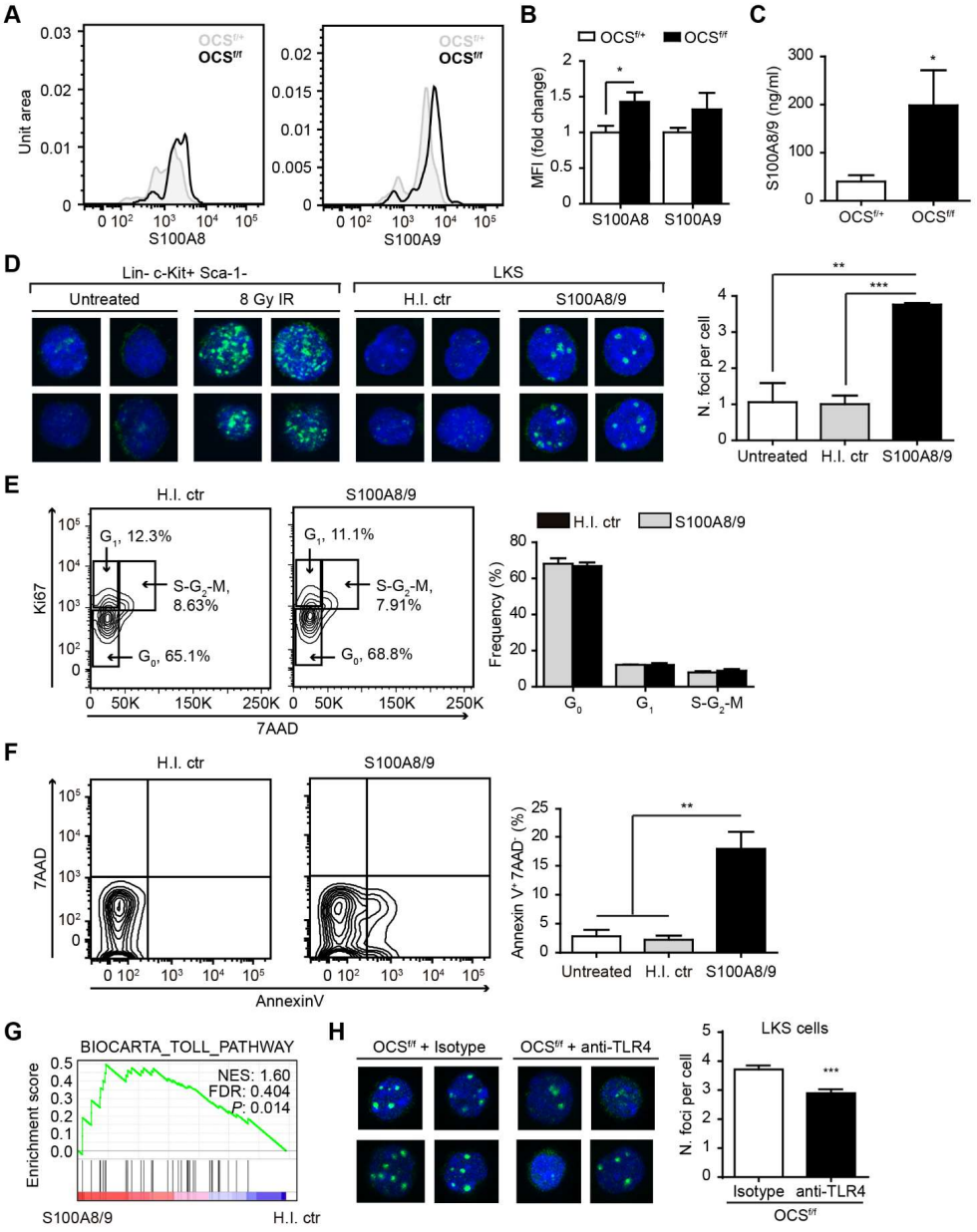
A
Unit area
OCS f/+
OCS f/f
S100A8
S100A9
B
OCS f/+
OCS f/f
MFI (fold change)
S100A8
S100A9
C
S100A8/9 (ng/ml)
OCS f/+
OCS f/f
D
Lin- c-Kit+ Sca-1-
LKS
Untreated
8 Gy IR
H.I. ctr
S100A8/9
N. foci per cell
Untreated
H.I. ctr
S100A8/9
E
H.I. ctr
S100A8/9
Ki67
G1, 12.3%
S-G2-M, 8.63%
G0, 65.1%
G1, 11.1%
S-G2-M, 7.91%
G0, 68.8%
7AAD
Frequency (%)
G0
G1
S-G2-M
F
H.I. ctr
S100A8/9
7AAD
AnnexinV
Annexin V+ 7AAD- (%)
Untreated
H.I. ctr
S100A8/9
G
BIOCARTA_TOLL_PATHWAY
NES: 1.60
FDR: 0.404
P: 0.014
Enrichment score
S100A8/9
H.I. ctr
H
OCS f/f + Isotype
OCS f/f + anti-TLR4
LKS cells
N. foci per cell
Isotype
anti-TLR4
OCS f/f

S100A8/9 expression in mesenchymal niche cells predicts clinical outcome in human low-risk MDS

To further define the biologic and clinical significance of these findings, we performed transcriptome sequencing of CD271$^+$ niche cells in a prospective, homogeneously treated cohort of low-risk MDS patients (*n* = 20, **Figure 6A**; **Table S6**). Expression of *S100A8* and *S100A9* was strongly correlated (**Figure 6B**), with a subgroup of MDS patients (6/20; 30%) demonstrating significant overexpression of *S100A8* and *S100A9* (Modified Thompson Tau outlier test) (**Figure 6B** and **6C**), independent of established prognostic factors as defined by the revised International Prognostic Scoring System (IPSS-R) and the MD Anderson risk score (LR-PSS) (**Table S6**). S100A8/9 overexpression in niche cells was strongly predictive of overall survival (median survival 8.95 vs 44.20 months) (**Figure 6D** and **Table S6**). All 6 patients in the S100A8/9$^+$ group died of MDS-related pathology such as bleeding or infection. Bone marrow analysis upon the course of disease was available in only 1/6 patients demonstrating leukemic evolution. Leukemic evolution was not observed in patients without elevated S100A8/9 expression in niche cells (*n* = 14), despite considerably longer follow-up.

DISCUSSION

Genomic stress and the ensuing DNA damage play a pivotal role in the attenuation of normal hematopoiesis in ageing and disease. Mutations accumulate in HSPCs over the lifespan of an organism, but the (patho)physiological sources of genomic stress in HSPCs and their relationship with human bone marrow failure remain incompletely understood. Here, we show that specific inflammatory signals from the mesenchymal niche can induce genotoxic stress in heterotypic stem/progenitor cells and relate this concept to the pathogenesis of two human bone marrow failure and leukemia predisposition syndromes, SDS and MDS.

Figure 5. S100A8/9 induces genotoxic stress in murine HSPCs through TLR4 signaling. (A-B) Increased S100A8 and S100A9 levels in OCS$^{f/f}$ GFP$^+$ cells. (A) representative plots. (B) MFI values (*n* = 5). (C) Increased plasma concentration of S100A8/9 by ELISA (OCS$^{f/+}$, *n* = 5; OCS$^{f/f}$, *n* = 4). (D) Left: representative γH2AX pictures after HSPCs in vitro exposure. Positive control: 8-Gy irradiated Lin$^-$ c-Kit$^+$ Sca-1$^-$ cells. Negative controls: heat-inactivated S100A8/9 (H.I. ctr). Right: number of γH2AX foci (*n* = 3). (E) S100A8/9 has no effect on cell cycle (*n* = 2). (F) Increased apoptosis in S100A8/9-exposed LKS (*n* = 3). (G) Activation of TLR signaling (GSEA). (H) TLR4-blocking antibodies limit DNA damage in OCS$^{f/f}$ mice (*n* = 4). **P*<0.05. **P*<0.01. ****P*<0.001. Data are mean ± SEM. See also Figure S2 and S5; Table S5.

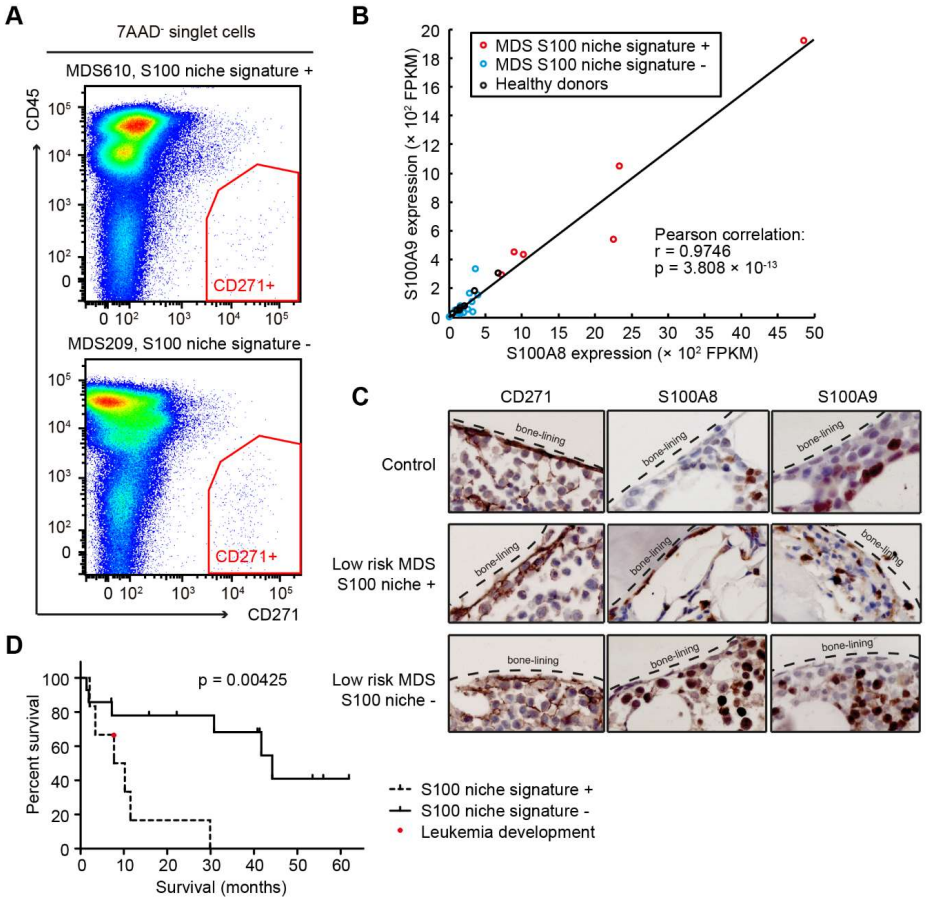

Figure 6. Expression of S100A8/9 in highly purified mesenchymal niche cells predicts clinical outcome in low-risk MDS. (A) Representative examples of FACS-isolated CD271$^+$ niche cells in human MDS. (B) Correlation plot of *S100A8* and *S100A9* expression levels in human low-risk MDS (*n* = 20) and normal controls (*n* = 7). (C) Representative staining of S100A8 and S100A9 in endosteal (CD271$^+$) stromal cells. Intramedullary staining reflects expression of S100A8/9 in myeloid cells. (D) Kaplan-Meier survival curve showing patient outcome. See also Table S6.

The data indicate that the mesenchymal niche may actively contribute to the formation of a 'mutagenic' environment, adding to our understanding of how a premalignant environment facilitates cancer initiation and evolution. The data argue that this may not only occur through facilitated selection and expansion of genetic clones that stochastically emerge in a permissive

environment, but that the mesenchymal niche may be an active participant in driving the genotoxic stress underlying tissue failure and malignant transformation of parenchymal cells.

Notably, leukemic transformation was not observed in mice with targeted deficiency of *Sbds* in mesenchymal cells. Earlier, in a related mouse model of targeted *Dicer1* deletion in MPCs, leukemic transformation was a rare event.[8] In the light of our current findings, these observations are likely explained by several factors. First, prolonged exposure to a mutagenic niche, beyond the limited lifespan of OCS mice, may be necessary for the accumulation of genetic damage required for full transformation. Additionally, the data argue that DNA repair-proficient HSPCs are able to cope with the mutagenic stress induced by their environment through activation of the DDR (as shown by molecular activation of cell cycle checkpoints and apoptosis), preventing the accumulation of stable genetic damage (as demonstrated by comet assays) and maintaining the functional integrity of HSPCs (as shown by repopulation assays). It will thus be of considerable interest to test the hypothesis that a mutagenic environment cooperates with aberrant HSPCs, compromised in their ability to cope with inflammatory genotoxic stress, in leukemic evolution. In this context, the propensity of *Sbds*-deficient cells to accumulate ROS[38] and their reduced ability to cope with various cellular stressors, such as mitotic spindle destabilizing agents, endoplasmic reticulum stress activators, topoisomerase inhibitors and UV irradiation,[39,40] is noteworthy.

The current findings add to emerging insights into the role of innate immune TLR-signaling in the pathogenesis of human MDS. TLR4 and other TLRs are overexpressed in HSPCs from MDS patients[41,42] and TLR4 expression was shown to correlate with apoptosis in $CD34^+$ hematopoietic cells. TLR signaling is constitutively activated in MDS mice with deletion of chromosome 5 (del5q)[43] and multiple TLR downstream signaling pathways have been shown to be activated in MDS and related to loss of progenitor cell function.[44]

Our findings implicate the DAMP S100A8/9 derived from the mesenchymal niche as a driver of TLR signaling in this disease. The unbiased identification of S100A8/9 seems to independently converge with an earlier report implicating S100A8/9 in the pathogenesis of MDS.[37] In this study it was shown that the plasma concentration of S100A9 was significantly increased in MDS patients and S100A8/9 was shown to drive expansion and activation of myeloid-derived suppressor cells (MDSCs), which contributed to cytopenia and myelodysplasia in a murine model of S100A9 overexpression through secretion of suppressive cytokines. It is therefore an intriguing possibility that additional, indirect, biologic effects of S100A8/9 contribute to the hematopoietic phenotype of OCS mice. This may include engagement of other cognate receptors of the protein, including expansion of MDSCs through CD33 signaling.[37] Similarly, it is conceivable that other ligands secreted from mesenchymal cells contribute to the induction of DNA damage in HSPCs in the mouse model. We found a striking abundance of transcripts encoding other DAMPs and cytotoxic

proteins in both the mouse model and mesenchymal elements isolated from SDS patients. Ongoing investigations will have to assess whether other selected ligands can evoke genomic stress in heterotypic HSPCs and in such a fashion contribute to the generation of a mutagenic environment in these disorders.

Finally, our findings establish molecular characteristics of the mesenchymal environment as an important determinant of disease outcome in humans. S100A8/9 expression in mesenchymal cells predicted overall survival in a cohort of homogeneously treated low-risk MDS patients. This is of considerable clinical relevance because low-risk MDS is a heterogeneous disease-entity with a subset of patients having a particular dismal prognosis not identified by current risk-stratification strategies.[45] Gene expression of S100A8/9 may identify a substantial subset of patients with an overall survival typically associated with 'high-risk' patients and, if confirmed in larger independent cohorts, could guide therapeutic decision making in MDS. The data thus provide a strong rationale for niche–instructed therapeutic targeting of inflammatory signaling in human preleukemic disease.

EXPERIMENTAL PROCEDURES

Mice and *in vivo* procedures

OCS and *Trp53*$^{f/f}$ mice have been previously described.[8,46] *Ptprc*^{a}*Pepc*^{b}*/BoyCrl* (B6.SJL) mice were purchased from Charles River. Animals were maintained in specific pathogen free conditions in the Experimental Animal Center of Erasmus MC (EDC). For *in vivo* cell cycle analysis, OCS mice received intraperitoneal injections of BrdU (1.5 mg in PBS, BD Biosciences) and sacrificed after 15 h. For TLR4 studies, 2 week-old mice were intraperitoneally injected with a double dose (100 µg and 35 µg, 48 h interval) of TLR4-neutralizing antibody (clone MTS510, eBioscience) or isotype control (clone eBR2a, eBioscience) and sacrificed after 60h. All mice were sacrificed by cervical dislocation. Animal studies were approved by the Animal Welfare/Ethics Committee of the EDC in accordance with legislation in the Netherlands (Approval No. EMC 2067, 2714, 2892, 3062).

µCT analysis

Femur bones were isolated, fixated in 3% PFA/PBS for 24 h and stored in 70% ethanol. µCT analysis was performed using a SkyScan 1172 system (SkyScan) using previously described settings.[47] Bone microarchitectural parameters relative to the trabecular and the cortical area were determined in the distal metaphysis and the mid-diaphysis of each femur, respectively, using software packages from Bruker MicroCT (NRecon, CtAn and Dataviewer).

Patient material

Bone marrow aspirates were obtained from SDS and DBA patients during routine follow-up. All low-risk MDS patients were treated with lenalidomide (10 mg/day, d 1-21 in a 4-week schedule) in the context of an ongoing prospective clinical trial (HOVON89; www.hovon.nl; www.trialregister.nl as NTR1825; EudraCT No. 2008-002195-10); bone marrow specimens were collected at study entry. As controls, bone marrow cells from allogeneic transplantation donors were used. Patients and healthy donor characteristics are described in **Table S4** and **S6**. All specimens were collected with informed consent, in accordance with the Declaration of Helsinki.

Gene expression profiling

Osx::GFP cells from bone cell suspensions of OCS mice were sorted in TRIzol Reagent (Life Technologies) and RNA was extracted according to the manufacturer's recommendations. Linear amplification of mRNA was performed using the Ovation Pico WTA System (NuGEN). cDNA was fragmented and labelled with Encore™ Biotin Module (NuGEN). The biotinylated cDNA was hybridized to the GeneChip Mouse Genome 430 2.0 Array (Affymetrix eBioscience). Signal was normalized and differential gene expression analysis was performed with the limma package.[48] RNA sequencing experiments were performed as previously described.[15] Human transcripts were aligned to the Ref Seq transcriptome (hg19) and analyzed with DESeq2,[49], while mouse transcripts were aligned to the Ensembl transcriptome (mm10) and analyzed with EdgeR[50] in the R environment. FPKM values were calculated using Cufflinks.[51] Principal component analysis was performed in the R environment on the raw fragment counts extracted from the BAM files by HTSeq-count.[52] For Gene Set Enrichment Analysis[53] (GSEA, Broad Institute), normalized intensity values (microarray data) and FPKM values (RNA sequencing) were compared to the curated gene sets (C2) and the Gene Ontology gene sets (C5) of the Molecular Signature Database (MsigDB) using the Signal2Noise metric and 1000 gene set-based permutations. For HSPCs GO-term analysis, genes with significantly differential expression (P<0.05) were interrogated using g:Profiler web-based software.[54,55]

Immunofluorescence microscopy

HSPCs were harvested in PBS+0.5%FBS, cytospun on a glass slide for 3 min at 500 rpm using a Cytospin 4 centrifuge (Thermo Scientific) and fixed in 3% PFA/PBS for 15 min on ice. After 3 washing steps in PBS, cells were permeabilized for 2 min in 0.15% Triton-X100/PBS. Aspecific binding sites were blocked by incubation in 1%BSA/PBS for 1 h at room temperature. Cells were

next stained overnight at 4°C with anti-phospho-histone H2A.X (Ser139) mouse monoclonal antibody (clone JBW301, Merck Millipore, diluted 1:1000 in 1%BSA/PBS). Slides were washed twice in PBS for 5 min and incubated for 1 h at 37°C with Alexa Fluor 488-conjugated goat anti-mouse antibody (Cat. A10667, Life Technologies, diluted 1:200 in 1%BSA/PBS). After 2 washes in PBS, slides were mounted in VECTASHIELD Mounting Medium with DAPI (Vector Laboratories). Z-series images were acquired with a Leica TCS SP5 confocal microscope (63X objective lens) using the LAS software (Leica Microsystems). γH2AX foci were counted manually from the maximum projection view.

Survival analysis

The low-risk MDS patient subgroup with S100 niche signature was defined by the Modified Thompson Tau test for outlier detection. In brief, *S100A8* statistics from the control cases were combined to define the rejection region, demarcating FPKM values to be considered as outliers. MDS cases with *S100A8* FPKM values within the rejection region were thus defined as niche-signature^{+}. Kaplan-Meier curves were next constructed for the two MDS patient subgroups with events defined as patient death or development of leukemia. Statistical significant difference was asserted with the log-rank test.

Statistics

Statistical analysis was performed using Prism 5 (GraphPad Software). Unless otherwise specified, unpaired, 2-tailed Student's t test (single test) or 1-way analysis of variance (multiple comparisons) were used to evaluate statistical significance, defined as $P<0.05$. All results in bar graphs are mean value ± standard error of the mean.

AUTHOR CONTRIBUTIONS

Conceptualization: N.A.Z. and M.H.G.P.R.; Methodology: N.A.Z., Z.P., S.C., K.J.G.K., E.M.J.B., B.V.D.E., M.A.M., J.P.T.M.V.L., R.K., T.V., and M.H.G.P.R.; Investigation: N.A.Z., Z.P., S.C., E.M.J.B., B.V.D.E., M.N.A., C.V.D.L., M.K., M.A.M., and T.V.; Resources: T.W.K., T.M.W., A.V.D.L., E.M.K., J.P.T.M.V.L, R.K., I.P.T. and T.V.; Data curation: M.A.S., R.M.H., T.W.K., T.M.W., A.V.D.L., and E.M.K.; Writing: N.A.Z. and M.H.G.P.R; Visualization: N.A.Z., Z.P., S.C, and R.H.M.; Supervision and Funding Acquisition: M.H.G.P.R.

ACKNOWLEDGEMENTS

Dr Pier Giorgio Mastroberardino and Dr Chiara Milanese provided reagents and assistance with mitochondrial analysis; Prof. Johanna M. Rommens donated *Sbds*-floxed mice; Dr Eric Braakman and Mariette ter Borg provided $CD34^+$ cells; Dr Elwin Rombouts, Onno Roovers, Paulette van Strien, Peter van Geel, Nicole van Vliet, Charlie Laffeber and Gert-Jan Kremers provided technical assistance; Dr Marc Bierings and Dr Valerie de Haas on behalf of the 'Stichting Kinderoncologie Nederland (SKION)' provided DBA samples; Pearl F.M. Mau Asam helped with SDS bone marrow collection; members of the Erasmus MC Department of Hematology provided scientific discussion; members of the Erasmus MC animal core facility EDC helped with animal care. This work was supported by grants from the Dutch Cancer Society (KWF Kankerbestrijding), Amsterdam, The Netherlands (grant EMCR 2010-4733 to M.H.G.P.R.), the Netherlands Organization of Scientific Research (NWO 90700422 to M.H.G.P.R.) and the Netherlands Genomics Initiative (Zenith grant no 40-41009-98-11062 to M.H.G.P.R.).

REFERENCES

1. Rossi DJ, Bryder D, Seita J, Nussenzweig A, Hoeijmakers J, Weissman IL. Deficiencies in DNA damage repair limit the function of haematopoietic stem cells with age. *Nature*. 2007;447(7145):725-729.
2. Jaiswal S, Fontanillas P, Flannick J, et al. Age-related clonal hematopoiesis associated with adverse outcomes. *N Engl J Med*. 2014;371(26):2488-2498.
3. Walkley CR, Olsen GH, Dworkin S, et al. A microenvironment-induced myeloproliferative syndrome caused by retinoic acid receptor gamma deficiency. *Cell*. 2007;129(6):1097-1110.
4. Arranz L, Sanchez-Aguilera A, Martin-Perez D, et al. Neuropathy of haematopoietic stem cell niche is essential for myeloproliferative neoplasms. *Nature*. 2014;512(7512):78-81.
5. Hanoun M, Zhang D, Mizoguchi T, et al. Acute myelogenous leukemia-induced sympathetic neuropathy promotes malignancy in an altered hematopoietic stem cell niche. *Cell Stem Cell*. 2014;15(3):365-375.
6. Medyouf H, Mossner M, Jann JC, et al. Myelodysplastic cells in patients reprogram mesenchymal stromal cells to establish a transplantable stem cell niche disease unit. *Cell Stem Cell*. 2014;14(6):824-837.
7. Schepers K, Campbell TB, Passegue E. Normal and leukemic stem cell niches: insights and therapeutic opportunities. *Cell Stem Cell*. 2015;16(3):254-267.
8. Raaijmakers MH, Mukherjee S, Guo S, et al. Bone progenitor dysfunction induces myelodysplasia and secondary leukaemia. *Nature*. 2010;464(7290):852-857.
9. Kode A, Manavalan JS, Mosialou I, et al. Leukaemogenesis induced by an activating beta-catenin mutation in osteoblasts. *Nature*. 2014;506(7487):240-244.
10. Boocock GR, Morrison JA, Popovic M, et al. Mutations in SBDS are associated with Shwachman-Diamond syndrome. *Nature Genetics*. 2003;33(1):97-101.
11. Finch AJ, Hilcenko C, Basse N, et al. Uncoupling of GTP hydrolysis from eIF6 release on the ribosome causes Shwachman-Diamond syndrome. *Genes & Development*. 2011;25(9):917-929.
12. Alter BP. Diagnosis, genetics, and management of inherited bone marrow failure syndromes. *Hematology Am Soc Hematol Educ Program*. 2007:29-39.
13. Donadieu J, Fenneteau O, Beaupain B, et al. Classification of and risk factors for hematologic complications in a French national cohort of 102 patients with Shwachman-Diamond syndrome. *Haematologica-the Hematology Journal*. 2012;97(9):1312-1319.
14. Rawls AS, Gregory AD, Woloszynek JR, Liu FL, Link DC. Lentiviral-mediated RNAi inhibition of Sbds in murine hematopoietic progenitors impairs their hematopoietic potential. *Blood*. 2007;110(7):2414-2422.
15. Zambetti NA, Bindels EM, Van Strien PM, et al. Deficiency of the ribosome biogenesis gene Sbds in hematopoietic stem and progenitor cells causes neutropenia in mice by attenuating lineage progression in myelocytes. *Haematologica*. 2015.
16. Toiviainen-Salo S, Mayranpaa MK, Durie PR, et al. Shwachman-Diamond syndrome is associated with low-turnover osteoporosis. *Bone*. 2007;41(6):965-972.
17. Aggett PJ, Cavanagh NPC, Matthew DJ, Pincott JR, Sutcliffe J, Harries JT. Shwachmans Syndrome - a Review of 21 Cases. *Archives of Disease in Childhood*. 1980;55(5):331-347.

18. Ginzberg H, Shin J, Ellis L, et al. Shwachman syndrome: phenotypic manifestations of sibling sets and isolated cases in a large patient cohort are similar. *Journal of Pediatrics*. 1999;135(1):81-88.
19. Mäkitie O, Ellis L, Durie PR, et al. Skeletal phenotype in patients with Shwachman-Diamond syndrome and mutations in SBDS. *Clinical Genetics*. 2004;65(2):101-112.
20. Li L, Li M, Sun C, et al. Altered hematopoietic cell gene expression precedes development of therapy-related myelodysplasia/acute myeloid leukemia and identifies patients at risk. *Cancer Cell*. 2011;20(5):591-605.
21. Murphy MP. How mitochondria produce reactive oxygen species. *Biochem J*. 2009;417(1):1-13.
22. Ito S. Encapsulation of a reactive core in neuromelanin. *Proc Natl Acad Sci U S A*. 2006;103(40):14647-14648.
23. Yahata T, Takanashi T, Muguruma Y, et al. Accumulation of oxidative DNA damage restricts the self-renewal capacity of human hematopoietic stem cells. *Blood*. 2011;118(11):2941-2950.
24. Walter D, Lier A, Geiselhart A, et al. Exit from dormancy provokes DNA-damage-induced attrition in haematopoietic stem cells. *Nature*. 2015.
25. Curtin NJ. DNA repair dysregulation from cancer driver to therapeutic target. *Nat Rev Cancer*. 2012;12(12):801-817.
26. Sahin E, Depinho RA. Linking functional decline of telomeres, mitochondria and stem cells during ageing. *Nature*. 2010;464(7288):520-528.
27. Raiser DM, Narla A, Ebert BL. The emerging importance of ribosomal dysfunction in the pathogenesis of hematologic disorders. *Leuk Lymphoma*. 2014;55(3):491-500.
28. Marino S, Vooijs M, van der Gulden H, Jonkers J, Berns A. Induction of medulloblastomas in p53-null mutant mice by somatic inactivation of Rb in the external granular layer cells of the cerebellum. *Genes & Development*. 2000;14(8):994-1004.
29. Tormin A, Li O, Brune JC, et al. CD146 expression on primary nonhematopoietic bone marrow stem cells is correlated with in situ localization. *Blood*. 2011;117(19):5067-5077.
30. Woloszynek JR, Rothbaum RJ, Rawls AS, et al. Mutations of the SBDS gene are present in most patients with Shwachman-Diamond syndrome. *Blood*. 2004;104(12):3588-3590.
31. Peddie CM, Wolf CR, McLellan LI, Collins AR, Bowen DT. Oxidative DNA damage in CD34+ myelodysplastic cells is associated with intracellular redox changes and elevated plasma tumour necrosis factor-alpha concentration. *Br J Haematol*. 1997;99(3):625-631.
32. Head DR, Jacobberger JW, Mosse C, et al. Innovative analyses support a role for DNA damage and an aberrant cell cycle in myelodysplastic syndrome pathogenesis. *Bone Marrow Res*. 2011;2011:950934.
33. Xiao Y, Wang J, Song H, Zou P, Zhou D, Liu L. CD34+ cells from patients with myelodysplastic syndrome present different p21 dependent premature senescence. *Leuk Res*. 2013;37(3):333-340.
34. Vlachos A, Rosenberg PS, Atsidaftos E, Alter BP, Lipton JM. Incidence of neoplasia in Diamond Blackfan anemia: a report from the Diamond Blackfan Anemia Registry. *Blood*. 2012;119(16):3815-3819.
35. Srikrishna G, Freeze HH. Endogenous damage-associated molecular pattern molecules at the crossroads of inflammation and cancer. *Neoplasia*. 2009;11(7):615-628.
36. Vogl T, Tenbrock K, Ludwig S, et al. Mrp8 and Mrp14 are endogenous activators of Toll-like receptor 4, promoting lethal, endotoxin-induced shock. *Nature Medicine*. 2007;13(9):1042-1049.

37. Chen X, Eksioglu EA, Zhou J, et al. Induction of myelodysplasia by myeloid-derived suppressor cells. *Journal of Clinical Investigation*. 2013;123(11):4595-4611.
38. Ambekar C, Das B, Yeger H, Dror Y. SBDS-deficiency results in deregulation of reactive oxygen species leading to increased cell death and decreased cell growth. *Pediatr Blood Cancer*. 2010;55(6):1138-1144.
39. Austin KM, Gupta ML, Jr., Coats SA, et al. Mitotic spindle destabilization and genomic instability in Shwachman-Diamond syndrome. *Journal of Clinical Investigation*. 2008;118(4):1511-1518.
40. Ball HL, Zhang B, Riches JJ, et al. Shwachman-Bodian Diamond syndrome is a multi-functional protein implicated in cellular stress responses. *Hum Mol Genet*. 2009;18(19):3684-3695.
41. Maratheftis CI, Andreakos E, Moutsopoulos HM, Voulgarelis M. Toll-like receptor-4 is up-regulated in hematopoietic progenitor cells and contributes to increased apoptosis in myelodysplastic syndromes. *Clin Cancer Res*. 2007;13(4):1154-1160.
42. Wei Y, Dimicoli S, Bueso-Ramos C, et al. Toll-like receptor alterations in myelodysplastic syndrome. *Leukemia*. 2013;27(9):1832-1840.
43. Starczynowski DT, Kuchenbauer F, Argiropoulos B, et al. Identification of miR-145 and miR-146a as mediators of the 5q- syndrome phenotype. *Nat Med*. 2010;16(1):49-58.
44. Ganan-Gomez I, Wei Y, Starczynowski DT, et al. Deregulation of innate immune and inflammatory signaling in myelodysplastic syndromes. *Leukemia*. 2015;29(7):1458-1469.
45. Bejar R, Stevenson KE, Caughey BA, et al. Validation of a prognostic model and the impact of mutations in patients with lower-risk myelodysplastic syndromes. *J Clin Oncol*. 2012;30(27):3376-3382.
46. Jonkers J, Meuwissen R, van der Gulden H, Peterse H, van der Valk M, Berns A. Synergistic tumor suppressor activity of BRCA2 and p53 in a conditional mouse model for breast cancer. *Nature Genetics*. 2001;29(4):418-425.
47. Tudpor K, van der Eerden BC, Jongwattanapisan P, et al. Thrombin receptor deficiency leads to a high bone mass phenotype by decreasing the RANKL/OPG ratio. *Bone*. 2015;72:14-22.
48. Ritchie ME, Phipson B, Wu D, et al. limma powers differential expression analyses for RNA-sequencing and microarray studies. *Nucleic Acids Res*. 2015;43(7):e47.
49. Love MI, Huber W, Anders S. Moderated estimation of fold change and dispersion for RNA-seq data with DESeq2. *Genome Biol*. 2014;15(12):550.
50. Robinson MD, McCarthy DJ, Smyth GK. edgeR: a Bioconductor package for differential expression analysis of digital gene expression data. *Bioinformatics*. 2010;26(1):139-140.
51. Trapnell C, Williams BA, Pertea G, et al. Transcript assembly and quantification by RNA-Seq reveals unannotated transcripts and isoform switching during cell differentiation. *Nat Biotechnol*. 2010;28(5):511-515.
52. Anders S, Pyl PT, Huber W. HTSeq--a Python framework to work with high-throughput sequencing data. *Bioinformatics*. 2015;31(2):166-169.
53. Subramanian A, Tamayo P, Mootha VK, et al. Gene set enrichment analysis: a knowledge-based approach for interpreting genome-wide expression profiles. *Proc Natl Acad Sci U S A*. 2005;102(43):15545-15550.

54. Reimand J, Kull M, Peterson H, Hansen J, Vilo J. g:Profiler--a web-based toolset for functional profiling of gene lists from large-scale experiments. *Nucleic Acids Research*. 2007;35(Web Server issue):W193-200.
55. Reimand J, Arak T, Vilo J. g:Profiler--a web server for functional interpretation of gene lists (2011 update). *Nucleic Acids Research*. 2011;39(Web Server issue):W307-315.

SUPPLEMENTAL DATA ITEMS

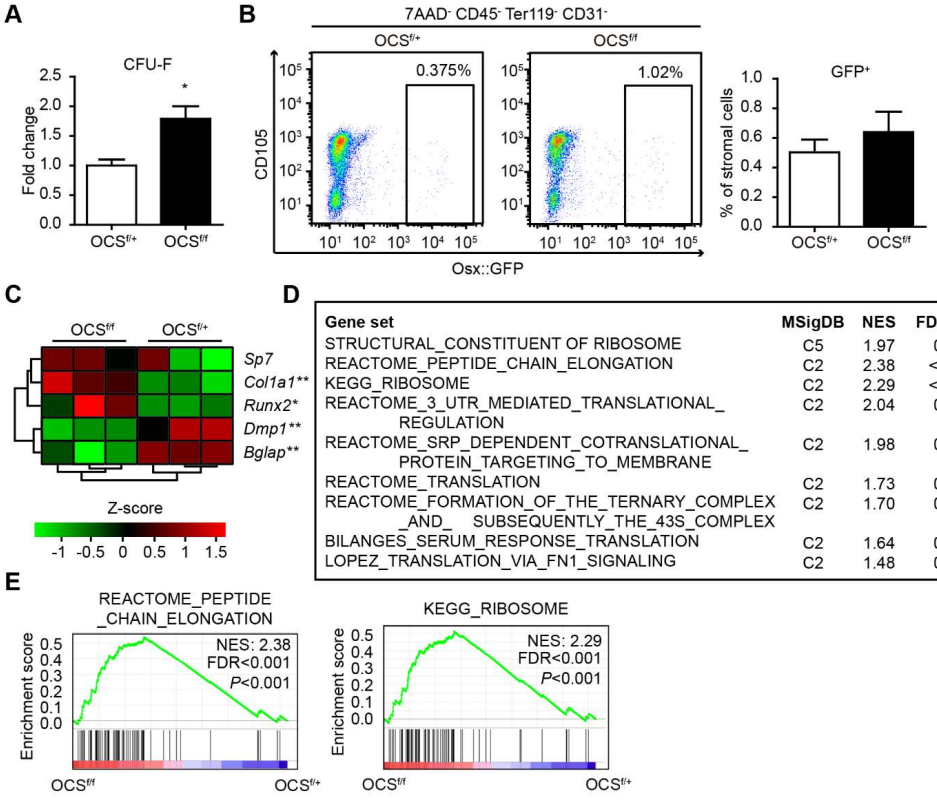

Gene set	MSigDB	NES	FDR q-val
STRUCTURAL_CONSTITUENT OF RIBOSOME	C5	1.97	0.214
REACTOME_PEPTIDE_CHAIN_ELONGATION	C2	2.38	<0.001
KEGG_RIBOSOME	C2	2.29	<0.001
REACTOME_3_UTR_MEDIATED_TRANSLATIONAL_REGULATION	C2	2.04	0.015
REACTOME_SRP_DEPENDENT_COTRANSLATIONAL_PROTEIN_TARGETING_TO_MEMBRANE	C2	1.98	0.020
REACTOME_TRANSLATION	C2	1.73	0.090
REACTOME_FORMATION_OF_THE_TERNARY_COMPLEX_AND_SUBSEQUENTLY_THE_43S_COMPLEX	C2	1.70	0.102
BILANGES_SERUM_RESPONSE_TRANSLATION	C2	1.64	0.135
LOPEZ_TRANSLATION_VIA_FN1_SIGNALING	C2	1.48	0.239

Figure S1. Related to Figure 1; Figure 4. Impairment of terminal osteogenic differentiation in OCS$^{f/f}$ mice. (A) Increased CFU-F numbers (n = 3) with (B) unaltered frequency of Osx::GFP$^+$ cells (n = 4) in OCS$^{f/f}$ mice. (C) Depletion of transcripts defining terminal osteogenic differentiation (osteocalcin, *Bglap*) and dentin matrix acidic phosphoprotein 1 (*Dmp1*), critical for proper mineralization of bone, and enrichment of markers of bone progenitors cells or early osteoblasts (*Runx2* and *Col1a1*) in GFP$^+$ cells from OCS$^{f/f}$ mice. (D) Significant (FDR<0.25) enrichment of ribosome and peptide chain elongation signatures in OCS$^{f/f}$ GFP$^+$ cells (GSEA) with (E) representative plots. *P<0.05. **P<0.01. Data are mean ± SEM.

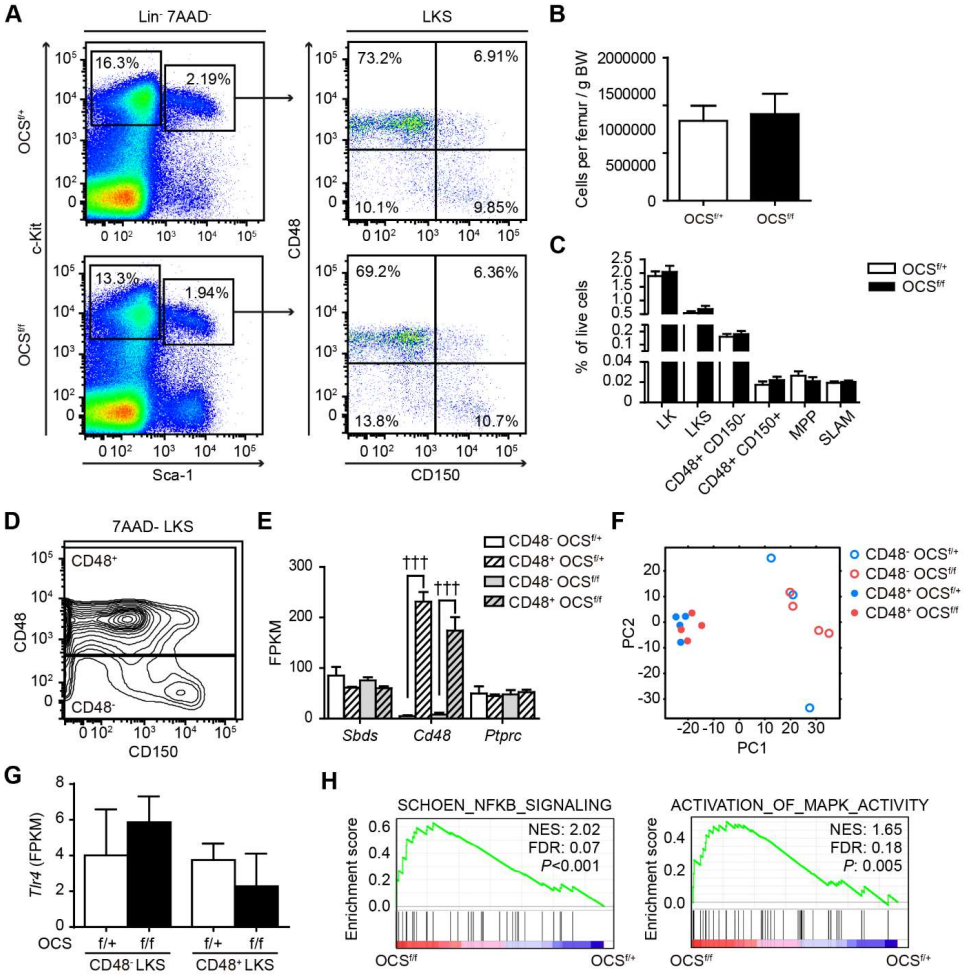

Figure S2. Related to Figure 2; Figure 5. Global preservation of the frequency and transcriptional landscape of HSPCs in OCS$^{f/f}$ mice. (A-C) unaltered HSPC numbers in OCS$^{f/f}$ mice: (A) representative FACS plots, (B) bone marrow cellularity and (C) subset frequency (OCS$^{f/+}$, *n* = 8 A-B, *n* = 7 C; OCS$^{f/f}$, *n* = 7). LK: Lin$^-$ c-Kit$^+$ Sca-1$^-$ cells. LKS: Lin$^-$ c-Kit$^+$ Sca-1$^+$ cells. MPP: multipotent progenitors, CD48$^-$ CD150$^-$ LKS cells. SLAM: CD48$^-$ CD150$^+$ LKS cells. (D) FACS isolation of CD48$^+$ and CD48$^-$ HSPC subsets for RNA-seq (OCS$^{f/+}$ CD48$^-$, *n* = 3; other groups, *n* = 4). (E) RNA-seq validation confirming CD48 and *Ptprc* (CD45) expression and the *Sbds*-proficient status of HSPCs from mutant mice. (F) Principal component analysis indicating global preservation of the transcriptome in HSPCs from OCS$^{f/f}$ mice. (G) TLR4 expression. (H) Activation of NF-κB and MAPK pathways in mutant HSPCs (GSEA). NES: normalized enrichment score. †††FDR-adjusted *P*<0.001. Data are mean ± SEM.

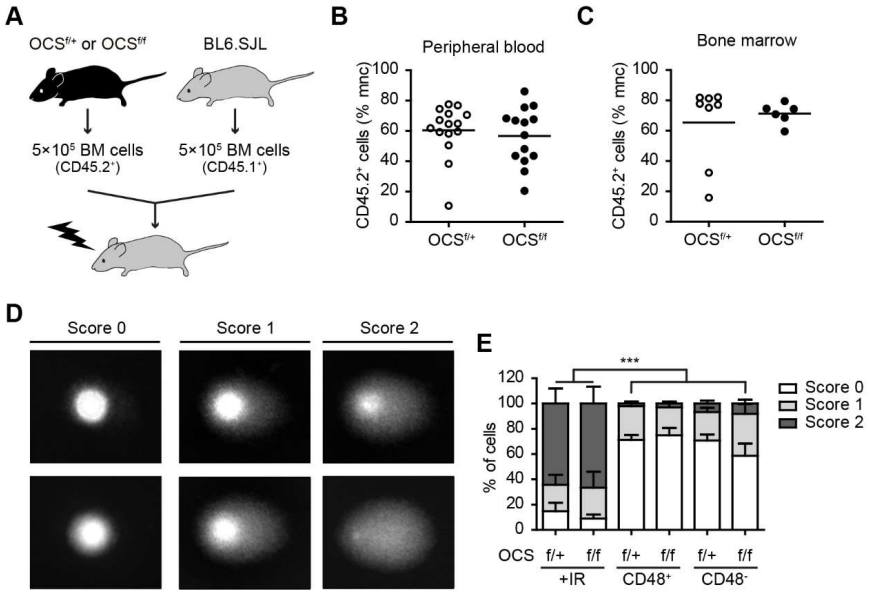

Figure S3. Related to Figure 2. Niche-induced DNA damage does not affect HSPC function. (A) Schematic representation of the competitive transplantation. BM: bone marrow. (B) Peripheral blood frequency of CD45.2$^+$ cells 16 weeks after transplantation. (C) Bone marrow frequency of CD45.2$^+$ cells (21-32 weeks after transplantation). Every circle represents one recipient mouse. (D) Manual scoring system applied to comet assay analysis. (E) Comet assay showing similar frequency of highly damaged HSPCs in OCS$^{f/+}$ and OCS$^{f/f}$ mice (n = 5). +IR: 8-10 Gy irradiated positive control (LK cells). ***P<0.001. Data are mean ± SEM.

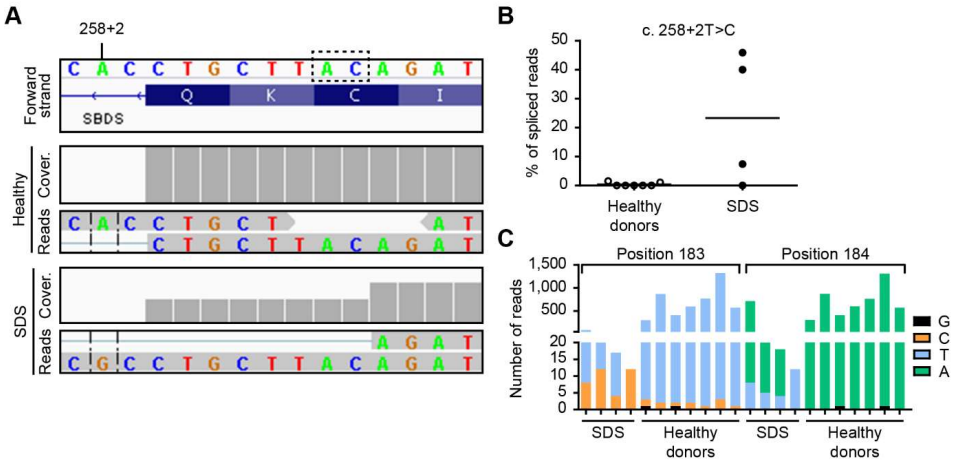

Figure S4. Related to Figure 4. *SBDS* mutations in mesenchymal cells from SDS patients. (A-B) Detection of 258+2 T>C mutation in SDS patients. (A) Representative IGV plot. Note that the coverage level after the cryptic site (dashed box) is reduced in SDS, indicating an 8-bp deletion. (B) Quantification of 258+2 T>C mutation as frequency of spliced reads with 8-bp deletion. Every circle represents a patient. (C) Nucleotide sequence in positions 183-184 from SDS patients and healthy donors.

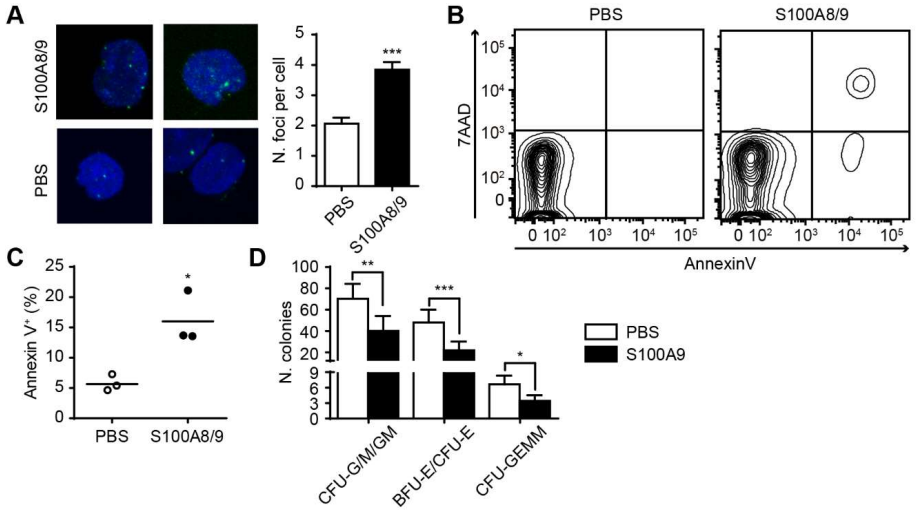

Figure S5. Related to Figure 5. S100A8/9 drives genomic stress in human HSPCs. (A-C) Treatment of human CD34^{+} HSPCs with recombinant S100A8/9. (A) Induction of γH2AX foci (*n* = 3). (B-C) Increased frequency of apoptotic cells. (B) Representative plot. (C) Quantification (*n* = 3). (D) Reduced colony forming capacity of HSPCs as assessed by CFU-C assay (*n* = 4 independent experiments in triplicate). Data are mean ± SEM. **P*<0.05. ***P*<0.01. ****P*<0.001.

Table S1. Related to Figure 2. Transcriptional profiling of OCS-derived HSPCs reveals dysregulation of signatures previously identified as predictive for leukemia evolution.

Gene set	MSigDB collection	CD48- NES	CD48- FDR	CD48+ NES	CD48+ FDR
Enriched in OCS mutants					
G-protein coupled receptors					
G_PROTEIN_COUPLED_RECEPTOR_PROTEIN_ SIGNALING_PATHWAY	C5			1.63	0.180
Cell adhesion-communication					
REACTOME_GAP_JUNCTION_ASSEMBLY	C2			1.84	0.170
PID_INTEGRIN_CS_PATHWAY	C2			1.78	0.213
SA_MMP_CYTOKINE_CONNECTION	C2			1.75	0.230
KEGG_CELL_ADHESION_MOLECULES_CAMS	C2			1.70	0.236
Enriched in OCS controls					
Mitochondria and oxidative phosphorylation					
MOOTHA_VOXPHOS	C2	-2.49	<0.001	-1.93	0.001
WONG_MITOCHONDRIA_GENE_MODULE	C2	-2.46	<0.001	-2.19	<0.001
REACTOME_RESPIRATORY_ELECTRON_TRANSPORT_A TP_SYNTHESIS_BY_CHEMIOSMOTIC_COUPLING_AND_ HEAT_PRODUCTION_BY_UNCOUPLING_PROTEINS	C2	-2.44	<0.001	-2.02	<0.001
REACTOME_RESPIRATORY_ELECTRON_TRANSPORT	C2	-2.43	<0.001	-1.91	0.002
KEGG_OXIDATIVE_PHOSPHORYLATION	C2	-2.37	<0.001	-1.75	0.012
REACTOME_MITOCHONDRIAL_PROTEIN_IMPORT	C2	-2.13	<0.001	-1.95	0.001
MOOTHA_MITOCHONDRIA	C2	-2.12	<0.001	-1.96	0.001
HOUSTIS_ROS	C2	-1.58	0.047	-1.34	0.211
REACTOME_RNA_POL_I_RNA_POL_III_AND_ MITOCHONDRIAL_TRANSCRIPTION	C2	-1.50	0.076		
GARGALOVIC_RESPONSE_TO_OXIDIZED_ PHOSPHOLIPIDS_TURQUOISE_DN	C2	-1.48	0.083		
MOOTHA_HUMAN_MITODB_6_2002	C2			-2.01	<0.001
GALLUZZI_PREVENT_MITOCHONDIAL_ PERMEABILIZATION	C2			-1.30	0.248
MITOCHONDRIAL_MEMBRANE_PART	C5	-2.21	<0.001	-1.83	0.016
MITOCHONDRIAL_INNER_MEMBRANE	C5	-2.15	<0.001	-1.99	0.003
MITOCHONDRIAL_PART	C5	-2.13	<0.001	-2.07	0.001
MITOCHONDRIAL_MEMBRANE	C5	-2.07	<0.001	-2.02	0.003
MITOCHONDRIAL_ENVELOPE	C5	-1.98	0.002	-2.01	0.003
MITOCHONDRIAL_MATRIX	C5	-1.97	0.002	-1.81	0.020
MITOCHONDRIAL_LUMEN	C5	-1.96	0.002	-1.81	0.019
MITOCHONDRIAL_RIBOSOME	C5	-1.87	0.008	-1.64	0.060

Table S1. Related to Figure 2. Transcriptional profiling of OCS-derived HSPCs reveals dysregulation of signatures previously identified as predictive for leukemia evolution. *(Continued)*

Gene set	MSigDB collection	CD48- NES	CD48- FDR	CD48+ NES	CD48+ FDR
Enriched in OCS controls					
Mitochondria and oxidative phosphorylation					
MITOCHONDRION	C5	-1.85	0.010	-2.01	0.002
MITOCHONDRIAL_RESPIRATORY_CHAIN	C5	-1.81	0.015	-1.87	0.013
MITOCHONDRION_ORGANIZATION_AND_BIOGENESIS	C5	-1.54	0.121	-1.50	0.133
ELECTRON_CARRIER_ACTIVITY	C5			-1.73	0.034
MITOCHONDRIAL_TRANSPORT	C5			-1.55	0.099
Ribosomes					
BILANGES_SERUM_RESPONSE_TRANSLATION	C2	-1.64	0.028		
REACTOME_DEADENYLATION_DEPENDENT_MRNA_ DECAY	C2	-1.63	0.032		
REACTOME_ELONGATION_ARREST_AND_RECOVERY	C2	-1.58	0.046		
REACTOME_TRANSLATION	C2	-2.47	<0.001		
KEGG_RIBOSOME	C2	-2.42	<0.001		
REACTOME_PEPTIDE CHAIN ELONGATION	C2	-2.42	<0.001		
REACTOME_NONSENSE_MEDIATED_DECAY_ ENHANCED_BY_THE_EXON_JUNCTION_COMPLEX	C2	-2.37	<0.001		
REACTOME_FORMATION_OF_THE_TERNARY_ COMPLEX_AND_SUBSEQUENTLY_THE_43S_COMPLEX	C2	-2.19	<0.001		
MCGOWAN_RSP6_TARGETS_UP	C2			-1.76	0.011
STRUCTURAL_CONSTITUENT_OF_RIBOSOME	C5	-2.33	<0.001		
RIBOSOME	C5	-2.04	0.001	-1.68	0.045
RIBOSOME_BIOGENESIS_AND_ASSEMBLY	C5	-2.02	0.001	-1.78	0.023
ORGANELLAR_RIBOSOME	C5	-1.89	0.007	-1.63	0.067
RIBONUCLEOPROTEIN_COMPLEX_BIOGENESIS_AND_ ASSEMBLY	C5	-1.83	0.012	-2.11	0.002
RIBOSOMAL_SUBUNIT	C5	-1.78	0.019	-1.62	0.071
TRANSLATION	C5	-1.56	0.118		
PROTEIN_POLYMERIZATION	C5	-1.53	0.126		
RIBONUCLEOPROTEIN_COMPLEX	C5			-2.09	0.001
PROTEIN_RNA_COMPLEX_ASSEMBLY	C5			-1.98	0.003
TRANSLATIONAL_INITIATION	C5			-1.73	0.034
TRANSLATION_REGULATOR_ACTIVITY	C5			-1.71	0.039
TRANSLATION_FACTOR_ACTIVITY_NUCLEIC_ACID_BIN DING	C5			-1.70	0.044
TRANSLATION_INITIATION_FACTOR_ACTIVITY	C5			-1.67	0.048

Table S1. Related to Figure 2. Transcriptional profiling of OCS-derived HSPCs reveals dysregulation of signatures previously identified as predictive for leukemia evolution. *(Continued)*

Gene set	MSigDB collection	CD48- NES	CD48- FDR	CD48+ NES	CD48+ FDR
Enriched in OCS controls					
Ribosomes					
REGULATION_OF_TRANSLATIONAL_INITIATION	C5			-1.55	0.100
tRNA biosynthesis					
REACTOME_CYTOSOLIC_TRNA_AMINOACYLATION	C2			-1.85	0.004
REACTOME_TRNA_AMINOACYLATION	C2			-1.72	0.015
KEGG_AMINOACYL_TRNA_BIOSYNTHESIS	C2			-1.64	0.030
TRNA_METABOLIC_PROCESS	C5			-1.69	0.044
Proteasomal pathway					
KEGG_PROTEASOME	C2	-2.18	<0.001	-1.99	0.001
REACTOME_AUTODEGRADATION_OF_THE_E3_ UBIQUITIN_LIGASE_COP1	C2	-2.07	<0.001	-2.01	<0.001
BIOCARTA_PROTEASOME_PATHWAY	C2	-1.92	0.002	-2.14	<0.001
WONG_PROTEASOME_GENE_MODULE	C2			-1.83	0.005
REACTOME_ANTIGEN_PROCESSING_UBIQUITINATION _PROTEASOME_DEGRADATION	C2			-1.42	0.138
PROTEASOME_COMPLEX	C5	-1.47	0.168	-1.52	0.113
Cell cycle regulation					
REACTOME_SYNTHESIS_OF_DNA	C2	-2.44	<0.001	-2.25	<0.001
REACTOME_S_PHASE	C2	-2.42	<0.001	-2.31	<0.001
CHICAS_RB1_TARGETS_LOW_SERUM	C2	-2.28	<0.001		
ISHIDA_E2F_TARGETS	C2	-2.27	<0.001	-2.11	<0.001
REACTOME_MITOTIC_G1_G1_S_PHASES	C2	-2.27	<0.001	-2.37	<0.001
REACTOME_G1_S_TRANSITION	C2	-2.26	<0.001	-2.31	<0.001
REACTOME_M_G1_TRANSITION	C2	-2.26	<0.001	-2.17	<0.001
REACTOME_DNA_STRAND_ELONGATION	C2	-2.23	<0.001	-2.05	<0.001
KEGG_DNA_REPLICATION	C2	-2.21	<0.001	-2.02	<0.001
RAHMAN_TP53_TARGETS_PHOSPHORYLATED	C2	-2.18	<0.001	-1.90	0.002
REACTOME_CDK_MEDIATED_PHOSPHORYLATION_ AND_REMOVAL_OF_CDC6	C2	-2.17	<0.001	-2.00	0.001
REACTOME_ASSEMBLY_OF_THE_PRE_REPLICATIVE_ COMPLEX	C2	-2.15	<0.001	-2.20	<0.001
KONG_E2F3_TARGETS	C2	-2.14	<0.001	-2.19	<0.001
REACTOME_DNA_REPLICATION	C2	-2.14	<0.001	-2.29	<0.001
REACTOME_CDT1_ASSOCIATION_WITH_THE_CDC6_ ORC_ORIGIN_COMPLEX	C2	-2.13	<0.001	-2.10	<0.001

Table S1. Related to Figure 2. Transcriptional profiling of OCS-derived HSPCs reveals dysregulation of signatures previously identified as predictive for leukemia evolution. *(Continued)*

Gene set	MSigDB collection	CD48- NES	CD48- FDR	CD48+ NES	CD48+ FDR
Enriched in OCS controls					
Cell cycle regulation					
REACTOME_CYCLIN_E_ASSOCIATED_EVENTS_DURING_G1_S_TRANSITION_	C2	-2.13	<0.001	-2.13	<0.001
MARKEY_RB1_ACUTE_LOF_DN	C2	-2.11	<0.001	-2.27	<0.001
REACTOME_CELL_CYCLE_CHECKPOINTS	C2	-2.10	<0.001	-2.11	<0.001
WHITFIELD_CELL_CYCLE_LITERATURE	C2	-2.08	<0.001	-2.25	<0.001
EGUCHI_CELL_CYCLE_RB1_TARGETS	C2	-2.03	<0.001	-1.97	0.001
REACTOME_REGULATION_OF_MITOTIC_CELL_CYCLE	C2	-2.03	<0.001		
REACTOME_CELL_CYCLE_MITOTIC	C2	-2.02	<0.001	-2.34	<0.001
REACTOME_LAGGING_STRAND_SYNTHESIS	C2	-2.02	<0.001	-1.88	0.003
REACTOME_CELL_CYCLE	C2	-2.01	<0.001	-2.18	<0.001
REACTOME_MITOTIC_M_M_G1_PHASES	C2	-2.00	<0.001	-2.23	<0.001
SCIAN_CELL_CYCLE_TARGETS_OF_TP53_AND_TP73_DN	C2	-1.98	0.001	-1.81	0.006
ZHOU_CELL_CYCLE_GENES_IN_IR_RESPONSE_24HR	C2	-1.90	0.002	-2.12	<0.001
KAUFFMANN_DNA_REPLICATION_GENES	C2	-1.87	0.003	-1.96	0.001
IGLESIAS_E2F_TARGETS_UP	C2	-1.86	0.003	-1.32	0.235
CHANG_CYCLING_GENES	C2	-1.85	0.004	-2.10	<0.001
TANG_SENESCENCE_TP53_TARGETS_DN	C2	-1.82	0.006	-1.86	0.003
MARKEY_RB1_CHRONIC_LOF_UP	C2	-1.78	0.008	-1.42	0.134
REACTOME_G2_M_CHECKPOINTS	C2	-1.78	0.008	-1.71	0.017
ZHOU_CELL_CYCLE_GENES_IN_IR_RESPONSE_6HR	C2	-1.77	0.009	-2.19	<0.001
REACTOME_CYCLIN_A_B1_ASSOCIATED_EVENTS_DURING_G2_M_TRANSITION	C2	-1.68	0.022	-1.39	0.160
REACTOME_E2F_MEDIATED_REGULATION_OF_DNA_REPLICATION	C2	-1.64	0.028	-1.88	0.003
MOLENAAR_TARGETS_OF_CCND1_AND_CDK4_DN	C2	-1.62	0.033	-2.32	<0.001
REACTOME_G1_S_SPECIFIC_TRANSCRIPTION	C2	-1.62	0.034	-1.94	0.001
BIOCARTA_P53_PATHWAY	C2	-1.59	0.044	-1.31	0.246
VERNELL_RETINOBLASTOMA_PATHWAY_UP	C2	-1.58	0.045	-1.96	0.001
REACTOME_MEIOTIC_RECOMBINATION	C2	-1.57	0.049		
KANNAN_TP53_TARGETS_DN	C2	-1.56	0.052		
IWANAGA_E2F1_TARGETS_INDUCED_BY_SERUM	C2	-1.54	0.059	-1.40	0.155
KEGG_CELL_CYCLE	C2	-1.51	0.068	-1.88	0.003
BIOCARTA_MCM_PATHWAY	C2	-1.49	0.079	-1.54	0.068

Table S1. Related to Figure 2. Transcriptional profiling of OCS-derived HSPCs reveals dysregulation of signatures previously identified as predictive for leukemia evolution. *(Continued)*

Gene set	MSigDB collection	CD48- NES	CD48- FDR	CD48+ NES	CD48+ FDR
Enriched in OCS controls					
Cell cycle regulation					
REACTOME_G0_AND_EARLY_G1	C2	-1.48	0.086	-1.86	0.003
PID_E2F_PATHWAY	C2	-1.47	0.088	-1.85	0.004
MARKEY_RB1_CHRONIC_LOF_DN	C2	-1.44	0.110		
CHICAS_RB1_TARGETS_GROWING	C2	-1.42	0.121	-1.72	0.015
REACTOME_MITOTIC_PROMETAPHASE	C2	-1.38	0.153	-1.84	0.004
REACTOME_G1_PHASE	C2	-1.37	0.155	-1.65	0.030
BIOCARTA_CELLCYCLE_PATHWAY	C2	-1.35	0.173	-1.65	0.029
HERNANDEZ_MITOTIC_ARREST_BY_DOCETAXEL_1_ DN	C2	-1.30	0.220		
WHITFIELD_CELL_CYCLE_G2	C2	-1.30	0.224	-1.60	0.044
SANCHEZ_MDM2_TARGETS	C2	-1.28	0.249		
BENPORATH_PROLIFERATION	C2			-2.15	<0.001
REACTOME_SCFSKP2_MEDIATED_DEGRADATION_OF_ P27_P21	C2			-2.14	<0.001
REACTOME_APC_C_CDC20_MEDIATED_ DEGRADATION_OF_MITOTIC_PROTEINS	C2			-2.03	<0.001
REN_BOUND_BY_E2F	C2			-1.89	0.002
REACTOME_PROCESSIVE_SYNTHESIS_ON_THE_ LAGGING_STRAND	C2	-1.92	0.001	-1.72	0.016
REACTOME_MITOTIC_G2_G2_M_PHASES	C2			-1.69	0.021
REACTOME_ACTIVATION_OF_THE_PRE_REPLICATIVE_ COMPLEX	C2	-1.93	0.001	-1.68	0.022
CEBALLOS_TARGETS_OF_TP53_AND_MYC_UP	C2			-1.67	0.025
REACTOME_RECRUITMENT_OF_MITOTIC_ CENTROSOME_PROTEINS_AND_COMPLEXES	C2			-1.63	0.033
REICHERT_MITOSIS_LIN9_TARGETS	C2			-1.61	0.039
PID_P53REGULATIONPATHWAY	C2			-1.59	0.047
BIOCARTA_G1_PATHWAY	C2			-1.55	0.060
SA_G1_AND_S_PHASES	C2			-1.51	0.082
WHITFIELD_CELL_CYCLE_G2_M	C2			-1.48	0.099
WHITFIELD_CELL_CYCLE_M_G1	C2			-1.48	0.099
WHITFIELD_CELL_CYCLE_G1_S	C2			-1.47	0.101
BIOCARTA_G2_PATHWAY	C2			-1.46	0.112
GEORGES_CELL_CYCLE_MIR192_TARGETS	C2			-1.45	0.116

Table S1. Related to Figure 2. Transcriptional profiling of OCS-derived HSPCs reveals dysregulation of signatures previously identified as predictive for leukemia evolution. *(Continued)*

Gene set	MSigDB collection	CD48- NES	CD48- FDR	CD48+ NES	CD48+ FDR
Enriched in OCS controls					
Cell cycle regulation					
WHITFIELD_CELL_CYCLE_S	C2			-1.40	0.155
REGULATION_OF_CYCLIN_DEPENDENT_PROTEIN_ KINASE_ACTIVITY	C5	-1.99	0.001		
REPLICATION_FORK	C5	-1.85	0.010	-1.45	0.169
DNA_REPLICATION	C5	-1.83	0.012	-1.58	0.088
CELL_CYCLE_PROCESS	C5	-1.74	0.031	-1.51	0.127
INTERPHASE	C5	-1.67	0.057	-1.45	0.171
CELL_CYCLE_PHASE	C5	-1.64	0.070	-1.40	0.209
CELL_CYCLE_GO_0007049	C5	-1.64	0.070	-1.43	0.174
MITOTIC_CELL_CYCLE	C5	-1.63	0.070	-1.51	0.122
DNA_DEPENDENT_DNA_REPLICATION	C5	-1.59	0.097	-1.52	0.113
INTERPHASE_OF_MITOTIC_CELL_CYCLE	C5	-1.58	0.104	-1.50	0.128
M_PHASE	C5	-1.54	0.122	-1.34	0.250
M_PHASE_OF_MITOTIC_CELL_CYCLE	C5	-1.52	0.125	-1.55	0.098
CELL_PROLIFERATION_GO_0008283	C5	-1.46	0.176		
MITOSIS	C5	-1.43	0.197	-1.56	0.096
DNA_METABOLIC_PROCESS	C5			-1.46	0.160
Metabolism					
REACTOME_TCA_CYCLE_AND_RESPIRATORY_ ELECTRON_TRANSPORT	C2	-2.19	<0.001	-2.08	<0.001
MOOTHA_TCA	C2	-1.67	0.024	-1.78	0.008
REACTOME_CITRIC_ACID_CYCLE_TCA_CYCLE	C2	-1.61	0.037	-1.87	0.003
KEGG_CITRATE_CYCLE_TCA_CYCLE	C2	-1.55	0.054	-1.79	0.007
REACTOME_GLUCOSE_METABOLISM	C2	-1.33	0.190		
REACTOME_PYRUVATE_METABOLISM_AND_CITRIC_ ACID_TCA_CYCLE	C2			-1.71	0.017
Hematopoietic stem cells					
IVANOVA_HEMATOPOIESIS_INTERMEDIATE_ PROGENITOR	C2	-1.67	0.023	-2.02	<0.001
BYSTRYKH_HEMATOPOIESIS_STEM_CELL_QTL_CIS	C2	-1.45	0.103		
PARK_HSC_AND_MULTIPOTENT_PROGENITORS	C2	-1.39	0.145	-1.53	0.070
BYSTRYKH_HEMATOPOIESIS_STEM_CELL_AND_BRAIN _QTL_CIS	C2			-1.32	0.227

Upregulation of G-protein-coupled receptors and cell adhesion-communication, and downregulation of mitochondrial oxidative phosphorylation, ribosome biogenesis, aminoacyl-tRNA synthetase activity, proteasomal degradation, citric acid cycle, cell cycle deregulation and hematopoietic stem cell programs. Normalized enrichment score (NES) and False Discovery Rate-adjusted q-value (FDR) are omitted when FDR > 0.25.

Table S2. Related to Figure 2. Stress and DNA damage dysregulation in the transcriptome of HSPCs from $OCS^{f/f}$ mice.

ID	Description	$CD48^-$ p-val	$CD48^+$ p-val
GO:0006310	DNA recombination	NS	4.68e-02
GO:0006950	response to stress	4.69e-05	1.31e-10
GO:0080134	regulation of response to stress	2.25e-03	9.78e-04
GO:0033554	cellular response to stress	5.53e-06	9.15e-05
GO:0080135	regulation of cellular response to stress	2.82e-02	NS
GO:0006974	cellular response to DNA damage stimulus	4.11e-03	1.96e-03
GO:0006281	DNA repair	3.86e-02	NS
GO:0006301	postreplication repair	NS	2.78e-02
REAC:5956042	Cell Cycle Checkpoints	1.27e-04	2.86e-04
REAC:5956049	Activation of ATR in response to replication stress	2.89e-02	4.10e-02
REAC:5956279	Gap-filling DNA repair synthesis and ligation in GG-NER	2.01e-02	NS
REAC:5956420	Gap-filling DNA repair synthesis and ligation in TC-NER	2.01e-02	NS

Genes with significantly different expression ($P<0.05$) between $OCS^{f/+}$ and $OCS^{f/f}$ mice within the $CD48^-$ or $CD48^+$ populations were interrogated for GO and Reactome term enrichment using g-profiler. P-val: p-value. NS: not significant ($P\geq0.05$).

Table S3. Related to Figure 2. Myc-related signatures depleted in OCS$^{f/f}$ HSPCs.

Gene set	Size	CD48$^-$ NES	CD48$^-$ FDR	CD 48$^+$ NES	CD48$^+$ FDR
DANG_MYC_TARGETS_UP	140	-2.3691	<0.0001	-2.3219	<0.0001
MENSSEN_MYC_TARGETS	52	-2.2803	<0.0001	-2.1716	<0.0001
YU_MYC_TARGETS_UP	40	-2.1026	<0.0001	-2.2127	<0.0001
ODONNELL_TARGETS_OF_MYC_AND_TFRC_DN	45	-1.9994	0.0004	-1.9883	0.0006
CAIRO_PML_TARGETS_BOUND_BY_MYC_UP	23	-1.9161	0.0015	-1.6278	0.0344
SCHUHMACHER_MYC_TARGETS_UP	80	-1.9014	0.0019	-2.2771	<0.0001
SCHLOSSER_MYC_TARGETS_REPRESSED_BY_SERUM	153	-1.8948	0.0021	-2.1315	0.0001
BENPORATH_MYC_TARGETS_WITH_EBOX	224	-1.8805	0.0025	-1.6005	0.0427
SANSOM_APC_TARGETS_REQUIRE_MYC	195	-1.8271	0.0049	-1.6294	0.0340
PID_MYC_ACTIVPATHWAY	77	-1.7735	0.0088	-1.7577	0.0107
MORI_EMU_MYC_LYMPHOMA_BY_ONSET_TIME_ UP	102	-1.7638	0.0098	-1.9423	0.0012
SCHLOSSER_MYC_AND_SERUM_RESPONSE_ SYNERGY	32	-1.7246	0.0142	-1.5919	0.0448
KIM_MYC_AMPLIFICATION_TARGETS_UP	192	-1.6787	0.0216	-1.8727	0.0027
DANG_REGULATED_BY_MYC_UP	69	-1.5696	0.0484	-1.7749	0.0091
COLLER_MYC_TARGETS_UP	25	-1.5656	0.0498	-2.0411	0.0003
ACOSTA_PROLIFERATION_INDEPENDENT_MYC_ TARGETS_UP	77	-1.4380	0.1081	-1.4098	0.1455
SCHLOSSER_MYC_TARGETS_AND_SERUM_ RESPONSE_DN	47	-1.4123	0.1260	-1.9374	0.0012
BILD_MYC_ONCOGENIC_SIGNATURE	193	-1.4101	0.1277	-1.3748	0.1735

Table S4. Related to Figure 4. Human normal donor and patient characteristics.

Sample ID	Disease status	Age	Sex
HD513	Healthy donor	40 y	M
HD723	Healthy donor	48 y	F
HD863	Healthy donor	42 y	M
HD237	Healthy donor	40 y	M
HD703	Healthy donor	39 y	M
HD066	Healthy donor	35 y	M
HD167	Healthy donor	48 y	M
SDS438	SDS patient[a]	9 y	M
SDS132	SDS patient[a]	14 y	M
SDS640	SDS patient[a]	4 y	M
SDS221	SDS patient[a]	18 y	M
MDS247	Low-risk MDS patient[b]	62 y	M
MDS006	Low-risk MDS patient[b]	63 y	F
MDS020	Low-risk MDS patient[b]	72 y	F
MDS159	Low-risk MDS patient[b]	75 y	F
MDS209	Low-risk MDS patient[b]	79 y	F
MDS222	Low-risk MDS patient[b]	66 y	F
MDS610	Low-risk MDS patient[b]	65 y	F
MDS627	Low-risk MDS patient[b]	80 y	M
MDS008	Low-risk MDS patient[b]	65 y	F
DBA044	DBA patient	1 y	F
DBA087	DBA patient	4 mo	M
DBA563	DBA patient	4 y	F

[a]All SDS patients were genetically characterized by compound heterozygosity c.183_184TA>CT/c.258+2T>C. Patients did not receive G-CSF treatment and were not diagnosed with MDS or AML at the time of bone marrow sampling. All patients presented with pancreatic insufficiency (serum trypsinogen level <6 µg/L) and growth retardation (≤ 2 SD). All patients but SDS438 were neutropenic at sampling (absolute neutrophil counts, ANC < 1.5×10^9/l); SDS438 had ANC = 1.62×10^9/l).

[b]See Table S6 for further patient characteristics.

Table S5. Related to Figure S5. In vitro exposure of HSPCs to S100A8/9 activates transcriptional signatures related to TLR signaling and cellular stress/apoptosis.

Gene set	NES	P-val	FDR q-val
Toll-like receptor signaling			
BIOCARTA_TOLL_PATHWAY	1.60	0.014	0.404
REACTOME_TOLL_RECEPTOR_CASCADES	1.53	0.005	0.365
PID_TOLL_ENDOGENOUS_PATHWAY 0.043	1.49	0.043	0.380
KEGG_TOLL_LIKE_RECEPTOR_SIGNALING_PATHWAY	1.46	0.012	0.428
REACTOME_ACTIVATED_TLR4_SIGNALLING	1.44	0.025	0.444
REACTOME_INNATE_IMMUNE_SYSTEM	1.56	0.0001	0.374
Activation of p53 and apoptosis pathways			
REACTOME_P53_DEPENDENT_G1_DNA_DAMAGE_RESPONSE	1.52	0.017	0.364
INGA_TP53_TARGETS	1.62	0.019	0.363
RASHI_RESPONSE_TO_IONIZING_RADIATION_1	1.68	0.005	0.326
DAZARD_UV_RESPONSE_CLUSTER_G2	1.69	0.006	0.314
AMUNDSON_GAMMA_RADIATION_RESISTANCE	1.71	0.009	0.316
KEGG_APOPTOSIS	1.74	0.001	0.260
KEGG_P53_SIGNALING_PATHWAY	1.78	0.001	0.217

Table S6. Related to Figure 6. MDS patient characteristics at beginning of treatment and clinical outcome. Provided as an Excel file. All patients were treated with lenalidomide in the context of an ongoing prospective clinical trial (details in Experimental Procedures). Patients were studied of which sufficient bone marrow material was available for analysis. Survival data are calculated from date of study-entry. [a]Not calculated, missing cytogenetics. Hb, hemoglobin. PLT, platelets. WBC, white blood cells. ANC, absolute neutrophil count. *S100A8* and *S100A9* expression is obtained by RNA-sequencing data. *P*-values were calculated by Mann-Whitney test.

Patient ID	WHO	Cytogenetics	IPSS	LR-PSS score	LR-PSS category	Outcome
S100 niche signature^{+}						
MDS020	RCMD-RS	46,XX[20]	0.5	4	2	Death
MDS267	RCMD	46,XY[20]	0.5	4	2	Death
MDS486	RAEB-1	46,XX,t(3;3)(q21;q26)[10]	0.5	4	2	Death
MDS610	RCMD-RS	46,XX[20]	0.5	3	2	Leukemia
MDS314	Del(5q)	46,XX,del(5)(q13q33)[25]/46,XX[5]	0	2	1	Death
MDS008	RCMD	46,XX[20]	0	4	2	Death
Mean (SD)						
S100 niche signature^{-}						
MDS247	RCMD-RS	46,XY[20]	0	3	2	Alive
MDS006	RAEB-1	46,XX[20]	1	5	3	Death
MDS118	RARS	46,XX[20]	0	1	1	Alive
MDS159	Del(5q)	46,XX,del(5)(q15q33)[10]	0	3	2	Death
MDS222	RARS	46,XX[21]	0	4	2	Alive
MDS209	RCMD-RS	46,XX[10]	0	3	2	Death
MDS025	RCMD-RS	46,XY[20]	0.5	3	2	Death
MDS146	RARS	46,XY[20]	0.5	4	2	Alive
MDS433	RCMD-RS	45,X,-Y[10]/46,XY[10]	0	2	1	Alive
MDS646	RAEB-1	46,yy[20]	1	5	3	Death
MDS893	RARS	46,XX[20]	0	3	2	Death
MDS111	RCMD	46,XX[20]	0.5	3	2	Alive
MDS623	RCMD	46,XY[20]	0.5	4	2	Alive
MDS067	RCMD-RS	not available	1	[a]	[a]	Alive
Mean (SD)						
MW P-value						

Table S6. Related to Figure 6. MDS patient characteristics at beginning of treatment and clinical outcome. Provided as an Excel file. *(Continued)* All patients were treated with lenalidomide in the context of an ongoing prospective clinical trial (details in Experimental Procedures). Patients were studied of which sufficient bone marrow material was available for analysis. Survival data are calculated from date of study-entry. [a]Not calculated, missing cytogenetics. Hb, hemoglobin. PLT, platelets. WBC, white blood cells. ANC, absolute neutrophil count. *S100A8* and *S100A9* expression is obtained by RNA-sequencing data. *P*-values were calculated by Mann-Whitney test.

Patient ID	Age (y)	Hb (mmol/l)	PLT ($x10^3$/ul)	WBC ($x10^3$/ul)	ANC (/ul)	Blasts (%)	S100A8 (FPKM)	S100A9 (FPKM)
***S100** niche signature*$^+$								
MDS020	72	8.1	69	5.5	76	1%	889	450
MDS267	80	5.7	153	10.3	57	3%	724	293
MDS486	66	5.3	530	12.4	65	1%	1016	436
MDS610	65	5.9	249	4.2	27	3%	4853	1921
MDS314	38	6.3	100	8.9	56	2%	2255	540
MDS008	65	4.8	153	5.0	36	2%	2330	1029
Mean (SD)	64 (14)	6.0 (1.1)	209 (169)	7.7 (3.3)	53 (18)	2% (0.9%)	2011 (1558)	778 (614)
S100 niche signature$^-$								
MDS247	62	4.0	587	4.0	56	0%	200	32
MDS006	63	5.1	73	2.8	14	5%	277	186
MDS118	56	4.3	391	3.8	39	0%	332	39
MDS159	75	5.4	327	8.4	55	1%	398	154
MDS222	66	5.0	185	15.7	70	2%	151	26
MDS209	79	5.2	240	3.5	52	0%	314	105
MDS025	85	5.4	264	2.6	50	1%	254	58
MDS146	85	5.5	163	3.9	33	1%	0,6	0
MDS433	58	4.8	248	4.5	56	1%	174	65
MDS646	74	5.3	65	3.4	18	5%	158	80
MDS893	85	6.0	501	5.3	59	1%	190	71
MDS111	62	4.2	118	2.8	51	3%	116	34
MDS623	73	5.8	74	7.6	83	2%	89	52
MDS067	74	6.1	107	2.7	62	2%	361	333
Mean (SD)	71 (10)	5.1 (0.6)	239 (163)	5.1 (3.5)	50 (19)	1.7%(1.6%)	215 (113)	88 (87)
MW P-value	0.4556	0.1040	0.6459	0.**0246**	0.6011	0.665	**<0.0001**	**<0.0001**

SUPPLEMENTAL EXPERIMENTAL PROCEDURES

Mice genotyping and sample collection

DNA was extracted from mouse toes with DirectPCR Lysis Reagent (Viagen Biotech). Genotyping and Cre-mediated recombination were verified on genomic DNA samples using the primers listed in the table below. Mouse bone marrow and bone fraction cells were isolated as previously described.[1] Red blood cells (RBC) were lysed with ACK lysing buffer (Lonza) before surface markers staining. Peripheral blood was collected from the submandibular vein in K_2EDTA-coated microtainers (BD) and analyzed using a Vet ABC counter (Scil Animal Care).

Genotyping primers used in the study.

Target	Allele	Primer ID	Sequence	Amplicon size (bp)
Sbds	Wild-type	a	CCAGGGTCACGTTAATACAAACC	329
		b	TGAGTTTCAATCCTCAGCATCC	
	Floxed	a	CCAGGGTCACGTTAATACAAACC	450
		b	TGAGTTTCAATCCTCAGCATCC	
	Recombined	c	TAAAACAAAGCTGCGGTCAAGA	319
		d	ATCCTCAGCATCCCGAACAA	
Sp7 (Osx)	Wild type	e	CTCTTCATGAGGAGGACCCT	No band
		f	GCCAGGCAGGTGCCTGGACAT	
	Cre	e	CTCTTCATGAGGAGGACCCT	500
		f	GCCAGGCAGGTGCCTGGACAT	
Trp53	Wild-type	10.1	GTTAAGGGGTATGAGGGACA	400
		10.2	GAAGACAGAAAAGGGGAGGG	
	Floxed	10.1	GTTAAGGGGTATGAGGGACA	600
		10.2	GAAGACAGAAAAGGGGAGGG	
	Recombined	1.1	CACAAAAACAGGTTAAACCCAG	612

Bone mineral density and 3-point bending test analysis

Cortical BMD was calculated from µCT cortical data on the basis of a calibration scanning obtained using two phantoms with known density (0.25 g/cm^3 and 0.75 g/cm^3; Bruker MicroCT) under identical conditions as for the femurs. For the bending test, femurs were placed in a custom-modified Single Column Lloyd LRX System bending device (Lloyd Instruments) and analyzed as previously reported (van der Eerden et al., 2013) using CtAnalyzer software (Bruker MicroCT).

Goldner's Masson trichrome staining

Femurs were embedded in methylmetacrylate as indicated before.[2] Sections of 6 µm were deacrylated, hydrated and stained accordingly to the previously described protocol.[3] Images of the metaphysial area were captured with a Nikon Eclipse E400 system (Nikon) using a 20X objective lens. Data was analyzed using Image J software (http://imagej.nih.gov/ij/). Briefly, the bone surface was manually selected and the perimeter length calculated. Osteoblasts were manually identified based on staining and morphology. The frequency of osteoblasts was calculated as percentage of osteoblast area in the bone surface and as number of osteoblasts per mm of bone.

CFU-F assay

Primary bone fraction cells were resuspended in growth medium, consistent of αMEM, 20% FBS (Life Technologies), and Penicillin-Streptomycin solution (Life Technologies), and cultured under hypoxic conditions (5% O_2, 5% CO_2) in 24-well plates (seeding density: 6.5 x 10^4 cells/cm^2). After 24h, the medium was changed to eliminate non-adherent cells. Colonies were stained after 7 days of culture. Briefly, medium was removed and cells were fixed 5' in methanol, stained in a 1:20 dilution of Giemsa staining (Merck Millipore) in distilled water and rinsed with tap water. Colonies were counted with an Olympus CK2 inverted microscope, using a 10X magnification.

Primary cell isolation and flow cytometry

All FACS antibodies incubations were performed in PBS+0.5%FCS for 20 min on ice. To identify hematopoietic stem and progenitor cells (HSPCs), bone marrow cells were first co-stained with a cocktail of biotin-labelled antibodies against the following lineage (Lin) markers: Gr1 (RB6-8C5), Mac1 (M1/70), Ter119 (TER-119), CD3e (145-2C11), CD4 (GK1.5), CD8 (53-6.7) and B220 (RA3-6B2) (all from BD Biosciences). After washing, cells were incubated with Pacific Orange-conjugated streptavidin (Life Technologies) and the following antibodies: Pacific Blue anti-Sca1 (D7), FITC or PE anti-CD48 (HM48-1), PE-Cy7 anti-CD150 (TC15-12F12.2) (all from Biolegend), APC anti-c-Kit (2B8, BD Biosciences).

To analyze differentiated cells and define chimerism, we used FITC anti-Gr1 (RB6-8C5), APC anti-Mac1 (M1/70), PE anti-B220 (RA3-6B2), APC-Cy7 anti-CD45.1 (A20), PE-Cy7 anti-CD45.2 (104), all from Biolegend. To identify stromal cells, bone fraction cell suspension was stained with the following antibodies: APC-Cy7 anti-CD45.2 (104), BV510 anti-Ter119 (TER-119), PE-Cy7 anti-CD105 (MJ7/18) (all from Biolegend), PE-CF594 anti-CD31 (MEC 13.3, BD Biosciences).

For human mesenchymal cell isolation, bone marrow aspirates were diluted 1:25 with red blood cell lysis solution (NH_4Cl 0.155 M, $KHCO_3$ 0.01 M, EDTA-Na2.2H2O 0.1 M, pH 7.4) and incubated for 10 min at room temperature. Cells were collected by centrifugation and washed once with PBS+0.5%FBS. For FACS sorting, immunostaining was performed with the same protocol used for murine bone marrow, using PE CD271 (ME20.4) and PE-Cy7 CD45 (HI30) antibodies (Biolegend). $CD271^+$ cells did not contain erythroid cells based on staining with BV421 CD235a (GA-R2, BD Biosciences).

Apoptosis was assayed with FITC Annexin V Apoptosis Detection Kit I (BD Biosciences) according to the recommendation of the manufacturer. Dead cells were excluded based on 7AAD staining.

The content of p53 in stromal cells was analyzed after cell surface antibody staining and cell permeabilization, obtained with Cytofix/Cytoperm Fixation/Permeabilization Solution Kit (BD Biosciences), by incubating cells with Alexa Fluor 647 anti-p53 (1C12) diluted in 1X Perm/Wash buffer (BD Biosciences).

All FACS events were recorded using a BD LSR II Flow Cytometer and analyzed with FlowJo 7.6.5 software (Tree Star). Cells were sorted with a BD FACSAria III.

SBDS mutation analysis

Mutations in *SBDS* were evaluated in the RNA sequencing data of SDS patients and healthy controls using the Integrative Genomics Viewer (IGV).[4] The c.183_184TA>CT mutation was quantified by annotating the number of reads presenting each of the four different nucleotides for both the positions 183 and 184. Because of its intronic position, the c.258+2T>C mutation was assessed by quantifying the usage of the 251-252 cryptic donor site.[5] Specifically, we quantified the fraction of spliced reads with an 8-bp deletion (nucleotides 251-258) as an indication of the mutated genotype.

Mitochondrial membrane potential quantification

After staining cells for surface antigens, cells were washed in PBS+0.5%FBS and centrifuged. Cells were resuspended in PBS+0.5%FBS and tetramethylrhodamine methyl ester (TMRM, Life Technologies) was added from a 10 µM stock solution in DMSO to a final non-quenching concentration of 100 nM. After incubation for 20 min at 37°C, cells were washed with PBS+0.5%FBS and analyzed. Cells treated with 1 µM p-trifluoromethoxy carbonyl cyanide phenyl hydrazone (FCCP) were used as positive control for membrane depolarization.

ROS detection

After surface antigen staining, cells washed in PBS+0.5%FBS and centrifuged. A stock solution of 2.5 µg/µl 5-(and-6)-chloromethyl-2',7'-dichlorodihydrofluorescein diacetate acetyl ester (CM-H2DCFDA, Life Technologies) in DMSO was diluted with PBS+0.5%FBS to a final concentration of 3 µg/µl. Cells were resuspended with the CM-H2DCFDA solution and stained for 20 min at 37°C, washed in PBS+0.5%FBS and analyzed.

Cell cycle analysis

Mice labeled in vivo by BrdU were sacrificed and bone marrow cells were stained for surface antigen. BrdU staining was performed using the FITC BrdU Flow Kit (BD Biosciences) following the manufacturer's instructions.

For in vitro cell cycle analysis, cultured cells were first stained for surface markers and then fixed and permeabilized with Cytofix/Cytoperm Fixation/Permeabilization Solution Kit (BD Biosciences). After washing, cells were incubated cells with FITC anti-Ki67 (B56, BD Biosciences) diluted in 1X Perm/Wash buffer (BD Biosciences) for 20 min and then washed. Cells were resuspended in PBS+0.5%FBS and 7AAD was added to detect DNA.

Alkaline comet assay

HSPCs were resuspended in 0.7% low melting agarose (Sigma-Aldrich) in PBS at a concentration of 10^5 cells/ml. 50 µl of cell suspension were spread on CometSlides (Trevigen) and the agarose was allowed to solidify for 30 min at 4°C. Slides were incubated for 1 h at 4°C in lysis buffer (1% Triton-X100 freshly added to 2.5M NaCl, 100 mM EDTA, 10 mM Tris/pH10 solution) protected from light and placed in an electrophoresis tray. After 20 min incubation in alkaline solution (200mM NaOH, 1mM EDTA, freshly prepared), unwound DNA was run in the same solution for 30 min at 1 V/cm. After electrophoresis, slides were washed twice in distilled water for 5 min, fixated in 70% ethanol for 5 min and allowed to dry at 37°C. DNA was stained for 5 min in SYBR Gold (Life Technologies), washed in distilled water and allowed to dry in the dark. Images were captured with a Leica DMRXA fluorescent microscope (10X magnification). DNA damage severity was manually quantified according to the score system depicted in Figure S3D.

Competitive transplantation

Bone marrow cells from OCS and BL6.SJL mice were isolated and RBC-depleted as described above. BL6.SJL cells were mixed in a 1:1 ratio with cells from $OCS^{f/+}$ of $OCS^{f/f}$ mice. 9 week-old B6.SJL mice were lethally irradiated (8.5Gy) and transplanted with a total of 10^6 bone marrow cells. Recipients received antibiotics in the drinking water for 2 weeks after transplantation.

S100A8/9 measurements

To quantify intracellular levels of S100A8/9 proteins, bone fraction cell suspensions were first stained for surface markers and next fixated and permeabilized with Cytofix/Cytoperm Fixation/Permeabilization Solution Kit (BD Biosciences) according to the manufacturer's instructions. Cells were then resuspended in 1X Perm/Wash buffer (BD Biosciences) and incubated for 20 min with polyclonal rabbit antibodies against mouse S100A8 or S100A9.[6] After washing, cells were incubated for 20 min with Pacific Orange-labelled goat anti-rabbit secondary antibody (Life Technologies) diluted in 1X Perm/Wash buffer, washed and resuspended in PBS+0.5%FBS and analyzed by FACS.

To analyze the concentration of S100A8/9 in the plasma, peripheral blood was collected in Microtainer PST tube (BD) and centrifuged to collect the plasma fraction. Samples were stored at -80°C until the moment of analysis. S100A8/9 was quantified by ELISA as previously described.[6]

Immunohistochemical staining of low-risk MDS and age-matched controls (biopsies obtained for disease staging from lymphoma patients without evidence of intramedullary localization) were performed on 5 µm bone marrow sections, which were deparaffinized in xylene and hydrated in a graded series of alcohol. Antigen retrieval was achieved by microwave treatment in citrate buffer (10mM pH 6.0) and blocking of the endogenous peroxidases was performed with 3% H_2O_2 in PBS. Sections were blocked using 10% normal human and goat serum (DAKO) in Teng-T solution followed by overnight incubation at 4°C with primary antibody anti-S100A8 and S100A9[6] diluted 1:500, CD271 (Sigma Aldrich) diluted 1:200, or normal rabbit immunoglobulin (DAKO) diluted accordingly. Immunoreactions were detected using biotinylated secondary antibody (goat anti-rabbit, 1:2000 dilution) with Vectastain ABC Elite Kit (Vector Laboratories) and 3,3'-diaminobenzidine tetrahydrochloride (Sigma Aldrich). For all stainings, nuclei were counterstained with haematoxylin (Vector Laboratories). Images of the stained tissue were acquired using a Leica DM5500B upright microscope with 40x lenses and LAS-AF image acquisition software.

HSPCs in vitro culture, S100A8/A9 exposure and CFU-C assay

LKS and Lin$^-$ c-Kit$^+$ Sca-1$^-$ cells were sorted from wild type C57BL/6 mice and cultured in a serum-free medium, with the following composition: X-Vivo 15 (Lonza), 1% detoxified BSA, 50 µM β-mercaptoethanol (Life Technologies), 1:100 GlutaMAX™ Supplement (Life Technologies), 20 ng/ml recombinant murine SCF (Peprotech), 100 ng/ml recombinant murine Flt3-Ligand (Peprotech), 1:100 penicillin-streptomycin mixture (Life Technologies). The medium was supplemented with recombinant murine S100A8/9, produced with the same methods described earlier,[7] at a final, clinically relevant concentration of 25-50 µg/ml, in the range of concentrations measured in the bone marrow supernatants of MDS patients[8]. A heat-inactivated control was obtained by incubating S100A8/9 at 80°C for 30 min; the protein was cooled-down and next added to the HSPC medium with the same concentration and volume as S100A8/9. LKS and Lin$^-$ c-Kit$^+$ Sca-1$^-$ cells were cultured in 96-well plates at a cell density of 2.5x10^4 cells/well.

For human studies, cryopreserved CD34$^+$ cells were used, which were isolated from cord blood obtained under informed consent by Ficoll gradient and MACS separation (Miltenyi Biotec). Thawed cells were resuspended in StemSpan SFEM II (STEMCELL Technologies) and recombinant human S100A8/9 was added (R&D systems) at a final concentration of 50 µg/ml. For the control medium, an equal volume of vehicle (PBS) was added. Cells were seeded in flat bottom 96 well-plates (5x10^4 cells/well).

For both mouse and human studies, cells were harvested at 4h for γH2AX and cell cycle studies and at 24 h for apoptosis assay.

To assess the effect of S100A9 on HSPC function, CD34$^+$ cord blood cells were resuspended in SFEM1 medium (Stemcell Technologies) containing SCF (50 ng/ml) and human recombinant S100A9 (2.5 µg/ml,ProSpec) or PBS control and seeded in 96-well plates (2x10^4 cells/well). After one week of preconditioning (37ºC, 5% CO_2), cells were pooled. 2,000 cells per condition were resuspended in 400 µl IMDM and transferred to 3.6 ml of MethoCult H84434 (Stemcell Technologies). Cells were plated in triplicate on 1 cm² petri-dishes (1 ml/dish) and incubated at 37ºC/5% CO2. Colonies were counted after 12-14 days.

SUPPLEMENTAL REFERENCES

1. Raaijmakers MH, Mukherjee S, Guo S, et al. Bone progenitor dysfunction induces myelodysplasia and secondary leukaemia. *Nature*. 2010;464(7290):852-857.
2. Derkx P, Nigg AL, Bosman FT, et al. Immunolocalization and quantification of noncollagenous bone matrix proteins in methylmethacrylate-embedded adult human bone in combination with histomorphometry. *Bone*. 1998;22(4):367-373.
3. Gruber HE. Adaptations of Goldner's Masson trichrome stain for the study of undecalcified plastic embedded bone. *Biotech Histochem*. 1992;67(1):30-34.
4. Robinson JT, Thorvaldsdottir H, Winckler W, et al. Integrative genomics viewer. *Nat Biotechnol*. 2011;29(1):24-26.
5. Boocock GR, Morrison JA, Popovic M, et al. Mutations in SBDS are associated with Shwachman-Diamond syndrome. *Nature Genetics*. 2003;33(1):97-101.
6. Vogl T, Eisenblatter M, Voller T, et al. Alarmin S100A8/S100A9 as a biomarker for molecular imaging of local inflammatory activity. *Nat Commun*. 2014;5:4593.
7. Vogl T, Leukert N, Barczyk K, Strupat K, Roth J. Biophysical characterization of S100A8 and S100A9 in the absence and presence of bivalent cations. *Biochim Biophys Acta*. 2006;1763(11):1298-1306.
8. List, A. (2014). Myeloid-Derived Suppressor Cells & Altered Innate Immunity in MDS Pathogenesis. http://www.mds-foundation.org/wp-content/uploads/manual/ASH2014/6ListMDSF-ASH-253 12-5-14.pdf

Chapter 4

Low-risk myelodysplastic syndromes are characterized by a molecular signature of mesenchymal stress and inflammation

Si Chen,[1] Noemi A. Zambetti,[1] Athina M. Mylona,[1] Maria N. Adisty,[1] Remco M. Hoogenboezem,[1] Eric M.J. Bindels,[1] Mathijs A. Sanders,[1] Eline M.P. Cremers,[3] Dicky J. Lindenbergh-Kortleve,[2] Janneke N. Samsom,[2] Arjan A. van de Loosdrecht[3] and Marc H.G.P, Raaijmakers1

[1]Department of Hematology, Erasmus MC Cancer Institute, Rotterdam, The Netherlands

[2]Laboratory of Pediatrics, Division of Gastroenterology and Nutrition, Erasmus MC Cancer Institute, Rotterdam, The Netherlands

[3]Department of Hematology, VU University Medical Center, Cancer Center Amsterdam, Amsterdam, The Netherlands

Manuscript submitted

ABSTRACT

Myelodysplastic syndromes (MDS) have long been considered hematopoietic cell-autonomous disorders in which disease initiation and progression is exclusively driven by hematopoietic cell intrinsic genetic events. Recent experimental findings have challenged this view, implicating mesenchymal elements in the bone marrow microenvironment in disease pathogenesis. Translation of experimental findings to human disease is complicated by a lack of insight in the molecular wiring of primary, non-expanded, mesenchymal cells in MDS. Here, we describe massive parallel sequencing of prospectively isolated mesenchymal elements from human low-risk MDS, revealing a common molecular signature, characterized by cellular stress, activation of the NF-κB inflammatory pathway and upregulation of senescence associated secreted factors, including known negative regulators of hematopoiesis. The data comprise, to our knowledge, the first comprehensive transcriptional network analysis of primary mesenchymal elements in a hematopoietic disorder. They provide human disease relevance to earlier findings in mouse models, implicating the mesenchyme in disease pathogenesis and stressing the relevance of considering the tissue context in understanding hematopoietic disease.

INTRODUCTION

Myelodysplastic syndromes (MDS) are a heterogeneous group of hematopoietic disorders characterized by ineffective hematopoiesis and predisposition to leukemic transformation. Profiling of transcriptional, genetic and epigenetic events in hematopoietic cells has contributed markedly to the understanding and prognostication of these diseases, but their pathogenesis remains incompletely understood. The inability to faithfully recapitulate and propagate disease in xenograft models, as well as longstanding observations of abnormalities in *ex vivo* expanded bone marrow derived mesenchymal cells, have sparked a continuing debate about a potential facilitating role of accessory elements in disease pathogenesis.[1] This notion has been substantiated by experimental support, providing proof of principle that components of the hematopoietic stem and progenitor cell (HSPC) niche have the ability to initiate and facilitate disease progression in mice.[2-4] Specifically, genetic perturbation of mesenchymal bone lineage cells has the ability to induce MDS and AML, establishing an experimental concept of 'niche-induced' oncogenesis.[3,4] Alternatively, primary alterations in hematopoietic cells have the ability to alter mesenchymal niche components such that niche cells facilitate disease propagation in the context of xenograft transplantation.[5]

Together, these observations challenge the view that ineffective hematopoiesis and leukemic progression is exclusively driven by hematopoietic cell-autonomous events in human MDS. Translating experimental concepts to human disease, however, critically depends on our ability to interrogate primary mesenchymal elements from the diseased marrow, which has hitherto not been performed. Molecular insights from mesenchymal cells in MDS have largely been derived from small-scale gene expression assessments in *ex vivo* expanded, plastic adherent mesenchymal cells with uncertain significance to *in vivo* hematopoiesis. Here, we describe massive parallel whole transcriptome sequencing of prospectively isolated primary mesenchymal elements from low-risk MDS. The data reveal a defining molecular signature of NF-κB-mediated inflammation, senescence and upregulation of known negative regulators of hematopoiesis, establishing human relevance to concepts and mechanisms proposed in mouse studies.

MATERIALS AND METHODS

Patient characteristics (median age: 65, range: 38-80) are shown in supplemental Table 1. Bone marrow was collected at diagnosis and control marrow was obtained from donors for allogeneic transplantation (median age: 45, range: 35-61), after written informed consent. The use of human samples was approved by the Institutional Review Board of Erasmus Medical Center, the Netherlands, in accordance with the declaration of Helsinki.

FACS data were acquired on FACSAria III systems (BDBioscience) and analyzed by FlowJo software (version 7). Gating strategy and antibodies used are described in the supplemental Methods. Cells were directly sorted in TRIzol (Ambion). Smarter Ultra Low RNA kit for Illumina Sequencing (Clonetech) was used for cDNA synthesis according to the manufacturer's protocol. Sample preparation, sequencing, demultiplexing and alignment were performed as previously described with modifications specific to the application of Smarter kit (Supplemental Methods).[6] Immunohistochemistry was performed as previously described (Supplemental Methods).[7]

RESULTS AND DISCUSSION

Mesenchymal cells were prospectively FACS-isolated from bone marrow aspirates of low-risk MDS patients at diagnosis (*n* = 12, **Table S1**) and normal controls (*n* = 10) using previously established markers of primary bone marrow mesenchymal cells[8] (**Figure 1A**). The frequency of $CD45^-$ $7AAD^-$ $CD235a^-$ $CD31^-$ $CD271^+$ $CD105^+$ mesenchymal cells in MDS was not significantly different from normal bone marrow (**Figure 1B**) (0.019% ± 0.0086% of mononuclear cells (MNCs) vs. 0.022% ± 0.0066%, *P* = 0.819 by unpaired student t-test), and these cells comprised a small subset of $CD45^-$ $7AAD^-$ $CD235a^-$ 'niche' cells (10.41% ± 4.086% vs. 12.30% ± 5.052, *P* = 0.771) with the major constituent being $CD31^+$ endothelial cells (43.80% ± 7.243% vs. 38.28% ± 9.424%, *P* = 0.816). Together, the data indicate that the cellular composition of the niche remains relatively intact in low-risk MDS in this particular experimental context. The mesenchymal nature of $CD45^-$ $7AAD^-CD235a^-$ $CD31^-$ $CD271^+$ $CD105^+$ cells was confirmed molecularly by whole transcriptome analysis demonstrating significant abundance of transcripts encoding the defining membrane proteins (**Figure 1C**), established markers of mesenchymal stem cells (**Figure 1D**)[8,9], essential 'niche' factors governing the behavior of HSPCs (**Figure 1E**) and osteolineage markers (**Figure 1F**) compared to endothelial cells. Together, the data indicate the feasibility of prospective isolation and molecular characterization of highly purified primary mesenchymal elements in MDS using massive parallel sequencing.

Figure 1. Prospective isolation and molecular characterization of mesenchymal cells in low-risk MDS. (A) Flow cytometry approach to identify and isolate $7AAD^-$ $CD45^-$ $CD235a^-$ $CD271^+$ $CD105^+$ mesenchymal cells. (B) Frequency of mesenchymal cells in normal and MDS samples. (C-F) Transcriptional validation of the mesenchymal nature of $7AAD^-$ $CD45^-$ $CD235a^-$ $CD271^+$ $CD105^+$ cells, showing differential expression in comparison to endothelial subsets of (C) defining cell surface markers (CD271, CD105, CD31), (D) known mesenchymal markers (CD73, CD90, CD146), (E) established hematopoiesis-supporting cytokines (*CXCL12, ANGPT1, KitL*) and (F) bone lineage markers (*BGLAP, RUNX2, SPP1* and *ALPL*). FPKM: fragments per kilobase of exon per million fragments mapped. Figure C to figure F: Normal samples (*n* = 10); MDS samples (*n* = 12). Black bar: $CD271^+$ mesenchymal cells; white bar: $CD31^+$ endothelial cells. *FDR < 0.05; **FDR < 0.01; ***FDR < 0.001.

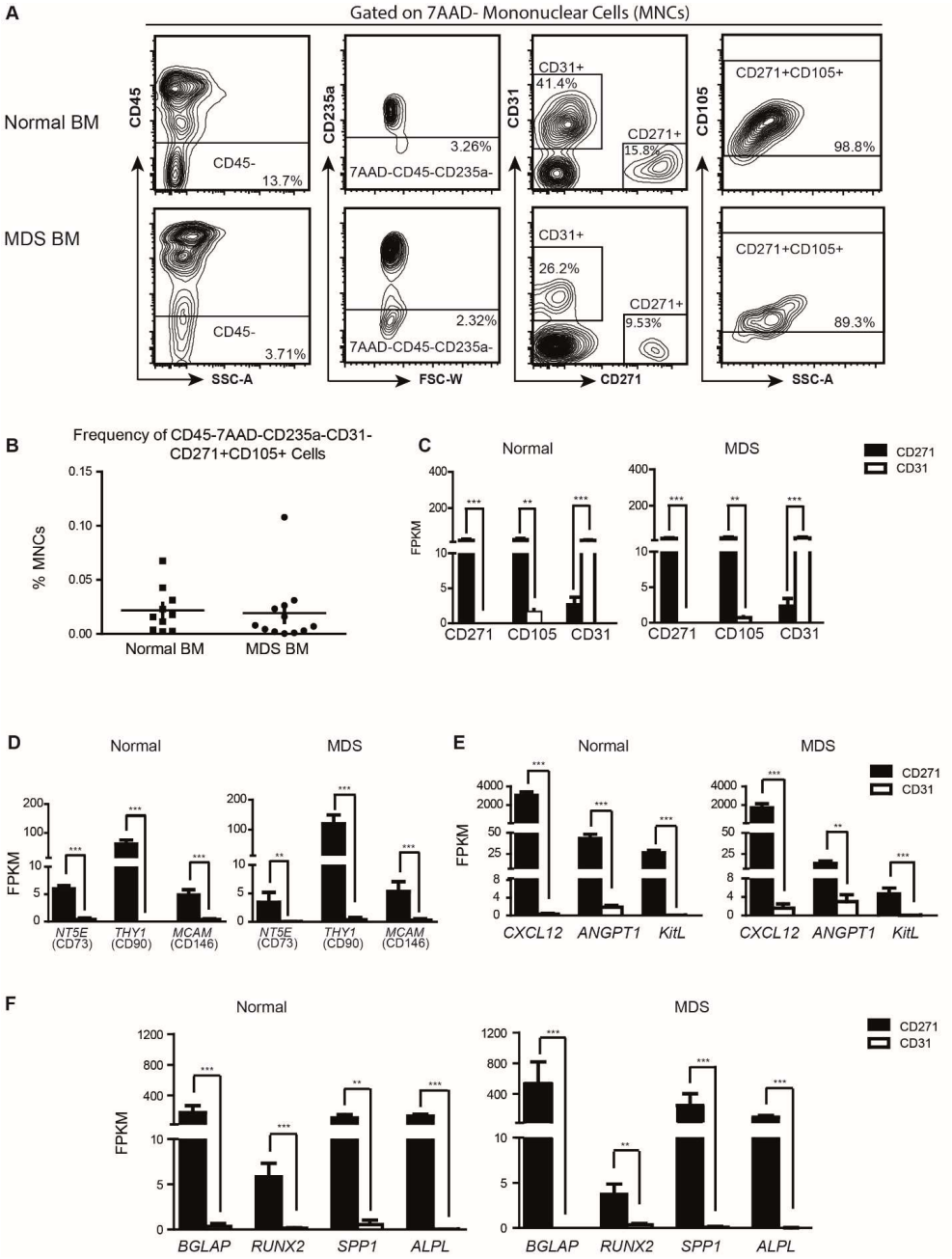
A
Gated on 7AAD- Mononuclear Cells (MNCs)
Normal BM
MDS BM
CD45
CD45-
13.7%
CD45-
3.71%
SSC-A
CD235a
3.26%
7AAD-CD45-CD235a-
2.32%
7AAD-CD45-CD235a-
FSC-W
CD31
CD31+
41.4%
CD271+
15.8%
CD31+
26.2%
CD271+
9.53%
CD271
CD105
CD271+CD105+
98.8%
CD271+CD105+
89.3%
SSC-A
B
Frequency of CD45-7AAD-CD235a-CD31-CD271+CD105+ Cells
% MNCs
Normal BM
MDS BM
C
Normal
MDS
CD271
CD31
FPKM
CD271
CD105
CD31
D
Normal
MDS
FPKM
NT5E (CD73)
THY1 (CD90)
MCAM (CD146)
E
Normal
MDS
CD271
CD31
FPKM
CXCL12
ANGPT1
KitL
F
Normal
MDS
CD271
CD31
FPKM
BGLAP
RUNX2
SPP1
ALPL

Principle component analysis (PCA) of transcriptomes demonstrated uniform clustering of normal mesenchymal cells, indicating transcriptional homogeneity (**Figure 2A**). Strikingly, distinct and more heterogeneous clustering of mesenchymal transcriptomes was found in low-risk MDS revealing that these cells are transcriptionally distinct from their normal counterparts. Distinct clustering remained present in an age-matched cohort (**Figure S1**), excluding the potential effect of age differences. Gene set enrichment analysis (GSEA) was then performed to define the molecular networks underlying the distinct transcriptional landscape in low-risk MDS. Gene sets associated with cellular stress induced by UV and ionizing radiation were remarkably enriched in low-risk MDS (**Figure 2B**; **Table S2**).

Cell cycle progression and metabolic signatures were significantly downregulated (**Table S2**), compatible with the view that these cells suffer from cellular stress, metabolic reprogramming, and may activate senescence programs. This notion is further supported by strong enrichment of transcriptional signatures of p53 activation and upregulation of several classic senescence-associated genes, including *CDKN1A* (p21) and *CDKN2D* (p19) (**Figure S2**).

Investigating potential pathways driving cellular stress, we found significant enrichment of inflammatory signatures (**Figure 2C**), in particular activation of the nuclear factor NF-κB family of transcription factors in low-risk MDS (**Figure 2C-D**; **Table S3**). Congruent with this finding, increased phosphorylation of p65, a component of the activated NF-κB complex, was found in bone-lining stromal cells, which were shown to be predominantly $CD271^+$ (**Figure S3**). Importantly, NF-κB activation in non-hematopoietic cells has been shown to induce 'MDS-like' disease in mice through upregulation of the Notch ligand Jagged-1[2]. Jagged-1, which drives hematopoietic abnormalities in another niche-induced mouse model of myeloid neoplasia,[4] was significantly overexpressed in mesenchymal cells from low-risk MDS (**Figure 2E**), thus directly relating mouse modeling to human disease.

Activation of NF-κB has recently been identified as a major driver of cellular senescence[10] and the senescence-associated secretory phenotype (SASP),[11,12] implicated in alteration of the tumor microenvironment and progression of (pre)malignant phenotypes.[13,14] Transcript abundance analysis revealed significant upregulation of numerous SASP factors (**Table S4**), such as the canonical IL-6 and IL-8 cytokines and a large number of other secreted factors including a wide variety of factors previously demonstrated to be negative regulators of hematopoiesis, in particular erythropoiesis and B-lymphopoiesis, cell lineages that are typically affected in low-risk MDS (**Table S5** and references herein).

The finding of NF-κB activation in mesenchymal cells complements recent findings implicating activation of the NF-κB pathway in $CD34^+$ cells in the pathogenesis of low-risk MDS.[15] The combined findings suggest that in low-risk MDS, activation of NF-κB occurs in both hematopoietic

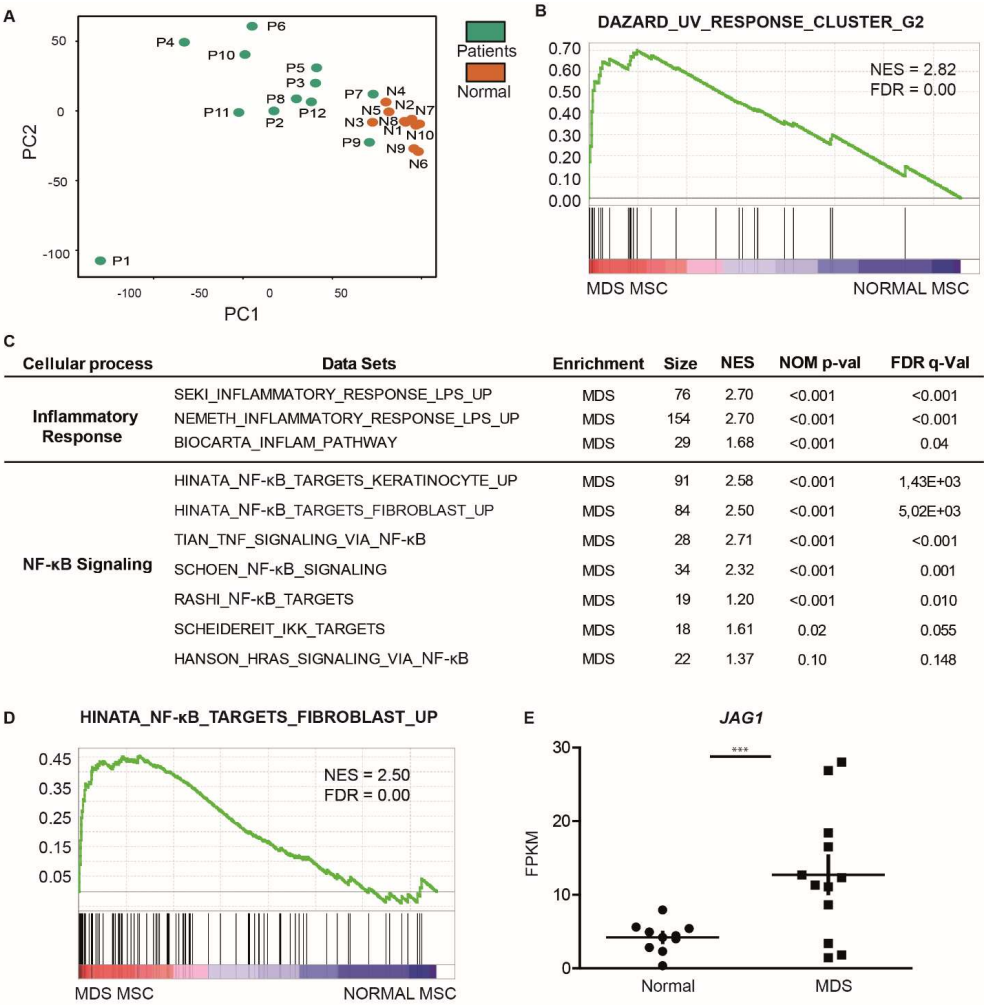

Cellular process	Data Sets	Enrichment	Size	NES	NOM p-val	FDR q-Val
Inflammatory Response	SEKI_INFLAMMATORY_RESPONSE_LPS_UP	MDS	76	2.70	<0.001	<0.001
	NEMETH_INFLAMMATORY_RESPONSE_LPS_UP	MDS	154	2.70	<0.001	<0.001
	BIOCARTA_INFLAM_PATHWAY	MDS	29	1.68	<0.001	0.04
NF-κB Signaling	HINATA_NF-κB_TARGETS_KERATINOCYTE_UP	MDS	91	2.58	<0.001	1,43E+03
	HINATA_NF-κB_TARGETS_FIBROBLAST_UP	MDS	84	2.50	<0.001	5,02E+03
	TIAN_TNF_SIGNALING_VIA_NF-κB	MDS	28	2.71	<0.001	<0.001
	SCHOEN_NF-κB_SIGNALING	MDS	34	2.32	<0.001	0.001
	RASHI_NF-κB_TARGETS	MDS	19	1.20	<0.001	0.010
	SCHEIDEREIT_IKK_TARGETS	MDS	18	1.61	0.02	0.055
	HANSON_HRAS_SIGNALING_VIA_NF-κB	MDS	22	1.37	0.10	0.148

Figure 2. Mesenchymal cells in low-risk MDS display a distinct molecular signature characterized by cellular stress and NF-κB-mediated inflammation. (A) PCA based on the entire transcriptome of normal and low-risk MDS mesenchymal cells. Patient numbers in the figure refer to MDS patient IDs (supplemental Table 1). (B) Representative GSEA plot demonstrating cellular stress in response to UV in low-risk MDS mesenchymal cells. (C) Summary of gene sets indicating inflammatory response and NF-κB activation in low-risk MDS mesenchymal cells. (D) Example of GSEA plot revealing activation of NF-κB signaling in the mesenchymal cells from low-risk MDS. (E) Expression level of *JAG1* (FPKM) in normal and low-risk MDS mesenchymal cells. Size: Data set gene size. NES: normalized enrichment score. FDR: false discovery rate. ***FDR < 0.001

and mesenchymal cells, likely through autocrine and paracrine feedback signaling networks, leading to overexpression of a repertoire of secreted negative hematopoietic regulators (**Figure S4**). Of interest, NF-κB mediated chronic tissue inflammation drives cancer initiation and progression in other systems,[16] warranting ongoing experiments defining the contribution of NF-κB activation to ineffective hematopoiesis and leukemic evolution in MDS.

Taken together, the data reveal a distinct transcriptional network of NF-κB activation-related inflammation and senescence characterizing the mesenchyme in low-risk MDS, translating findings in mouse models to human disease. The data comprises, to our knowledge, the first whole transcriptome analysis of highly purified, prospectively isolated, primary mesenchymal cells in a hematopoietic disorder, stressing its relevance in generating a comprehensive understanding of disease, considering the tissue context in addition to molecular and genetic events in hematopoietic cells. The findings further open the perspective that mesenchymal factors, in addition to hematopoietic cell autonomous characteristics, may be therapeutically targeted in low risk MDS.

ACKNOWLEDGEMENTS

The authors thank P. van Geel and Dr. W.J.C. Chikhovskaya - Rombouts for their technical support and prof. I. Touw for helpful comments on the manuscript. This work was supported by grants received from the Netherlands Organization for Scientific Research (NWO) (40-41009-98-11062) and the Dutch Cancer Society (2010-4733).

AUTHORSHIP

S.C. and M.H.G.P.R. designed studies; S.C., A.M.M., D.J.L.K. and M.N.A. performed experiments and acquired data; S.C., R.M.H., E.M.J.B., and M.A.S. provided technical guidance and bioinformatical analysis; J.N.S. provided helpful insights in immunohistochemical data analysis; E.M.P.C. and A.V.D.L. provided patient material; S.C. and M.H.G.P.R. wrote the manuscript; all authors were involved in data interpretation and manuscript reviewing, M.H.G.P.R. supervised the study.

Conflict-of-interest disclosure: The authors declare no competing financial interests

REFERENCES

1. Raaijmakers MH. Myelodysplastic syndromes: revisiting the role of the bone marrow microenvironment in disease pathogenesis. *Int J Hematol*. 2012;95:17-25.
2. Rupec RA, Jundt F, Rebholz B, et al. Stroma-mediated dysregulation of myelopoiesis in mice lacking I kappa B alpha. *Immunity*. 2005;22:479-491.
3. Raaijmakers MHGP, Mukherjee S, Guo SQ, et al. Bone progenitor dysfunction induces myelodysplasia and secondary leukaemia. *Nature*. 2010;464:852-U858.
4. Kode A, Manavalan JS, Mosialou I, et al. Leukaemogenesis induced by an activating beta-catenin mutation in osteoblasts. *Nature*. 2014;506:240-244.
5. Medyouf H, Mossner M, Jann JC, et al. Myelodysplastic cells in patients reprogram mesenchymal stromal cells to establish a transplantable stem cell niche disease unit. *Cell Stem Cell*. 2014;14:824-837.
6. Groschel S, Sanders MA, Hoogenboezem R, et al. A single oncogenic enhancer rearrangement causes concomitant EVI1 and GATA2 deregulation in leukemia. *Cell*. 2014;157:369-381.
7. van Dieren JM, Simons-Oosterhuis Y, Raatgeep HC, et al. Anti-inflammatory actions of phosphatidylinositol. *Eur J Immunol.* 2011;41:1047-1057.
8. Tormin A, Li O, Brune JC, et al. CD146 expression on primary nonhematopoietic bone marrow stem cells is correlated with in situ localization. *Blood*. 2011;117:5067-5077.
9. Dominici M, Le Blanc K, Mueller I, et al. Minimal criteria for defining multipotent mesenchymal stromal cells. The International Society for Cellular Therapy position statement. *Cytotherapy.* 2006;8:315-317.
10. Rovillain E, Mansfield L, Caetano C, et al. Activation of nuclear factor-kappa B signalling promotes cellular senescence. *Oncogene.* 2011;30:2356-2366.
11. Freund A, Patil CK, Campisi J. p38MAPK is a novel DNA damage response-independent regulator of the senescence-associated secretory phenotype. *EMBO J*. 2011;30:1536-1548.
12. Salminen A, Kauppinen A, Kaarniranta K. Emerging role of NF-kappaB signaling in the induction of senescence-associated secretory phenotype (SASP). *Cell Signal.* 2012;24:835-845.
13. Ohanna M, Giuliano S, Bonet C, et al. Senescent cells develop a PARP-1 and nuclear factor-{kappa}B-associated secretome (PNAS). *Genes Dev.* 2011;25:1245-1261.
14. Coppe JP, Desprez PY, Krtolica A, Campisi J. The senescence-associated secretory phenotype: the dark side of tumor suppression. *Annu Rev Pathol.* 2010;5:99-118.
15. Wei Y, Chen R, Dimicoli S, et al. Global H3K4me3 genome mapping reveals alterations of innate immunity signaling and overexpression of JMJD3 in human myelodysplastic syndrome CD34+ cells. *Leukemia.* 2013;27:2177-2186.
16. DiDonato JA, Mercurio F, Karin M. NF-kappaB and the link between inflammation and cancer. *Immunol Rev.* 2012;246:379-400.

SUPPLEMENTAL METHODS

Flow Cytometry Procedure and Cell Sorting

Bone marrow cells from patients and normal donors were stained on ice in dark with the following antibodies using optimized dilutions: CD45-PE-Cy7 (1:200), CD235a-BV421-A (1:100), CD271-PE (1:100), CD105-APC (1:50), CD31-APC-Cy7 (1:50). The indicated populations of interest were sorted using FACS ARIAIII Cell Sorter (BD) and the cells were directly sorted in Trizol (Ambion) (800 µl) for RNA isolation step. The RNAse-free non-stick Eppendorf tubes (Ambion) were used to prevent pre-digestion of RNA. Dead cells were gated out using 7AAD (Stem-Kit Reagents) after mononuclear cell selection and doublets exclusion.

RNA Extraction and RNA Quality Control

Total sample RNA isolation was performed according to the standard protocol of RNA isolation with Trizol and GenElute LPA (Sigma). Next, the RNA pellet was resuspended in 7.5 µl RNAse free water (Qiagen) and 1.2 µl was taken to check the quality and quantity of the total RNA with 2100 Bio-analyzer (Agilent) using the Agilent RNA 6000 Pico Kit. Samples were selected based on the quality of total RNA using Bio-analyzer RNA Integrity Number of 4 as cut-off. The whole procedure was performed in an RNAse free environment.

RNA Sequencing and Gene Expression Profiling

SMARTer Ultra Low RNA Kit (Clontech) for Illumina Sequencing was used to prepare the cDNA library. Before starting the library preparation, specific dilution of total RNA from each sample was carried out to ensure a comparable amount of starting material. cDNA library preparation steps were performed according to the user manual in a PCR-clean room to avoid contamination. The Agilent 2100 Bio-analyzer and the High Sensitivity DNA kit were applied to check the quality of the cDNA library. Once the cDNA libraries were obtained, the subsequent sample preparation steps, sequencing and alignments were performed as previously described.[1] Prior to sequence alignment, the SMARTer adapters were trimmed using the cutadapt program.[2] The resulting sequences were aligned to the human RefSeq transcriptome using TopHat2.[3] Sequences that could not be aligned to the RefSeq transcriptome were aligned to the reference genome (hg19). Normalization and quantification was performed using Cufflinks.[4] The resulting gene expression values are measured as FPKM. Differential expression analysis was performed on the fragment counts using the DESeq2[5] package in the R environment and the FDR multiple testing correction was applied. The required per-gene fragment counts were measured using the htseq-count

program using the strict intersection option. Principle component analysis was also performed on the fragment counts using the R environment. For all of the mentioned analysis, the RefSeq gene database was used. Finally we also performed GSEA on the gene expression values using the curated C2 collection of MSigDB.[6]

Immunohistochemistry

Immunohistochemical staining of low-risk MDS and age-matched controls were performed on 5 µm bone marrow sections, which were deparaffinized in xylene and hydrated in a graded series of alcohol. Antigen retrieval was achieved by microwave treatment in citrate buffer (10mM PH 6.0) and blocking of the endogenous peroxidases was performed with 3% H_2O_2 in PBS. Sections were blocked using 10% normal human and goat serum (DAKO) in Teng-T solution followed by overnight incubation at 4°C with primary antibody: serine 276 phosphorylated p65 (p-p65, active form; Santa Cruze Biotechonology) diluted 1:400, CD271 (Sigma Aldrich) diluted 1:200, or normal rabbit immunoglobulin (DAKO) diluted accordingly. Immunoreactions were detected using biotinylated secondary antibody (goat anti-rabbit, 1:2000 dilution) with Vectastain ABC Elite Kit (Vector Laboratories) and 3,3'-diaminobenzidine tetrahydrochloride (Sigma Aldrich). In all stainings, nuclei were counterstained with haematoxylin (Vector Laboratories). Images of the stained tissue were acquired using a Leica DM5500B upright microscope with 40x lenses and LAS-AF image acquisition software. The number of phospho-p65+ bone lining cells were manually quantitated using ImageJ software on x40 photomicrographs of blindly selected trabecular bone area. Unpaired t-test was performed and $P < 0.05$ was used to define significance.

SUPPLEMENTAL TABLES

Table S1. Patient Characteristics

Patient ID	Age	WHO	Cytogenetics	BM blasts	IPSS
MDS01	62	RCMD-RS	46, XY[20]	0%	0
MDS02	63	RAEB-1	46, XX[20]	5%	1
MDS03	72	RCMD-RS	46, XX[20]	1%	0.5
MDS04	75	Del(5q)	46, XX, del(5)(q15q33)[10]	1%	0
MDS05	79	RCMD-RS	46, XX[10]	0%	0
MDS06	66	RARS	46, XX[21]	2%	0
MDS07	56	RARS	46, XX[20]	0%	0
MDS08	80	RCMD	46, XY[20]	3%	0.5
MDS09	65	RCMD-RS	46, XX[20]	3%	0.5
MDS10	58	RCMD-RS	46, X, -Y[10]/46, XY[10]	1%	0
MDS11	38	Del(5q)	46, XX, del(5)(q13q33)[25]/46, XX[5]	2%	0
MDS12	65	RCMD	46, XX[20]	2%	0

The patient ID, age, WHO category (MDS WHO classification 2008), cytogenetic abnormalities, level of bone marrow blasts and the international prognostic scoring system (IPSS) of each patient are listed above (*n* = 12). BM blasts: bone marrow blasts.

Table S2. Transcriptional signatures reflecting cellular stress in mesenchymal cells from low-risk MDS patients

Data Set	Enrichment	Size	NES	NOM p-val	FDR q-val
DNA Damage and Stress Response					
GHANDHI_DIRECT_IRRADIATION_UP	MDS	106	2.40	<0.001	0.064
GHANDHI_BYSTANDER_IRRADIATION_UP	MDS	83	2.30	<0.001	0.001
DAZARD_UV_RESPONSE_CLUSTER_G24	MDS	26	2.26	<0.001	0.001
DAZARD_UV_RESPONSE_CLUSTER_G4	MDS	21	2.08	<0.001	0.006
DAZARD_UV_RESPONSE_CLUSTER_G28	MDS	20	2.44	<0.001	0.004
RASHI_RESPONSE_TO_IONIZING_RADIATION_1	MDS	45	1.68	<0.001	0.040
RASHI_RESPONSE_TO_IONIZING_RADIATION_2	MDS	127	2.42	<0.001	0.006
GENTILE_UV_LOW_DOSE_UP	MDS	27	2.68	<0.001	<0.001
GENTILE_UV_HIGH_DOSE_UP	MDS	25	2.26	<0.001	0.001
SESTO_RESPONSE_TO_UV_C3	MDS	20	2.13	<0.001	0.004
SESTO_RESPONSE_TO_UV_C1	MDS	72	1.95	<0.001	0.011
SESTO_RESPONSE_TO_UV_C5	MDS	46	1.79	<0.001	0.026
SESTO_RESPONSE_TO_UV_C0	MDS	107	1.42	<0.001	0.126
SMIRNOV_RESPONSE_TO_IR_2HR_UP	MDS	50	2.62	<0.001	0.049
SMIRNOV_RESPONSE_TO_IR_6HR_UP	MDS	163	1.65	<0.001	<0.001
MURAKAMI_UV_RESPONSE_6HR_UP	MDS	37	1.35	0.09	0.159
TSAI_RESPONSE_TO_RADIATION_THERAPY	MDS	32	2.25	<0.001	0.002
TSAI_RESPONSE_TO_IONIZING_RADIATION	MDS	149	1.81	<0.001	0.024
Cell Cycle and DNA Replication					
KEGG_DNA_REPLICATION	Normal	36	-1.67	<0.001	0.030
REACTOME_G2_M_CHECKPOINTS	Normal	41	-1.68	0.001	0.035
REACTOME_M_G1_TRANSITION	Normal	78	-1.67	<0.001	0.041
REACTOME_MITOTIC_M_M_G1_PHASES	Normal	169	-1.63	<0.001	0.057
REACTOME_DNA_REPLICATION	Normal	189	-1.63	<0.001	0.060
REACTOME_CELL_CYCLE_CHECKPOINTS	Normal	112	-1.60	0.002	0.075
REACTOME_REGULATION_OF_MITOTIC_CELL_CYCLE	Normal	77	-1.58	<0.001	0.096
REACTOME_CELL_CYCLE_MITOTIC	Normal	312	-1.50	<0.001	0.177
REACTOME_S_PHASE	Normal	106	-1.50	0.005	0.178
REACTOME_G1_S_TRANSITION	Normal	107	-1.48	0.005	0.203

The size of each individual gene set, normalized enrichment score (NES), nominal p-value (NOM p-val) and false discovery rate (FDR q-val) values are as listed.

Table S2. Transcriptional signatures reflecting cellular stress in mesenchymal cells from low-risk MDS patients *(Continued)*

Data Set	Enrichment	Size	NES	NOM p-val	FDR q-val
Metabolic Activities					
KEGG_PROPANOATE_METABOLISM	Normal	32	-1.52	0.011	0.152
KEGG_CITRATE_CYCLE_TCA_CYCLE	Normal	30	-1.52	0.029	0.155
KEGG_PYRIMIDINE_METABOLISM	Normal	97	-1.50	0.001	0.179
KEGG_FATTY_ACID_METABOLISM	Normal	42	-1.88	<0.001	0.002
KEGG_TRYPTOPHAN_METABOLISM	Normal	40	-1.70	0.001	0.030
KEGG_BUTANOATE_METABOLISM	Normal	34	-1.70	0.001	0.031
REACTOME_CITRIC_ACID_CYCLE_TCA_CYCLE	Normal	20	-1.59	0.010	0.082
REACTOME_SULFUR_AMINO_ACID_METABOLISM	Normal	24	-1.56	0.020	0.110

The size of each individual gene set, normalized enrichment score (NES), nominal p-value (NOM p-val) and false discovery rate (FDR q-val) values are as listed.

Table S3. Differential expression of bona fide downstream targets of NF-κB signaling in low-risk MDS mesenchymal cells

NF-κB target gene	Signature	Fold-change	FDR/*P*[a]
CXCL3	GSEA-Derived NF-κB Targets[7-12]	6.21	0.026
CXCL10	GSEA-Derived NF-κB Targets[7-12]	4.00	0.034
CCL5	GSEA-Derived NF-κB Targets[7-12]	2.71	0.036
CD83	GSEA-Derived NF-κB Targets[7-12]	4.27	0.034
CEACAM6	GSEA-Derived NF-κB Targets[7-12]	-2.48	0.024*
DUSP6	GSEA-Derived NF-κB Targets[7-12]	2.58	<0.001
DAPK1	GSEA-Derived NF-κB Targets[7-12]	-1.78	0.016*
FN1	GSEA-Derived NF-κB Targets[7-12]	2.00	0.037
GADD45A	GSEA-Derived NF-κB Targets[7-12]	1.80	0.010
IER3	GSEA-Derived NF-κB Targets[7-12]	3.60	0.020
IL8	GSEA-Derived NF-κB Targets[7-12]	7.24	<0.001
IL6	GSEA-Derived NF-κB Targets[7-12]	5.09	0.005
LITAF	GSEA-Derived NF-κB Targets[7-12]	407	<0.001
MAP3K8	GSEA-Derived NF-κB Targets[7-12]	2.18	0.001
NFKBIA	GSEA-Derived NF-κB Targets[7-12]	4.47	<0.001
NFKBIE	GSEA-Derived NF-κB Targets[7-12]	2.88	0.036
PLK2	GSEA-Derived NF-κB Targets[7-12]	2.16	0.020
SERPINB1	GSEA-Derived NF-κB Targets[7-12]	2.75	0.006
SOD2	GSEA-Derived NF-κB Targets[7-12]	3.18	0.002
VEGFA	GSEA-Derived NF-κB Targets[7-12]	2.67	<0.001
VIM	GSEA-Derived NF-κB Targets[7-12]	-1.93	0.028
BCL2L11	Online Database[13]	2.90	0.034
BMP2	Online Database[13]	4.83	0.017
BCL3	Online Database[13]	2.35	0.026
CD44	Online Database[13]	3.90	0.002
CCL3	Online Database[13]	4.21	0.022
CXCL9	Online Database[13]	6.73	0.023
CD69	Online Database[13]	6.26	0.023
EMR1	Online Database[13]	6.06	0.006*
FTH1	Online Database[13]	2.02	0.015
HIF1A	Online Database[13]	4.54	<0.001
IER2	Online Database[13]	3.60	0.020

Significantly differentially expressed genes in low-risk MDS mesenchyme were compared to experimentally defined NF-κB targets derived from GSEA signatures listed in Figure 2C[7-12] and online database.[13] FDR: false discovery rate. [a]The differential expression of these genes is *P*-significant instead of FDR-significant.

Table S3. Differential expression of bona fide downstream targets of NF-κB signaling in low-risk MDS mesenchymal cells *(Continued)*

NF-κB target gene	Signature	Fold-change	FDR/*P*[a]
INHBA	Online Database[13]	8.08	0.026
KDM6B (JMJD3)	Online Database[13]	5.21	<0.001
NR4A2	Online Database[13]	2.11	0.030
LTF	Online Database[13]	6.58	0.017
MYC	Online Database[13]	3.66	0.010
SLC16A1	Online Database[13]	3.24	0.012
S100A10	Online Database[13]	2.95	<0.001
S100A6	Online Database[13]	3.06	0.006
SOX9	Online Database[13]	6.11	0.001
SLC3A2	Online Database[13]	2.64	0.008
TMOD2	Online Database[13]	2.00	0.004

Significantly differentially expressed genes in low-risk MDS mesenchyme were compared to experimentally defined NF-κB targets derived from GSEA signatures listed in Figure 2C[7-12] and online database.[13] FDR: false discovery rate. [a]The differential expression of these genes is *P*-significant instead of FDR-significant.

Table S4. Upregulation of SASP factors in low-risk MDS mesenchymal cells

SASP factor gene	Fold-change	FDR/*P*[a]
Soluble factors and chemokines (CXCL, CCL)		
IL6 (interleukin 6)	5.10	0.005*
IL8 (interleukin 8)	7.24	<0.001
CCL3 (chemokine C-C motif ligand 3, MIP-1a)	4.21	0.022
CCL7 (chemokine C-C motif ligand 7, MCP-3)	9.65	0.006*
CXCL4 (chemokine C-X-C motif ligand 4, PF4)	6.96	0.005
CXCL14 (chemokine C-X-C motif ligand 14)	5.54	0.023
CXCL3 (chemokine C-X-C motif ligand 3)	6.23	0.026
Growth factors and regulators		
VEGFA (vascular endothelial growth factor A)	6.36	<0.001
IGFBP3 (insulin-like growth factor binding protein 3)	2.53	0.010*
IGFBP4 (insulin-like growth factor binding protein 4)	2.17	0.004*
IGFBP7 (insulin-like growth factor binding protein 7)	2.00	0.016*
Proteases and regulators		
TIMP1 (tissue inhibitor of metalloproteinases 1)	2.22	0.012
ISG15 (ISG15 ubiquitin-like modifier)	2.45	0.014*
SERPINB2 (serpin peptidase inhibitor, member 2)	4.11	0.029*
SMURF2 (SMAD specific E3 ubiquitin protein ligase 2)	2.46	0.029*
Soluble or shed receptors and ligands		
ICAM1 (intercellular adhesion molecule 1)	2.51	0.010
PLAUR (plasminogen activator, urokinase receptor, uPAR)	3.36	<0.001
Insoluble factors (ECM)		
FN1 (fibronectin 1)	2.00	0.037*
COL1A1 (collagen, type 1, alpha 2)	3.27	0.005
Other		
CLTB (clathrin, light chain, Lcb)	3.20	0.009*
CRYAB (crystalline, alpha B)	3.18	0.012
CYP1B1 (cytochrome P450, family 1, subfamily B, polypeptide 1)	2.22	0.004*
MAP1LC3B (microtubule-associated protein 1 light chain 3, beta)	2.75	0.016
NME2 (NME/NM23 nucleus diphosphate kinase 2)	1.83	0.020
RAC1 (Ras-related C3 botulinum toxin substrate 1, Rho family, small GTP binding protein)	1.75	0.020*
VIM (vimentin)	2.00	0.003*
MDM2 (Mdm2 p53 binding protein homolog)	2.13	0.029*

The differential expression of canonical SASP factors[14-16] is listed. FDR: false discovery rate. [a]The differential expression of these genes is *P*-significant instead of FDR-significant.

Table S5 Negative regulators of hematopoiesis upregulated in low-risk MDS mesenchymal cells

Gene name	Effect on hematopoiesis	FC	FDR/*P*[a]
TGFB1	Negative Regulator of Hematopoiesis[17]	4.44	0.048
S100A8	Negative Regulator of Erythropoiesis[18-19, 24]	4.44	0.024
S100A9	Negative Regulator of Erythropoiesis[18-19, 24]	4.56	0.028
CCL3	Negative Regulator of Erythropoiesis[18-19, 24]	4.21	0.022
IL8	Negative Regulator of Erythropoiesis[18-19, 24]	7.24	<0.001
INHBA	Negative Regulator of B-lymphopoiesis[20]	8.08	0.026
FTH1	Myelosuppressive Effects[21]	2.02	0.015
LTF	Myelosuppressive Effects[21]	6.58	0.017
CCL5	Myelosuppressive Effects[21]	2.71	0.036*
IL8	Myelosuppressive Effects[21]	7.24	<0.001
PF4 (CXCL4)	Negative Regulator of Megakaryopoiesis and HSCs activity[22-23]	6.96	0.005

The differential expression of known secreted negative regulators of hematopoiesis[17-24] is listed. FC: Fold change; FDR: false discovery rate. [a]The differential expression of these genes is *P*-significant instead of FDR-significant.

SUPPLEMENTAL FIGURES

A

Patient ID	Age	Median (range)
MDS01	62	58 (38-63)
MDS02	63	
MDS07	56	
MDS10	58	
MDS11	38	
Normal Donor	**Age**	**Median (range)**
N10410 (N1)	58	58 (48-61)
N14207 (N5)	61	
N08276 (N8)	58	
N12723 (N3)	48	
N14167 (N9)	48	

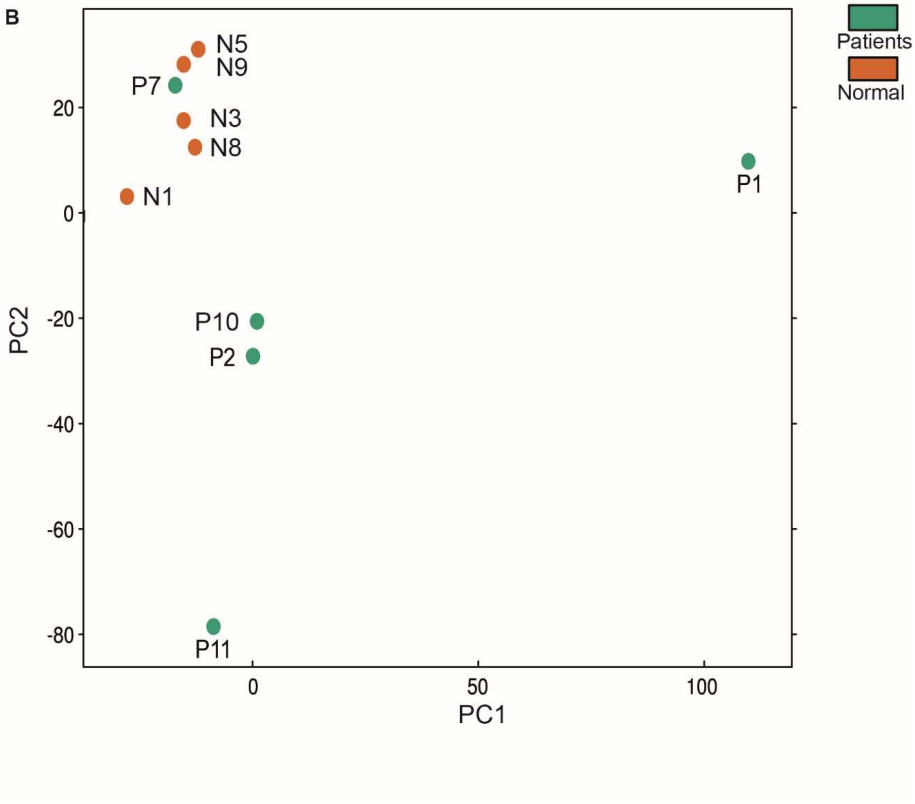

Figure S1. Principle component analysis (PCA) of an age-matched cohort of low-risk MDS and normal mesenchymal cells. (A) Patient and control characteristics. (B) PCA plot.

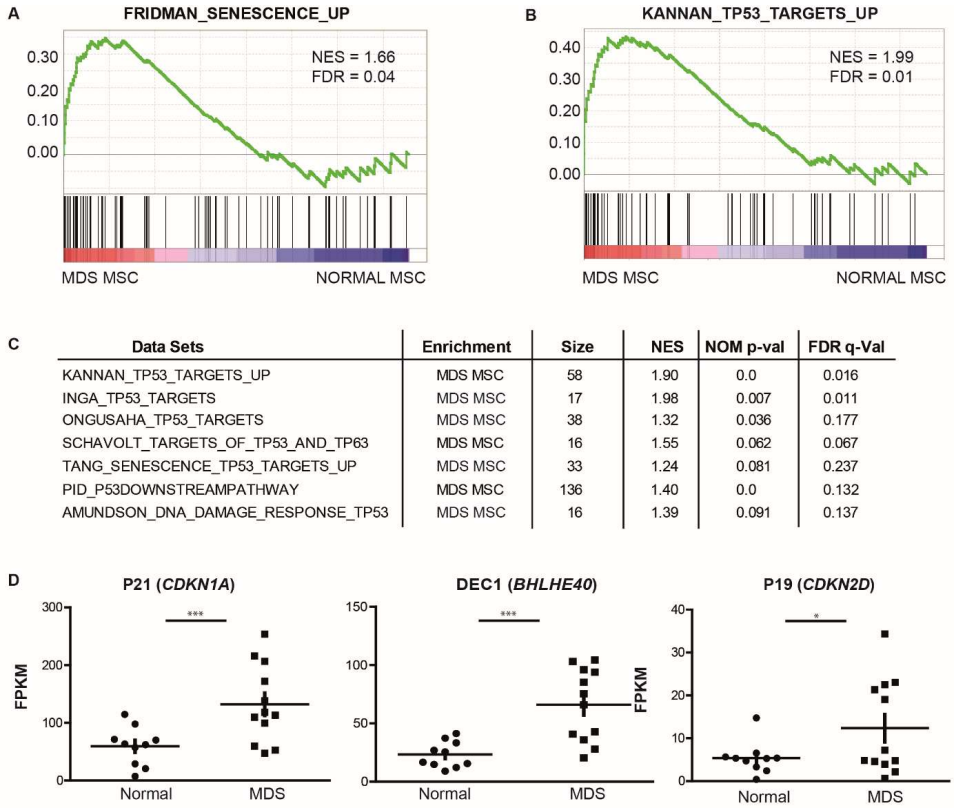

C

Data Sets	Enrichment	Size	NES	NOM p-val	FDR q-Val
KANNAN_TP53_TARGETS_UP	MDS MSC	58	1.90	0.0	0.016
INGA_TP53_TARGETS	MDS MSC	17	1.98	0.007	0.011
ONGUSAHA_TP53_TARGETS	MDS MSC	38	1.32	0.036	0.177
SCHAVOLT_TARGETS_OF_TP53_AND_TP63	MDS MSC	16	1.55	0.062	0.067
TANG_SENESCENCE_TP53_TARGETS_UP	MDS MSC	33	1.24	0.081	0.237
PID_P53DOWNSTREAMPATHWAY	MDS MSC	136	1.40	0.0	0.132
AMUNDSON_DNA_DAMAGE_RESPONSE_TP53	MDS MSC	16	1.39	0.091	0.137

Figure S2 (up). Transcriptional activation of p53 and senescence pathways in mesenchymal cells from low-risk MDS. (A-B) Representative GSEA plot of gene sets demonstrating enrichment of senescence programs (A) and p53 activation (B). (C) Significantly upregulated gene sets indicating activation of p53 signaling. (D) Expression level of senescence marker p19 and canonical downstream p53-mediated senescence markers p21 and DEC1.[25] NES: normalized enrichment score; FDR: false discovery rate. *FDR < 0.05; **FDR < 0.01; ***FDR < 0.001.

Figure S3 (right). NF-κB activation in CD271$^+$ endosteal cells in low-risk MDS. (A) Representative photomicrographs (original magnification x40) of the distribution of CD271$^+$ mesenchymal cells identified by immunohistochemistry (brown). CD271$^+$ cells are enriched at the endosteal surface and have a spindle-shaped morphology. (B) Representative immune-histochemical analysis (original magnification x40) of phospho-p65 (brown) in low-risk MDS (n = 2) (bottom panel) and age-matched controls (n = 2) (top panel), demonstrating NF-κB activation of spindle-shaped endosteal cells in low-risk MDS. (C) The percentage of phospho-p65$^+$ bone lining cells as a fraction of the total bone lining cells in low-risk MDS compared to age-matched controls. *P < 0.05

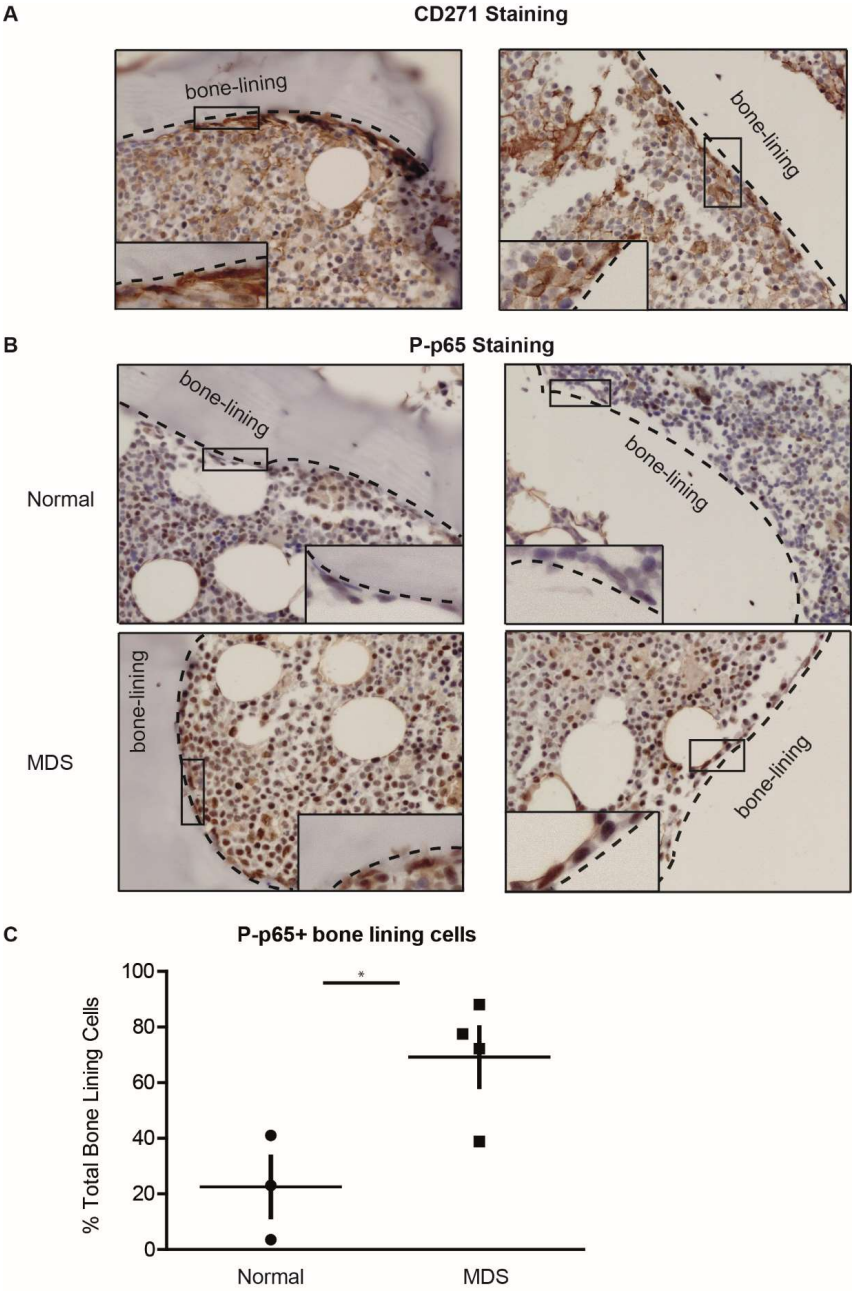
A
CD271 Staining
bone-lining
bone-lining
B
P-p65 Staining
Normal
bone-lining
bone-lining
MDS
bone-lining
bone-lining
C
P-p65+ bone lining cells
% Total Bone Lining Cells
100
80
60
40
20
0
*
Normal
MDS

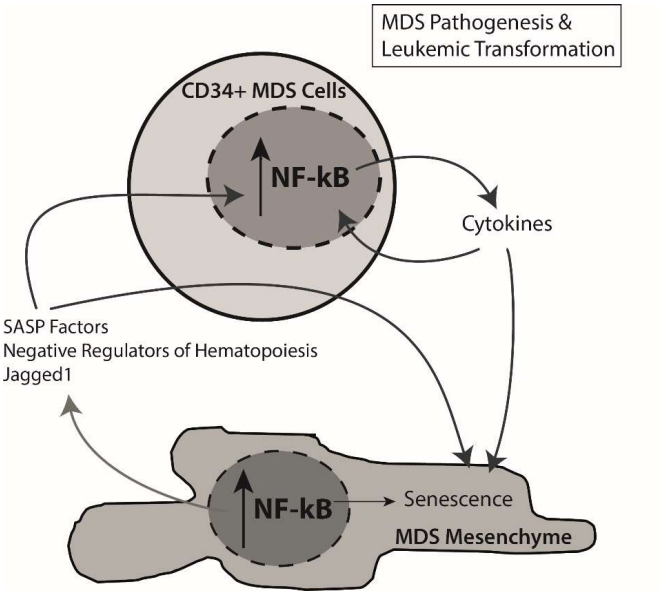

Figure S4. A working model of mesenchyme involvement in low-risk MDS pathogenesis: integration of transcriptional networking in human disease and mouse modeling. Activation of NF-κB in mesenchymal cells induces ineffective hematopoiesis and promotes malignant transformation through secretion of Jagged-1 and senescence associated factors, negatively affecting hematopoiesis and driving leukemic transformation. NF-κB activation may be maintained by autocrine/paracrine feedback signaling networks.

SUPPLEMENTAL REFERENCES

1. Groschel S, Sanders MA, Hoogenboezem R, et al. A single oncogenic enhancer rearrangement causes concomitant EVI1 and GATA2 deregulation in leukemia. *Cell*. 2014;157:369-381.
2. Martin M. Cutadapt removes adapter sequences from high-throughput sequencing reads. *EMBnet journal.* 2011;17:pp. 10-12.
3. Kim D, Pertea G, Trapnell C, Pimentel H, Kelley R, Salzberg SL. TopHat2: accurate alignment of transcriptomes in the presence of insertions, deletions and gene fusions. *Genome Biol.* 2013;14:R36.
4. Trapnell C, Roberts A, Goff L, et al. Differential gene and transcript expression analysis of RNA-seq experiments with TopHat and Cufflinks. *Nat Protoc*. 2012;7:562-578.
5. Anders S, Huber W. Differential expression analysis for sequence count data. *Genome Biol.* 2010;11:R106.
6. Subramanian A, Tamayo P, Mootha VK, et al. Gene set enrichment analysis: a knowledge-based approach for interpreting genome-wide expression profiles. *Proc Natl Acad Sci U S A.* 2005;102:15545-15550.
7. Hinata K, Gervin AM, Jennifer Zhang Y, Khavari PA. Divergent gene regulation and growth effects by NF-kappa B in epithelial and mesenchymal cells of human skin. *Oncogene.* 2003;22:1955-1964.
8. Hanson JL, Hawke NA, Kashatus D, Baldwin AS. The nuclear factor kappaB subunits RelA/p65 and c-Rel potentiate but are not required for Ras-induced cellular transformation. *Cancer Res.* 2004;64:7248-7255.
9. Tian B, Nowak DE, Jamaluddin M, Wang S, Brasier AR. Identification of direct genomic targets downstream of the nuclear factor-kappaB transcription factor mediating tumor necrosis factor signaling. *J Biol Chem*. 2005;280:17435-17448.
10. Rashi-Elkeles S, Elkon R, Weizman N, et al. Parallel induction of ATM-dependent pro- and antiapoptotic signals in response to ionizing radiation in murine lymphoid tissue. *Oncogene*. 2006;25:1584-1592.
11. Schon M, Wienrich BG, Kneitz S, et al. KINK-1, a novel small-molecule inhibitor of IKKbeta, and the susceptibility of melanoma cells to antitumoral treatment. *J Natl Cancer Inst*. 2008;100:862-875.
12. Scheidereit C. IkappaB kinase complexes: gateways to NF-kappaB activation and transcription. *Oncogene*. 2006;25:6685-6705.
13. Boston University Gene Source: NF-kB Target Genes. http://www.bu.edu/nf-kb/gene-resources/target-genes/. Accessed January 2, 2015
14. Coppe JP, Patil CK, Rodier F, et al. A human-like senescence-associated secretory phenotype is conserved in mouse cells dependent on physiological oxygen. *PLoS One*. 2010;5:e9188.
15. Coppe JP, Patil CK, Rodier F, et al. Senescence-associated secretory phenotypes reveal cell-nonautonomous functions of oncogenic RAS and the p53 tumor suppressor. *PLoS Biol*. 2008;6:2853-2868.
16. Coppe JP, Desprez PY, Krtolica A, Campisi J. The senescence-associated secretory phenotype: the dark side of tumor suppression. *Annu Rev Pathol*. 2010;5:99-118.
17. Kim SJ, Letterio J. Transforming growth factor-beta signaling in normal and malignant hematopoiesis. *Leukemia*. 2003;17:1731-1737.

18. Chen X, Eksioglu EA, Zhou J, et al. Induction of myelodysplasia by myeloid-derived suppressor cells. *J Clin Invest*. 2013;123:4595-4611.
19. Broxmeyer HE, Cooper S, Lu L, Miller ME, Langefeld CD, Ralph P. Enhanced stimulation of human bone marrow macrophage colony formation in vitro by recombinant human macrophage colony-stimulating factor in agarose medium and at low oxygen tension. *Blood*. 1990;76:323-329.
20. Nishihara T, Ohsaki Y, Ueda N, Koseki T, Eto Y. Induction of apoptosis in B lineage cells by activin A derived from macrophages. *J Interferon Cytokine Res*. 1995;15:509-516.
21. Broxmeyer HE, Cooper S, Hangoc G, Kim CH. Stromal cell-derived factor-1/CXCL12 selectively counteracts inhibitory effects of myelosuppressive chemokines on hematopoietic progenitor cell proliferation in vitro. *Stem Cells Dev*. 2005;14:199-203.
22. Lambert MP, Rauova L, Bailey M, Sola-Visner MC, Kowalska MA, Poncz M. Platelet factor 4 is a negative autocrine in vivo regulator of megakaryopoiesis: clinical and therapeutic implications. *Blood*. 2007;110:1153-1160.
23. Bruns I, Lucas D, Pinho S, et al. Megakaryocytes regulate hematopoietic stem cell quiescence through CXCL4 secretion. *Nat Med.* 2014;20:1315-1320.
24. Dimicoli S, Wei Y, Bueso-Ramos C, et al. Overexpression of the toll-like receptor (TLR) signaling adaptor MYD88, but lack of genetic mutation, in myelodysplastic syndromes. *PLoS One*. 2013;8:e71120.
25. Qian Y, Zhang J, Yan B, Chen X. DEC1, a basic helix-loop-helix transcription factor and a novel target gene of the p53 family, mediates p53-dependent premature senescence. *J Biol Chem*. 2008;283:2896-2905.

Chapter 5

SUMMARY AND GENERAL DISCUSSION

1. SUMMARY OF THE RESULTS

The bone marrow microenvironment supports and regulates the activity of hematopoietic stem cells (HSCs). Recent work in experimental mouse models has shown that genetic manipulation of mesenchymal elements within the niche is sufficient for the development of leukemia.[1,2] However, the molecular mechanisms underlying the concept of niche-induced leukemogenesis and their relevance for human disease have remained elusive. This thesis adopted the human leukemia predisposition disorder Shwachman-Diamond syndrome (SDS) as a model disease to address these open questions, as an involvement of the HSC niche in the pathogenesis of this disease could be hypothesized based on several aspects. These included the presence of pathognomonic mutations in mesenchymal cells (due to the congenital nature of SDS), the existence of skeletal defects in SDS patients, and the lack of leukemic transformation in mice with hematopoietic-restricted *Sbds* deficiency.[3]

To unravel niche contributions to SDS hematological phenotypes, two tissue-specific conditional knock-out mouse models were used, which allowed to dissect hematopoietic cell intrinsic and extrinsic effects of *Sbds* deficiency. In **chapter 2**, the cell intrinsic effects were considered. The chapter described the generation and characterization of the first mouse model of neutropenia in SDS, obtained by targeted deletion of *Sbds* in *Cebpa*$^{+}$ hematopoietic stem and progenitor cells (HSPCs). Although homozygous deletion of *Sbds* produced a lethal phenotype, transplantation of fetal liver cells from *Sbds*$^{f/f}$ *Cebpa*$^{cre/+}$ *R26*$^{EYFP/+}$ embryos into lethally irradiated recipients induced profound neutropenia. Bone marrow analysis revealed that progression through the myelocyte stage was impaired in *Sbds*$^{f/f}$ *Cebpa*$^{cre/+}$ recipients, leading to decreased numbers of terminally differentiated neutrophils with a reactive expansion of myeloid progenitor cells. Molecularly, activation of the p53 tumor suppressor pathway and increased apoptosis characterized late stages of myelopoiesis. The data revealed a critical dependency of a specific cell type in the hematopoietic hierarchy on SBDS, while, unanticipatedly, rapidly cycling progenitor populations were not functionally affected by loss of the protein.

While intrinsic *Sbds* deficiency in hematopoietic cells was sufficient to recapitulate SDS-associated bone marrow failure (BMF) in this model, no clear indication of myelodysplasia and no signs of leukemia were observed in the transplanted mice throughout the experimental follow-up. Conversely, myelodysplastic features were previously described in *Sbds*$^{f/f}$ Osx-cre mice (OCS$^{f/f}$), in which *Sbds* is deleted from osterix-expressing mesenchymal progenitor cells, suggesting that the progression of SDS to myelodysplasia (MDS) and acute myeloid leukemia (AML) may depend on specific cues from the bone marrow microenvironment.[1]

Consequently, in **chapter 3**, the OCS mouse model was used to investigate how HSPC biology is influenced by a *Sbds*-deficient niche. First, it was shown that OCS$^{f/f}$ mice, like SDS patients, develop low-turnover osteoporosis, associated with impaired terminal differentiation in the bone

lineage. Further, exposure to the *Sbds*-deficient microenvironment altered specific aspects of HSPC biology. In particular, mitochondrial dysfunction and accumulation of reactive oxygen species (ROS) were observed in $OCS^{f/f}$-derived HSPCs. Oxidative stress was associated with DNA damage (accumulation of γH2AX foci) and related cell cycle arrest, revealing a novel concept of niche-induced DNA damage in the hematopoietic system. However, the attenuation of HSPCs genomic integrity did not affect their function in competitive transplantation assays, suggesting that a *Sbds*-deficient niche is not sufficient for the malignant transformation of DNA-repair proficient HSPCs. Searching for the molecular events underlying the phenotype of $OCS^{f/f}$ mice, two putative mechanisms were evaluated: the activation of the p53 pathway in Osx^{+} cells (and their progeny) and the secretion of inflammatory ligands. Genetic deletion of p53 from Osx^{+} cells rescued osteoporosis, but it did not alter ROS accumulation in HSPCs. To discover candidate secreted proteins driving the hematopoietic stress, an unbiased whole transcriptome analysis of niche cells was subsequently employed in search for molecular overlaps between the mouse model and human SDS. This identified the alarmins S100A8 and S100A9 as proteins capable to elicit DNA damage repair programs in murine and human HSPCs, suggesting a functional link between alarmin-mediated stress signaling from the niche and establishment of a HSPC-genotoxic environment. Importantly, abundant *S100A8* and *S100A9* transcript levels also identified a subgroup of low-risk MDS patients with significantly impaired survival. Globally, the results in this chapter provide evidence for a direct role of *Sbds*-deficient niche cells in driving osteoporosis in SDS, and reveal a concept of mesenchymal niche-induced attenuation of genomic integrity through inflammatory S100A8/9 signaling in the context of human preleukemic disease.

After having examined how mesenchymal cells can induce hematopoietic dysfunction in preleukemic syndromes, **chapter 4** describes the first transcriptome-wide analysis of primary mesenchymal cells in the human preleukemic condition MDS. Immunophenotypical analysis of bone marrow samples from 12 low-risk MDS patients revealed global preservation of the niche architecture. However, gene expression profiles obtained by massive parallel RNA sequencing distinguished prospectively isolated mesenchymal cells from normal and MDS individuals in hierarchical clustering, unveiling a profound alteration in the transcriptional programs of stromal cells in MDS, with enrichment of signatures for cellular stress, DNA damage and p53 activation. Transcriptional evidence for senescence (GSEA data) was congruent with upregulated senescence-associated secretory phenotype (SASP) genes in MDS $CD271^{+}$ cells and with the enrichment of signatures for cell cycle progression and metabolic activity in control samples, derived from healthy individuals. In line with its proposed role as driver of SASP,[4] activation of NF-κB was observed, as indicated by supporting transcriptional data and by increased phospho-p65 staining in bone lining stromal cells. Finally, increased expression of the Notch ligand Jagged-1 and of a group of negative regulators of hematopoiesis were observed in the MDS niche. In conclusion, impaired hematopoiesis in low-risk MDS is associated with a remarkable molecular alteration of the microenvironment. While the functional relevance of this changes remains to be

shown, previous literature suggests a possible implication of NF-κB,[5,6] senescence[7,8] and Jagged-1[2,9] pathways in the progression of MDS to overt cancer, while the expression of negative regulators of hematopoiesis by CD271$^+$ cells indicates that the niche may contribute to cytopenias in MDS.

2. NOVEL INSIGHTS ON THE PATHOGENESIS OF SDS

The first chapters of this dissertation focused on SDS, chosen as model disease to study the role of the HSC niche in BMF and leukemogenesis. Much of the current knowledge on SDS pathogenesis has been generated in the last decade, starting with the identification of loss-of-function mutations in the ribosome biogenesis gene *SBDS* as drivers of this disease.[10] In spite of several *in vitro* and few *in vivo* studies, little is known about the cellular and molecular events leading to bone marrow failure and MDS/AML predisposition in this syndrome, with main proposed mechanisms being cellular stress in rapidly cycling progenitors in association to some cytoskeletal dysfunction.[11] Even more obscure is the reason behind tissue specificity of symptoms in this ribosomopathy. The findings illustrated in chapters 2 and 3 provide new insights on SDS pathogenesis while offering possible explanations to the conundrum of ribosomopathies tissue specificity.

Molecular mechanisms in SDS: activation of p53 tumor suppressor pathway

As indicated in **chapter 1**, experimental data supports the view that ribosome biogenesis defects determine activation of the p53 tumor suppressor pathway due to the inhibitory binding of free ribosomal proteins to the p53 negative regulator, MDM2. Activation of p53 could explain the hypoplastic phenotypes observed in ribosomopathies as it induces transcriptional programs of cell cycle arrest, cellular senescence or apoptosis, limiting cell proliferation. In the context of SDS, the contribution of p53 to disease pathogenesis is still controversial. While a developmental model of SDS in zebrafish showed no rescue of pancreatic hypoplasia and myeloid defects upon loss of p53 function,[12] the genetic ablation of *Trp53* in mouse models of *Sbds* deficiency partially restored the exocrine pancreatic function by blocking cellular senescence programs.[13] Deficiency of p53 also determined an increase in the number of hematopoietic progenitors in *Sbds$^{R126T/R126T}$* embryos.[13]

In this dissertation, the activation of the p53 pathway was analyzed in both hematopoietic (**chapter 2**) and stromal (**chapter3**) cells in the context of disease-relevant mouse models. The data demonstrates that *Sbds* deficiency in myeloid and mesenchymal cells equally determines an

accumulation of the p53 protein and the upregulation of its transcriptional targets, indicating activation of this tumor suppressor pathway. In the *Cebpa*-Cre model, p53 activation was further experimentally supported by an increased frequency of apoptotic cells at late stages of myelopoiesis, characterized by p53 accumulation, with a corresponding dramatic loss of terminally differentiated neutrophils (**chapter 2**). The finding is consistent with previous *in vitro* data showing high apoptotic rates upon *Sbds* knockdown in human $CD34^+$ cells[14] and in different cell lines (32Dcl3,[15] TF-1,[16] K562[14] and Hela[16,17]), as well as in SDS patient-derived iPSC lines differentiated towards the pancreatic or the hematopoietic lineage.[18]

To assess whether p53 activation is critical for the pathogenesis of SDS, genetic and pharmacological inhibition of this tumor suppressor pathway were considered. Deletion of *Trp53* in mesenchymal cells rescued the osteoporotic phenotype of OCS mice (**chapter 3**), providing direct experimental support for a role of p53 in SDS bone pathology. Concerning bone marrow failure, due to the genetic complexity of the *Sbds*-flox *Cebpa*-Cre R26EYFP model, crossings with *Trp53*-flox mice are still ongoing while this thesis is being written. A pharmacological approach was however tested to preliminarily assess the relevance of p53 activation in this model. Pifithrin α (PFTα) is a small molecule which blocks p53-mediated transcriptional activation.[19] A two month-treatment of *Sbds f/f* recipients with PFTα partially rescued bone marrow cellularity, but failed to ameliorate the progression through the myelocyte stage and thus the production of mature neutrophils (**Figure 1 A-C**). Of note, while the lack of effects on p53 protein levels (**Figure 1D**) was predicted (PFTα targets p53 transcriptional activity rather than its stability),[20] the expression of p53 downstream targets was unexpectedly not or modestly reduced (**Figure 1E**) and the apoptotic phenotype was not rescued (**Figure 1F**). An incomplete targeting of p53 transcriptional activity by PFTα treatment likely explains the findings, and compels the use of genetic models to clearly define whether p53 activation is necessary for development of neutropenia in SDS.

In conclusion, mouse models investigated here highlight clear activation of p53 by *Sbds* deficiency, but the functional relevance of this tumor suppressor pathway for SDS pathogenesis needs further assessment. At the same time, data from this thesis also indicate that some aspects of disease pathology may be p53-independent. Specifically, the abnormal regulation of HSPCs by *Sbds*-deficient niche cells did not appear to be – at least completely – dependent on p53 activation, as no rescue of oxidative stress was observed in $p53^{f/f}$ $OCS^{f/f}$ mice (**chapter 3**). A more complex model where p53 activation is necessary for some, but not all, aspects of SDS pathogenesis may also help explaining the conflicting results of studies targeting p53 activation in SDS models previously reported in literature.[12,13]

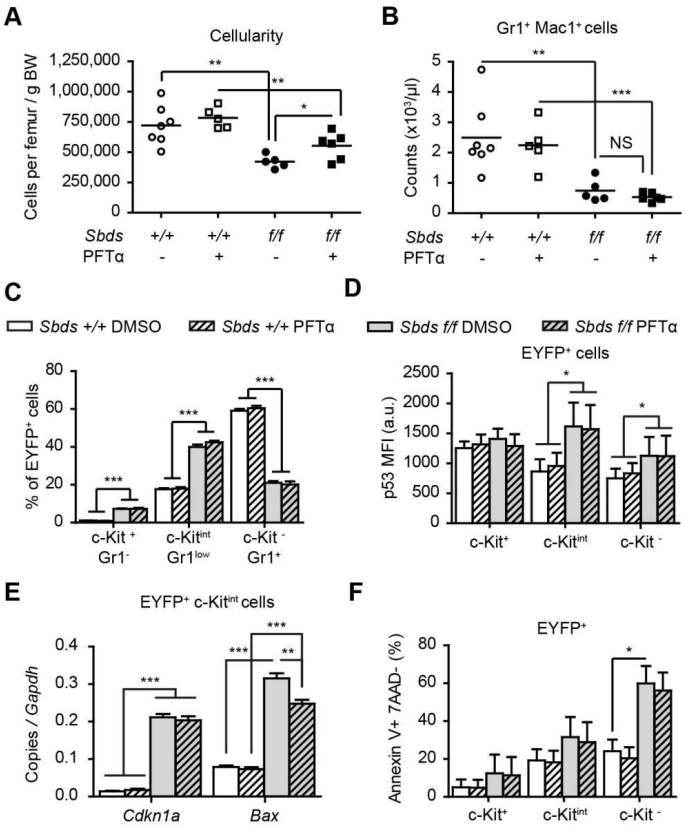

Figure 1. Treatment with pifithrin α does not rescue neutropenia in *Sbds*$^{f/f}$ *Cebpa*$^{cre/+}$ recipients. (A) Partial increase in cellularity in PFTα treated *Sbds f/f* recipients. Treatment with PFTα does not rescue (B) neutropenia or (C) arrest of myeloid lineage progression (n = 5). (D) PFTα does not alter the protein levels of p53 (n = 4). (E) Quantitative RT-PCR shows decreased mRNA levels of *Bax* but not p21 in *Sbds* deficient, PFTα treated myelocytes (n = 5). (F) PFTα treatment is not sufficient to limit apoptosis rate in *Sbds f/f* recipients (n = 4). Data in bar graph is mean ± s.e.m. *P < 0.05. **P < 0.01. ***P < 0.001.

Cytotoxic granules: a common theme in SDS tissue specificity?

While functioning ribosomes are required in every cells of the body, ribosomal defects in SDS seem to specifically affect the exocrine pancreas, the skeleton and the bone marrow. Similar to other ribosomopathies, the cellular and molecular determinants of this specificity have remained elusive. For SDS, a major obstacle in the study of tissue specificity has been the limited availability of models recapitulating the hallmarks of this disease. In particular, while *Ptf1a*-cre *Sbds*-flox mice

were described as consistently developing exocrine pancreatic failure,[13,21] a model of SDS neutropenia in vivo was lacking,[3] and the skeletal phenotype observed in SDS patients was only partially recapitulated in a *LysM*-cre-based model of *Sbds* deficiency,[22] with complete absence of SDS-associated growth defects. This dissertation addressed these experimental gaps by introducing the first mouse model of *Sbds* deficiency-induced neutropenia (**chapter 2**) and defining skeletal abnormalities in the previously described *Sbds*-flox *Osx*-cre mice[1] (**chapter 3**). With the whole spectrum of SDS symptoms modeled, it is now possible to compare findings and advance hypotheses on the mechanisms underlying tissue specificity in SDS symptoms.

The *Cebpa*-cre model presented in **chapter 2** indicates that *Sbds* deficiency critically affects myeloid lineage development at the myelocyte-to-metamyelocyte transition. This developmental stage is characterized by the production of so-called secondary and tertiary granules, which contain a number of cytotoxic molecules and matrix-remodeling peptidases essential for the immune function of neutrophils. Transcript levels for these granules components were found reduced in *Sbds*-deficient c-Kit^{int} cells, while transcripts for primary granule components – produced from promyelocytes – were enriched, likely reflecting arrested lineage progression at the myelocyte stage. Interestingly, the exocrine function of the pancreas also includes the secretion of potentially cytotoxic molecules, among which proteases, lipases and the pancreatic amylase, produced by acinar pancreatic cells. Similar to myelocytes/metamyelocytes, acinar cells coordinate the production of pancreatic enzymes and their storage in (zymogen) granules, thus preventing cellular digestion and severe organ damage. Defective zymogen granule production was described in different *in vitro* and *in vivo* model of SDS pancreatic disease.[12,18,21]

Unexpectedly, the transcriptional analysis of Osx::GFP$^+$ cells showed that *Sbds*-deficient mesenchymal progenitor cells, critical for the osteoporotic phenotype of OCS mice, overexpress genes implicated in inflammation and innate immunity (**chapter 3**). These genes included cytotoxic molecules, metallopeptidases and transmembrane proteins typically found in the membrane of myeloid granules (**Table 1**). Indeed, transcriptional analysis revealed enriched signatures for myeloid granules in OCS$^{f/f}$-derived Osx::GFP$^+$ cells (**Figure 2A**). Staining of sorted Osx::GFP$^+$ cells confirmed the existence of a mesenchymal subpopulation characterized by cytoplasmic granules (**Figure 2B**), although their exact content still needs to be assessed.

Given their 'osteoblast-like' morphology (eccentric nucleus, prominent Golgi apparatus, eosinophilic cytoplasm), and because they were observed both in OCS mutants and controls, it is attractive to hypothesize that granule-containing Osx::GFP$^+$ cells represent a naturally occurring stage in osteoblast differentiation, perhaps with a particular sensitivity to ribosomal stress. In line with this, it is interesting to point out that some granule components were proposed to play a role in bone metabolism (**Table 2**), and thus their production may be functional for bone-depositing cells. If this were the case, the granule component signature in OCS$^{f/f}$ Osx::GFP$^+$ cells

Table 1. Transcripts for myeloid granule components are increased in Osx^{+} cells from OCS$^{f/f}$ mice.

Gene	Description	Myeloid granule	P value	FC	MNI OCS$^{f/f}$	MNI OCS$^{f/+}$
Fpr2	formyl peptide receptor 2	SG, GG	0.000001	14.20	4785.48	1892.93
Lcn2	lipocalin 2	SG	0.000284	7.50	4180.05	1948.51
Prg2	proteoglycan 2	EG	0.000307	11.81	1686.42	698.49
Ear2	eosinophil-associated, ribonuclease A family, member 2	EG	0.000599	7.83	5028.02	2302.59
Slpi	secretory leukocyte peptidase inhibitor	SG	0.002701	2.09	515.44	247.14
Cybb	cytochrome b-245, beta polypeptide	SG, GG	0.000364	6.64	2147.14	1031.02
Lyz2	lysozyme 2	AG, SG; GG	0.003925	5.52	11836.58	6011.45
Fpr1	formyl peptide receptor 1	SG, GG	0.010926	3.94	270.92	155.68
Ctsg	cathepsin G	AG	0.014213	15.08	3748.10	1483.49
Ltf	lactoferrin	SG	0.017512	4.29	4808.99	2694.00
Mmp8	matrix metallopeptidase 8	SG, GG	0.019802	13.95	1055.14	417.60
Prg3	proteoglycan 3	EG	0.021057	32.59	131.89	46.55
Elane	elastase, neutrophil expressed	AG	0.035623	9.37	693.25	290.65
Ear1	eosinophil-associated, ribonuclease A family, member 1	EG	0.039260	19.61	2875.52	1085.90
Ear3	eosinophil-associated, ribonuclease A family, member 3	EG	0.039671	16.83	407.79	159.07
Itgam[a]	integrin, alpha M		0.130952	2.62	44.30	16,94
Sp7[b]	Sp7 transcription factor 7		0.161034	1.23	2979.80	2428.06

Microarray data from Osx^{+} cells (n = 3); the typical myeloid granule localization is indicated. [a]CD11b (*Itgam*) is shown as negative control. [b]Osx (*Sp7*) expression serves as positive control. Experimental details are described in chapter 3. FC: fold change. MNI: mean normalized intensity. AG: azurophilic granules. SG: specific granules. GG: gelatinase granules. EG: eosinophilic granules.

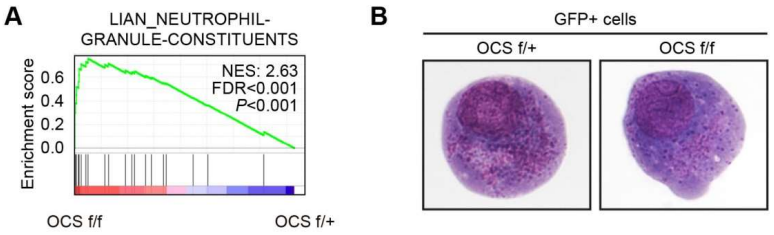

Figure 2. Molecular and morphological analysis suggests the presence of granules in a subpopulation of Osx^{+} cells. (A) GSEA data showing enrichment of signatures for neutrophil granule constituents in Osx::GFP^{+} cells from OCS$^{f/f}$ mice. NES: normalized enrichment score. FDR: false discovery rate. (B) Sorted GFP^{+} cells were cytospun and stained (May-Grünwald Giemsa). GFP^{+} cells have an osteoblast/progenitor-like phenotype with granular morphology observed in 10-33% of cells (*n* = 3).

Table 2. Myeloid granule constituents in mesenchymal cell biology

Gene	Expression	Function
Fpr1	Human MSC[23] Expression increases upon osteogenesis[24]	Mobilization intracellular calcium; cell adhesion and chemotaxis[23] Promotes osteoblast differentiation.[25]
Fpr2	Human MSC[23]	Mobilization intracellular calcium; cell adhesion and chemotaxis[23]
Lcn2	Human MSC under oxidative stress[26] BMSC of mice subjected to reduced bone load[27]	Increases human MSC proliferation[26] Inhibits mouse osteogenesis[27]
Ltf	Human fetal osteoblasts[28]	Promotes bone anabolism[29]
Mmp8	Rat embryonic osteolineage cells[30]	Not characterized
Slpi	Decreased expression in osteoblasts in a mouse model of impaired osteoblast differentiation (*Bgn*$^{-/-}$)[31]	Not characterized

Experimental evidence of myeloid granule components expression from literature (references are in apex). MSC: plastic adherent mesenchymal stromal cells.

could be explained by an impairment in bone lineage progression with enrichment of transcripts for earlier stages of differentiation, reminiscent of the imbalance between transcripts for primary and secondary/tertiary granules in *Sbds*-deficient cKit^{int} cells (**chapter 2**). Indeed, a terminal osteogenic differentiation defect was proposed in OCS$^{f/f}$ mice based on the reduced expression of late- and the increased expression of early osteolineage markers (**chapter 3**). While surely intriguing, this hypothesis awaits a formal experimental validation.

In conclusion, data from this thesis suggest that *Sbds* deficiency critically impairs lineage progression through granule production stages in each of the tissues affected in SDS, perhaps explaining tissue specificity in this ribosomopathy (**Figure 3**). This notion is supported by our experimental data in myelopoiesis, while its validity for bone lineage cells remains to be formally demonstrated. Likewise, more experimental insight is needed to understand what are the molecular consequences of *Sbds* deficiency in granule-producing cells, although it was earlier proposed that this may lead to the activation of cytotoxic molecules with consequent organ damage.[18,21] Further exploring these concepts is of utmost importance for the field, as it could instruct tailored therapeutic strategies targeting at once all tissues specifically affected by SDS.

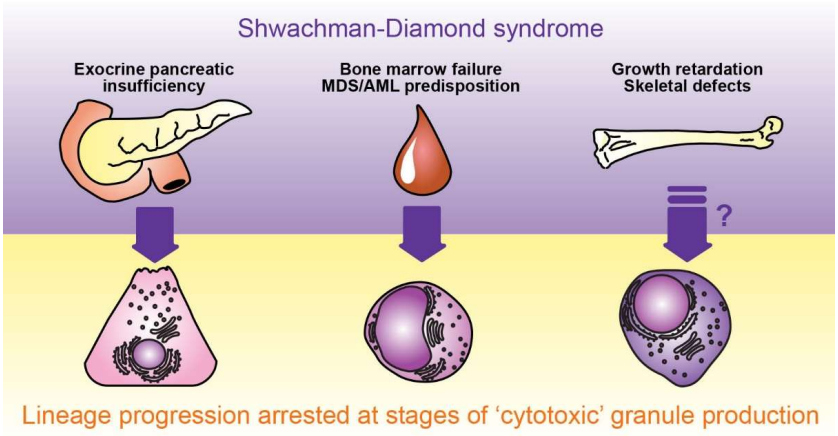

Figure 3. A working model for tissue specificity in SDS. Data from this thesis and previously published work suggest that *Sbds* deficiency impairs lineage progression at stages characterized by the production of granules containing cytotoxic molecules. Unanticipatedly, this concept may apply not only to the pancreatic and myeloid, but also to the osteoblastic lineage.

Unfolded protein response as a novel candidate mechanism in SDS pathogenesis

When postulating lineage progression arrest at granule producing-stages as a common feature of cells critically affected in SDS, a fundamental question that arises is how *Sbds* deficiency would affect such granule-containing cells.

The production of granules and secretory vesicles is a complex process that involves several organelles. Nascent proteins destined for secretion translocate co-translationally from ribosomes to the lumen of the endoplasmic reticulum (ER), a specialized environment for protein folding. Next, they move to the Golgi apparatus, where a sorting takes place between constitutively secreted proteins and those routed for the regulated secretory pathway, which will be eventually stored in granules. The whole process of granule production is tightly regulated, and a crucial quality control exists for protein folding in the ER. Accumulation of unfolded proteins determines the activation of three main sensors, namely inositol-requiring protein 1α (IRE1α), protein kinase RNA-like ER kinase (PERK) and activating transcription factor 6 (ATF6). The so-called 'unfolded protein response' (UPR) thus activated allows buffering of the ER stress by improving ER folding capacity, reducing the translation and folding load, degrading misfolded proteins, and inducing the digestion of malfunctioning ERs by autophagy.

Unfolded or misfolded proteins may accumulate in the ER in different conditions, including nutrient deprivation, impaired redox balance, and increased secretory protein synthesis.[32] Specialized secretory cells show in fact a natural propensity for protein folding stress.[33] Importantly, UPR in granule-producing cells underlies another inherited bone marrow failure syndrome, i.e. severe congenital neutropenia (SCN). Like SDS, SCN is characterized by a profound decrease in mature neutrophil counts due to different inherited mutations, of which the most common affect the gene encoding the neutrophil elastase (*ELANE*).[34] In SCN, myeloid differentiation is arrested at the stage of promyelocytes, which – like myelocytes – are characterized by intense production of (primary) granules. Mechanistically, *ELANE* mutations in SCN are thought to cause mistrafficking of the protein and its accumulation in the ER. The resulting ER stress determines the activation of the UPR, ultimately leading to cellular apoptosis.[35-37] Given that SDS, like SCN, appears to affect granule-producing cells, resulting in bone marrow failure, it is reasonable to hypothesize that *Sbds* deficiency equally determines ER stress and UPR activation, perhaps through inefficient translation and processing of secretable proteins.

Recent studies already demonstrated the activation of UPR upon ribosomal stress. In zebrafish, loss of an essential component of the rRNA small subunit processome, *kri1l*, resulted in inefficient protein synthesis and accumulation of misfolded proteins, triggering PERK activity.[38] Of note, inhibition of PERK rescued hematopoietic failure observed in *kri1l* mutants. Similarly, RPL22

inactivation in T cell precursors, which is observed in ~10% of pediatric T-ALL patients,[39] was recently reported to activate the PERK-EIF2a-ATF4 stress pathway (Patel *et al.*, Cancer Res 2015;75(15 Suppl):Abstract nr 1269). Importantly, this finding could reflect the direct dependency of ATF4 translation on the availability of functional ribosomes.

The translation of the key UPR transcription factors ATF4 is in fact normally inhibited by the presence of two upstream open reading frames (uORF) in its mRNA (reviewed in [40]). During normal conditions, after the first uORF is translated, the 60S abandons the mRNA, but can rapidly be recruited to translate the second uORF. As the latter overlaps with the main coding sequence of ATF4, but has a different reading frame, this results in the inhibition of ATF4 translation. However, in conditions of scarce availability of 60S subunits, the recruiting of the latter on the second uORF is delayed. This results in bypassing the second uORF in favor of the main coding sequence, thus allowing the expression of ATF4. It is conceivable that RPL22 inactivation, or *Sbds* deficiency, similarly reduce the availability of 60S subunits and activate ATF4 expression.

Although at this moment no study formally addressed the role of UPR in *Sbds*-deficiency, a study in HeLa cells showed that *Sbds*-knockdown induces hypersensitivity to tunicamycin, an ER stress inducer.[41] Moreover, work from this thesis provides preliminary data supporting the concept of UPR activation in SDS (**Figure 4**). The gene expression profiling of c-Kit^{int} cells described in chapter 2, besides proving lineage progression arrest and p53 activation, also unraveled an enrichment of signatures for UPR in *Sbds*-deficient myelocytes (**Figure 4A**-**C**), including PERK regulated gene expression and transcriptional activation mediated by ATF4. RNA sequencing also showed a modest, although not significant, increase in the spliced isoform of X box-binding protein 1 (Xbp1s) (**Figure 4D**), which is induced by activated IRE1 and drives the expression of several UPR targets. Finally, upregulation of specific UPR genes, including two activators of UPR sensors, *Hspa5*/BiP and calreticulin (*Calr*), characterized *Sbds f/f* myelocytes (**Figure 4E**).

In conclusion, transcriptional evidence from the *Cebpa*-Cre model strongly suggests that *Sbds* deficiency may determine ER stress and activation of the UPR in granule producing cells. Importantly, UPR may also contribute to the increased rate of apoptosis observed in mutant myeloid cells, as programmed cell death is a possible outcome of irreversible ER stress. In this sense, it is important to consider that UPR induction also increases the binding of free ribosomal proteins to MDM2,[42] thus ER stress may reinforce p53 activation to induce cell death and impaired differentiation in SDS affected lineages. Additional experiments to interrogate the role of UPR in the pathogenesis of SDS are ongoing in our laboratory.

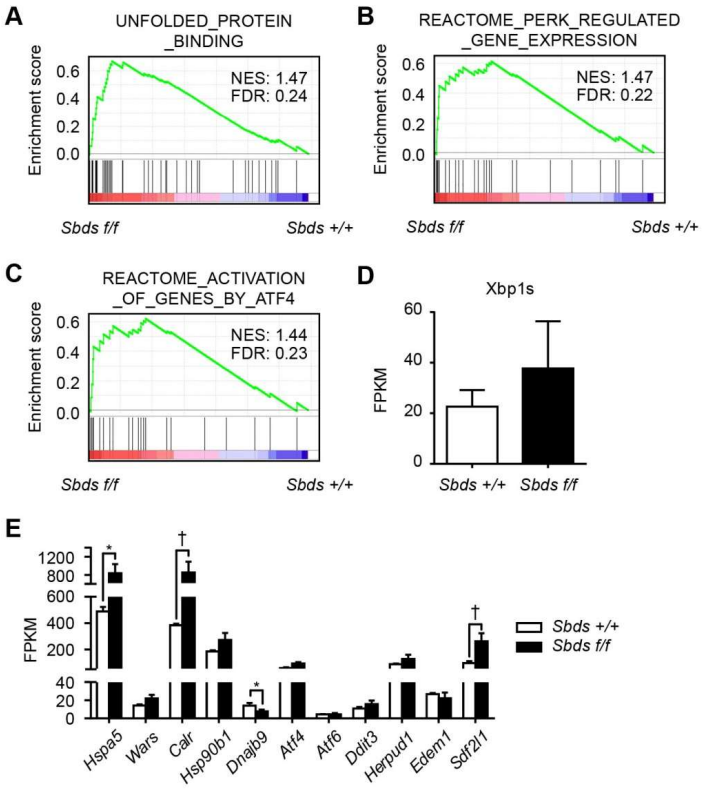

Figure 4. *Sbds* deficient myelocytes are characterized by a signature of activated unfolded protein response (UPR). (A-C) Gene Set Enrichment Analysis plots indicating enrichment of data sets for UPR (A) and transcriptional regulation by PERK (B) and ATF4 (C). NES: normalized enrichment score. FDR: false discovery rate. (D) Tendency for upregulation of Xbp1 short isoform (Xbp1s, $P = 0.17$ by T test). (E) RNA sequencing data showing upregulation of different UPR genes. Data is mean ± s.e.m ($n = 4$). *$P < 0.05$. † FDR-adjusted $P < 0.05$.

3. A ROLE FOR THE MICROENVIRONMENT IN LEUKEMIA PREDISPOSITION SYNDROMES

The homeostasis of the hematopoietic tissue is guaranteed by the presence of hematopoietic stem cells (HSCs), but their maintenance and fate specification depends on signals from the bone marrow microenvironment (**Figure 5A**). Based on this notion, and on seminal work in

experimental mouse models,[1,2,43] this thesis evaluated the possibility that HSC niche cells contribute to two human pre-leukemic syndromes, SDS and MDS.

First, by analyzing separately the effects of *Sbds* deficiency in hematopoietic and mesenchymal cells, it was possible to unravel a distinct contribution of the HSC niche to SDS pathogenesis. Specifically, the findings indicate that cell-autonomous events underlie bone marrow failure (neutropenia) in SDS, but do not readily explain leukemia predisposition. In fact, while all recipients of *Sbds*-deficient hematopoietic cells developed neutropenia, none of them progressed to MDS/AML, and only a benign and probably reactive expansion of myeloid progenitors was observed (**chapter 2** and **Figure 5B**). On the contrary, in the OCS model, exposure of HSPCs to *Sbds*-deficient mesenchymal cells not only induced myelodysplasia,[1] but caused oxidative and genotoxic stress in HSPCs (**Figure 5C**), thus supporting a concept of heterotypic contribution to the emergence of (malignant) mutations in SDS hematopoietic cells.

Notably, however, the function of *Sbds*-proficient HSPCs was preserved in transplantation assays. Given also the absence of persistent DNA lesions in comet assays, the finding was explained in terms of rapid resolution of the damage and/or elimination of affected cells. However, the effect of a genotoxic microenvironment may be different on *Sbds*-deficient HSPCs. Previous *in vitro*

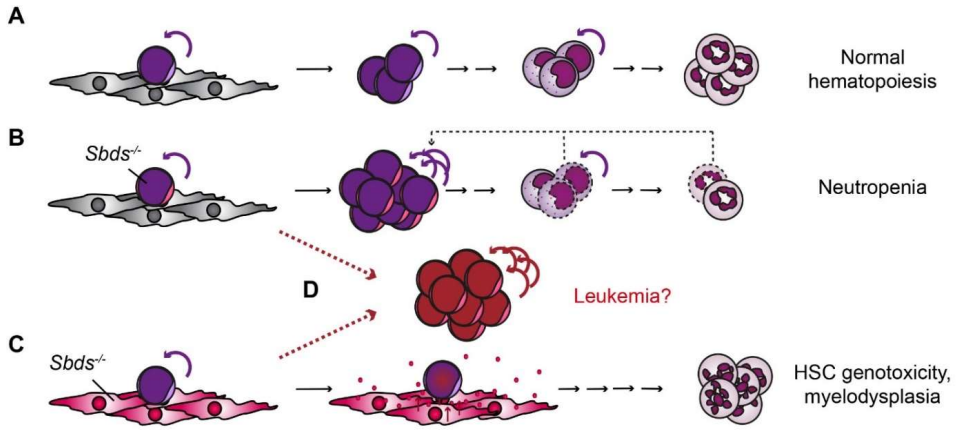

Figure 5. A working model for hematopoietic and mesenchymal contributions to SDS pathogenesis. (A) In normal hematopoiesis, hematopoietic cells are supported by a healthy bone marrow niche and differentiate to secure the production of mature neutrophils. (B) *Sbds* deficiency in the hematopoietic lineage induces neutropenia and a reactive expansion of proliferating progenitors. This expansion, combined with genotoxic signals from *Sbds*-deficient mesenchymal cells (C), may predispose hematopoietic stem and progenitor cells to malignant transformation (D).

studies indicate in fact that *Sbds* deficiency reduces the ability of human cell lines to cope with DNA damaging agents.[41] Moreover, *Sbds* knockdown was associated with accumulation of reactive oxygen species in myeloid cell lines,[16] opening the possibility that intrinsic and extrinsic sources of oxidative stress combine in SDS hematopoietic cells, leading to stronger genotoxic insults. Therefore, it is intriguing to hypothesize that the coexistence of *Sbds* loss of function in the hematopoietic cells and their niche, combining environmental genotoxicity with an increased intrinsic sensitivity to DNA damage (with a possible further challenge represented by reactive progenitor proliferation), result in neoplastic transformation, thus explaining AML predisposition in the human disease (**Figure 5D**). Combining the two mouse models presented in this dissertation by genetic (*Cebpa*$^{cre/+}$;*Osx*$^{cre/+}$ double knockout system) or transplantation experiments (*Cebpa*$^{cre/+}$ *Sbds*$^{f/f}$ fetal liver cells transplanted in OCS mutant mice or S100-overexpressing mice[44]) will be required to fully demonstrate the codependency of hematopoietic and niche contributions to leukemogenesis in SDS.

The second human pre-leukemic syndrome analyzed in this dissertation is MDS and, in particular, the subset associated with low-risk prognosis. Massive parallel RNA sequencing indicated that the gene expression programs of bone marrow niche cells are profoundly reshaped in low-risk MDS, with enriched signatures for cellular stress and senescence (**chapter 4**). More importantly, the same molecules proposed to underlie the genotoxic effects of the microenvironment on HSPCs in SDS, S100A8 and S100A9, were found overexpressed in a subset of low-risk MDS patients characterized by poor survival (**chapter 3**). These findings indicate a possible prognostic value of niche cell analysis in MDS (yet still to be demonstrated in larger cohorts of patients), and suggest that the genotoxic effect of the microenvironment on HSPCs may be of broader relevance to human leukemic predisposition syndromes.

In summary, this thesis unraveled a new model of niche contribution to hematologic diseases via attenuation of genomic integrity of HSPCs. The study reinforces the importance of stromal cells for the homeostasis of the bone marrow and suggests that leukemogenesis should be interpreted at the tissue level (the bone marrow), rather than focusing solely on HSPCs. This notion, relatively novel for the hematology field, actually echoes the old concept of 'field carcinogenesis'. Already in the late 50s, skin graft experiments demonstrated that the exposure of the dermal stroma to carcinogens was necessary to transform epithelial cells, while exposing epithelial cells alone was not sufficient to their transformation.[45]

Carcinogenesis was thus proposed to result from "field effects" of chemical compounds on the whole tissue[45-47] rather than from the genetic transformation of single cell types. From the first elaboration of the field carcinogenesis hypothesis, a body of literature has shown the importance of stromal elements in the field of solid tumors, with the remarkable emergence of so-called "cancer associated fibroblast", shown to contribute to tumorigenesis and disease progression.[48]

Data from this thesis similarly propose that mesenchymal cells may be important for leukemogenesis, at least in pre-leukemic syndromes, thus shifting the focus of hematology/oncology from the 'cellular' level (the HSC) to the 'ecosystem' level, i.e., the entire hematopoietic tissue.

The S100A8/9 DAMPs as inducers of genotoxicity

An important objective of this dissertation was to investigate the cellular and molecular mechanisms underlying the concept of niche-induced leukemogenesis. In **chapter 1**, two non-mutually exclusive models were proposed to explain this phenomenon. According to the first, the niche would facilitate carcinogenesis by selecting premalignant HSC clones naturally emerging in the bone marrow, thus promoting disease progression to overt cancer. This 'Darwinian' model seems congruent with a number of studies demonstrating that niche cells in premalignant mouse models are able to maintain aberrant hematopoietic clones, while offering limited support to normal hematopoiesis (reviewed in [49]). The second model considered instead the possibility that the very emergence of (pre)malignant clones, rather than their selection, directly depends on aberrant niche cells. This thesis demonstrated that this principle could be relevant for the human disorders SDS and MDS (**chapter 3**).

The DAMP molecules S100A8 and S100A9 were found overexpressed both in a niche-restricted mouse model of SDS and in primary niche cells from human SDS and MDS patients. S100A8/9 signaling was independently able to induce DNA damage in cultured murine and human HSPCs. Blockade of S100A8/9 receptor TLR4 was sufficient to rescue DNA damage in OCS mutant-derived HSPCs, demonstrating the critical role of these DAMPs in establishing a genotoxic microenvironment for hematopoietic cells. By destabilizing genomic integrity, S100A8/9 may promote accumulation of somatic mutations in SDS/MDS-derived HSPCs potentially favoring the emergence of leukemic clones, in agreement with the model of niche cells as inducers of leukemogenesis.

The observation that single molecules from the microenvironment can destabilize the genomic integrity of parenchymal cells is not limited to the hematology field. In breast oncology, a similar scenario was described, demonstrating a role for the matrix metalloproteinase 3 (MMP3, or stromelysin) in inducing genomic instability of breast epithelial cells. While MMP3 is normally produced by stromal cells during mammary development, inducing its overexpression *in vivo* determined epithelial-to-mesenchymal transition (EMT) and development of tumors characterized by non-random cytogenetic changes.[50] Subsequent *in vitro* studies further demonstrated that epithelial cells exposed to soluble MMP3 activate the GTPase Rac1, which in turn induces mitochondrial dysfunction, with consequent oxidative stress and DNA damage.[51] The

OCS models present evident parallels with this study: like MMP3,[52,53] also S100A8/9 DAMPs bind parenchymal cells (via their interaction with TLR4) and induce DNA damage via mitochondrial oxidative stress induction. Importantly, work from this thesis not only identified molecules with genotoxic potential in a preleukemic mouse model, but verified their expression in primary niche cells from human patients and described their relation with disease outcome in the context of low-risk MDS.

In conclusion, parallels between this thesis and previous work in breast cancer models suggest that niche-induced genotoxicity may unexpectedly be a common theme in oncology, and the prevalence and relevance of this phenomenon in human disease is worth to be tested. Equally important is trying to define what drives the expression of genotoxic molecules in niche cells and how they elicit mitochondrial dysfunction and DNA damage. The following sections will provide insights on these issues.

What drives S100A8/9 expression in niche cells?

The DAMP proteins S100A8 and S100A9 were found overexpressed in primary niche cells from SDS and a subgroup of low-risk MDS patients. At this moment, it is still unclear why upregulation of these molecules would characterize stromal cells in two related yet distinct pre-leukemic disorders.

Because low risk MDS subtypes include the 5q- syndrome, which like SDS is a ribosomopathy, it is reasonable to hypothesize that S100A8/9 induction in the two diseases reflects stress signaling from (hematopoietic) cells with impaired ribosome biogenesis. However, this hypothesis seems confuted by the fact that the two patients with del(5q) in the investigated MDS cohort were equally distributed between the high and low S100A8/9 expression subgroups.

A likelier hypothesis is that different stress signals in SDS and MDS niche cells converge to the activation of common pathways determining the overexpression of DAMP molecules. Signatures for p53 pathway activation were for instance observed in niche cells from both OCS mice (**chapter 3**) and human low-risk MDS patients (**chapter 4**). Interestingly, the *S100A9* promoter contains putative p53 binding sites and was proposed to be a novel p53 target based on luciferase reporter assays.[54] It is thus possible that S100A8/9 overexpression in the two pre-leukemic disorders reflects common activation of the p53 pathway in niche cells. While in the SDS model p53 activation likely depends on ribosomal biogenesis stress associated with *Sbds* deficiency, in MDS it could reflect activation of senescence programs, as suggested by the upregulation of SASP factors and NF-κB targets.

The same activation of NF-κB pathway could be sufficient to induce S100A8/9 expression, as shown in a model of hepatocellular carcinoma, where production of the DAMP molecules was observed upon overexpression of p65.[55] It is interesting to note that three out of the four patients with low-risk MDS investigated by immunohistochemistry showed abundant P-p65 staining in stromal cells, while the frequency of P-p65$^+$ bone lining cells in a fourth patient was comparable to controls (**chapter 4**). It would be interesting to test S100A8/9 expression in these samples to verify whether the induction of alarmins correlates with P-p65 staining and thus with NF-κB activation.

A wider body of evidence from the literature links S100A8/9 expression to inflammation signaling. S100A8/9 were initially discovered as associated with acute and chronic inflammatory diseases[56-58] and are now considered biomarkers of inflammation.[59] Although they are abundant in immune cells, most notably in neutrophils, they are also expressed in non-hematopoietic cells upon stimulation with inflammation factors, such as PGE2[60] and IL-1β.[61] Importantly, high *Il1b* transcript levels characterized Osx::GFP$^+$ cells from OCS mutants (fold change 6.34, P = 0.006), and inflammation cytokines *IL6* and *IL8* were overexpressed in niche cells from low-risk MDS patients (**chapter 4**). Interestingly, the latter also showed enriched signatures for response to UV irradiation, which was shown to induce *S100A8* expression in keratinocytes.[62,63]

In conclusion, inflammation and cellular stress could be responsible for increased S100A8/9 production in the HSPC niche of SDS and MDS patients. The presence of low-risk MDS patients with high and low S100A8/9 expression in the niche offers the opportunity to further explore the molecular pathways leading to DAMP signaling. A differential expression analysis between the transcriptomes of the two subgroups could in fact lead to the definition of candidate molecules for S100A8/9 production. Blocking DAMP expression from the niche could represent a novel strategy to control progression of pre-leukemic disorders.

How do S100A8/9 proteins establish a genotoxic microenvironment?

Another insufficiently understood aspect of niche-induced genotoxicity is how S100A8/9 can drive DNA damage in HSPCs. Because in HSPCs from OCS mutants high levels of reactive oxygen species (ROS) were found associated with an increase in γH2AX foci, it was hypothesized that DNA damage resulted from oxidative stress. As neutrophil cytosolic molecules, S100A8/9 proteins are well-known ROS inducers via binding and activation of the NADPH oxidase,[64] and this function was reported in some non-myeloid tumor cell lines as well.[65] Also extracellular stimulation with S100A9 directly increases the production of ROS in neutrophils[66] and different cell lines,[67] and a proposed mechanism to explain this phenomenon is the formation of permeability pores in the outer membrane of mitochondria,[67] which induce the release of ROS as well as the activation of

endogenous apoptotic programs. Although this dissertation shows a similar apoptotic effect of S100A8/9 (**chapter 3**), the presence of hyperpolarized mitochondria in HSPCs from OCS mutants is hard to reconcile with the model of mitochondrial permeability. Other mechanisms of S100-induced genotoxicity should therefore be explored.

Notably, the effects of S100A8/9 on DNA damage were rescued by treating OCS mice with a blocking anti-TLR4 antibody, indicating that the genotoxic signaling depends on this pattern recognition receptor (**chapter 3**). Interestingly, stimulation of TLR4 with its well-known ligand lipopolysaccharide was recently reported to induce HSC exhaustion in a ROS-dependent manner and with an associated accrual of DNA damage in HSCs (Takizawa et al., ASH meeting 2014, abstract 604). An intriguing hypothesis is that S100A8/9 may similarly elicit ROS production in HSPCs via direct stimulation of TLR4.

The TLR4-mediated genotoxic effects of S100A8/9 may equally depend on indirect effects due to a signal amplification in HSPCs. A major effect of the S100A8/9 binding to its receptors TLR4 and RAGE is the activation of NF-κB and the consequent secretion of proinflammatory molecules,[68-71] including TNF-α, TGF-β, IL-1β, and metalloproteinases.[44,70,72] In addition to recruiting immune cells, which reinforce S100A8/9 secretion,[73] inflammation factors may be relevant for HSPC genotoxicity. For instance, lipocalin-2 (*Lcn2*), which is upregulated upon S100A8 stimulation,[74] was recently shown to promote oxidative stress and DNA damage of hematopoietic cells in myeloproliferative syndromes.[75,76] Interestingly, *Lcn2* was among the most upregulated genes in niche cells from both $OCS^{f/f}$ mice and SDS patients (**chapter 3**) and thus represents another candidate genotoxic factor in human pre-leukemic syndromes.

In summary, direct stimulation and indirect effects mediated through the establishment of inflammatory milieus may contribute to the genotoxicity of S100A8/9. Further exploring the mechanisms of S100A8/9-mediated DNA damage may be of broader interest to the oncology field, as abundant expression of these DAMPs is found in numerous cancer types,[77] and characterizes tumor cells as well as immune infiltrating cells and tumor-supporting stroma.[55,78,79] Attenuation of genomic integrity could represent a novel paradigm for the role of S100A8/9 in carcinogenesis, adding to previously established contributions to tumor cell growth,[80] immune protection[81] and metastasis.[71,82]

Contribution of inflammation to bone marrow failure and leukemogenesis

While analyzing niche cells in OCS mice, as well as human SDS and low-risk MDS patients, a recurring theme was the presence of inflammatory signatures. Osx::GFP^{+} cells from $OCS^{f/f}$ mice overexpressed a number of molecules involved in inflammation (**chapter 3** and **Table 1**), including

the master regulators of the inflammasome cascade caspase 1 (fold-change 4.66, *P* = 0.03) and IL-1β (fold-change 6.34, *P* = 0.006). Importantly, of the ~25 common differentially expressed genes between niche cells from the OCS model and human SDS patients, 15 were related to inflammation and immunity (**chapter 3**). Signatures for inflammation also characterized $CD271^+$ cells from low-risk MDS patients, probably resulting from NF-κB-mediated senescence signaling (**chapter 4**). Finally, the S100A8/9-TLR4 axis, typically marking local inflammatory activity,[59] characterized the studied pre-leukemic syndromes, with a proposed role in inducing DNA damage in HSPCs. Collectively, these findings suggest that inflammation may play a role in the pathogenesis of preleukemic disease.

Further support for this concept comes from recent publications. In particular, it was reported that myelodysplastic syndromes often coexist with inflammatory manifestations, such as rheumatic disorders, arthritis and inflammatory bowel disease.[83] Additionally, inflammation factors such as TNF-α and IFN-γ proteins accumulate in the bone marrow of MDS patients,[84] with a proposed role in inducing TLR-4 upregulation in hematopoietic cells.[85] As previously indicated (**chapter 3**, Discussion), the same TLR signaling pathway is often active in MDS[86] and probably contributes to BMF and AML development in the 5q- syndrome subgroup.[87] Finally, the proinflammatory molecules IFN-γ and TNF-α were found overexpressed in the bone marrow of patients affected by Fanconi anemia (FA), another BMF and AML predisposition syndrome.[88] Of these factors, TNF-α appeared to play a role in impairing erythroid differentiation of patient bone marrow cells,[88] and it stimulated ROS accumulation and leukemogenesis in the *Fancc*$^{-/-}$ FA mouse model.[89]

Collectively, these observations indicate that inflammation is not only a trademark of preleukemic syndromes, but it may indeed have functional relevance for the pathogenesis of these disorders, including tumorigenesis. Leukemia predisposition syndromes thus reinforce the longstanding relationship between inflammation and cancer. Already in the 19th century, Rudolf Virchow hypothesized, based on the presence of leukocyte infiltrates in tumors, that cancer develops on inflamed tissues.[90] Chronic inflammation is now considered a major risk factor of cancer development.[91] Moreover, different tumors are characterized by inflammatory milieus, with secretion of cytokines, chemokines and tissue remodeling factors, the presence of which led some to refer to tumors as “wounds that do not heal”.[92]

An emerging question is how inflammation milieus are established in pre-leukemic syndromes. In the context of low-risk MDS, proinflammation molecules produced by the niche coincide with a senescence-associated secretion profile (SASP), as suggested by this thesis (**chapter 4**) and by previous reports analyzing plastic-adherent stromal cultures from MDS patients.[93-95] Moreover, especially in low-risk MDS, senescence programs are not limited to the mesenchymal compartment, but also characterize hematopoietic cells, including HSPCs.[96,97] It cannot be

therefore excluded that senescence is initially established in the hematopoietic compartment, primarily affected by MDS, and next propagated to the bone marrow microenvironment via the SASP.[98] Establishment of senescent milieus could next contribute to disease progression. In the context of solid tumors, it was already shown that senescent stromal cells sustain the growth of parenchymal cells,[99-101] and promote malignant transformation, invasion and metastasis.[102,103] Whether a similar role is played by senescent niche cells in human MDS remains to be proven.

Another intriguing hypothesis to explain inflammation phenotypes in preleukemic syndromes is that the presence of cytopenias contributes directly to sustained inflammation in these diseases. Peripheral cell deficiencies may mimic the elimination of differentiated cells observed upon infections, thus eliciting the release of proinflammatory molecules that signal directly to HSPCs to induce their mobilization, proliferation and differentiation.[104-107] While these activation signals rapidly terminate upon elimination of pathogens, in BMF the inflammation would persist due to genetically-determined impairment of mature hematopoietic cell production. Chronic 'sterile' inflammation may thus lead to exhaustion of the stem cell pool and bone marrow failure,[108] ultimately contributing to hematopoietic dysfunction. Moreover, the exit from dormancy of HSCs was recently shown to induce oxidative stress and DNA damage,[109] promoting malignant transformation. Data from this thesis suggest that inflammatory molecules in the microenvironment may equally contribute to HSPC DNA damage.

In conclusion, while work described in this thesis demostrated that niche cells can directly induce genotoxic stress in hematopoietic cells, it is also possible that diseased hematopoietic clones contribute to niche reprogramming by establishing inflammatory environments (**Figure 6**). This model can explain why, in disorders such as MDS, mesenchymal cells would be affected even in the apparent absence of a primary genetic mutation.

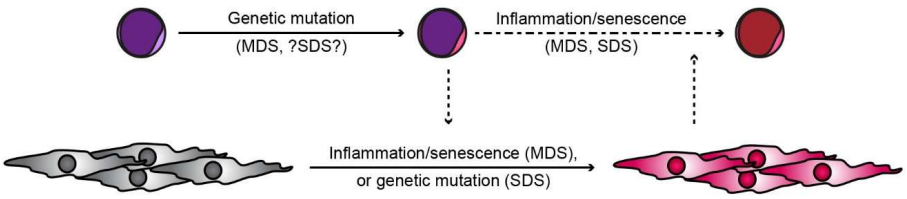

Figure 6. A model for inflammation contributions to human preleukemic syndromes. In MDS, a primary genetic event in HSPCs may drive establishment of a senescent/proinflammatory environment that reshapes the bone marrow niche. This alteration may be genetically determined in inherited BMF syndromes such as SDS. Inflammation and SASP factors coming from the microenvironment may next contribute to progression of preleukemic HSPC clones to overt malignant transformation.

CONCLUSIONS AND PERSPECTIVES

The worked described in this thesis was aimed at studying SDS and MDS pathogenesis with a particular focus on the role of HSPC niche cells in leukemia predisposition. Important conclusions can be drawn from the data presented. A first conclusion concerns the pathogenesis of SDS. In particular, it was shown that ribosome biogenesis defects do not affect all (proliferating) cells, but that the type and extent of ribosomopathy-induced stress strictly depends on the affected cellular types and their differentiation stage, with *Sbds* deficiency critically impairing the myelocyte-to-metamyelocyte transition in the myeloid lineage. The availability of a transplantation model of neutropenia offers the opportunity to better investigate the molecular mechanisms underlying attenuated lineage progression in myelopoiesis. However, developing an *in vitro* model faithfully recapitulating cellular defects at the myelocyte stage would be of tremendous help, allowing the use of high-throughput screenings before engaging in transplantation studies, with evident advantages in terms of ethics, time and finances.

A second major finding in this dissertation was the discovery that *S100A8* and *S100A9* mRNA levels in primary niche cells from low-risk MDS patients correlate with poor disease outcome, regardless of the mutational status of MDS clones, while previously established classification methods failed to identify patients with dismal prognosis.[110] This finding suggests that S100A8/9 levels in the niche could be used as prognostic markers in low-risk MDS. Notably, the prognostic value of S100A8 expression was already proposed in AML, with high S100A8 in myeloblasts predicting poor outcome.[111] Moreover, the use of stromal cell signatures as prognostic factors has been already proposed in solid tumors, such as breast cancer, non-small cell lung carcinoma and intrahepatic cholangiocarcinoma.[112-115] Importantly, a first report in hematology has shown that increased numbers of immunophenotypically-defined mesenchymal subsets in bone marrow aspirates predict relapse in AML patients.[116] Given these precedents, future work will be aimed at confirming the prognostic value of *S100A8* and *S100A9* niche expression in extended cohorts of MDS patients, as well as developing diagnostic tests tailored for daily clinical practice.

Finally, this thesis reports on a novel contribution of niche cells to leukemogenesis via induction of genotoxic milieus for HSPCs, thus potentially contributing to the occurrence of oncogenic mutations. Important follow-up studies should first clarify whether the crosstalk between preleukemic clones and aberrant niches results in leukemogenesis. As previously indicated, genetic or transplantation studies may help elucidating this aspect. If leukemia development is observed in such studies, it will be equally important to verify if increased S100A8/9 secretion from the niche is required for leukemogenesis. This could be achieved either by using anti-TLR4 antibodies, as shown in **chapter 3**, or by using small molecule inhibitors blocking the capacity of S100A8/9 heterodimer to bind its receptor. Molecules of this type, namely quinolone-3-carboxamide derivatives (ABR-215050 and ABR-215757), are currently tested as potential

treatment of prostate cancer and inflammatory diseases.[117-119] Administering such molecules to established mouse models of MDS progression to leukemia will be seminal in exploring the feasibility of niche-targeting therapies in human disease.

REFERENCES

1. Raaijmakers MH, Mukherjee S, Guo S, et al. Bone progenitor dysfunction induces myelodysplasia and secondary leukaemia. *Nature*. 2010;464(7290):852-857.
2. Kode A, Manavalan JS, Mosialou I, et al. Leukaemogenesis induced by an activating beta-catenin mutation in osteoblasts. *Nature*. 2014;506(7487):240-244.
3. Rawls AS, Gregory AD, Woloszynek JR, Liu FL, Link DC. Lentiviral-mediated RNAi inhibition of Sbds in murine hematopoietic progenitors impairs their hematopoietic potential. *Blood*. 2007;110(7):2414-2422.
4. Rovillain E, Mansfield L, Caetano C, et al. Activation of nuclear factor-kappa B signalling promotes cellular senescence. *Oncogene*. 2011;30(20):2356-2366.
5. DiDonato JA, Mercurio F, Karin M. NF-kappaB and the link between inflammation and cancer. *Immunol Rev*. 2012;246(1):379-400.
6. Wei Y, Chen R, Dimicoli S, et al. Global H3K4me3 genome mapping reveals alterations of innate immunity signaling and overexpression of JMJD3 in human myelodysplastic syndrome CD34+ cells. *Leukemia*. 2013;27(11):2177-2186.
7. Coppe JP, Desprez PY, Krtolica A, Campisi J. The senescence-associated secretory phenotype: the dark side of tumor suppression. *Annu Rev Pathol*. 2010;5:99-118.
8. Ohanna M, Giuliano S, Bonet C, et al. Senescent cells develop a PARP-1 and nuclear factor-{kappa}B-associated secretome (PNAS). *Genes Dev*. 2011;25(12):1245-1261.
9. Rupec RA, Jundt F, Rebholz B, et al. Stroma-mediated dysregulation of myelopoiesis in mice lacking I kappa B alpha. *Immunity*. 2005;22(4):479-491.
10. Boocock GR, Morrison JA, Popovic M, et al. Mutations in SBDS are associated with Shwachman-Diamond syndrome. *Nature Genetics*. 2003;33(1):97-101.
11. Ruggero D, Shimamura A. Marrow failure: a window into ribosome biology. *Blood*. 2014;124(18):2784-2792.
12. Provost E, Wehner KA, Zhong XG, et al. Ribosomal biogenesis genes play an essential and p53-independent role in zebrafish pancreas development. *Development*. 2012;139(17):3232-3241.
13. Tourlakis ME, Zhang S, Ball HL, et al. In Vivo Senescence in the Sbds-Deficient Murine Pancreas: Cell-Type Specific Consequences of Translation Insufficiency. *PLoS Genet*. 2015;11(6):e1005288.
14. Sen S, Wang H, Nghiem CL, et al. The ribosome-related protein, SBDS, is critical for normal erythropoiesis. *Blood*. 2011;118(24):6407-6417.
15. Yamaguchi M, Fujimura K, Toga H, Khwaja A, Okamura N, Chopra R. Shwachman-Diamond syndrome is not necessary for the terminal maturation of neutrophils but is important for maintaining viability of granulocyte precursors. *Exp Hematol*. 2007;35(4):579-586.
16. Ambekar C, Das B, Yeger H, Dror Y. SBDS-deficiency results in deregulation of reactive oxygen species leading to increased cell death and decreased cell growth. *Pediatr Blood Cancer*. 2010;55(6):1138-1144.
17. Rujkijyanont P, Adams SL, Beyene J, Dror Y. Bone marrow cells from patients with Shwachman-Diamond syndrome abnormally express genes involved in ribosome biogenesis and RNA processing. *British Journal of Haematology*. 2009;145(6):806-815.

18. Tulpule A, Kelley JM, Lensch MW, et al. Pluripotent stem cell models of Shwachman-Diamond syndrome reveal a common mechanism for pancreatic and hematopoietic dysfunction. *Cell Stem Cell*. 2013;12(6):727-736.
19. Dutt S, Narla A, Lin K, et al. Haploinsufficiency for ribosomal protein genes causes selective activation of p53 in human erythroid progenitor cells. *Blood*. 2011;117(9):2567-2576.
20. Komarov PG, Komarova EA, Kondratov RV, et al. A chemical inhibitor of p53 that protects mice from the side effects of cancer therapy. *Science*. 1999;285(5434):1733-1737.
21. Tourlakis ME, Zhong J, Gandhi R, et al. Deficiency of Sbds in the Mouse Pancreas Leads to Features of Shwachman-Diamond Syndrome, With Loss of Zymogen Granules. *Gastroenterology*. 2012;143(2):481-492.
22. Leung R, Cuddy K, Wang Y, Rommens J, Glogauer M. Sbds is required for Rac2-mediated monocyte migration and signaling downstream of RANK during osteoclastogenesis. *Blood*. 2011;117(6):2044-2053.
23. Viswanathan A, Painter RG, Lanson NA, Jr., Wang G. Functional expression of N-formyl peptide receptors in human bone marrow-derived mesenchymal stem cells. *Stem Cells*. 2007;25(5):1263-1269.
24. Shin MK, Jang YH, Yoo HJ, et al. N-formyl-methionyl-leucyl-phenylalanine (fMLP) promotes osteoblast differentiation via the N-formyl peptide receptor 1-mediated signaling pathway in human mesenchymal stem cells from bone marrow. *J Biol Chem*. 2011;286(19):17133-17143.
25. Arai F, Hirao A, Ohmura M, et al. Tie2/angiopoietin-1 signaling regulates hematopoietic stem cell quiescence in the bone marrow niche. *Cell*. 2004;118(2):149-161.
26. Bahmani B, Roudkenar MH, Halabian R, Jahanian-Najafabadi A, Amiri F, Jalili MA. Lipocalin 2 decreases senescence of bone marrow-derived mesenchymal stem cells under sub-lethal doses of oxidative stress. *Cell Stress Chaperones*. 2014;19(5):685-693.
27. Rucci N, Capulli M, Piperni SG, et al. Lipocalin 2: a new mechanoresponding gene regulating bone homeostasis. *J Bone Miner Res*. 2015;30(2):357-368.
28. Ieni A, Barresi V, Grosso M, Rosa MA, Tuccari G. Lactoferrin immuno-expression in human normal and neoplastic bone tissue. *J Bone Miner Metab*. 2009;27(3):364-371.
29. Naot D, Grey A, Reid IR, Cornish J. Lactoferrin--a novel bone growth factor. *Clin Med Res*. 2005;3(2):93-101.
30. Sasano Y, Zhu JX, Tsubota M, et al. Gene expression of MMP8 and MMP13 during embryonic development of bone and cartilage in the rat mandible and hind limb. *J Histochem Cytochem*. 2002;50(3):325-332.
31. Bi Y, Nielsen KL, Kilts TM, et al. Biglycan deficiency increases osteoclast differentiation and activity due to defective osteoblasts. *Bone*. 2006;38(6):778-786.
32. Rutkowski DT, Kaufman RJ. A trip to the ER: coping with stress. *Trends Cell Biol*. 2004;14(1):20-28.
33. Hetz C. The unfolded protein response: controlling cell fate decisions under ER stress and beyond. *Nat Rev Mol Cell Biol*. 2012;13(2):89-102.
34. Dale DC, Person RE, Bolyard AA, et al. Mutations in the gene encoding neutrophil elastase in congenital and cyclic neutropenia. *Blood*. 2000;96(7):2317-2322.

35. Kollner I, Sodeik B, Schreek S, et al. Mutations in neutrophil elastase causing congenital neutropenia lead to cytoplasmic protein accumulation and induction of the unfolded protein response. *Blood*. 2006;108(2):493-500.
36. Grenda DS, Murakami M, Ghatak J, et al. Mutations of the ELA2 gene found in patients with severe congenital neutropenia induce the unfolded protein response and cellular apoptosis. *Blood*. 2007;110(13):4179-4187.
37. Nayak RC, Trump LR, Aronow BJ, et al. Pathogenesis of ELANE-mutant severe neutropenia revealed by induced pluripotent stem cells. *J Clin Invest*. 2015.
38. Jia XE, Ma K, Xu T, et al. Mutation of kri1l causes definitive hematopoiesis failure via PERK-dependent excessive autophagy induction. *Cell Res*. 2015;25(8):946-962.
39. Rao S, Lee SY, Gutierrez A, et al. Inactivation of ribosomal protein L22 promotes transformation by induction of the stemness factor, Lin28B. *Blood*. 2012;120(18):3764-3773.
40. Barbosa C, Peixeiro I, Romão L. Gene expression regulation by upstream open reading frames and human disease. *PLoS Genet*. 2013;9(8):e1003529.
41. Ball HL, Zhang B, Riches JJ, et al. Shwachman-Bodian Diamond syndrome is a multi-functional protein implicated in cellular stress responses. *Hum Mol Genet*. 2009;18(19):3684-3695.
42. Zhang F, Hamanaka RB, Bobrovnikova-Marjon E, et al. Ribosomal stress couples the unfolded protein response to p53-dependent cell cycle arrest. *J Biol Chem*. 2006;281(40):30036-30045.
43. Walkley CR, Olsen GH, Dworkin S, et al. A microenvironment-induced myeloproliferative syndrome caused by retinoic acid receptor gamma deficiency. *Cell*. 2007;129(6):1097-1110.
44. Chen X, Eksioglu EA, Zhou J, et al. Induction of myelodysplasia by myeloid-derived suppressor cells. *Journal of Clinical Investigation*. 2013;123(11):4595-4611.
45. Orr JW. The mechanism of chemical carcinogenesis, with particular reference to the time of development of irreversible changes in the epithelial cells. *Br Med Bull*. 1958;14(2):99-101.
46. Smithers DW. An attack on cytologism. *Lancet*. 1962;1(7228):493-499.
47. Bissell MJ, Radisky D. Putting tumours in context. *Nat Rev Cancer*. 2001;1(1):46-54.
48. Kalluri R, Zeisberg M. Fibroblasts in cancer. *Nat Rev Cancer*. 2006;6(5):392-401.
49. Schepers K, Campbell TB, Passegue E. Normal and leukemic stem cell niches: insights and therapeutic opportunities. *Cell Stem Cell*. 2015;16(3):254-267.
50. Sternlicht MD, Lochter A, Sympson CJ, et al. The stromal proteinase MMP3/stromelysin-1 promotes mammary carcinogenesis. *Cell*. 1999;98(2):137-146.
51. Radisky DC, Levy DD, Littlepage LE, et al. Rac1b and reactive oxygen species mediate MMP-3-induced EMT and genomic instability. *Nature*. 2005;436(7047):123-127.
52. Talhouk RS, Bissell MJ, Werb Z. Coordinated expression of extracellular matrix-degrading proteinases and their inhibitors regulates mammary epithelial function during involution. *J Cell Biol*. 1992;118(5):1271-1282.
53. Lund LR, Romer J, Thomasset N, et al. Two distinct phases of apoptosis in mammary gland involution: proteinase-independent and -dependent pathways. *Development*. 1996;122(1):181-193.
54. Li C, Chen H, Ding F, et al. A novel p53 target gene, S100A9, induces p53-dependent cellular apoptosis and mediates the p53 apoptosis pathway. *Biochem J*. 2009;422(2):363-372.

55. Nemeth J, Stein I, Haag D, et al. S100A8 and S100A9 are novel nuclear factor kappa B target genes during malignant progression of murine and human liver carcinogenesis. *Hepatology*. 2009;50(4):1251-1262.
56. Odink K, Cerletti N, Bruggen J, et al. Two calcium-binding proteins in infiltrate macrophages of rheumatoid arthritis. *Nature*. 1987;330(6143):80-82.
57. Wilkinson MM, Busuttil A, Hayward C, Brock DJ, Dorin JR, Van Heyningen V. Expression pattern of two related cystic fibrosis-associated calcium-binding proteins in normal and abnormal tissues. *J Cell Sci*. 1988;91 (Pt 2):221-230.
58. Kelly SE, Jones DB, Fleming S. Calgranulin expression in inflammatory dermatoses. *J Pathol*. 1989;159(1):17-21.
59. Vogl T, Eisenblatter M, Voller T, et al. Alarmin S100A8/S100A9 as a biomarker for molecular imaging of local inflammatory activity. *Nat Commun*. 2014;5:4593.
60. Miao L, Grebhardt S, Shi J, Peipe I, Zhang J, Mayer D. Prostaglandin E2 stimulates S100A8 expression by activating protein kinase A and CCAAT/enhancer-binding-protein-beta in prostate cancer cells. *Int J Biochem Cell Biol*. 2012;44(11):1919-1928.
61. Rahimi F, Hsu K, Endoh Y, Geczy CL. FGF-2, IL-1beta and TGF-beta regulate fibroblast expression of S100A8. *FEBS J*. 2005;272(11):2811-2827.
62. Grimbaldeston MA, Geczy CL, Tedla N, Finlay-Jones JJ, Hart PH. S100A8 induction in keratinocytes by ultraviolet A irradiation is dependent on reactive oxygen intermediates. *J Invest Dermatol*. 2003;121(5):1168-1174.
63. Lee YM, Kim YK, Eun HC, Chung JH. Changes in S100A8 expression in UV-irradiated and aged human skin in vivo. *Arch Dermatol Res*. 2009;301(7):523-529.
64. Kerkhoff C, Nacken W, Benedyk M, Dagher MC, Sopalla C, Doussiere J. The arachidonic acid-binding protein S100A8/A9 promotes NADPH oxidase activation by interaction with p67phox and Rac-2. *FASEB J*. 2005;19(3):467-469.
65. Benedyk M, Sopalla C, Nacken W, et al. HaCaT keratinocytes overexpressing the S100 proteins S100A8 and S100A9 show increased NADPH oxidase and NF-kappaB activities. *J Invest Dermatol*. 2007;127(8):2001-2011.
66. Simard JC, Simon MM, Tessier PA, Girard D. Damage-associated molecular pattern S100A9 increases bactericidal activity of human neutrophils by enhancing phagocytosis. *J Immunol*. 2011;186(6):3622-3631.
67. Ghavami S, Eshragi M, Ande SR, et al. S100A8/A9 induces autophagy and apoptosis via ROS-mediated cross-talk between mitochondria and lysosomes that involves BNIP3. *Cell Res*. 2010;20(3):314-331.
68. Turovskaya O, Foell D, Sinha P, et al. RAGE, carboxylated glycans and S100A8/A9 play essential roles in colitis-associated carcinogenesis. *Carcinogenesis*. 2008;29(10):2035-2043.
69. Gebhardt C, Riehl A, Durchdewald M, et al. RAGE signaling sustains inflammation and promotes tumor development. *J Exp Med*. 2008;205(2):275-285.
70. Vogl T, Tenbrock K, Ludwig S, et al. Mrp8 and Mrp14 are endogenous activators of Toll-like receptor 4, promoting lethal, endotoxin-induced shock. *Nature Medicine*. 2007;13(9):1042-1049.
71. Hiratsuka S, Watanabe A, Sakurai Y, et al. The S100A8-serum amyloid A3-TLR4 paracrine cascade establishes a pre-metastatic phase. *Nature Cell Biology*. 2008;10(11):1349-1355.

72. van Lent PL, Grevers L, Blom AB, et al. Myeloid-related proteins S100A8/S100A9 regulate joint inflammation and cartilage destruction during antigen-induced arthritis. *Ann Rheum Dis*. 2008;67(12):1750-1758.
73. Ehrchen JM, Sunderkotter C, Foell D, Vogl T, Roth J. The endogenous Toll-like receptor 4 agonist S100A8/S100A9 (calprotectin) as innate amplifier of infection, autoimmunity, and cancer. *J Leukoc Biol*. 2009;86(3):557-566.
74. Ichikawa M, Williams R, Wang L, Vogl T, Srikrishna G. S100A8/A9 activate key genes and pathways in colon tumor progression. *Mol Cancer Res*. 2011;9(2):133-148.
75. Kagoya Y, Yoshimi A, Tsuruta-Kishino T, et al. JAK2V617F+ myeloproliferative neoplasm clones evoke paracrine DNA damage to adjacent normal cells through secretion of lipocalin-2. *Blood*. 2014;124(19):2996-3006.
76. Lu M, Xia L, Liu YC, et al. Lipocalin produced by myelofibrosis cells affects the fate of both hematopoietic and marrow microenvironmental cells. *Blood*. 2015;126(8):972-982.
77. Bresnick AR, Weber DJ, Zimmer DB. S100 proteins in cancer. *Nat Rev Cancer*. 2015;15(2):96-109.
78. Li MX, Xiao ZQ, Liu YF, et al. Quantitative proteomic analysis of differential proteins in the stroma of nasopharyngeal carcinoma and normal nasopharyngeal epithelial tissue. *J Cell Biochem*. 2009;106(4):570-579.
79. Choi JH, Shin NR, Moon HJ, et al. Identification of S100A8 and S100A9 as negative regulators for lymph node metastasis of gastric adenocarcinoma. *Histol Histopathol*. 2012;27(11):1439-1448.
80. Ghavami S, Rashedi I, Dattilo BM, et al. S100A8/A9 at low concentration promotes tumor cell growth via RAGE ligation and MAP kinase-dependent pathway. *J Leukoc Biol*. 2008;83(6):1484-1492.
81. Cheng P, Corzo CA, Luetteke N, et al. Inhibition of dendritic cell differentiation and accumulation of myeloid-derived suppressor cells in cancer is regulated by S100A9 protein. *J Exp Med*. 2008;205(10):2235-2249.
82. Hiratsuka S, Watanabe A, Aburatani H, Maru Y. Tumour-mediated upregulation of chemoattractants and recruitment of myeloid cells predetermines lung metastasis. *Nature Cell Biology*. 2006;8(12):1369-1375.
83. Ganan-Gomez I, Wei Y, Starczynowski DT, et al. Deregulation of innate immune and inflammatory signaling in myelodysplastic syndromes. *Leukemia*. 2015;29(7):1458-1469.
84. Kitagawa M, Saito I, Kuwata T, et al. Overexpression of tumor necrosis factor (TNF)-alpha and interferon (IFN)-gamma by bone marrow cells from patients with myelodysplastic syndromes. *Leukemia*. 1997;11(12):2049-2054.
85. Maratheftis CI, Andreakos E, Moutsopoulos HM, Voulgarelis M. Toll-like receptor-4 is up-regulated in hematopoietic progenitor cells and contributes to increased apoptosis in myelodysplastic syndromes. *Clin Cancer Res*. 2007;13(4):1154-1160.
86. Wei Y, Dimicoli S, Bueso-Ramos C, et al. Toll-like receptor alterations in myelodysplastic syndrome. *Leukemia*. 2013;27(9):1832-1840.
87. Starczynowski DT, Kuchenbauer F, Argiropoulos B, et al. Identification of miR-145 and miR-146a as mediators of the 5q- syndrome phenotype. *Nat Med*. 2010;16(1):49-58.
88. Dufour C, Corcione A, Svahn J, et al. TNF-alpha and IFN-gamma are overexpressed in the bone marrow of Fanconi anemia patients and TNF-alpha suppresses erythropoiesis in vitro. *Blood*. 2003;102(6):2053-2059.

89. Li J, Sejas DP, Zhang X, et al. TNF-alpha induces leukemic clonal evolution ex vivo in Fanconi anemia group C murine stem cells. *J Clin Invest*. 2007;117(11):3283-3295.
90. Balkwill F, Mantovani A. Inflammation and cancer: back to Virchow? *Lancet*. 2001;357(9255):539-545.
91. Coussens LM, Werb Z. Inflammation and cancer. *Nature*. 2002;420(6917):860-867.
92. Dvorak HF. Tumors: wounds that do not heal. Similarities between tumor stroma generation and wound healing. *N Engl J Med*. 1986;315(26):1650-1659.
93. Geyh S, Oz S, Cadeddu RP, et al. Insufficient stromal support in MDS results from molecular and functional deficits of mesenchymal stromal cells. *Leukemia*. 2013;27(9):1841-1851.
94. Fei C, Zhao Y, Guo J, Gu S, Li X, Chang C. Senescence of bone marrow mesenchymal stromal cells is accompanied by activation of p53/p21 pathway in myelodysplastic syndromes. *Eur J Haematol*. 2014;93(6):476-486.
95. Kim Y, Jekarl DW, Kim J, et al. Genetic and epigenetic alterations of bone marrow stromal cells in myelodysplastic syndrome and acute myeloid leukemia patients. *Stem Cell Res*. 2015;14(2):177-184.
96. Wang YY, Cen JN, He J, et al. Accelerated cellular senescence in myelodysplastic syndrome. *Exp Hematol*. 2009;37(11):1310-1317.
97. Xiao Y, Wang J, Song H, Zou P, Zhou D, Liu L. CD34+ cells from patients with myelodysplastic syndrome present different p21 dependent premature senescence. *Leuk Res*. 2013;37(3):333-340.
98. Hoare M, Narita M. Transmitting senescence to the cell neighbourhood. *Nat Cell Biol*. 2013;15(8):887-889.
99. Krtolica A, Parrinello S, Lockett S, Desprez PY, Campisi J. Senescent fibroblasts promote epithelial cell growth and tumorigenesis: a link between cancer and aging. *Proc Natl Acad Sci U S A*. 2001;98(21):12072-12077.
100. Bavik C, Coleman I, Dean JP, Knudsen B, Plymate S, Nelson PS. The gene expression program of prostate fibroblast senescence modulates neoplastic epithelial cell proliferation through paracrine mechanisms. *Cancer Res*. 2006;66(2):794-802.
101. Coppe JP, Boysen M, Sun CH, et al. A role for fibroblasts in mediating the effects of tobacco-induced epithelial cell growth and invasion. *Mol Cancer Res*. 2008;6(7):1085-1098.
102. Parrinello S, Coppe JP, Krtolica A, Campisi J. Stromal-epithelial interactions in aging and cancer: senescent fibroblasts alter epithelial cell differentiation. *J Cell Sci*. 2005;118(Pt 3):485-496.
103. Liu D, Hornsby PJ. Senescent human fibroblasts increase the early growth of xenograft tumors via matrix metalloproteinase secretion. *Cancer Res*. 2007;67(7):3117-3126.
104. Zhao JL, Ma C, O'Connell RM, et al. Conversion of danger signals into cytokine signals by hematopoietic stem and progenitor cells for regulation of stress-induced hematopoiesis. *Cell Stem Cell*. 2014;14(4):445-459.
105. Challen GA, Boles NC, Chambers SM, Goodell MA. Distinct hematopoietic stem cell subtypes are differentially regulated by TGF-beta1. *Cell Stem Cell*. 2010;6(3):265-278.
106. Maeda K, Malykhin A, Teague-Weber BN, Sun XH, Farris AD, Coggeshall KM. Interleukin-6 aborts lymphopoiesis and elevates production of myeloid cells in systemic lupus erythematosus-prone B6.Sle1.Yaa animals. *Blood*. 2009;113(19):4534-4540.
107. Mossadegh-Keller N, Sarrazin S, Kandalla PK, et al. M-CSF instructs myeloid lineage fate in single haematopoietic stem cells. *Nature*. 2013;497(7448):239-243.

108. Schuettpelz LG, Link DC. Regulation of hematopoietic stem cell activity by inflammation. *Front Immunol*. 2013;4:204.
109. Walter D, Lier A, Geiselhart A, et al. Exit from dormancy provokes DNA-damage-induced attrition in haematopoietic stem cells. *Nature*. 2015.
110. Bejar R, Stevenson KE, Caughey BA, et al. Validation of a prognostic model and the impact of mutations in patients with lower-risk myelodysplastic syndromes. *J Clin Oncol*. 2012;30(27):3376-3382.
111. Nicolas E, Ramus C, Berthier S, et al. Expression of S100A8 in leukemic cells predicts poor survival in de novo AML patients. *Leukemia*. 2011;25(1):57-65.
112. Finak G, Bertos N, Pepin F, et al. Stromal gene expression predicts clinical outcome in breast cancer. *Nat Med*. 2008;14(5):518-527.
113. Farmer P, Bonnefoi H, Anderle P, et al. A stroma-related gene signature predicts resistance to neoadjuvant chemotherapy in breast cancer. *Nat Med*. 2009;15(1):68-74.
114. Edlund K, Lindskog C, Saito A, et al. CD99 is a novel prognostic stromal marker in non-small cell lung cancer. *Int J Cancer*. 2012;131(10):2264-2273.
115. Sulpice L, Rayar M, Desille M, et al. Molecular profiling of stroma identifies osteopontin as an independent predictor of poor prognosis in intrahepatic cholangiocarcinoma. *Hepatology*. 2013;58(6):1992-2000.
116. Kim JA, Shim JS, Lee GY, et al. Microenvironmental remodeling as a parameter and prognostic factor of heterogeneous leukemogenesis in acute myelogenous leukemia. *Cancer Res*. 2015;75(11):2222-2231.
117. Armstrong AJ, Haggman M, Stadler WM, et al. Long-term survival and biomarker correlates of tasquinimod efficacy in a multicenter randomized study of men with minimally symptomatic metastatic castration-resistant prostate cancer. *Clin Cancer Res*. 2013;19(24):6891-6901.
118. Yan L, Bjork P, Butuc R, et al. Beneficial effects of quinoline-3-carboxamide (ABR-215757) on atherosclerotic plaque morphology in S100A12 transgenic ApoE null mice. *Atherosclerosis*. 2013;228(1):69-79.
119. Helmersson S, Sundstedt A, Deronic A, Leanderson T, Ivars F. Amelioration of experimental autoimmune encephalomyelitis by the quinoline-3-carboxamide paquinimod: reduced priming of proinflammatory effector CD4(+) T cells. *Am J Pathol*. 2013;182(5):1671-1680.

ADDENDUM

LIST OF ABBREVIATIONS

µCT	Micro-computed tomography
AD	Anauxetic dysplasia
AG	Azurophilic granule
AML	Acute myeloid leukemia
ANC	Absolute neutrophil count
BCS	Bowen-Conradi syndrome
BMF	Bone marrow failure
CAR	CXCL12-abundant reticular
CFU-C	Colony forming unit culture
CFU-F	Fibroblast colony forming unit
CHH	Cartilage-hair hypoplasia
CLP	Common lymphoid progenitor
CMP	Common myeloid progenitor
DAMP	Damage-associated molecular pattern
DBA	Diamond-Blackfan anemia
DC	Dendritic cell
DCL	Donor cell leukemia
DDR	DNA damage response
EG	Eosinophilic granule
EMT	Epithelial-mesenchymal transition
ER	Endoplasmic reticulum
ES	Enrichment score
FA	Fanconi anemia
FC	Fold change

FDR	False discovery rate
FPKM	Fragments per kilobase of exon per million fragments mapped
GG	Gelatinase granule
GMP	Granulocyte-macrophage progenitor
GSEA	Gene set enrichment analysis
Hb	Hemoglobin
HSC	Hematopoietic stem cell
HSPC	Hematopoietic stem and progenitor cell
IBMFS	Inherited bone marrow failure syndrome
ICA	Isolated congenital asplenia
iPSC	Induced pluripotent stem cell
IPSS	International prognostic scoring system
IRES	Internal ribosome entry site
LR-PSS	Lower-risk prognostic scoring system
MB	Myeloblast
MC	Myelocyte
MCV	Mean corpuscular volume
MDS	Myelodysplastic syndrome
MDSC	Myeloid-derived suppressor cell
MEP	Megakaryocyte–erythroid progenitor
MFI	Mean fluorescence intensity
MM	Metamyelocyte
MPC	Mesenchymal progenitor cell
MPP	Multipotent progenitor
MSC	Mesenchymal stromal cell
MSigDB	Molecular signature database

NAIC	North American Indian childhood cirrhosis
NES	Normalized enrichment score
NET	Neutrophil extracellular trap
NK	Natural killer
OCS	Osx-cre *Sbds*-flox strain
PCA	Principal component analysis
PLT	Platelet
PM	Promyelocyte
RBC	Red blood cell
ROS	Reactive oxygen species
SASP	Senescence-associated secretory profile
SC	Segmented cell
SCN	Severe congenital neutropenia
SDS	Shwachman-Diamond syndrome
SEM	Standard error of the mean
SG	Specific granule
SLAM	Signaling lymphocyte activation molecule
T-ALL	T-cell acute lymphoblastic leukemia
TCS	Treacher Collins syndrome
uORF	Upstream open reading frame
UPR	Unfolded protein response
WBC	White blood cell
X-DC	X-linked dyskeratosis congenita

ENGLISH SUMMARY

The white blood cells, red blood cells and platelets circulating in the human blood are necessary for the survival of the entire organism, but their lifespan is limited. Sustaining a continuous production of new blood cells, or hematopoiesis, is the function of the so-called hematopoietic stem cells (HSC), located in the bone marrow. HSCs are undifferentiated, pluripotent cells capable of concurrently generating by cell division one differentiation-committed cell and another HSC, thus maintaining the hematopoietic potential throughout the lifespan of an organism. However, because sustained proliferation may result in the accumulation of genetic mutations, HSCs are often kept in a non-dividing, quiescent state to protect the genomic integrity in the blood lineage.

The balance between HSC quiescence, proliferation and differentiation depends both on intrinsic programs and on signals coming from regulatory non-hematopoietic cells in the bone marrow microenvironment, cells which are collectively referred to as the HSC niche. The niche comprises several cell types among which mesenchymal progenitor cells. Disruption of the delicate mechanism regulating HSCs may lead to the development of acute myeloid leukemia, a form of cancer characterized by uncontrolled proliferation of immature myeloid cells that fail to fully differentiate.

While numerous studies have focused on identifying genetic mutations in leukemic cells that intrinsically explain their malignant behavior, investigations on possible extrinsic contributions to HSC transformation have been so far limited. Genetically engineered mouse models have shown that aberrant niche cells can promote leukemogenesis, but the underlying molecular mechanisms, as well as their relevance to human disease states, remain to be elucidated.

The aim of this thesis was to shed further light on these key issues, seeking answers to the following questions:

1. What is the contribution of niche cells to leukemogenesis?
2. What molecular mechanisms drive such contributions?
3. What is the relevance of these concepts and mechanisms to human disease?

To this end, two human bone marrow failure disorders were analyzed which confer a significantly increased risk of developing leukemia: Shwachman-Diamond syndrome (SDS) and the myelodysplastic syndromes (MDS).

The first part of this thesis focuses on SDS, which was chosen as ‘index disease’ based on several considerations. First, as an inherited monogenic disorder, SDS is particularly suitable for experimental modeling. Moreover, SDS patients, besides suffering from severe neutropenia and leukemia predisposition, present skeletal abnormalities and osteoporosis, thus it was hypothesized that mesenchymal lineage cells may be involved in SDS pathogenesis. Finally, it was

previously shown that mice with reduced hematopoietic expression of *Sbds*, the ribosome biogenesis gene mutated in SDS, do not develop leukemia, suggesting that *Sbds* deficiency in hematopoietic cells is not sufficient for leukemia predisposition.

In this thesis, cell intrinsic and extrinsic contributions to SDS pathogenesis were dissected using two conditional *Sbds* knockout mouse models targeting hematopoietic and niche cells, respectively.

Chapter 2 describes the development and characterization of a hematopoietic lineage-specific mouse model, obtained by transplanting wild type mice with *Sbds*-deficient hematopoietic cells. *Sbds* deficiency in hematopoietic cells was achieved by deleting the gene through a cre-loxP system expressed under the control of the *Cebpa* promoter. *Cebpa* encodes for a hematopoietic transcription factor expressed in a subset of immunophenotypic hematopoietic stem and progenitor cells (HSPCs) and critical for myeloid development. Validation experiments on the transplanted mice confirmed highly efficient deletion of *Sbds* from HSPCs and throughout all hematopoietic differentiation stages, including the vast majority of myeloid-committed progenitor cells. Importantly, while previous attempts to recapitulate SDS disease characteristics in mice failed to induce neutropenia, all mice transplanted with *Sbds*-deficient cells demonstrated a profound reduction of circulating granulocytes, thus recapitulating for the first time SDS-associated neutropenia in a mouse model.

Analysis of this model subsequently allowed investigating the mechanisms linking *Sbds* deficiency to bone marrow failure. The general view on SDS and other 'ribosomopathies' is that ribosome biogenesis defects should mostly affect dividing progenitor cells due to the high demand of protein synthesis connected to cellular proliferation. At odds with this view, analysis of transplanted mice revealed that hematopoietic progenitor cells tolerate *Sbds* deficiency, while cells at terminal stages of myeloid differentiation respond to it with p53 activation and programmed cell death, thus providing cellular insights into the specific development of neutropenia in SDS. A final observation from transplanted mice was the fact that none of them showed signs of leukemia, further suggesting that non-hematopoietic cells may contribute to malignant transformation of HSPCs in SDS.

In **chapter 3** this hypothesis was tested in a second SDS mouse model, previously developed, where *Sbds* gene deletion is confined to mesenchymal progenitor cells in the bone marrow microenvironment. Mice with mesenchymal cell-restricted *Sbds* deficiency presented growth retardation and osteoporosis as observed in SDS patients. Low numbers of osteoblasts and reduced expression of late osteoblast markers in mutant mice suggested that, much like in the hematopoietic lineage, *Sbds* impairs terminal stages of mesenchymal differentiation.

It was earlier reported that mutant mice display myelodysplastic alterations and increased frequency of apoptotic HSPCs, as observed in the human disease. To better understand the cellular and molecular basis for these hematopoietic alterations, a series of additional investigations was performed. These demonstrated that the exposure to the *Sbds*-deficient niche induces mitochondrial dysfunction, accumulation of free oxygen radicals and DNA damage in HSPCs, with consequent activation of cell cycle checkpoints. These findings reveal a concept of niche-induced genotoxic stress in HSPCs, perhaps contributing to the acquisition of genetic alterations and leukemic evolution in SDS.

To identify candidate mechanisms for the niche genotoxic effects on HSPCs, the transcriptome of *Sbds*-deficient mesenchymal progenitors was profiled. Like in the myeloid lineage, *Sbds* deficiency was associated with p53 activation, however deletion of p53 did not improve the hematopoietic phenotype of mutant mice, while it rescued osteoporosis. Other candidate mechanisms were searched by comparing the transcriptome of mesenchymal cells from the mouse model and human patients suffering from SDS and other preleukemic conditions, namely low risk MDS and Diamond-Blackfan anemia.

The damage-signaling molecules S100A8 and S100A9 were found upregulated both in the mouse model and in the two conditions mostly associated with leukemia progression, SDS and MDS. These molecules were able to directly induce DNA damage and apoptosis in HSPCs and blockade of their signaling through the TLR4 receptor was sufficient to partially rescue niche-induced genotoxicity in the mouse model. High mesenchymal expression of *S100A8* and *S100A9* identified low-risk MDS patients with poor outcome independently of known prognostic factors, indicating that increased S100A8/9 mesenchymal expression may represent a potential prognostic marker of human MDS.

Collectively, the investigations in chapter 3 reveal a concept of mesenchymal niche-induced genotoxic stress in heterotypic stem and progenitor cells through inflammatory signaling as an actionable determinant of disease outcome in human preleukemia. They provide proof of principle that concepts derived from studies in mice may be relevant to human disease and stress the potential importance of detailed insights into the molecular wiring of mesenchymal cells in human disease to guide prognostification and therapeutic strategies. However, thus far, insights into the molecular wiring of mesenchymal cells in human hematopoietic disease have been derived from *ex vivo*-expanded mesenchymal stromal cells, with unknown relevance to their actual transcriptional activity in the diseased tissue.

Chapter 4 describes the first whole-transcriptome analysis of niche elements directly isolated from the marrow of low-risk MDS patients. A method was developed, optimized and validated to perform massive parallel sequencing on these rare cells. Downstream transcriptional network analyses indicated that niche cells from MDS patients are transcriptionally distinct from those of

normal individuals and characterized by upregulation of DNA damage, cellular stress and inflammation-associated pathways. Transcript analysis and immunohistochemistry also suggested that senescence characterizes niche cells in low-risk MDS. In particular, a number of transcripts for senescence-associated secretable molecules with known inflammatory potential were found upregulated in the MDS niche. The elucidation of the mesenchymal niche cell transcriptome is anticipated to facilitate the experimental definition of the molecular programs upstream of S100A8/9 activation and the identification of other pathways involved in the disruption of hematopoiesis in MDS.

In conclusion, the experiments described in this thesis provided novel insights into the contribution of niche cells to impaired hematopoiesis in preleukemic conditions and the underlying molecular mechanisms. They established human disease relevance of concepts and mechanisms uncovered in murine studies and stressed the view that alterations in HSPCs and in their niche may work in concert to drive leukemogenesis in human preleukemic disorders. The findings pave the way to future analyses determining whether such microenvironmental contributions are necessary for leukemogenesis and raise the perspective of niche-instructed therapeutic targeting to delay or prevent leukemogenesis in human preleukemic disorders.

DUTCH SUMMARY

Nederlandse samenvatting

De witte bloedcellen, rode bloedcellen en bloedplaatjes die circuleren in het menselijk bloed zijn noodzakelijk voor de overleving van het gehele organisme, maar hun levensduur is beperkt. Behoud van een continue productie van nieuwe bloedcellen (hematopoiese), is de taak van de zogenaamde hematopoietische stamcellen (HSC), gelegen in het beenmerg. HSC zijn ongedifferentieerde, pluripotente cellen die in staat zijn zichzelf te delen in zowel een andere HSC als een meer uitgerijpte cel. Hierdoor blijven HSC gedurende het gehele leven intact en vormen ze de basis van de bloedcelvorming.

Omdat aanhoudende celdeling kan resulteren in de opstapeling van afwijkingen in het DNA (mutaties) worden HSC overwegend in een niet-delende, rustende toestand gehouden om te voorkomen dat er DNA schade ontstaat. Het evenwicht tussen HSC rust, celdeling en differentiatie wordt bepaald door zowel cel-intrinsieke factoren als signalen van regulerende, niet-hematopoietische, cellen in de beenmerg micro-omgeving, de zogenaamde HSC niche. De niche omvat verschillende celtypes, waaronder mesenchymale cellen. Verstoring van de delicate regelmechanisme van HSC (zowel intrinsiek als extrinsiek) kan leiden tot de ontwikkeling van acute myeloïde leukemie (AML), een vorm van bloedkanker gekenmerkt door een ongecontroleerde proliferatie van onrijpe cellen die niet volledig differentiëren.

Hoewel een veelheid aan studies een belangrijke rol hebben aangetoond voor genetische afwijkingen in hematopoietische cellen in het ontstaan van AML, is het aantal studies wat heeft gekeken naar de rol van extrinsieke factoren beperkt. Recent hebben studies in genetisch gemanipuleerde muismodellen aangetoond dat afwijkende niche-cellen het ontstaan van leukemie kunnen bevorderen, maar de onderliggende moleculaire mechanismen en hun relevantie voor menselijke ziektetoestanden, moeten nog worden opgehelderd.

Het doel van dit proefschrift was om meer licht te werpen op deze belangrijke kwesties, op zoek naar antwoorden op de volgende vragen:

1. Wat is de bijdrage van niche cellen aan leukemie?
2. Welke moleculaire mechanismen zijn verantwoordelijk voor deze bijdragen?
3. Wat is de relevantie van deze concepten en mechanismen voor menselijke ziekte?

Hiertoe werden twee beenmergziekten geanalyseerd die een significant verhoogd risico op het ontwikkelen van leukemie in zich dragen: Shwachman-Diamond Syndroom (SDS) en myelodysplastische syndromen (MDS).

Het eerste deel van dit proefschrift richt zich op SDS. Deze ziekte leek bijzonder geschikt voor het onderzoek naar niche bijdragen aan het ontstaan van leukemie om de volgende redenen: ten

eerste wordt de ziekte veroorzaakt door een mutatie die leidt tot verlies van functie van een enkel gen (genaamd *SBDS*) in alle cellen van het lichaam, wat het goed mogelijk maakt de ziekte na te bootsen in muizen. Bovendien hebben SDS patiënten naast afwijkingen in bloedcellen (met name lage aantallen witte bloedcellen (granulocyten), neutropenie genoemd) en een verhoogde kans op leukemie, ook skeletafwijkingen, wat een direct verband legt tussen bloed en bot-niche cellen. Tenslotte werd eerder aangetoond in muizen dat mutatie van het *Sbds* gen in bloedcellen *alleen,* onvoldoende is voor het ontwikkelen van leukemie, wat suggereert dat andere cellen wellicht een rol spelen in het ontstaan hiervan.

In dit proefschrift, werden cel intrinsieke en extrinsieke bijdragen aan het ontstaan van SDS ontleed met behulp van muismodellen waarin het *Sbds* gen specifiek werd aangedaan in bloedcellen danwel botcellen.

Hoofdstuk 2 beschrijft de ontwikkeling van het muizenmodel met verlies van het *Sbds* gen, specifiek in bloedcellen, verkregen door het transplanteren van normale muizen met *Sbds*-deficiënte bloedcellen. *Sbds* deficiëntie in hematopoietische cellen werd bereikt door het uitknippen van het gen via een zogenaamd Cre-loxP-systeem, wat aan wordt gezet door een gen wat specifiek in hematopoietische cellen tot expressie komt (*Cebpa*). *Cebpa* codeert een hemopoëtische transcriptiefactor die tot expressie komt in een deel van de HSC en in voorlopercellen van de witte reeks. Dit leidt tot verlies van het *Sbds* gen in de gehele lijn van bloedcellen die uiteindelijk leiden tot gedifferentieerde granulocyten. Verlies van het gen in al deze celtypen werd experimenteel bevestigd en de muizen ontwikkelden een uitgesproken neutropenie, waarmee we het eerste muismodel van neutropenie in SDS ontwikkeld hebben.

Analyse van dit model stelde ons in staat onderzoek te doen naar de mechanismen die ten grondslag liggen aan neutropenie in SDS. Dit is belangrijk omdat neutropenie een ernstige ziektemanifestatie is die leidt tot ernstige infecties bij aangedane patienten. Over het algemeen wordt aangenomen dat in SDS, maar ook in andere ziekten die gepaard gaan met defecten in ribosomen, met name snel delende cellen zijn aangedaan omdat delende voorlopercellen een hoge behoefte hebben aan de aanmaak van eiwitten (de taak van ribosomen).

In tegenstelling tot deze aanname, liet analyse van de getransplanteerde muizen zien dat snel delende hematopoietische voorlopercellen *Sbds* deficiëntie tolereren, terwijl cellen later in de uitrijping naar granulocyten reageren met p53 activatie en geprogrammeerde celdood. Deze specificiteit voor de ontwikkeling van witte bloedcellen is in overeenstemming met de observatie dat met name deze cellen zijn aangedaan in SDS. Een andere belangrijke observatie was dat getransplanteerde muizen geen leukemie ontwikkelden, wat verder suggereert dat niet-hematopoïetische cellen mogelijk een noodzakelijke bijdrage leveren aan leukemische transformatie van HSC in SDS.

In **hoofdstuk 3** werd deze hypothese getoetst in een tweede SDS muismodel, waarbij het *Sbds* gen specifiek werd verwijderd uit mesenchymale cellen in het beenmerg micro-milieu. Deze muizen hadden een groeiachterstand en botontkalking (osteoporose), zoals waargenomen in SDS patiënten. De osteoporose werd veroorzaakt door een stoornis in de ontwikkeling richting uitgerijpte botvormende cellen (osteoblasten). Bloedvormende cellen in het beenmerg die blootgesteld werden aan dit micromilieu ontwikkelden mitochondriale dysfunctie, ophoping van vrije zuurstofradicalen en DNA schade. Deze bevindingen beschrijven een concept van 'niche-geïnduceerde genotoxische stress' in HSC, waarbij veranderingen in het micromilieu leiden tot toegenomen schade aan het DNA van bloedcellen. Het is voorstelbaar dat dit concept bijdraagt aan de ophoping van genetische schade in bloedvormende cellen die nodig is voor leukemische evolutie.

Om dit verder uit te werken en kandidaat mechanismen voor de niche-geinduceerde genotoxische effecten op HSC te identificeren, werd het transcriptoom (genexpressieprofiel) van *Sbds*-deficiënte mesenchymale cellen bestudeerd. Net als in hematopoietische cellen van de witte reeks, was *Sbds*-deficiëntie geassocieerd met p53 activatie. Genetische deletie van p53 leidde tot herstel van de botafwijkingen en osteoporose, maar niet tot herstel van de DNA schade in bloedcellen. Andere kandidaat-mechanismen werden gezocht door het vergelijken van de genexpressie in mesenchymale cellen uit het muizenmodel met de expressie van genen in mesenchymale cellen geisoleerd uit patienten met SDS en een andere preleukemische ziekte, myelodysplastisch syndroom (MDS).

De ontstekings-gerelateerde moleculen S100A8 en S100A9 bleken verhoogd tot expressie te komen in zowel het muismodel als deze beide preleukemische ziekten. Blootstelling van HSC aan S100A8/A9 leidde tot DNA schade en celdood via activatie van de TLR4 receptor en blokkade van deze receptor in de muizen verminderde de DNA schade. Hoge expressie van *S100A8* en *S100A9* in mesenchymale cellen was bovendien sterk geassocieerd met de overleving van MDS-patiënten, onafhankelijk van bekende prognostische factoren, wat aangeeft dat verhoogde *S100A8/A9* expressie een potentiële prognostische marker in MDS is.

Samengevat onthult het onderzoek, beschreven in hoofdstuk 3, een nieuw concept van niche-geïnduceerde genotoxische stress in HSC via ontstekings-gerelateerde eiwitten, waaronder S100A8 en S100A9, via TLR4 receptor-activatie. De relatie met de overleving in MDS suggereert verder dat dit nieuwe mechanisme belangrijk is voor de pathogenese van MDS en opent de mogelijkheid dat het remmen van deze signalering zou kunnen leiden tot verbetering van de overleving in deze ziekte.

Om meer inzicht te krijgen in de biologie van mesenchymale cellen in MDS werd in **Hoofdstuk 4** de moleculaire opmaak van deze cellen bestudeerd. Een methode (RNA sequencing) werd ontwikkeld, geoptimaliseerd en gevalideerd om mesenchymale cellen direct afkomstig uit het

beenmerg te bestuderen. Dit is een belangrijke aanvulling op bestaand onderzoek waarin deze cellen eerst buiten het lichaam worden gekweekt en dan onderzocht. Transcriptionele netwerk analyse liet zien dat deze cellen fundamenteel verschillen van normale mesenchymale cellen. Deze verschillen werden gekenmerkt door respons op DNA-schade, cellulaire stress en ontsteking-relateerde veranderingen.

Concluderend hebben de experimenten beschreven in dit proefschrift nieuwe inzichten gegenereerd in de bijdrage van niche cellen aan de verstoring van de bloedvorming in preleukemische ziekten. De onderzoekingen brachten nieuwe moleculaire mechanismen aan het licht en lieten relevantie zien van deze bevindingen voor humane ziekten. Op grond van de resultaten hypothetiseren we dat ontsteking van mesenchymale cellen leidt tot uitscheiding van ontstekings (gerelateerde) eiwitten die de normale bloedvorming remmen en bijdragen aan het ontstaan van leukemie door het induceren van DNA schade.

De uitkomsten passen in het beeld dat veranderingen in HSC en hun niche kunnen samenwerken in het ontstaan van leukemie. Toekomstige onderzoekingen zullen uit moeten maken of deze niche-bijdragen noodzakelijk zijn voor het ontstaan van leukemie en of in dat geval de moleculaire mechanismen geremd kunnen worden om het ontstaan van leukemie te verhinderen of uit te stellen.

ITALIAN SUMMARY
Riassunto in italiano

I globuli bianchi, i globuli rossi e le piastrine che circolano nel sangue umano sono necessari alla sopravvivenza dell'intero organismo, ma tali cellule restano in vita per un periodo di tempo limitato. Garantire una produzione continuata di nuove cellule sanguigne, o emopoiesi, è la funzione delle cosiddette cellule staminali emopoietiche (CSE), situate nel midollo osseo.

Le CSE sono cellule indifferenziate pluripotenti capaci di generare contemporaneamente, per divisione cellulare, una cellula destinata al differenziamento e un'ulteriore CSE, mantenendo quindi il potenziale emopoietico per tutta la durata di vita dell'organismo. Tuttavia, poiché una proliferazione cellulare continuata può causare a lungo andare l'accumulo di mutazioni genetiche, le CSE sono mantenute spesso in uno stato di non divisione (quiescenza) per proteggere l'integrità genomica nella linea emopoietica.

Il bilancio tra quiescenza, proliferazione e differenziazione delle CSE dipende sia da programmi cellulari intrinseci, sia da segnali esterni provenienti da cellule regolatorie non emopoietiche situate nel microambiente midollare, cellule chiamate collettivamente 'nicchia' della CSE. La nicchia comprende diversi tipi cellulari, tra cui i progenitori mesenchimali. Un'alterazione del delicato meccanismo di regolazione delle CSE può portare allo sviluppo della leucemia mieloide acuta, un tumore maligno caratterizzato da proliferazione incontrollata di cellule mieloidi immature che non riescono a differenziarsi completamente. Mentre numerose ricerche si sono concentrate sull'identificazione delle mutazioni genetiche che spiegano a livello intrinseco il carattere tumorale delle cellule leucemiche, gli studi sui possibili contributi estrinseci alla trasformazione delle CSE sono stati finora limitati. Esperimenti su topi geneticamente modificati hanno dimostrato che cellule della nicchia anomale possono promuovere lo sviluppo di leucemie (leucemogenesi), ma rimangono da chiarire sia i meccanismi molecolari alla base di questo fenomeno, sia la sua rilevanza per l'uomo.

Lo scopo di questa tesi è stato quello di far luce su tali punti chiave, cercando una risposta ai seguenti quesiti:

1. Qual è il ruolo delle cellule della nicchia nello sviluppo della leucemia?
2. Quali sono i relativi meccanismi molecolari?
3. Come si applicano tali concetti all'uomo?

A questo scopo, sono state analizzate due sindromi di aplasia midollare che conferiscono un alto rischio di sviluppare la leucemia mieloide acuta: la sindrome di Shwachman-Diamond (SSD) e la sindrome mielodisplastica (SMD). La prima parte di questa tesi si occupa della SSD, scelta come paradigma sulla base di diverse considerazioni. In primo luogo, essendo la SSD una malattia

ereditaria monogenica, essa è particolarmente adatta ad essere riprodotta in modelli sperimentali. Per di più, i pazienti con SSD, oltre a soffrire di neutropenia severa e predisposizione alla leucemia, presentano anomalie scheletriche e osteoporosi, per cui è ipotizzabile che la linea mesenchimale sia coinvolta nella patogenesi della SSD. Inoltre, è stato in precedenza dimostrato che topi con ridotta espressione emopoietica del gene per la biogenesi dei ribosomi *Sbds,* mutato nella SSD, non sviluppano leucemie, il che suggerisce che il deficit di *Sbds* nelle sole cellule emopoietiche non è sufficiente per la trasformazione delle CSE stesse.

In questa tesi, i fattori patogenetici intrinseci ed estrinseci per la SSD sono stati analizzati separatamente tramite l'uso di due topi *conditional knockout* in cui il gene *Sbds* è stato deleto rispettivamente nelle cellule emopoietiche e nella nicchia. Il **capitolo 2** descrive lo sviluppo di un modello murino specifico per la linea emopoietica, ottenuto trapiantando cellule epatiche fetali con deficit di *Sbds* in topi *wild type*. Tali cellule sono state ottenute inducendo la delezione del gene *Sbds* tramite un sistema 'cre-loxP' espresso sotto il controllo del promotore di *Cebpa*. Il gene *Cebpa* codifica un fattore di trascrizione emopoietico espresso in una frazione di cellule staminali e progenitrici emopoietiche (CSPE), definite in base al loro immunofenotipo, e critico per il differenziamento mieloide. L'efficiente delezione del gene *Sbds* nei topi trapiantati è stata verificata sperimentalmente nelle CSPE e in ogni fase del differenziamento emopoietico, compresi i progenitori mieloidi. Mentre i tentativi precedenti di ottenere un modello murino per la neutropenia associata alla SSD erano risultati fallimentari, tutti i topi trapiantati hanno sviluppato una forte riduzione dei granulociti nel sangue, riproducendo quindi per la prima volta gli effetti della SSD sulla linea mieloide in un modello murino. L'analisi di tale modello ha successivamente permesso di analizzare i possibili meccanismi che legano il deficit di *Sbds* all'aplasia midollare. È opinione diffusa che, nella SSD come in altre 'ribosomopatie', i difetti della biogenesi dei ribosomi colpiscano maggiormente le cellule progenitrici a causa dell'alta richiesta di sintesi proteica di quest'ultime, connessa al loro elevato tasso di proliferazione. L'analisi dei topi trapiantati ha dimostrato invece come i progenitori emopoietici tollerino il deficit di *Sbds*, mentre cellule nelle fasi terminali del differenziamento mieloide vi rispondano con l'attivazione di p53 e la morte cellulare programmata, fornendo quindi un meccanismo cellulare per lo specifico sviluppo della neutropenia nella SSD. Un'ultima osservazione effettuata sui topi trapiantati è stata il fatto che nessuno di essi ha mostrato segni di leucemia, suggerendo nuovamente che cellule non ematopoietiche possono contribuire alla trasformazione delle CSE nella SSD.

Nel **capitolo 3** questa ipotesi è stata testata in un secondo modello murino, sviluppato precedentemente, dove la delezione del gene *Sbds* è confinata alle cellule progenitrici mesenchimali nel microambiente midollare. Come i pazienti con SSD, anche i topi con deficit di *Sbds* circoscritto alle cellule mesenchimali presentano ritardo di crescita e osteoporosi. Il basso numero di osteoblasti e la ridotta espressione di marker per osteoblasti terminalmente

differenziati hanno indicato che, proprio come osservato nella linea emopoietica, il deficit di *Sbds* colpisce le fasi finali del differenziamento mesenchimale.

Era stato precedentemente riportato in letteratura che i topi con deficit mesenchimale di *Sbds* presentano alterazioni mielodisplastiche ed alto tasso di apoptosi nelle CSPE, proprio come osservato nella malattia umana. Una serie di analisi descritte in questa tesi hanno permesso una migliore comprensione dei meccanismi cellulari e molecolari alla base di queste osservazioni. Si è infatti dimostrato che l'esposizione a una nicchia con deficit di *Sbds* induce disfunzione mitocondriale, accumulo di radicali liberi dell'ossigeno e danno al DNA in CSPE, con conseguente attivazione dei *checkpoint* del ciclo cellulare. Questi risultati introducono il concetto di genotossicità della nicchia per le CSPE, genotossicità che forse contribuisce all'acquisizione di mutazioni genetiche e alla progressione verso la leucemia nella SSD.

Per identificare possibili meccanismi alla base degli effetti genotossici sulle CSPE, si è poi analizzato il trascrittoma dei progenitori mesenchimali *Sbds*-deleti. Come nella linea mieloide, il deficit di *Sbds* è risultato associato all'attivazione di p53, tuttavia proprio la delezione di p53, pur attenuando il fenotipo osteoporotico dei topi mutanti, non è sembrata migliorare le alterazioni del tessuto emopoietico. Si sono quindi investigati altri possibili meccanismi patogenetici comparando il trascrittoma di cellule mesenchimali del modello murino e di pazienti che soffrono di SSD ed altre condizioni preleucemiche, nella fattispecie la SMD a basso rischio e l'anemia di Diamond-Blackfan. Le molecole di segnale del danno S100A8 e S100A9 sono risultate overespresse sia nel modello murino che nelle due sindromi più associate con leucemia mieloide acuta, la SSD e la SMD. Si è poi dimostrato come queste molecole siano capaci di indurre direttamente danno al DNA e apoptosi nelle CSPE e il blocco del loro recettore TLR4 è stato sufficiente a limitare la genotossicità indotta dalla nicchia nel modello murino. Inoltre, un'alta espressione di *S100A8* e *S100A9* ha identificato, tra i pazienti con SMD a basso rischio, quelli con decorso sfavorevole, indipendentemente da fattori prognostici già noti, per cui l'elevata espressione di S100A8/9 nella nicchia potrebbe rappresentare un nuovo marker di prognosi nella SMD umana.

Complessivamente, gli esperimenti descritti nel capitolo 3 rivelano come la nicchia possa indurre stress genotossico in cellule staminali e progenitrici eterotipiche attraverso segnali infiammatori. Questo concetto, critico per il decorso clinico della malattia preleucemica nell'uomo, rappresenta al contempo un possibile target d'intervento clinico. Data tale rilevanza per la malattia umana, è quindi importante ottenere una visione dettagliata dei segnali molecolari provenienti dalla nicchia nelle sindromi preleucemiche, al fine di guidare la loro prognosi e le relative strategie terapeutiche. Tuttavia, le conoscenze attuali sulla nicchia di soggetti malati derivano da studi effettuati su cellule mesenchimali stromali espanse *ex vivo*, mentre non è noto in quale misura tale sistema rispecchi lo stato delle cellule nel contesto del tessuto malato.

Il **capitolo 4** descrive la prima analisi trascrittomica delle cellule della nicchia isolate direttamente dal midollo osseo di pazienti con SMD a basso rischio. È stato sviluppato, ottimizzato e validato un nuovo metodo per permettere il sequenziamento di nuova generazione (*massive parallel sequencing*) delle rare cellule della nicchia. Successivamente, l'analisi dei *network* trascrizionali ha indicato che le cellule della nicchia di pazienti con SMD hanno un profilo di espressione genica distinto da quello di individui sani e caratterizzato dall'attivazione di *pathway* associati a danno al DNA, stress cellulare e infiammazione. L'analisi trascrittomica ed esperimenti di immunoistochimica hanno anche indicato che le cellule della nicchia di pazienti con SMD a basso rischio possono essere soggette a senescenza cellulare. In particolare, diverse molecole tipicamente secrete da cellule senescenti e con note proprietà proinfiammatorie sono risultate overespresse nella nicchia dei pazienti con SMD. Si prevede che lo studio del trascrittoma delle cellule della nicchia aiuterà a definire sperimentalmente i programmi molecolari alla base dell'overespressione di S100A8/9 e ad identificare altri *pathway* che alterano l'emopoiesi nella SMD.

In conclusione, gli esperimenti descritti in questa tesi hanno dimostrato che cellule della nicchia contribuiscono al fenotipo emopoietico delle sindromi preleucemiche, identificando al contempo i relativi meccanismi molecolari. I concetti elaborati sulla base del modello murino sono risultati applicabili alla malattia umana ed hanno evidenziato come possa esistere una sinergia tra le alterazioni nelle CSPE e nella loro nicchia, sinergia che può guidare lo sviluppo delle leucemie nelle sindromi preleucemiche umane. Questi risultati rappresentano la base per analisi future volte a determinare se il contributo della nicchia sia sufficiente alla leucemogenesi, e aprono al contempo nuove prospettive per terapie nicchia-specifiche che ritardino o prevengano la comparsa delle leucemie nelle sindromi preleucemiche.

AUTHOR'S CURRICULUM VITAE

Noemi Zambetti was born in Bari, Italy, in 1985. After receiving her high school diploma in foreign languages from Cartesio Licei (Triggiano, Italy), she studied health and pharmaceutical biotechnologies at the University of Bari, where she obtained her bachelor degree *cum laude* in 2007 presenting a thesis on the use of molecular cytogenetics to detect genetic amplifications. She then pursued her master in Medical Biotechnology and Molecular Medicine at the University of Bari. After completing a one-year research internship at the Department of Genetics at University "Sapienza" in Rome (Italy), she succesfully defended her thesis '*Construction and characterization of interfering lentiviral vectors for the study of genes implicated in telomeric metabolism*' and graduated in Bari in 2010 with the awarding of *cum laude* honors. In May 2010 she was appointed as PhD candidate in the research group of Dr. Marc Raaijmakers. From May 2010 to July 2010 her research was conducted under the supervision of Dr. Raaijmakers in the laboratory of Prof. David Scadden at the Harvard Stem Cell Institute/Massachusetts General Hospital in Boston (United States). She next moved to the Netherlands, where she continued her doctoral training at the department of Hematology, Erasmus Medical Center (Rotterdam). Here, she studied the regulation of normal and malignant hematopoiesis by mesenchymal niche cells, with a specific focus on how stromal cells contribute to the pathogenesis of inherited bone marrow failure syndromes.

Awards

- Best BA in Biotechnology, University of Bari (2007)
- Best MSc in Medical Biotechnologies and Molecular Medicine, University of Bari (2010)
- Best presentation award, Dutch Society for Stem Cell Research (2014)
- Outstanding Abstract Achievement Award, American Society of Hematology (2014)

List of publications

- **Noemi A. Zambetti**, Marc H. G. P. Raaijmakers. 'Selectin' endothelium to protect blood stem cells. *Haematologica*. 2013 Jan;98(1):1.
- **Noemi A. Zambetti**, Eric M. J. Bindels, Paulina M. H. Van Strien, Marijke G. Valkhof, Maria N. Adisty, Remco M. Hoogenboezem, Mathijs A. Sanders, Johanna M. Rommens, Ivo P. Touw, and Marc H. G. P. Raaijmakers. Deficiency of the ribosome biogenesis gene *Sbds* in hematopoietic stem and progenitor cells causes neutropenia in mice by attenuating lineage progression in myelocytes. *Haematologica*. 2015 Oct;100(10):1285-93.
- **Noemi A. Zambetti***, Zhen Ping*, Si Chen*, Keane J. G. Kenswil, Maria A. Mylona, Mathijs A. Sanders, Remco M. Hoogenboezem, Eric M. J. Bindels, Maria N. Adisty, Cindy S. van der Leije,

Theresia M. Westers, Eline M. P. Cremers, Johannes P. T. M. van Leeuwen, Bram C. J. van der Eerden, Ivo P. Touw, Taco W. Kuijpers, Roland Kanaar, Arjan A. van de Loosdrecht, Thomas Vogl, and Marc H. G. P. Raaijmakers. Mesenchymal inflammation induces genotoxic stress in hematopoietic stem and progenitor cells in leukemia predisposition syndromes. *Manuscript submitted*.

- Si Chen, **Noemi A. Zambetti**, Athina M. Mylona, Maria N. Adisty, Remco M. Hoogenboezem, Eric M.J. Bindels, Mathijs A. Sanders, Eline M.P. Cremers, Dicky J. Lindenbergh-Kortleve, Janneke N. Samsom, Arjan A. van de Loosdrecht and Marc H.G.P, Raaijmakers. Low-risk myelodysplastic syndromes are characterized by a molecular signature of mesenchymal stress and inflammation. *Manuscript submitted.*

Erasmus MC
Universitair Medisch Centrum Rotterdam

PhD Portfolio

Summary of PhD training and teaching

Name PhD student: N. A. Zambetti Erasmus MC Department: Hematology Research School: Molecular Medicine	PhD period: May 2010 – May 2015 Promotor(s): Prof. Dr. Ivo P. Touw Supervisor: Dr. Marc H. G. P. Raaijmakers

1. PhD training

	Year	Workload (Hours/ECTS)
General courses		
Laboratory Animal Science (Art.9)	2010	4.2
Biomedical Research Techniques	2010	1.2
Get-out-of-your-lab Days	2011	0.6
Biomedical English Writing Course	2014	2
In-depth courses and workshops		
Basic Introduction Course on SPSS	2011	1
Photoshop and Illustrator Workshop	2011	0.3
Basic Course on R	2013	0.7
Analysis of microarray and RNA data	2013	1
Scientific meetings Department of Hematology		
Work discussions	2010-2015	10
Erasmus Hematology Lectures	2010-2015	2.5
PhD lunch with seminar speaker	2010-2015	2.5
AIO/PostDoc meeting	2010-2015	2.5
Literature discussions	2010-2015	7.5
AIO/PostDoc Career Event	2015	0.1
(Inter)national conferences		
ESH scientific workshop “Anti-inflammatory & Immune Modulatory Properties of Mesenchymal Stromal Cells”	2012	0.6
Dutch Society for Stem Cell Research Annual Meeting (2X)	2013-2014	0.6
MolMed Day (2X)	2013, 2015	0.6
Dutch Hematology Congress	2014	0.3

Annual conference American Society of Hematology	2014	1
Molecular Aspects of Hematological Disorders (2X)	2014-2015	1.4
International Conference on The Tumour Microenvironment in the Haematological Malignancies and its Therapeutic Targeting	2015	0.6
International Society for Stem Cell Research annual meeting	2015	1
Presentations		
AIO/PostDoc meeting (Oral, 4X)	2012-2014	2
Journal Club (Oral, 3X)	2011-2014	1.5
Workdiscussion (Oral, 9X)	2011-2014	4.5
Daniel Den Hoed Day (Oral, 1X)	2012	1
Molecular Medicine Day (Poster, 1X; Oral, 1X)	2013, 2015	2
Dutch Hematology Congress (Oral, 1X)	2014	1
Dutch Society for Stem Cell Research annual meeting (Oral, 1X)	2014	1
Molecular Aspects of Hematological Disorders (Oral, 2X)	2014-2015	2
Annual conference American Society of Hematology (Oral, 1X)	2015	1
International Society for Stem Cell Research annual meeting (Poster, 1X)	2015	1
2. Teaching		
	Year	**Workload (Hours/ECTS)**
Supervising practicals and excursions, Tutoring		
Organization and supervision PhD lunch with seminar speaker	2012-2013	0.2
Organization and supervision AIO/PostDoc Career Event	2014	0.1
Supervising Master's theses		
Master Student Biomedical Sciences (LUMC)	2012-2013	3
3. Total		62.5

ACKNOWLEDGMENTS

When I started writing my thesis, I was well aware that it was going to be a difficult job. All along my doctorate, I observed fellow PhD students facing this moment and I knew what to expect: late nights, anxiety, grammar dilemmas and, every now and then, an attack of the so-called 'impostor syndrome' (i.e., thinking "I am not knowledgeable-smart-good enough for this"). However, no one really mentioned to me how hard it would be to start writing my acknowledgements! So many people helped me during these years, with my experiments, with administration, or simply reminding me that sometimes the best solution to your problem is to laugh about it! Definitely a lot of people to acknowledge, and so little space to do it, but let's get started!

The first on my list is for sure my supervisor, Marc Raaijmakers. Dear **Marc**, you taught me so much, not only about hematology, but really about being a scientist. I know now that this job is not about digging to discover something, but "to make sure that no one else has to dig there". I learned that 'done' is often better than 'perfect'. I learned that sometimes is not about being fair, as much as being kind and helpful. Working with you, I had the privilege to witness the hard task of creating a new research group, and the even harder job of keeping it functional and productive. Thank you for giving me this great opportunity, and thanks for helping me out in every step, from searching an accommodation for me in Boston, to teaching me how to work with mice, to always making room for my "five minutes questions" that obviously took longer than expected. I will always keep fond memories of our discussions in the yellow chair room, struggling with some weird results and deciding how to proceed. Lastly, thank you so much for dealing with my hot-blooded Italian personality! We had passionate discussions these years, but I hope it came clear that this is just a Southern European demonstration of caring enough! I really hope that I was up to the expectations you had when you first hired me, and I wish you all the luck in the world in your career.

My heartfelt thanks to my promoter, Prof. Ivo Touw. Dear **Ivo**, I felt honored when I learned that you accepted being my promotor. I have always admired you as a scientist, but working closer to you, I had the opportunity to appreciate your qualities as a mentor as well. Thank you so much for your collaboration on the C/EBP-α project, for your guidance in obtaining my PhD and for supporting my career development.

I would like to express my gratitude to the members of my inner doctoral committee for helping me improving my thesis and most importantly for giving me the opportunity to look at my results from different angles. Dear **Marieke**, your contagious energy and enthusiasm are truly inspiring! Thank you for motivating me to deepen my knowledge into the complex world of translational regulation! Dear **Ruud**, during these years I appreciated your efforts in promoting collaboration among hematology researchers. Thank you for giving me the opportunity to contribute to the 'Molecular Aspects of Hematology Research' seminars, and obviously thanks for your thought-

provoking comments to my thesis! Dear **Sjaak**, although we do not know each other much, you agreed on being part of my inner committee. Thank you for your responsiveness and thoughtful suggestions. I would also like to thank all members of my large committee for their time and commitment to my defense ceremony, and special thanks to professors **Hans** van Leeuwen and **Roland** Kanaar for collaborating with us on our niche project.

My warmest thanks go to Prof. Bob Löwenberg, who took part to my job interview six years ago. Dear **Bob**, I never had the chance to thank you for that positive feedback! Thank you also for your suggestions on our manuscripts and for precious insights on all aspects of hematology. To all the PIs of the Hematology Department (previous and past), including **Jan**, **Eric**, **Tom**, **Pieter**, **Mojca**, **Peter**, **Frank**, **Dick**, **Moniek**, **Anita**, **Stefan** and **Miranda**: thank you all! Your questions and positive criticism helped me to grow as a scientist and I hope there will be the chance to keep collaborating in the future.

This thesis would not have seen the light of the day without the help of my lab members. Dear Zhen, or shall I say Mr. **Ping**? Collaborating with you has been a learning experience for me. Your passion for science combines with uncommon kindness and a great heart...and makes you a true workaholic! I will be forever grateful for all the late nights you spent in the lab working on the project, and I wish you all the best in your career, starting from getting our niche paper published very soon! This wish is obviously extended to our paper's co-first author and my desk-mate, Si Chen! Dear **Si**, you brought such a fresh vibe in our lab, and tons of food in our drawer! We shared the fun moments, we shared the many hard times, and I couldn't ask for a better colleague and friend. Thank you very much for all your help! And then there's my lab godson! Dear **Keane**, it was a pleasure to help you during your internship, and I was so happy learning you were staying for a PhD position. I saw your transformation from a promising student to a brilliant researcher and I'm sure your talent will bring you far! Thanks for your help in the lab, and for organizing such memorable karaoke nights!

A special thanks to the past members of the lab. Dear **Athina**, without you we would have no RNA-seq protocol for our niche cells! You were one of the pioneers in our lab and I thank you deeply for all the suggestions you gave me along the years. Dear **Niken**, my favorite Indonesian, thanks for bringing some order in our messy lab, and thanks for your help with RNA sequencing. I look forward to visiting you in Indo…I need your saoto soup recipe after all! Dear **Adrian**, you crazy Ecuadorian! I will never forget your video-shooting technique when you first arrived! Thanks for your daily doctor tips, not to mention you great barbeques! To everyone else who passed by, **Shikhar**, **Sam**, **Titia**, **Uttara**, **Marwa**, **Sjoerd**, **Niels**…thank you all and good luck in your careers!

I cannot forget to acknowledge all the other people that helped me to produce and analyze the data in this dissertation. Talking about data (the big type), thank you **Remco** and **Mathijs** for your support with bioinformatics and statistics. You guys were always ready to re-analyze our datasets

from different angles, and to explain us 'math-illiterate' how to approach our results. Thank you so much for your efforts! Of course every RNA-seq experiment required also the help of Eric Bindels. Dear **Eric**, I bet you hate being on the spotlight right now, but I want to thank you officially for your hard work, including your support with the C/EBP-α project. You always kept a 'listening ear' to my troubles and were a great counselor. All the best in your career! Dear **Elwin** and **Peter** van Geel, with your help setting up a flow cytometry experiment and sorting cells was never a problem. Thank you both very much! I extend my acknowledgements to the other members of the **BMT lab** (including past member **Hannie**) for their help with normal bone marrow samples and for teaching me the tricks of human CFU-C analysis.

The work described in this thesis required the help of many external collaborators as well. Dear **Bram**, thank you for introducing me to the world of bone metabolism! It was a fun experience, and a fruitful one. Thank you **Cindy**, **Marijke**, **Andrea** and **Tanja** for your help with bone assays. Cindy, I consider myself invited for a tour of your new home! Dear **Taco** Kuijpers and **Arjan** van de Loosdrecht, thank you for your interest in our SDS projects. It was a wonderful opportunity being able to work on patient material and you made that possible. Dear **Thomas** Vogl, thanks for your amazing help with the S100A8/9 experiments. You were so responsive and always ready to share material and knowledge with us, thank you so much for that. Dear **Pier Giorgio** and **Chiara**, although the mitochondria world will always be a bit mysterious to me, with your guidance I managed to perform all ROS analyses! Grazie di cuore ad entrambi!

Animal experiments are taken very seriously in the Netherlands, but my job was made easier thanks to the members of the EDC and the article 14 team. Dear **Amélie**, **Henk**, **Mathieu**, **Miranda** and **Thea**, thanks for your help with administrative and ethical aspects of our work. Dear **Kim**, **Jessica**, **Ingeborg**, **Eva**, **Vincent**, and the other workers of the EDC: thanks for taking good care of our mouse colonies!

I would like to take the time to thank now my two awesome paranymphs. Dear **Paulette**, I worked side by side with you on the C/EBP-α project, and what a success it was! I have no words to express my gratitude for teaching me all the tricks of transplantation and for managing the strain with such precision. Everyone knows how devoted you are to your job and I knew I could count on you for my thesis as well. Thanks for all your help, very much appreciated! Dear **Katarzyna**, Kasia, Kasienka, Kaska (yes, all of your personalities!). My colleague, friend and life coach! The one and only who can work over 15 hours and still find the energy to organize coffee dates, dinners, parties… Our lives crossed on the 13th floor and I am so glad they did. You have been through a lot these years, but you accepted difficulties and tried to stay positive and that was truly inspiring. Thanks for sharing those 'rose-colored glasses' with me! I wish you an amazing career because…wouldn't that be "super super nice"?

During these years as a PhD student I was lucky enough to share my office with great colleagues from the Wagemaker, Delwel, Rijneveld/Valk and Sonneveld lab. Dear **Helen**, you were my first desk-mate and the first who really welcomed me in this department. You helped me out with administration when I couldn't understand Dutch language, you invited me in the Wagemaker lunch groups (featuring the famous **Trui**!) and in no time you became a dear friend. I am so grateful I got to enjoy that friendship once you came back from Boston. Thanks to you and to **Eric** for great game dates (Arkham is a safer city thanks to us!) and look forward to see you both very soon. Dear **Yvette**, thanks for your help with managing the blood counter. You're always welcome to visit for a Magic card game session! Dear **Merel**, we both found more than career development on this department and I'm so proud of all your achievements, professional and not! Thanks to you and to **Roel** for fun nights featuring mysterious murders! Dear **Rana**, thanks for sharing delicious treats at any given occasion and good luck with your papers and thesis. Dear **Leonie**, your work promoting science is really admirable. Thank you for giving me the opportunity to contribute to the Discovery Festival. Dear **Niek**, I'm glad your career proceeds well in Utrecht. Thank you for all your suggestions on lentiviral transduction. Dear **Carla** and **Anikó**, you girls make a great teamwork: always happy and very motivated. Anikó, thanks for your help in arranging the career workshop. Dear **Tim** and **Sophie**, I regret the opportunity to know you better but I wish you good luck in your PhD track!

It is a true blessing when your colleagues become your dearest friends. I already mentioned quite a few of them, but I have more members of the 'crazy 13' club to thank! Dear **Roberto**, in spite of your reserved personality we managed to become dear friends. We are similar in many ways, and we similarly missed the warm Southern European vibe in the Netherlands. Thank you so much for many long and interesting conversations. I truly believe you are one of the most brilliant PhDs I have met in my journey, and I do not need to wish you success because that's a given. Dear **Onno**, where shall I start thanking you from? Shall I be professional and mention your help with imaging and computer-related issues? Honestly, I prefer instead to thank you for all the fun you brought to us PhD student by organizing beerclubs, roadtrips, theme-nights and other memorable events. You are really the glue that kept us all together! I hope you will be visiting often…we need your help preparing party concoctions in the US! Dear **Jana**, I am close to my PhD defense and still I cannot find the birds! All joking aside, I am so happy to have met you and become your friend. Thanks for showing me that no matter what happens in the lab, you can still manage to be positive and relaxed…you just need to stroke a furry wall! Dear **Joyce**, regardless of your lab moving to the new building you never abandoned us, luckily! Thank you for all the fun times we had together, from preparing the Joker's minion masks to the many dinners (also the ones in which I self-invited) and of course our little trip to Helmond! Dear **Julia**, my concert-pal! No matter how grumpy you try to be, you cannot help being helpful and kind. Thanks for your tips with many experiments and I look forward to the next metal music event together! Dear **Patricia** Olofsen, we knew each other for little time but still you shared a lot with me, from the laughter to some

tears. Thanks for being a great friend, I am sure wonderful things await in your life! Dear Julien, Monica and Patricia Aparicio, you guys made me feel less lonely in my late sorting nights…because you were next to me waiting for the Aria to become available! Dear **Patricia**, thanks for all the tips in arranging my thesis! **Monica**, I regret not having spent more time with you. Let's fix it when the Señora Tomasa is in town again! And obviously good luck in wrapping up your PhD! Dear **Julien**, I will try to bring some sun to Rotterdam for my defense…so we can all meet up in your garden again! Good luck with your career, and remember, Marseille is close! Dear **Davine**, the only one who can understand my need of focaccia! It was great finding someone who knew my city in the middle of the Netherlands, you made me feel at home! Thanks for your help with the career event and the many tips about Stockholm! Looking forward to having you as a guest in Bari!

Dear **Ferry**, **Farshid**, **Mark**, **Shiraaz**, **Shirley**, **Adil**, **Avinash**, thank you all for being amazing colleagues and good luck in your research! Dear **Claudia**, **Marije**, **Marijke**, **Hans**, **Jasper** and all the department analysts, thank you all for your help! I was often running around in search of a reagent or some technical advice, and you always made time for me. I also want to express my gratitude to the supporting personnel, **Jan**, **Egied**, **Natasha**, **Tomasia**, and especially the secretaries **Ans**, **Leenke** and **Annelies**. Dear Annelies, you made it possible for me to arrange my thesis while staying in Italy. Thank you so much!

Now would you please excuse a temporary language switch to thank my Italian friends and family.

Care **Claudia**, **Alessia** e **Katia**, probabilmente non avrete modo di essere con me per la mia tesi di dottorato, e se ci riusciste forse vi annoiereste a morte. Ciononostante, vorrei ringraziarvi per essermi sempre state vicine, anche solo con una chiamata o un messaggio veloce. Questi anni lontano da casa non sono stati sempre facili e con il vostro aiuto mi sono sentita meno sola. Grazie per aver ritagliato un momento per incontrarci ogni volta che scendevo a Bari (o a Lisbona!). Non vedo l'ora che giugno arrivi per ricreare il gruppo. Vi voglio bene!

Caro **Manuel**, il tempo passa ma la nostra amicizia cresce e si rinforza. Abbiamo sopportato e stiamo ancora sopportando insieme le difficoltà che nascono dall'essere ricercatori, dal duro lavoro all'insicurezza sul nostro futuro. Grazie per il tuo ascoltare ogni mio sfogo, anche se…diciamocelo…mi lamento sempre per le stesse cose! Grazie anche per avermi spronato ad uscire ogni volta che ero nei dintorni. È strano essere lontani da casa, torni e gli amici nel tuo gruppo cambiano, o ridono per eventi passati cui ovviamente non hai partecipato. Ecco, tu hai sempre fatto in modo che quei momenti non mi pesassero. Sei un grande amico, e sono sicuro che lo sarai anche con un oceano di mezzo.

Cari **mamma**, **papà** e **Lorenzo**. Incredibile a dirsi, anche questa è fatta! Sembra ieri quando mi avete lasciato nella 'casa con il bidet nel giardino', ed eccomi qui a scrivere le ultime pagine della mia tesi. So che è stato difficile accettare l'idea che avrei vissuto in un altro Paese, ma suvvia…ve

la siete cercata quando avete deciso di passare ogni estate girovagando per l'Europa in camper! Scherzi a parte, vi ringrazio davvero per avermi supportato (e sopportato) durante questi anni di lontanza. Grazie per i pacchi pieni di bontà 'terroniche', dall'olio buono, alla salsiccia barese, alla mozzarella, ai pacchi di pasta…anche se, a dirla tutta, a volte era proprio troppa roba! Grazie per aver ascoltato i miei sfoghi su Skype ogni volta che c'era un problema in casa o sul lavoro. Grazie per aver speso soldi e tempo per venirmi a trovare (anche se mi sorge il dubbio che Dino's contribuiva molto alla vostra scelta!). E grazie per avermi riaccolto a casa mentre scrivevo la tesi. Per quanto possa spaventarmi l'idea di partire per l'America, sapere che potrò ancora contare su di voi mi rincuora! E chissà…magari questa Italia cambia rotta e ci permette di riunirci definitivamente! Incrociamo le dita!

Sometimes life has unexpected plans for you. I moved to the Netherlands to pursue professional development, and I found love. These last words of thanks are for the person that rearranged my life plans and convinced me to move 10,000 kilometers (sorry, 6,500 miles) away from home. Dear **Marshall**, I could not have made it without you. You always believed that I would succeed as a researcher, and you encouraged me to go on and finish my PhD even when I was about to give up. You shared your own difficulties to remind me that I was not alone in this journey. You made me laugh when I was homesick and made your best to make me feel at home in Rotterdam. When I was running late in the lab, you got on your bike and came back to Erasmus MC just to share dinner with me. You were my safe haven and my peace sanctuary in all these years. I have no words to say how thankful I am to have you in my life. I do not know what my job will be, or where I will live, but as long as we are together, I will always look forward to our next great adventure.

"The sky grew darker, painted blue on blue, one stroke at a time,
into deeper and deeper shades of night."
Haruki Murakami, Dance Dance Dance.